(12) INTERNATIONAL APPLICATION PUBLISHED UNDER THE PATENT COOPERATION TREATY (PCT)

(19) World Intellectual Property Organization
International Bureau

(43) International Publication Date
21 February 2013 (21.02.2013)

WIPO | PCT

(10) International Publication Number
WO 2013/024040 A2

(51) International Patent Classification:
A61K 38/19 (2006.01)

(21) International Application Number:
PCT/EP2012/065716

(22) International Filing Date:
10 August 2012 (10.08.2012)

(25) Filing Language: English

(26) Publication Language: English

(30) Priority Data:
61/522,728 12 August 2011 (12.08.2011) US

(71) Applicant *(for all designated States except US)*: **B.S.R.C. ALEXANDER FLEMING** [GR/GR]; P.O. Box 74145, GR-166 02 Varkiza (GR).

(72) Inventors; and

(75) Inventors/Applicants *(for US only)*: **NTOUNI, Eleni** [GR/GR]; Mikinaikon Tafon 19, GR-190 04 Spata (GR). **KOLLIAS, Georgios** [GR/GR]; Agiou Ioannou 89, GR-153 42 Aghia Paraskevi (GR).

(74) Agent: **JANSEN, C.M.**; Johan de Wittlaan 7, NL-2517 JR Den Haag (NL).

(81) Designated States *(unless otherwise indicated, for every kind of national protection available)*: AE, AG, AL, AM, AO, AT, AU, AZ, BA, BB, BG, BH, BN, BR, BW, BY, BZ, CA, CH, CL, CN, CO, CR, CU, CZ, DE, DK, DM, DO, DZ, EC, EE, EG, ES, FI, GB, GD, GE, GH, GM, GT, HN, HR, HU, ID, IL, IN, IS, JP, KE, KG, KM, KN, KP, KR, KZ, LA, LC, LK, LR, LS, LT, LU, LY, MA, MD, ME, MG, MK, MN, MW, MX, MY, MZ, NA, NG, NI, NO, NZ, OM, PE, PG, PH, PL, PT, QA, RO, RS, RU, RW, SC, SD, SE, SG, SK, SL, SM, ST, SV, SY, TH, TJ, TM, TN, TR, TT, TZ, UA, UG, US, UZ, VC, VN, ZA, ZM, ZW.

(84) Designated States *(unless otherwise indicated, for every kind of regional protection available)*: ARIPO (BW, GH, GM, KE, LR, LS, MW, MZ, NA, RW, SD, SL, SZ, TZ, UG, ZM, ZW), Eurasian (AM, AZ, BY, KG, KZ, RU, TJ, TM), European (AL, AT, BE, BG, CH, CY, CZ, DE, DK, EE, ES, FI, FR, GB, GR, HR, HU, IE, IS, IT, LT, LU, LV, MC, MK, MT, NL, NO, PL, PT, RO, RS, SE, SI, SK, SM, TR), OAPI (BF, BJ, CF, CG, CI, CM, GA, GN, GQ, GW, ML, MR, NE, SN, TD, TG).

Published:

— *without international search report and to be republished upon receipt of that report (Rule 48.2(g))*

WO 2013/024040 A2

(54) Title: TNF SUPERFAMILY TRIMERIZATION INHIBITORS

(57) Abstract: The invention relates to methods and compositions for inhibiting the trimerization of ligands belonging to the TNF superfamily. In particular, the invention relates to inhibiting RANKL trimerization. Accordingly, the methods and compositions provided herein can be used to treat disorders associated with increased RANK signalling, in particular those related to bone loss. Novel compounds that inhibit trimerization of ligands belonging to the TNF superfamily are also provided.

Title: TNF superfamily trimerization inhibitors

FIELD OF THE INVENTION

The invention relates to methods and compositions for inhibiting the trimerization of ligands belonging to the TNF superfamily. In particular, the invention relates to inhibiting RANKL trimerization. Accordingly, the methods and compositions provided herein can be used to treat disorders associated with increased RANK signalling, in particular those related to bone loss.

BACKGROUND OF THE INVENTION

Bone remodeling is a constant process through the synthesis of bone matrix by osteoblasts and the coordinate bone resorption by osteoclasts [1,2]. Normally, osteoblastic and osteoclastic activities are balanced so that skeletal integrity is preserved. Perturbations in bone remodeling can result in skeletal abnormalities such as osteopetrosis and osteoporosis which are characterized by excessive or decreased bone mass, due to impaired or enhanced osteoclast activity. RANKL is the primary mediator of osteoclast-induced bone resorption [3] and belongs to the TNF superfamily [4,5] that is characterized by homotrimerization. It is a type II transmembrane protein that consists of a short N-terminal cytoplasmic domain and a conserved extracellular domain forming an antiparallel ß-sheet that is predicted to assemble into a trimer required for receptor activation [6,7]. Soluble RANKL is generated either by proteolytic processing of the transmembrane form or by alternative splicing [8,9]. RANKL is expressed on activated T lymphocytes [4,5] as well as on stromal cells [10,11] and binds as a trimer to its receptor RANK that is expressed on the surface of osteoclast precursors and mature osteoclasts. This interaction is necessary for osteoclast differentiation, activity and survival [10,12], which subsequently lead to bone resorption. Osteoprotegerin (OPG), a

decoy receptor of RANKL, inhibits the binding of RANKL to RANK and thereby limits osteoclastogenesis [11]. Genetic ablations of both RANKL [13,14] and RANK [15,16] result in severe osteopetrosis due to complete lack of osteoclast formation demonstrating that RANKL and RANK are indispensable for osteoclastogenesis. Absence of OPG causes increased osteoclastogenesis and osteopenia [17]. While RANKL is best known for its role in bone resorption, it also plays multiple roles in immune system [4,5,13,18,19], mammary gland development during pregnancy [20], thermoregulation [21], cancer metastasis [22], and hormone-derived breast development [23].

As a result of its effects on the skeleton, RANKL is a major therapeutic target for the suppression of bone resorption in osteoporosis, rheumatoid arthritis and cancer metastasis [24]. Indeed, clinical trials with denosumab, a fully human monoclonal antibody against RANKL, showed an increased bone mass and reduced incidence of fractures in postmenopausal women with osteoporosis [25] and in prostate cancer patients receiving androgen-deprivation therapy [26]. This antibody has been recently approved in the USA and EU for the treatment of patients with osteoporosis and in prostate cancer patients undergoing hormonal ablation therapy. On the other hand, a variety of mutations localized within the extracellular domain of RANKL have been recently reported in children with autosomal recessive osteopetrosis (ARO) (OMIM 602642), an incurable rare genetic disease [27]. However, animal models bearing functional mutations in the *Rankl* gene have not been reported yet, hampering not only the identification of critical residues involved in RANKL function but also the elucidation of the molecular pathogenic mechanisms underlying ARO.

SUMMARY OF THE INVENTION

One aspect of the disclosure provides a method for inhibiting trimerization of a TNF superfamily member polypeptide comprising contacting said polypeptide with a trimerization inhibitor selected from

- a) a dominant negative TNF superfamily member polypeptide or fragment thereof, preferably having a dominant negative mutation in the trimerization domain,

- b) a compound that binds to said TNF superfamily member polypeptide in the F beta-strand of said polypeptide, preferably at the glycine residue that corresponds to position 279 in human RANKL, provided that when the trimerization inhibitor is 6,7-Dimethyl-3-[[methyl[2-[methyl[[1-[3-(trifluoromethyl)phenyl]-1H-indol-3-yl]methyl]amino]ethyl]amino]methyl]-(4H-1-Benzopyran-4-one), said TNF superfamily member polypeptide is not TNF-alpha. Preferably, when the trimerization inhibitor is a compound of formula 1 as described herein, or a stereoisomer thereof, tautomer thereof, or mixture thereof in any ratio; a pharmaceutically acceptable salt, pharmaceutically acceptable solvate, or pharmaceutically acceptable polymorph thereof; said TNF superfamily member polypeptide is not TNF-alpha. More preferably, when the trimerization inhibitor is a compound that binds to said TNF superfamily member polypeptide in the F beta-strand, said TNF superfamily member polypeptide is not TNF-alpha. Preferably, the TNF superfamily member polypeptide or fragment thereof comprises a mutation in the F beta-strand, preferably in the glycine residue that corresponds to position 279 in human RANKL. In some embodiments, the method is an in vitro method.

Preferably a method is provided for inhibiting trimerization of a TNF superfamily member polypeptide comprising contacting said polypeptide with T23 or a functional derivative thereof, or a functional derivative of 6,7-Dimethyl-3-[[methyl[2-[methyl[[1-[3-(trifluoromethyl)phenyl]-1H-indol-3-yl]methyl]amino]ethyl]amino]methyl]-(4H-1-Benzopyran-4-one); preferably selected from PRA123, PRA224, PRA333, PRA738, and PRA828, most preferably PRA224.

Preferably a method is provided for inhibiting TNF-induced cell death comprising contacting a cell susceptible of TNF-induced cell death with T23 or a functional derivative thereof, or a functional derivative of 6,7-Dimethyl-3-[[methyl[2-[methyl[[1-[3-(trifluoromethyl)phenyl]-1H-indol-3-yl]methyl]amino]ethyl]amino]methyl]-(4H-1-Benzopyran-4-one); preferably selected from PRA123, PRA224, PRA333, PRA738, and PRA828, most preferably PRA224. In some embodiments, the method is an in vitro method. In some embodiments, the cell is a non-human cell.

Preferably a method is provided for reducing TNF-induced matrix metalloproteinase release comprising contacting a cell susceptible of TNF-induced matrix metalloproteinase release with T23 or a functional derivative thereof, or a functional derivative of 6,7-Dimethyl-3-[[methyl[2-[methyl[[1-[3-(trifluoromethyl)phenyl]-1H-indol-3-yl]methyl]amino]ethyl]amino]methyl]-(4H-1-Benzopyran-4-one); preferably selected from PRA123, PRA224, PRA333, PRA738, and PRA828, most preferably PRA224. Preferably, said cell is a synovial fibroblast. In some embodiments, the method is an in vitro method. In some embodiments, the cell is a non-human cell.

Another aspect of the disclosure provides for a method for inhibiting osteoclast formation or decreasing bone loss in an individual, comprising administering to an individual in need thereof a therapeutically effective amount of a compound that inhibits trimerization of RANKL selected from

- a) a dominant negative RANKL polypeptide or fragment thereof, preferably having a dominant negative mutation in the trimerization domain,
- b) a compound that binds to said TNF superfamily member polypeptide in the F beta-strand of said polypeptide, preferably at the glycine residue that corresponds to position 279 in human RANKL. Preferably, the RANKL polypeptide or fragment thereof comprises a mutation in the F beta-strand, preferably at the glycine residue that corresponds to position 279 in human

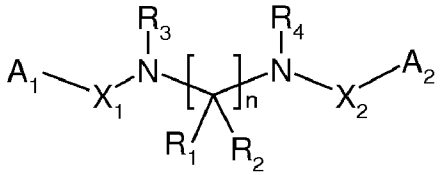
RANKL. Preferably the compound is T23 or a functional derivative thereof, or a functional derivative of 6,7-Dimethyl-3-[[methyl[2-[methyl[[1-[3-(trifluoromethyl)phenyl]-1H-indol-3-yl]methyl]amino]ethyl]amino]methyl]-(4H-1-Benzopyran-4-one); preferably selected from PRA123, PRA224, PRA333, PRA738, and PRA828, most preferably PRA224.

Another aspect of the disclosure provides for a method for preventing, treating, or reducing symptoms in an individual afflicted with osteoporosis, rheumatoid arthritis, multiple myeloma, bone metastasis, juvenile osteoporosis, osteogenesis imperfecta, hypercalcemia, hyperparathyroidism, osteomalacia, osteohalisteresis, osteolytic bone disease, osteonecrosis, Paget's disease of bone, bone loss due to rheumatoid arthritis, inflammatory arthritis, osteomyelitis, periodontal bone loss, bone loss due to cancer, age-related loss of bone mass, osteopenia, and inflammatory bowel syndrome, comprising administering to a individual in need thereof a therapeutically effective amount of a compound that inhibits trimerization of RANKL selected from

- a) a dominant negative RANKL polypeptide or fragment thereof, preferably having a dominant negative mutation in the trimerization domain,
- b) a compound that binds to said TNF superfamily member polypeptide in the F beta-strand of said polypeptide, preferably at the glycine residue that corresponds to position 279 in human RANKL. Preferably, the RANKL polypeptide or fragment thereof comprises a mutation in the F beta-strand, preferably at the glycine residue that corresponds to position 279 in human RANKL. Preferably the compound is T23 or a functional derivative thereof, or a functional derivative of 6,7-Dimethyl-3-[[methyl[2-[methyl[[1-[3-(trifluoromethyl)phenyl]-1H-indol-3-yl]methyl]amino]ethyl]amino]methyl]-(4H-1-Benzopyran-4-one); preferably selected from PRA123, PRA224, PRA333, PRA738, and PRA828, most preferably PRA224.

In preferred embodiments of the above methods, the compound that binds to said TNF superfamily member polypeptide is a compound as depicted in Figure 23 or a stereoisomer thereof, tautomer thereof, or mixture thereof in any ratio; a pharmaceutically acceptable salt, pharmaceutically acceptable solvate, or pharmaceutically acceptable polymorph thereof. Preferably the compound is compound 1 of Figure 23 (T23).

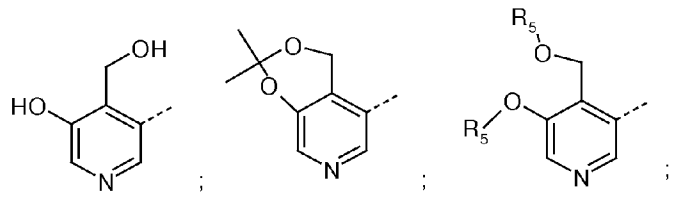
In preferred embodiments of the above methods, the compound that binds to said TNF superfamily member polypeptide is a compound of formula 1, or a stereoisomer thereof, tautomer thereof, or mixture thereof in any ratio; a pharmaceutically acceptable salt, pharmaceutically acceptable solvate, or pharmaceutically acceptable polymorph thereof;

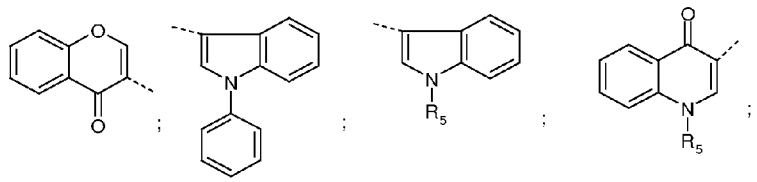


Formula 1

wherein:

A_1 and A_2 are independently a substituted or unsubstituted heterocyclic system selected from;





wherein the dotted line indicates the point of attachment, R_5 is hydrogen or (C_1-C_4)- alkyl group and the rings of the heterocyclic systems herein above may be substituted with groups selected from (C_1-C_4)-alkyl, (C_1-C_4)-alkoxy, hydroxyl, hydroxy-(C_1-C_4)-alkyl (e.g., hydroxymethyl or 1 -hydroxyethyl or 2-hydroxyethyl), and fluoroalkyl (e.g., CF_3);

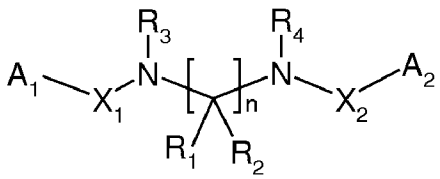
X_1 and X_2 are independently a carbonyl group or a methylene (-CH_2-) group; n is an integer from 2-4;

R_1 and R_2 are independently, hydrogen or (C_1-C_4)-alkyl group;

R_3 and R_4 are independently, hydrogen or (C_1-C_4)-alkyl group; and

R_3 and R_4 can optionally form a ring system; with a proviso that when A_1 and A_2 are 1 -(3-(thfluoromethyl)phenyl)-1 H-indole and 6,7-dimethyl-4H-chromen-4-one respectively and X_1 and X2 are independently a methylene (-CH_2-) group, R_3 and R_4 form a ring system, preferably, wherein said compound is 6,7-Dimethyl-3-[[methyl[2-[methyl[[1-[3-(trifluoromethyl)phenyl]-1H-indol-3-yl]methyl]amino]ethyl]amino]methyl]-(4H-1-Benzopyran-4-one), also known as SPD304.

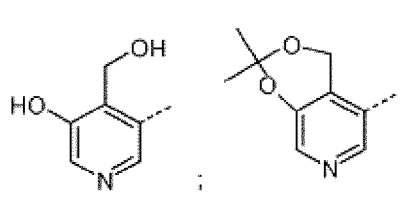
In preferred embodiments of the above methods, the compound that binds to said TNF superfamily member polypeptide is a compound of formula 1, or a stereoisomer thereof, tautomer thereof, or mixture thereof in any ratio; a pharmaceutically acceptable salt, pharmaceutically acceptable solvate, or pharmaceutically acceptable polymorph thereof;

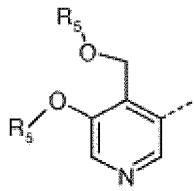
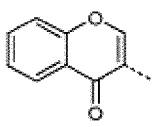
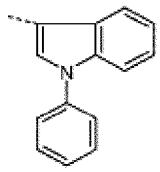
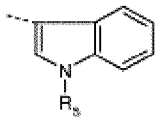
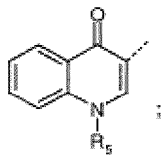


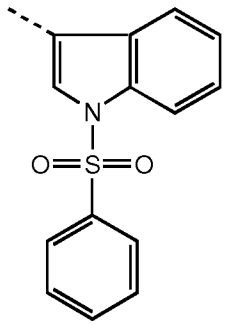
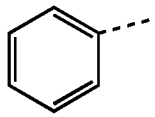
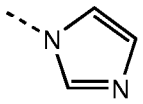
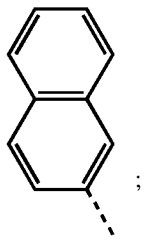
Formula 1

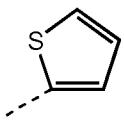
wherein:

A_1 and A_2 are independently a substituted or unsubstituted heterocyclic system selected from;





wherein the dotted line indicates the point of attachment, R_5 is hydrogen or (C_1-C_4)- alkyl group and the rings of the heterocyclic systems herein above are unsubstituted or substituted with one or more groups selected from (C_1-C_4)-alkyl, (C_1-C_4)-alkoxy, hydroxyl, hydroxy-(C_1-C_4)-alkyl (e.g., hydroxymethyl or 1 -hydroxyethyl or 2-hydroxyethyl), fluoroalkyl (e.g., CF_3), halide (e.g. fluoro); nitro (NO_2) and amino (NH_2);

X_1 and X_2 are independently a carbonyl group or a methylene (-CH_2-) group; n

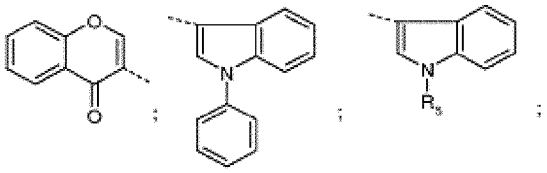
is an integer from 2-4;

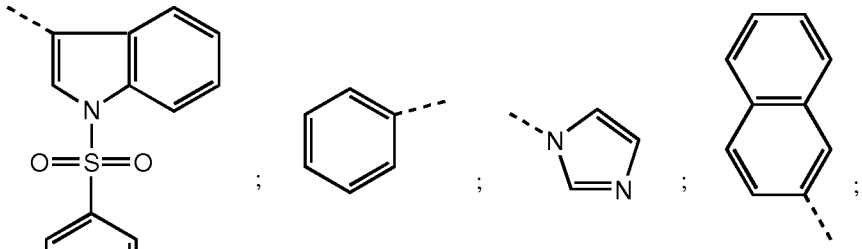
R_1 and R_2 are independently, hydrogen or (C_1-C_4)-alkyl group;

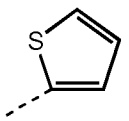
R_3 and R_4 are independently, hydrogen or (C_1-C_4)-alkyl group;

or wherein R_3 and R_4 are a single (C_1-C_8)-hydrocarbon group connecting the two nitrogen atoms of formula 1, which group may be selected from saturated hydrocarbon (*e.g.* C_2H_4) and aromatic hydrocarbon (*e.g.* phenyl).

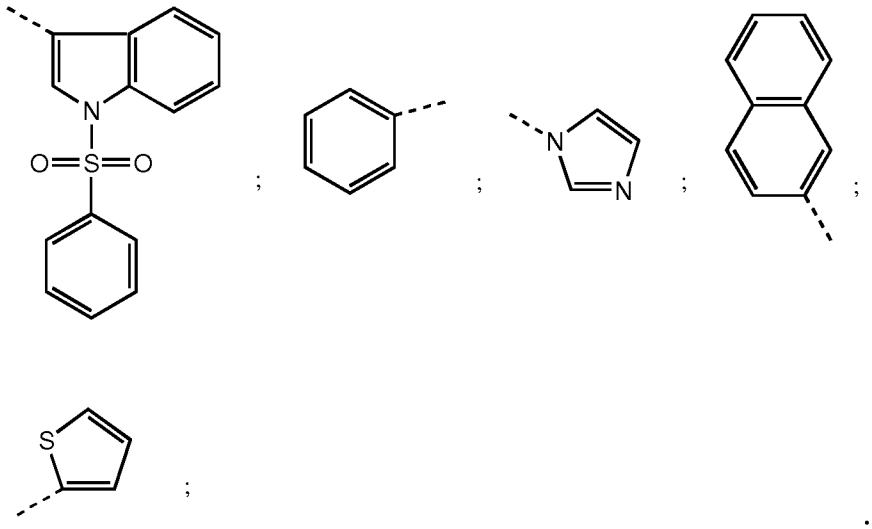
Preferably, the rings of the heterocyclic systems are unsubstituted or substituted with one or more groups selected from trifluoromethyl (CF_3), fluoro (F); nitro (NO_2) and amino (NH_2). Preferably, A_1 and A_2 are selected from;



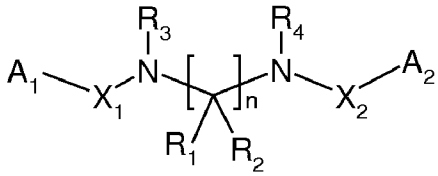




more preferably selected from



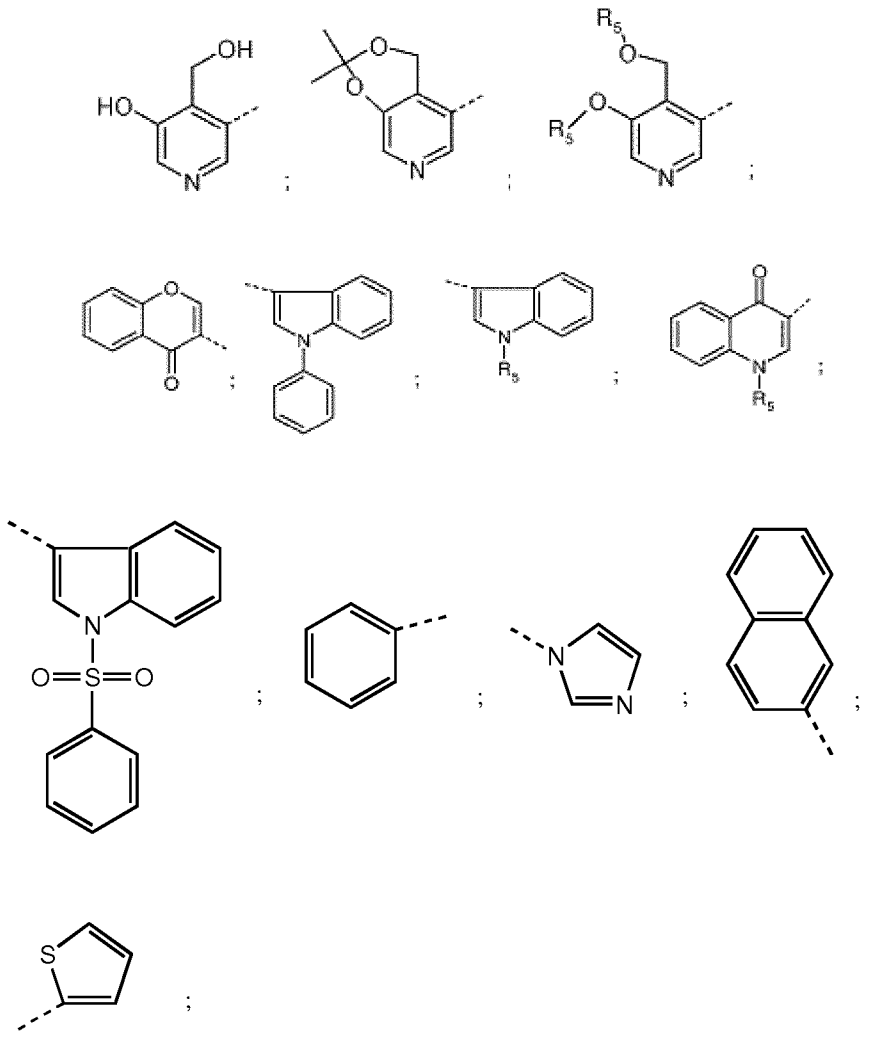
In a further aspect, novel compounds are provided having formula 1, or a stereoisomer thereof, tautomer thereof, or mixture thereof in any ratio; a pharmaceutically acceptable salt, pharmaceutically acceptable solvate, or pharmaceutically acceptable polymorph thereof;



Formula 1

wherein:

A_1 and A_2 are independently a substituted or unsubstituted heterocyclic system selected from;



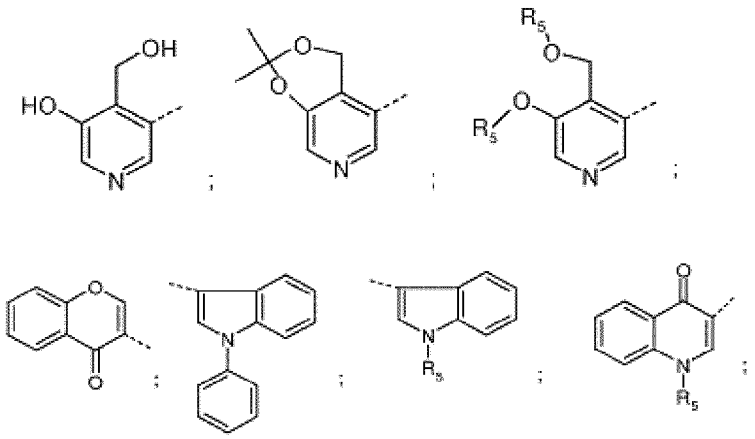
wherein the dotted line indicates the point of attachment, R_5 is hydrogen or (C_1-C_4)- alkyl group and the rings of the heterocyclic systems herein above are unsubstituted or substituted with one or more groups selected from (C_1-C_4)-alkyl, (C_1-C_4)-alkoxy, hydroxyl, hydroxy-(C_1-C_4)-alkyl (e.g., hydroxymethyl or 1 -hydroxyethyl or 2-hydroxyethyl), fluoroalkyl (e.g., CF_3), halide (e.g. fluoro); nitro (NO_2) and amino (NH_2);

X_1 and X_2 are independently a carbonyl group or a methylene (-CH_2-) group; n is an integer from 2-4;

R_1 and R_2 are independently, hydrogen or (C_1-C_4)-alkyl group;

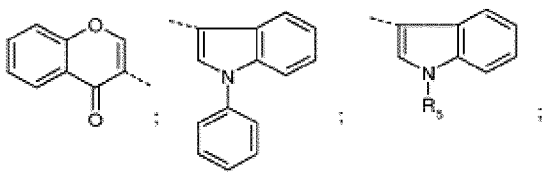
R_3 and R_4 are independently, hydrogen or (C_1-C_4)-alkyl group;

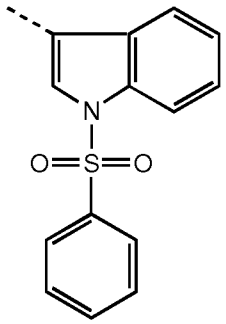
or wherein R_3 and R_4 are a single (C_1-C_8)-hydrocarbon group connecting the two nitrogen atoms of formula 1, which group may be selected from saturated hydrocarbon (*e.g.* C_2H_4) and aromatic hydrocarbon (*e.g.* phenyl);
with the proviso that when A_1 and A_2 are both selected from;

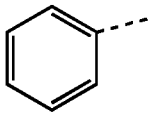
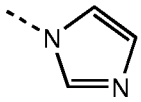


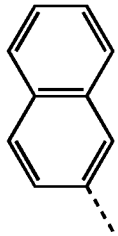
then at least one of the heterocyclic systems is substituted with one or more groups selected from halide (e.g. fluoro); nitro (NO_2) and amino (NH_2).

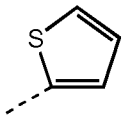
Preferably, the rings of the heterocyclic systems are unsubstituted or substituted with one or more groups selected from trifluoromethyl (CF_3), fluoro (F); nitro (NO_2) and amino (NH_2). Preferably, A_1 and A_2 are selected from;





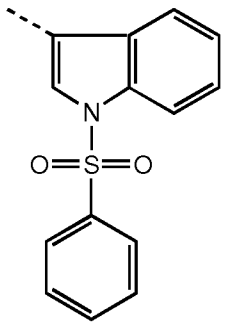
;

;


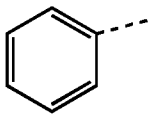
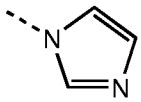
;

;

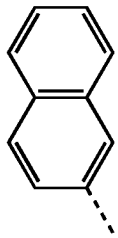


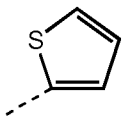
;

more preferably selected from



;

;


;

;



;

.

Preferably, a compound is provided selected from the compounds listed in Figure 22. Preferably, the compound is selected from PRA123, PRA224, PRA333, PRA738, and PRA828; more preferably selected from PRA828, most preferably PRA224. The compounds disclosed above are particularly useful in the methods disclosed herein.

A further aspect of the disclosure provides a TNF superfamily member polypeptide or fragment thereof that inhibits trimerization of said TNF

superfamily member. As used herein, said polypeptide or fragment thereof has a "dominant negative effect".

Preferably, said polypeptide or fragment thereof has a dominant negative mutation in the trimerization domain, preferably comprising a mutation in F beta-strand, more preferably in the glycine residue that corresponds to position 279 in human RANKL.

In preferred embodiments, the TNF superfamily member polypeptide or a functional fragment thereof comprises an amino acid sequence having at least 80% sequence identity to K L E A Q P F A H L T I N A T D I P S G S H K V S L S S W Y H D R G W A K I S N M T F S N G K L I V N Q D G F Y Y L Y A N I C F R H H E T S G D L A T E Y L Q L M V Y V T K T S I K I P S S H T L M K G G S T K Y W S G N S E F H F Y S I N V G X F F K L R S G E E I S I E V S N P S L L D P D Q D A T Y F G A F K V R D I D (SEQ ID NO:3), wherein X is not glycine.

A further aspect of the disclosure provides a fragment of a wild-type TNF superfamily member polypeptide that has a dominant negative effect. Such a fragment is also useful for the methods of inhibiting trimerization and for treating RANKL related disorders as described herein.

A further aspect of the disclosure provides an isolated nucleic acid encoding the TNF superfamily member polypeptide or fragment thereof as described herein; a non-human animal comprising said nucleic acid, preferably comprising a nucleic acid encoding for an amino acid sequence having at least 95% identity to SEQ ID NO:2 or SEQ ID NO:3; a vector comprising a nucleic acid as described herein; and a cell comprising said nucleic acid or said cell.

Another aspect of the disclosure provides a pharmaceutical composition comprising the TNF superfamily member polypeptide or fragment thereof as described herein, compounds of formula I, or T23, and a pharmaceutically acceptable carrier. The disclosure also provides a liposome comprising the TNF superfamily member polypeptide or fragment thereof as described herein. Said pharmaceutical compositions and liposomes are particularly useful for treating a bone disorder or a disease having bone disorder as a symptom. Preferred disorders include, osteoporosis, rheumatoid arthritis, multiple myeloma, bone metastasis, juvenile osteoporosis, osteogenesis imperfecta, hypercalcemia, hyperparathyroidism, osteomalacia, osteohalisteresis, osteolytic bone disease, osteonecrosis, Paget's disease of bone, bone loss due to rheumatoid arthritis, inflammatory arthritis, osteomyelitis, periodontal bone loss, bone loss due to cancer, age-related loss of bone mass, osteopenia, and inflammatory bowel syndrome, more preferably postmenopausal associated osteoporosis.

The disclosure provides TNF superfamily trimerization inhibitors for use in the preparation of a medicament for inhibiting osteoclast formation or decreasing bone loss; for preventing, treating, or reducing symptoms in an individual afflicted with osteoporosis, rheumatoid arthritis, multiple myeloma, bone metastasis, juvenile osteoporosis, osteogenesis imperfecta, hypercalcemia, hyperparathyroidism, osteomalacia, osteohalisteresis, osteolytic bone disease, osteonecrosis, Paget's disease of bone, bone loss due to rheumatoid arthritis, inflammatory arthritis, osteomyelitis, periodontal bone loss, bone loss due to cancer, age-related loss of bone mass, osteopenia, and inflammatory bowel syndrome.

BRIEF DESCRIPTION OF THE DRAWINGS

Figure 1. Severe osteopetrosis in *tles/tles* mice. (A) Representative von Kossa-stained proximal tibia sections are shown for 4-wk-old WT and *tles/tles* mice (n=6). (B) Representative serial sections of distal femurs stained with hematoxylin/eosin (H/E) and hematoxylin/TRAP (H/TRAP) (n=6). (C) TRAP staining of osteoclast cultures derived from BM cells or splenocytes (SP) treated with M-CSF and RANKL. (D) TRAP staining of cocultures between BM cells and primary calvarial osteoblasts (OB) in the presence of $1,25(OH)_2$ vitamin D3 and PGE2. Representative data of three experiments performed in triplicate. Bars: (A) 200µm; (B, C and D) 100 µm.

Figure 2. Mapping, identification and representation of the *tles* mutation. (A) Based on genome-wide genetic analysis, the causal mutation was mapped to chromosome 14. (B) DNA sequencing of the *Rankl* gene in WT control, *tles/+* heterozygous and *tles/tles* homozygous mice revealed that the mutation corresponds to a G to A transition (asterisk) causing a glycine to arginine substitution at residue 278. (C) Ribbon diagram of the RANKL trimer viewed down the threefold symmetry axis represents a trimer consisting of two WT monomers containing G278 (orange) and one monomer containing the G278R mutated residue (yellow). (D) Space filling diagram of the RANKL monomer viewed towards the trimer interface with the mutation G278R (yellow chickenwire) in place. Hydrophobic aminoacids are colored purple, polar in green and charged (+/-) in blue/red respectively. (E) The sequence of the extracellular F beta-strand of the murine RANKL is aligned to the beta strand of human TNF family cytokines RANKL, TNF, CD40L, TRAIL, BAFF, APRIL, and LTα. The degree of homology correlates with grey scaling, 0-50% conservation (no color), 50-70% (grey), 70-90% (dark grey), >90% (black). Asterisk indicates the residue which corresponds to mouse G278.

Figure 3. Genetic confirmation of the RANKL G278R mutation. (A) Serial sections of tibiae from 3-wk-old *Rankl*$^{-/tles}$ compound heterozygous mice were stained with hematoxylin and TRAP (H/TRAP). Bar: 100µm. (B) Representative femur trabecular areas from *Rankl*$^{+/+}$, *Rankl*$^{-/-}$ and *Rankl*$^{tles/tles}$ mice scanned with microCT (n=6 per group). (C) Histomorphometric analysis of structural bone parameters of femurs from *Rankl*$^{+/+}$ (n=12), *Rankl*$^{+/-}$ (n=6), *Rankl*$^{-/-}$ (n=6), *Rankl*$^{tles/+}$ (n=6), and *Rankl*$^{tles/tles}$ (n=6) littermate mice at 4 wks of age. BV/TV, bone volume/ total volume; NOc/T.Ar, number of osteoclasts/total area; NOc/B.Pm, number of osteoclasts/bone perimeter/mm; Tr.Th, trabecular thickness (mm); Tr.N. trabecular number/mm; Tr.S, trabecular separation/mm3. ***P<0.0001 and **P <0.001 when *Rankl*$^{-/-}$ and *Rankl*$^{tles/tles}$ mice were compared to the rest groups. (D) Osteoclast formation is restored by recombinant RANKL administration. Daily subcutaneous injections of recombinant RANKL at 150 µg/kg in *Rankl*$^{tles/tles}$ mice (n=4) induce formation of TRAP+ cells in trabecular bones. Representative TRAP staining of distal femur sections are shown. Scale bar: 50µm.

Figure 4. RANKL^{G278R} fails to trimerize and bind to RANK but interacts with WT RANKL. (A) Recombinant WT GST-RANKL and GST-RANKL^{G278R} were resolved either on native or SDS reduced polyacrylamide gel electrophoresis (PAGE) and detected by western blotting using monoclonal (mono) or polyclonal (poly) antibodies against RANKL or against GST. (B) Soluble WT RANKL and RANKL^{G278R} proteins were crosslinked with DSS (+) or PBS (-), run on 12% SDS-PAGE and detected by western blot using an anti-RANKL polyclonal antibody. (C) HEK 293FT cells were transfected with full-length WT RANKL-FLAG, WT RANKL-Myc and/or RANKL^{G278R}-Myc. Lysates were analyzed in native gels followed by western blot using an anti-Myc antibody. The protein input was determined in denatured acrylamide gels and westerns using antibodies against FLAG, Myc and actin. (D) The levels of soluble RANKL were quantified in supernatants of transfected HEK 293FT

cells displayed in 4C. Data shown as mean ± SEM of three experiments in duplicate. ***p<0.0001 when compared to WT RANKL-expressing cells. (E) Lysates of transfected HEK 293FT cells were immunoprecipitated with a Myc-specific antibody, and immunoblotted with an anti-FLAG antibody. The protein input was determined in western blots using antibodies against FLAG, Myc and actin. A representative figure of three independent experiments is shown for western blots. (F) Different concentrations of RANK-Fc were added to plates coated with either WT GST-RANKL, GST-RANKL^{G278R} or GST and the binding was monitored by fluorescence detection of PE-conjugated goat anti-human IgG. Data shown as mean ± SEM of three experiments performed in duplicate.

Figure 5. Dose-dependent suppression of RANKL-induced osteoclast formation by RANKL^{G278R}. (A) Representative TRAP stain of osteoclast cultures from WT BM cells treated with M-CSF and GST-RANKL in the absence (1:0) or presence of GST-RANKL^{G278R} at various concentrations including 100ng/ml (1:2), 50 ng/ml (1:1), 25 ng/ml (2:1), or 12.5 ng/ml (4:1). Bar: 100 µm. (B) The number of TRAP+ multinucleated (≥ 3 nuclei) cells was calculated per well (24 well plate). (C) The nuclei number in TRAP+ multinucleated cells was also calculated. Data shown as mean ± SEM of three experiments in duplicate. Each group was compared to that of GST-RANKL (1:0) (**p<0.001, ***p<0.0001).

Figure 6. G122R substitution abrogates TNF trimer formation, binding to TNFR and bioactivity. (A) Soluble WT TNF and TNF^{G122R} proteins were crosslinked with DSS (+) or PBS (-), run on 12% SDS-PAGE and detected by western blot using an anti-TNF polyclonal antibody. (B) Different concentrations of p75TNFR-Fc (1-160 ng/ml) were added to plates coated with either soluble TNF, or TNF^{G122R} and the binding was monitored by detection of HRP-conjugated goat anti-human IgG. Data shown as mean ± SEM of a

representative experiment performed in triplicate. (C) L929 cytotoxicity assay was performed in the presence of WT GST-TNF or GST-TNF^{G122R} at serial dilutions (0.03-4ng/ml). Data shown as mean ± SEM of three experiments performed in triplicate.

Figure 7. SPD304 inhibits RANKL-induced osteoclastogenesis. (A) Representative TRAP stain of osteoclast cultures from WT BM cells treated with M-CSF and GST-RANKL in the presence of 0.25-2µM SPD304. Bar: 100 µm. (B) The number of TRAP+ multinucleated (≥ 3 nuclei) cells was quantitated per well (48 well plate). (C) The nuclei number in TRAP+ multinucleated cells was also calculated. Data shown as mean ± SEM of three experiments performed in duplicate. The effect of SPD304 on osteoclast formation was compared to that of untreated cells (*p<0.05, **p<0.001, ***p<0.0001).

Figure 8. Phenotypic characteristics of osteopetrotic *tles/tles* mice. (A). Failure of tooth eruption in *tles/tles* mice. (B). Kaplan–Meier survival curve of control +/+ and *tles*/+ littermates (n=68), and *tles/tles* mice (n=20) analyzed in a total of 88 progeny derived from intrecrosses between heterozygous *tles*/+ mice.

Figure 9. Osteoclast precursor cells from *tles/tles* mice differentiate into osteoclasts. (A) Numbers of TRAP+ multinucleated osteoclasts per well (24 well plate) derived from BM cultures presented in figure 1C. Data shown as mean ± SEM of two experiments (n=4) (P>0.05). (B) TRAP staining of cocultures between splenocytes and primary calvarial osteoblasts (OB) in the presence of 1,25$(OH)_2$ vitamin D3 and PGE2. Representative data of three experiments performed in triplicate. Bar: 100µm.

Figure 10. G278R substitution allows normal RANKL protein production. Total extracts from thymus (T), spleen (S), and bone (B) of WT (*Rankl*+/+) and *Rankl*$^{tles/tles}$ mice were prepared and analyzed by western blotting with specific antibodies against RANKL and actin. The transmembrane form of RANKL (tmRANKL) (45 kD) as well as the soluble form of RANKL (sRANKL) (31 kD) are indicated.

Figure 11. G122R substitution abrogates TNF multimer formation. Recombinant WT GST-TNF and GST-TNF^{G122R} were resolved on native gel and detected by western blotting using polyclonal antibodies against RANKL or GST.

Figure 12. Alignment of several members of the TNF superfamily.

Figure 13. Effect of SDP304 on RANKL structure.
(**A**) RANKL dimer with SPD304 located on optimum binding position. G278 is shown with spacefilled atoms and SPD304 with doted surface. Cyan and green ribbons represent the two RANKL monomers. Diagram created using PYMOL v1.3. (**B**) Recombinant WT soluble mouse RANKL (60ng) was preincubated for 1h at 37°C either with SPD304 at various concentrations from 6-200µM or without SPD304 (-), resolved on native gel and detected by western blotting using a polyclonal antibody against RANKL. (**C**) Recombinant soluble mouse RANKL was preincubated with SPD304 at increasing concentrations from 6-100µM, was crosslinked with DSS, run on 12% SDS-PAGE and detected by western blot using an anti-RANKL polyclonal antibody. A representative figure of three independent experiments is shown for western blots.

Figure 14. The effect of small molecule inhibitors on RANKL activity.
(A) SPD304 at 2µM inhibits human RANKL activity in osteoclastogenesis assays but induces toxicity in osteoclast precursors (IC50=3.4 µM) as shown in

MTT survival assays. **(B)** SPD304 derivatives and T23 at 5μM inhibit RANKL activity in osteoclastogenesis assays. **(C)** The toxic effect of SPD304 derivatives and T23 is examined in MTT survival assays of osteoclast precursors. Data shown are representative of at least three experiments.

Figure 15. Small molecules disrupt RANKL trimers. PRA224 and T23 were preincubated at various ratios with recombinant soluble human RANKL, were cross linked and analyzed in 12% PAGE. The RANKL forms were detected using a polyclonal anti-RANKL antibody in western blots. Data shown are representative of at least three experiments.

Figure 16. The effect of RANKL peptides on RANKL inhibition. (A) Peptides 1 and 2 at 50 μM inhibit human RANKL activity in osteoclastogenesis assays. **(B)** Peptide 1 inhibits RANKL trimerization at 50:1 ratio as shown in western blotting. **(C)** RANKL peptides inhibit binding of human RANKL to its receptor RANK in a dose dependent manner. Data shown are representative of at least three experiments.

Figure 17 Inhibition of TNF-induced death in L929 cells. Increasing concentrations of the two compounds (a. compound 1=T23; b. compound 2=PRA224) were used to pre-incubate human TNF before addition to cells for 18 hours. Shown are mean values (n = 3) relative to controls (TNF pre-incubated with DMSO). Data shown are representative of at least three experiments. In parallel experiments, the toxicity of the compounds was tested also in L929 cells using the same approach but omitting TNF and actinomycin D from the experimental set-up (c. compound 1; d. compound 2). Shown are mean values (n = 3) relative to controls (DMSO-treated cells). Data shown are representative of at least three experiments.

Figure 18. Disruption of the TNF/TNF-R1 interaction by PRA224. Increasing concentrations of compound 2 (PRA224) were used to pre-incubate human TNF before addition on a TNF-R1 substrate. Binding was measured by ELISA. Shown are mean values (n = 2) of one experiment, representative of at least three repeats.

Figure 19. Reduction of TNF-induced MMP9 release in synovial fibroblasts. Increasing concentrations of the compounds were used to pre-incubate human TNF before used as a stimulus in cultured wild-type synovial fibroblasts for 18 hours (a). Supernatants were collected and MMP activity was visualised by gelatin zymography. The compounds were also used to treat synovial fibroblasts isolated from the human TNF-transgenic mouse, which release MMP9 without stimulation (b). In both (a) and (b) DMSO was used as a control.

Figure 20. TNF cross-linking experiment. Human TNF was incubated with different molar ratios of the compounds, or DMSO as a control, cross-linked with BS3, and subjected to SDS-PAGE. This was followed by western blotting to detect the various TNF multimers.

Figure 21. G249R substitution abrogates BAFF trimer formation and binding to BAFF receptor. (**A**)Various amount (1.2, 0.6, 0.3µg) of soluble WT BAFF and $BAFF^{G249R}$ proteins were cross linked with DSS (+) or PBS (-), run on 12% SDS-PAGE and detected by western blot using an anti-BAFF polyclonal antibody. (**B**) Different concentrations of BAFF receptor (3-400 ng/ml) were added to plates coated with either soluble BAFF, or $BAFF^{G249R}$. The RANKL binding to RANK was monitored by detection of HRP-conjugated goat anti-human IgG. Data shown as mean ± SEM of a representative experiment.

Figure 22. Structure of SPD304 analogues

Figure 23. Structure of T23 and derivatives. Compound 1 corresponds to T23.

DETAILED DESCRIPTION OF THE DISCLOSED EMBODIMENTS

The invention relates to the identification of a functional amino acid critical for ligand trimerization and bioactivity within the TNF ligand superfamily. A conserved glycine residue was found to be involved in RANKL trimer assembly. It is further demonstrated that RANKL trimerization can be inhibited by mutating an amino acid in the RANKL trimerization domain or by providing a compound that binds to said trimerization domain.

The present disclosure describes a chemically induced recessive mutation in the *Rankl* gene that causes severe osteopetrosis in mice similar to *Rankl* deficient mice. This loss-of-function mutation induces a glycine to arginine substitution (G278R) at the inner hydrophobic F beta-strand of the RANKL monomer that not only inhibits trimer assembly but also exerts a dominant negative effect on the wild-type (WT) RANKL assembly and function.

Although it has been previously proposed that RANKL trimerization involves intersubunit interactions among 43 residues, scattered mainly within the ten highly conserved beta-strands of each monomer [6], it is shown here for first time that a single amino acid substitution is sufficient to completely disrupt trimer assembly. Previous attempts at identifying functional RANKL residues have been based on predictions made on the crystal structure of RANKL/RANK. Such studies have been exclusively concentrated in amino acids interacting with the RANK receptor such as the Glu225, Arg222, and Asp299 residues [36], where their substitution leads to a dramatic decrease on binding to RANK and subsequent inability to promote osteoclast formation. The forward genetics approach described in the present disclosure is the first to identify and characterize a critical amino acid substitution that results in protein inactivation and subsequently to osteopetrosis *in vivo*.

RANKL is a member of the TNF (Tumor Necrosis Factor) superfamily. TNF superfamily proteins are important regulators of innate and adaptive immune responses and developmental events and proteins constitute an important class of cytokines that participate in a variety of cellular and intracellular signaling processes. The cognate receptors of the TNF superfamily ligands make up a related superfamily of receptors

The TNF superfamily proteins are synthesized as type 2 membrane proteins and fold into conserved beta-pleated sheet structures. The three-dimensional structures of TNF superfamily members are very similar, made up of a sandwich of two anti-parallel beta-sheets each formed by five anti-parallel beta strands with the "jelly roll" or Greek key topology. The inner sheet is formed from beta strands A, A', H, C, and F, while the outer sheet is formed from beta strands B, B', D, E, and G.

In addition, all characterized members of the family assemble into noncovalently associated trimers. The biologically active trimers exist in both membrane-bound and soluble cleaved forms. Most TNF superfamily members form homotrimers, although lymphotoxin-beta, for example, can form heterotrimers with lymphotoxin-alpha. Similarly, APRIL and BAFF also form both homotrimers and heterotrimers together (Daridon et al. Autoimmunity Reviews Volume 7, Issue 4, February 2008, Pages 267-271).

The $RANKL^{G278R}$ mutation identified herein is located at the hydrophobic F beta-strand, which is 100% conserved between human and mouse RANKL. The F beta-strand is part of the inner A'AHCF ß-sheet that is involved in intersubunit association. The introduction of a positive charge as well as a long side chain is expected to disrupt the hydrophobic interface and create steric hindrances causing packing inefficiencies (Figure 2D). Biochemical analysis on recombinant soluble RANKL has revealed that functional trimers or

multimers are not detected for the RANKL^{G278R} protein, confirming our structure-based prediction regarding the trimerization inability of RANKL^{G278R}. Instead, the studies described herein reveal the presence of monomers as well as the formation of RANKL^{G278R} aggregates. Since formation of a functional RANKL trimer is prerequisite for receptor binding, RANKL^{G278R} is unable to bind and activate RANK that is required for the stimulation of the downstream signaling cascades leading to osteoclast differentiation, activation and survival.

The sequence identity between members of the TNF superfamily is around 20-30% and members share a number of conserved residues as depicted in Figure 12. Interestingly, the glycine residue identified in RANKL for its involvement is trimerization is conserved among the TNF superfamily. This residue is also conserved among several members of the C1q family, which also trimerize, such as C1qA, C1Qb, C1Qc, Precerebellin, and CollVIIIa2 (see Figure 2 of Bodmer et al. 2002 Trends in Biochemical Sciences which is hereby incorporated by reference). The present disclosure further demonstrates that a similar residue substitution in TNF, G122R, abrogates TNF trimer formation, binding to the p75TNF receptor and bioactivity, highlighting its importance within the TNF superfamily.

Accordingly, one aspect of the disclosure provides a method for inhibiting trimerization of a TNF superfamily member polypeptide comprising contacting said polypeptide with a compound that inhibits trimerization of said polypeptide, herein referred to as a "trimerization inhibitor". Said polypeptide may be any polypeptide belonging to the TNF superfamily which forms a trimer, for example, TNF-alpha, lymphotoxin-alpha, lymphotoxin-beta, Fas ligand (FasL), TRAIL, CD40 ligand (CD40L), CD30 ligand, CD27 ligand, Ox40 ligand, APRIL, BAFF (BLyS), 4-IBBL, BAFF, and RANKL. Preferably, said polypeptide is TNF-alpha or RANKL.

Said polypeptide may also belong to a related family, such as the C1q family. Many of these proteins--which also form trimers or multimers of trimers--have been implicated in development, and immunological and physiological homeostasis. Preferred members of the C1q family are C1qA, C1Qb, C1Qc, Precerebellin, and CollVIIIa2.

Preferably, said method comprises contacting a cell expressing a TNF superfamily member polypeptide with a trimerization inhibitor. Preferably, said cell is a mammalian cell, more preferably a human cell. In some embodiments, the method is carried out in vitro. The trimerization inhibitors as described herein may therefore be used as tools to study the TNF superfamily signalling pathways.

Preferably the trimerization inhibitor binds a TNF superfamily, or related family, member polypeptide at the F beta-strand. The present disclosure provides a number of trimerization inhibitors including compounds and derivatives of formula I, TNF superfamily polypeptide or fragments thereof, and T23. "F beta-strand" binders are useful in the methods described herein.

Preferably, the trimerization inhibitor as described herein is selected from a) a compound that binds to said TNF superfamily, or related family, member polypeptide at the F beta-strand, preferably at the glycine residue that corresponds to position 279 in human RANKL and b) a TNF superfamily, or related family, member polypeptide or fragment thereof, preferably having a dominant negative mutation in the trimerization domain (herein referred to as the "dominant negative polypeptide"). Preferably, said trimerization inhibitor also induces the disassociation of already formed trimers.

Preferably, the trimerization inhibitor is 6,7-Dimethyl-3-[[methyl[2-[methyl[[1-[3-(trifluoromethyl)phenyl]-1H-indol-3-yl]methyl]amino]ethyl]amino]methyl]-

(4H-1-Benzopyran-4-one) (also known as SPD304) or functional derivatives thereof. As used herein, a functional derivative can bind a TNF superfamily polypeptide and act as a trimerization inhibitor. Preferably, the derivatives are selected from PRA123, PRA224, PRA333, PRA738, and PRA828, more preferably PRA828, most preferably PRA224.

The formation or disassociation of trimers can be measured by any number of assays known to one of skill in the art, including mass spectrometry (see, e.g., [35]), intrinsic fluorescence measurements, dynamic light scattering, and the assays described in the Examples (Example 4). The effect on trimerization can also be observed by measuring the binding of a TNF superfamily ligand to its congnate receptor, as receptor binding is dependent of ligand trimerization, or by measuring receptor activity (see, e.g., Examples 4 and 5). In some embodiments, said compound is provided to a cell. Preferably, the provision of said compound to a cell inhibits trimerization of said TNF superfamily, or related family, member polypeptide by at least 10, at least 20, at least 30, at least 40, at least 50, at least 60, at least 70, at least 80, or at least 90%.

The inhibition of trimerization also encompasses the induction of non-functional RANKL aggregates and/or the increase of monomers. Accordingly, the detection of an increase in aggregates indicates an inhibition of trimerization. This increase in aggregates can also be detected as a decrease in soluble RANKL (see Figure 4D). In a preferred embodiment, the inhibition of trimerization results in the decrease of trimeric soluble RANKL protein by at least 30, at least 40, at least 50, at least 60, at least 70, at least 80, or at least 90%.

In a further aspect of the disclosure, methods are provided for inhibiting osteoclast formation or decreasing bone loss in an individual comprising administering an effective amount of a compound that inhibits trimerization of

RANKL. Preferably, said trimerization inhibitor is used to treat inflammation-induced and/or immune-mediated loss of bone and/or cartilage and/or RANKL-mediated osteoporosis.

The trimerization inhibitor may be administered prophylactically, i.e., before bone loss occurs, in order to prevent bone loss or it may be administered after bone loss has occurred in order to decrease further bone loss. Preferably, said trimerization inhibitor is administered to an individual such that bone loss is decreased by at least 5, 10, 20, 30, 40, 50, or 60% compared to non-treatment.

In a further aspect of the disclosure, methods are provided for preventing, treating, or reducing symptoms in an individual afflicted with osteoporosis, preferably postmenopausal osteoporosis, rheumatoid arthritis, multiple myeloma, bone metastasis, juvenile osteoporosis, osteogenesis imperfecta, hypercalcemia, hyperparathyroidism, osteomalacia, osteohalisteresis, osteolytic bone disease, osteonecrosis, Paget's disease of bone, bone loss due to rheumatoid arthritis, inflammatory arthritis, osteomyelitis, periodontal bone loss, bone loss due to cancer, age-related loss of bone mass, osteopenia, and inflammatory bowel syndrome comprising administering an effective amount of a compound that inhibits trimerization of RANKL.

Preferably, said individual is a mammal, more preferably a human.

Rheumatoid arthritis (RA) is a chronic systemic inflammatory disorder with an unknown cause characterized by invasive synovial hyperplasia leading to progressive joint destruction. Bone erosion begins in the early stages of the disease and results in severe deformity of the affected joints which impairs the normal activity and quality of life of patients. Rheumatoid arthritis can be associated with elevated RANKL in T-cells, synovial fibroblasts, and bone marrow stroma;

The BXD2 mouse strain develops arthritis with bone erosions, synovial hyperplasia with mononuclear cell infiltration, and joint deformation. These mice also have high levels of rheumatoid factor and anti-DNA auto-antibodies. In this model, inhibition of RANKL completely prevented bone loss and partially protected against cartilage loss (Wu Y. et al., 2005, Arthritis Rheum, 52:3257-3268).

Periodontal diseases are chronic infectious inflammatory diseases characterized by increased leukocyte infiltration into the periodontal lesions. This infiltration results in the secretion of a number of cytokines, which leads to the destruction of periodontal tissues including alveolar bone (Taubman M A et al., 2001, Crit. Rev Oral Biol Med., 12:125-135).

RANKL expressed by either osteoblasts or infiltrating T cells in response to bacterial infection is involved in alveolar bone destruction in periodontal diseases. RANKL messenger RNA is upregulated in gums from patients with severe periodontitis.

Periprosthetic bone loss leading to aseptic loosening of implants is one of the most challenging complications of joint replacement surgeries. Osteoclast-like multinucleated cells are observed in the bone-implant interface of the loosened joints and the fibroblastic cells in the perioprosthetic tissues have been shown to induce the differentiation of normal human peripheral blood mononuclear cells into mature osteoclasts by a mechanism that involves both RANKL and TNF-.alpha. (Sabokbar A. et al., 2005, J Orthop Res., 23:511-519).

Hypercalcemia is a late stage complication of cancer, disrupting the body's ability to maintain normal levels of calcium, resulting in calcium deposit in the kidneys, heart conditions and neural dysfunction and occurs most frequently

in patients with cancers of the lung and breast. Hypercalcemia also occurs in patients with multiple myeloma, cancers of the head and neck, sarcoma, cancers of unknown primary origin, lymphoma, leukemia, melanoma, renal cancer, and gastrointestinal cancers (e.g. esophageal, stomach, intestinal, colon and rectal cancers). RANK and RANKL play a role in bone loss associated with cancers. When RANKL+ myeloma cells are injected into C57BL mice, the mice develop bone disease characterized by a marked decrease in cancellous bone volume in the tibial and femoral metaphyses, increased osteoclast formation, and radiologic evidence of osteolytic bone lesions.

Specific blockade of RANKL prevents the skeletal complications in various animal models of myeloma and suppressed bone resorption in patients with myeloma bone disease. Treatment of myelomatous SCID-human mice with a RANK-Fc fusion protein reduced myeloma-induced bone resorption and resulted in a greater than 80% reduction in paraprotein. Treatment resulted in a reduced number of osteoclasts, but had no effect on the apoptosis and proliferation of myeloma cells, suggesting that the anti-myeloma effect of RANKL inhibitors is associated with inhibition of osteoclast activity (Yaccodby et al., 2002, Br. J. Haematol., 116:278-290).

Other cancer indications, which the compounds described herein can treat include, but are not limited to: hematologic neoplasias and neoplastic-like conditions for example, Hodgkin's lymphoma; non-Hodgkin's lymphomas (Burkitt's lymphoma, small lymphocytic lymphoma/chronic lymphocytic leukemia, mycosis fungoides, mantle cell lymphoma, follicular lymphoma, diffuse large B-cell lymphoma, marginal zone lymphoma, hairy cell leukemia and lymphoplasmacytic leukemia), tumors of lymphocyte precursor cells, including B-cell acute lymphoblastic leukemia/lymphoma, and T-cell acute lymphoblastic leukemia/lymphoma, thymoma, tumors of the mature T and NK cells, including peripheral T-cell leukemias, adult T-cell leukemia/T-cell

lymphomas and large granular lymphocytic leukemia, Langerhans cell histocytosis, myeloid neoplasias such as acute myelogenous leukemias, including AML with maturation, AML without differentiation, acute promyelocytic leukemia, acute myelomonocytic leukemia, and acute monocytic leukemias, myelodysplastic syndromes, and chronic myeloproliferative disorders, including chronic myelogenous leukemia.

Some primary tumors and metastatic malignant tumors, such as breast cancer and lung cancer, invade bone tissues. Osteoclasts are primarily responsible for the osteolysis observed in these patients and there's evidence that in patients with severe osteolysis, the RANKL/OPG ratio is increased (Wittrant Y et al., Biochim Biophys Acta, 2004, 1704:49-57; Greimaud E et al., 2003, Am J Pathol., 163:2021-2031).

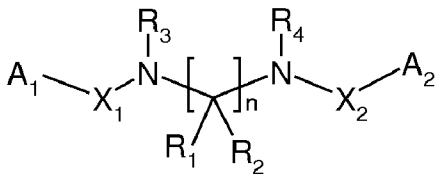
The RANKL/RANK/OPG system has also been reported to be involved in bone destruction in breast cancer cells, prostate cancer cells, and other metastatic bone tumors (Kitazawa S. et al., 2002, J. Pathol., 198:228-236; Park H R et al., 2003, J Korean Med Sci, 18:541-546; Zhang J et al., 2001, J Clin Invest., 107:1235-1244; Keller E T et al., 2001, Cancer Metastasis Rev., 20:333-349).

Some patients with Juvenile Paget's Disease have mutations in the OPG gene which result in undetectable serum levels of OPG and large increases in soluble RANKL levels. This disorder is a rare disease with an autosomal inheritance pattern, and it displays various deformities of long bones and vertebral column, which increase in severity during adolescence. (Whyte M P et al., 2002, N Engl J Med., 347:175-184; Cundy T et al., 2002, Hum Mol Genet., 11:2119-2127; Chong B. et al., 2003, J Bone Miner Res., 18:2095-2104).

Compounds that bind to TNF superfamily, or related family, member polypeptides at the glycine residue that corresponds to position 279 in human

RANKL and their method of preparation are described, for example, in WO2008/142623, which is hereby incorporated by reference.

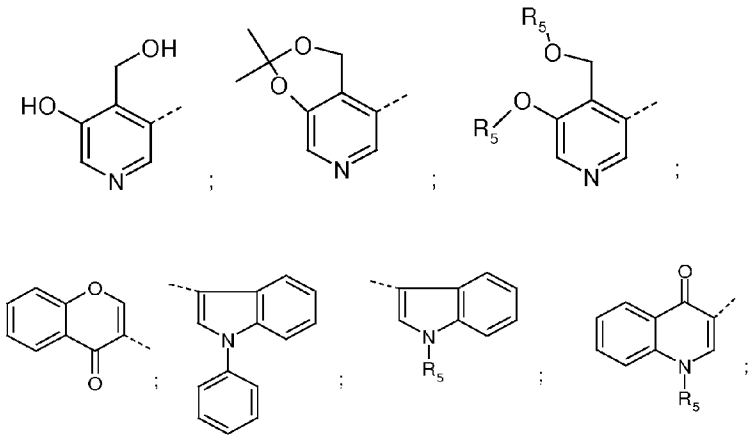
Said compounds include a compound of formula 1, or a stereoisomer thereof, tautomer thereof, or mixture thereof in any ratio; a pharmaceutically acceptable salt, pharmaceutically acceptable solvate, or pharmaceutically acceptable polymorph thereof;



Formula 1

wherein:

A_1 and A_2 are independently a substituted or unsubstituted heterocyclic system selected from;



wherein the dotted line indicates the point of attachment, R_5 is hydrogen or $(C_1\text{-}C_4)$- alkyl group and the rings of the heterocyclic systems herein above may be substituted with groups selected from $(C_1\text{-}C_4)$-alkyl, $(C_1\text{-}C_4)$-alkoxy, hydroxyl, hydroxy-($C_1\text{-}C_4$)-alkyl (e.g., hydroxymethyl or 1 -hydroxyethyl or 2-hydroxyethyl), and fluoroalkyl (e.g., CF_3);

X_1 and X_2 are independently a carbonyl group or a methylene (-CH_2-) group; n

is an integer from 2-4;
R_1 and R_2 are independently, hydrogen or (C_1-C_4)-alkyl group;
R_3 and R_4 are independently, hydrogen or (C_1-C_4)-alkyl group; and
R_3 and R_4 can optionally form a ring system; with a proviso that when A_1 and A_2 are 1 -(3-(thfluoromethyl)phenyl)-1 H-indole and 6,7-dimethyl-4H-chromen-4-one respectively and X_1 and X2 are independently a methylene (-CH_2-) group, R_3 and R_4 form a ring system.

Preferably, A_1 and A_2 are independently a substituted or unsubstituted phenyl group wherein the substituents on the phenyl ring are selected from (C_1-C_4)-alkyl, fluoroalkyl such as CF_3, hydroxyl, (C_1-C_4)-alkoxy, benzyloxy and hydroxy-(C_1-C_4)-alkyl; X_1 and X_2 are independently a carbonyl group or a methylene (-CH_2-) group; n is an integer from 2-4; R_1 and R_2 are independently, hydrogen or (C_1-C_4)-alkyl group;
R_3 and R_4 are independently, hydrogen or (C_1-C_4)-alkyl group; and
R_3 and R_4 can optionally form a ring system.

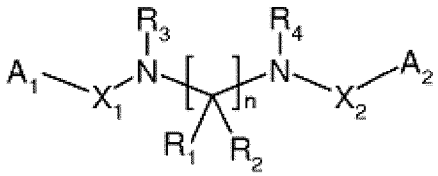
Preferably, said compound is selected from 3,3'-(ethane-1 ,2-diylbis(methylazanediyl))bis(methylene)bis(6,7-dimethyl-4H- chromen-4-one) dihydrochloride;
5,5'-(ethane-1 ,2-diylbis(methylazanediyl))bis(methylene)bis(4-(hydroxymethyl)-2- methylpyridin-3-ol) dihydrochloride;
6,7-Dimethyl-3-((methyl(2-(methyl((2,2,8-trimethyl-4H-[1 ,3]dioxino[4,5-c]pyhdin-5- yl)methyl)amino)ethyl)amino)methyl)-4H-chromen-4-one dihydrochloride;
1 ,4-Bis((1 -(3-(trifluoromethyl) phenyl)-1 H-indol-3-yl)methyl)piperazine dihydrochloride;
6,7-Dimethyl-3-((4-((1 -(3-(trifluoromethyl) phenyl)-1 H-indol-3-yl) methyl)piperazin-1-yl)methyl)-4H-chromen-4-one dihydrochloride;
N_1,N_2-bis(4-(benzyloxy)-3-methoxybenzyl)ethane-1,2-diamine dihydrochloride;

N,N'-(ethane-1 ,2-diyl) bis (2-hydroxybenzamide) dihydrochloride;
N,N'-(propane-1 ,3-diyl) bis (2-hydroxybenzamide) dihydrochloride;
and 4-Hydroxy-N-(2-(2-hydroxybenzamido)ethyl)-3-methoxybenzamide dihydrochloride.

Most preferably, said compound is 6,7-Dimethyl-3-[[methyl[2-[methyl[[1-[3-(trifluoromethyl)phenyl]-1H-indol-3-yl]methyl]amino]ethyl]amino]methyl]-(4H-1-Benzopyran-4-one) (also known as SPD304) or functional derivatives thereof.

In order to identify compounds with improved properties, particularly lower toxicity, new SPD304 derivatives were synthesized and tested for their ability to inhibit TNF and RANKL in vitro. Figure 22 depicts active compounds.

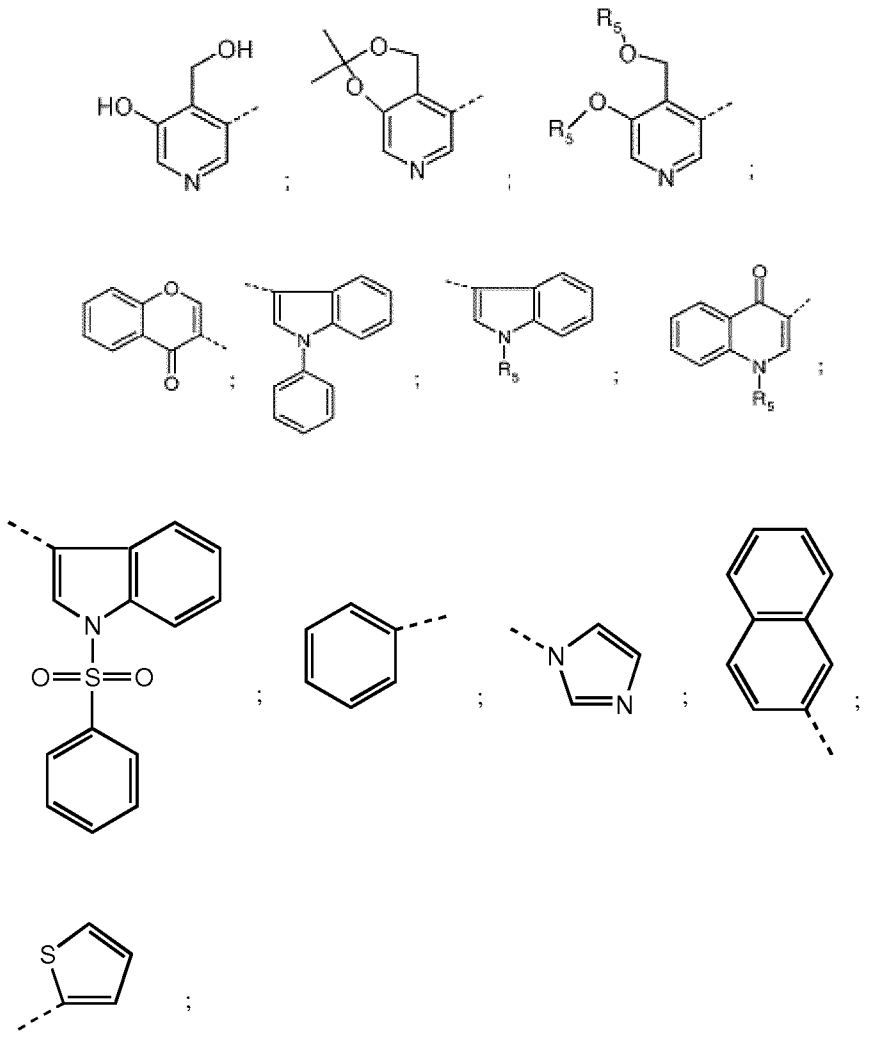
The present disclosure thus also includes new compounds not disclosed in WO2008/142623. Such compounds include those having formula 1



Formula 1

wherein:

A_1 and A_2 are independently a substituted or unsubstituted heterocyclic system selected from;



wherein the dotted line indicates the point of attachment, R_5 is hydrogen or (C_1-C_4)- alkyl group and the rings of the heterocyclic systems herein above are unsubstituted or substituted with one or more groups selected from (C_1-C_4)-alkyl, (C_1-C_4)-alkoxy, hydroxyl, hydroxy-(C_1-C_4)-alkyl (e.g., hydroxymethyl or 1 -hydroxyethyl or 2-hydroxyethyl), fluoroalkyl (e.g., CF_3), halide (e.g. fluoro); nitro (NO_2) and amino (NH_2);

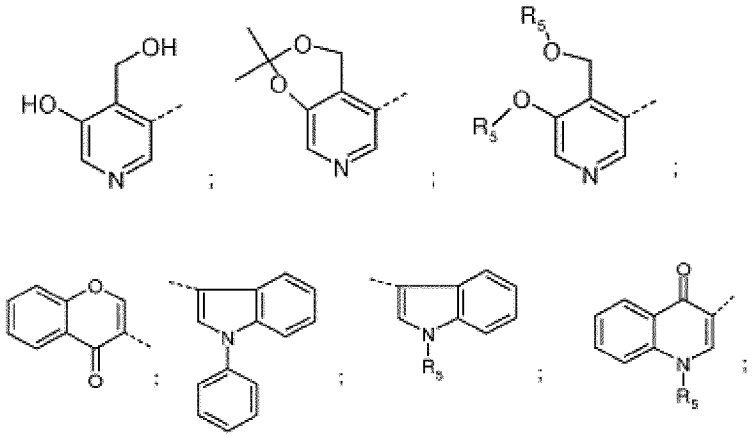
X_1 and X_2 are independently a carbonyl group or a methylene (-CH_2-) group; n is an integer from 2-4;

R_1 and R_2 are independently, hydrogen or (C_1-C_4)-alkyl group;

R_3 and R_4 are independently, hydrogen or (C_1-C_4)-alkyl group;

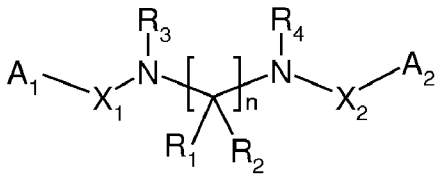
or wherein R_3 and R_4 are a single (C_1-C_8)-hydrocarbon group connecting the two nitrogen atoms of formula 1, which group may be selected from saturated hydrocarbon (*e.g.* C_2H_4) and aromatic hydrocarbon (*e.g.* phenyl);

with the proviso that when A_1 and A_2 are independently a substituted or unsubstituted heterocyclic system selected from;



the heterocyclic systems are substituted with one or more groups selected from halide (e.g. fluoro); nitro (NO_2) and amino (NH_2).

In the methods disclosed herein, a compound of formula 1, or a stereoisomer thereof, tautomer thereof, or mixture thereof in any ratio; a pharmaceutically acceptable salt, pharmaceutically acceptable solvate, or pharmaceutically acceptable polymorph thereof may be used, including;

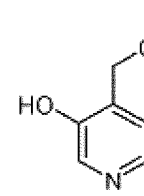
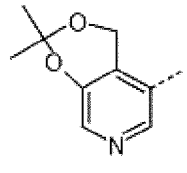
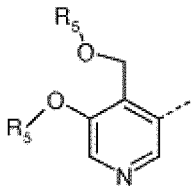
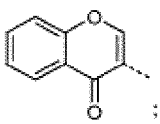
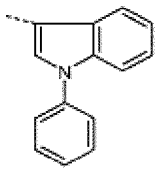
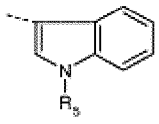
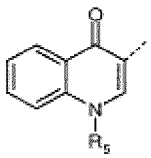
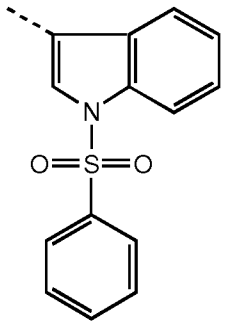
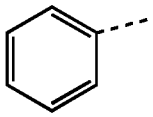
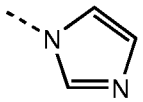
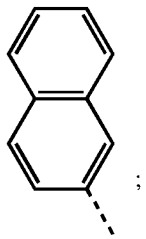
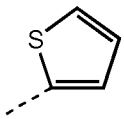


Formula 1

wherein:

A_1 and A_2 are independently a substituted or unsubstituted heterocyclic

system selected from;

wherein the dotted line indicates the point of attachment, R_5 is hydrogen or (C_1-C_4)- alkyl group and the rings of the heterocyclic systems herein above are unsubstituted or substituted with one or more groups selected from (C_1-C_4)-alkyl, (C_1-C_4)-alkoxy, hydroxyl, hydroxy-(C_1-C_4)-alkyl (e.g., hydroxymethyl or 1-hydroxyethyl or 2-hydroxyethyl), fluoroalkyl (e.g., CF_3), halide (e.g. fluoro); nitro (NO_2) and amino (NH_2);

X_1 and X_2 are independently a carbonyl group or a methylene (-CH_2-) group; n is an integer from 2-4;

R_1 and R_2 are independently, hydrogen or (C_1-C_4)-alkyl group;
R_3 and R_4 are independently, hydrogen or (C_1-C_4)-alkyl group;
or wherein R_3 and R_4 are a single (C_1-C_8)-hydrocarbon group connecting the two nitrogen atoms of formula 1, which group may be selected from saturated hydrocarbon (*e.g.* C_2H_4) and aromatic hydrocarbon (*e.g.* phenyl).

It has been previously shown that the small molecule SDP304, which interacts with TNF at the glycine residue at position 122, effectively inhibits TNF trimerization and function [35]. Accordingly, when SDP304 is used as the trimerization inhibitor, the TNF superfamily member is not TNF-alpha. Preferably, when the trimerization inhibitor is a compound of formula 1 as described above, or a stereoisomer thereof, tautomer thereof, or mixture thereof in any ratio; a pharmaceutically acceptable salt, pharmaceutically acceptable solvate, or pharmaceutically acceptable polymorph thereof; said TNF superfamily member polypeptide is not TNF-alpha. More preferably, when the trimerization inhibitor is a compound that binds to said TNF superfamily member polypeptide in the F beta-strand, said TNF superfamily member polypeptide is not TNF-alpha.

The present disclosure demonstrates that 6,7-Dimethyl-3-[[methyl[2-[methyl[[1-[3-(trifluoromethyl)phenyl]-1H-indol-3-yl]methyl]amino]ethyl]amino]methyl]-(4H-1-Benzopyran-4-one) effectively inhibits RANKL-induced *ex vivo* osteoclast formation, suggesting a surprising possible common mechanism of action to that of TNF inhibition.

In one aspect, T23 and its functional derivatives are provided as TNF superfamily inhibitors. T23 was identified based on in silico screening method to identify molecules which bind the F-strand of the TNF superfamily. As demonstrated in the examples, T23 (compound 1 of Figure 23) inhibits trimerization of both RANKL and TNF. Functional derivatives of T23 are

further provided (compound 2-1000 of Figure 23). As used herein, functional derivatives of T23 bind a TNF superfamily polypeptide, preferably TNF or RANKL, preferably the F-strand of said polypeptide, and inhibit its trimerization. The functional derivatives of T23 were identified by searching a chemical database for neighbours of T23 in the chemical space. These derivatives are predicted to have similar binding and, therefore, similar functional properties as T23.

It will be appreciated by those skilled in the art that the compounds described herein may also be provided in the form of their pharmaceutically acceptable salts or solvates thereof. The pharmaceutically acceptable salts of the compounds are in particular salts which are non-toxic, or which can be used physiologically. The present invention furthermore includes all solvates of the compounds, for example hydrates, and the solvates formed with other solvents of crystallization, such as alcohols, ethers, ethyl acetate, dioxane, DMF, or a lower alkyl ketone, such as acetone, or mixtures thereof.

In one aspect of the disclosure, a dominant negative TNF superfamily, or related family, member polypeptide or fragment thereof is provided (i.e., "dominant negative polypeptide") is provided. Preferably, said dominant negative polypeptide comprises a mutation in the trimerization domain. Preferably, said dominant negative polypeptide is a wild-type TNF superfamily peptide.

As used herein, a dominant negative polypeptide refers to a polypeptide that affects the function of the normal, wild-type form of said polypeptide. In preferred embodiments, said dominant negative polypeptides adversely affect the ability of wild-type TNF family polypeptides to form trimers. It has been previously shown that trimer assembly within the TNF ligand family constitutes a dynamic process, where subunits can be exchanged [40].

Although not wishing to be bound by theory, this phenomenon could explain the dominant negative effect exerted by the RANKL^{G278R} variant.

Dominant negative polypeptides are useful as trimerization inhibitors of the TNF superfamily or related families such as members of the C1q family that forms trimers. Preferably, said dominant negative polypeptide is selected from TNF-alpha, lymphotoxin-alpha, lymphotoxin-beta, Fas ligand (FasL), TRAIL, CD40 ligand (CD40L), CD30 ligand, CD27 ligand, Ox40 ligand, APRIL, BAFF (BLyS), 4-IBBL, BAFF, TWEAK, ectodysplasin-1, ectodysplasin-2, LIGHT, and RANKL, more preferably, said polypeptide is TNF-alpha or RANKL.

Preferably, said dominant negative polypeptide is non-naturally occurring.

Preferably, said dominant negative polypeptide is provided as an isolated and/or purified polypeptide. As used herein, "isolated" means that the polypeptides are separated from other components of either (a) a natural source, such as a plant or cell, preferably bacterial culture, or (b) a synthetic organic chemical reaction mixture. Preferably, via conventional techniques, the compounds of the invention are purified. As used herein, "purified" means that when isolated, the isolate contains at least about 80%, preferably at least about 90%, more preferably at least about 95% and even more preferably at least about 98%, of said polypeptide by weight of the isolate.

Preferably, the dominant negative polypeptide is the same family member as the TNF superfamily member whose trimerization is to be inhibited. It is contemplated that dominant negative polypeptides of one species, e.g., RANKL from mouse, can be used to inhibit the trimerization of a TNF superfamily polypeptide in another species, e.g., RANKL from human. A skilled person will appreciate that cross-species inhibition is possible based on the conservation of

sequence between species. Preferably, said dominant negative polypeptide is from the same species as the TNF superfamily member to be inhibited.

Preferably, the dominant negative polypeptide comprises at least one amino acid mutation in its trimerization domain that inhibits the ability of said polypeptide to form trimers. The mutation may be an amino acid deletion, insertion, or substitution, preferably the mutation is a substitution. Preferred amino acid residues in the trimerization domain include the tyrosine residue that corresponds to position 307 in human RANKL (Y227 in human TNF-alpha and Y151 in soluble human TNF-alpha), the asparagine, valine, glycine, and glycine residues that correspond to positions 276-279 in human RANKL (195-198 in human TNF-alpha and 119-122 in soluble human TNF-alpha), as well as the leucine residue that corresponds to position 57 in soluble human TNF-alpha, the tyrosine residue that corresponds to position 59 in soluble human TNF-alpha, the serine residue that corresponds to position 60 in soluble human TNF-alpha, and the glutamine residue that corresponds to position 61 in soluble human TNF-alpha. It is clear to a skilled person that mutations can be made in other TNF superfamily, and related family, members at positions that correspond to those described in RANKL and TNF-alpha.

Preferably, the dominant negative polypeptide comprises a mutation in the glycine residue that corresponds to position 279 in human RANKL. This position corresponds to 215 in APRIL, 295 in TWEAK, 348 in Ectodysplasin-1, 350 in Ectodysplasin-2, 249 in BAFF, 246 in TRAIL, 227 in CD40L, 198 in TNF-alpha, 122 in soluble human TNF, 205 in LIGHT, and 209 in Lymphotoxin. Preferably, the mutation is an amino acid substitution, more preferably a non-conservative amino acid substitution.

Preferably, the dominant negative polypeptide comprises non-conservative modifications (e.g. substitutions). By "nonconservative" modification herein is meant a modification in which the wild type residue and the mutant residue differ significantly in one or more physical properties, including hydrophobicity, charge, size, and shape. For example, modifications from a polar residue to a nonpolar residue or vice-versa, modifications from positively charged residues to negatively charged residues or vice versa, and modifications from large residues to small residues or vice versa are nonconservative modifications. For example, substitutions may be made which more significantly affect: the structure of the polypeptide backbone in the area of the alteration; the charge or hydrophobicity of the molecule at the target site; or the bulk of the side chain. The substitutions which in general are expected to produce the greatest changes in the polypeptide's properties are those in which (a) a hydrophilic residue, e.g. seryl or threonyl, is substituted for (or by) a hydrophobic residue, e.g. leucyl, isoleucyl, phenylalanyl, valyl or alanyl; (b) a cysteine or proline is substituted for (or by) any other residue; (c) a residue having an electropositive side chain, e.g. lysyl, arginyl, or histidyl, is substituted for (or by) an electronegative residue, e.g. glutamyl or aspartyl; or (d) a residue having a bulky side chain, e.g. phenylalanine, is substituted for (or by) one not having a side chain, e.g. glycine. In a preferred embodiment, the dominant negative polypeptide comprises a mutation in the glycine residue that corresponds to position 279 in human RANKL, wherein glycine is substituted for arginine, lysine, histidine, ornithine, methyllysine, or acetyllysine. Preferably, said glycine is substituted for arginine.

It is also contemplated that the dominant negative polypeptide as disclosed herein may include one or more amino acid analogs such as D-amino acid, di-amino acid, and/or beta-amino acid.

The dominant negative polypeptides may also contain additional amino acid modifications that those related to disrupting trimerization. Examples include amino acid substitutions introduced to enable soluble expression in E. coli, amino acid substitutions introduced to optimize protein stability, and amino acid substitutions introduced to modulate immunogenicity. Said polypeptides may also comprise epitope or purification tags or be fused to other therapeutic proteins or proteins such as Fc or serum albumin for pharmacokinetic purposes.

As used herein, dominant negative polypeptides include non-full length polypeptides such as the soluble form of said polypeptides, i.e., lacking the transmembrane domain. An exemplary soluble polypeptide is the RANKL soluble polypeptide: KLEAQPFAHLTINATDIPSGSHKVSLSSWYHDRGWAKISNMTFSNGKLIVN QDGFYYLYANICFRHHETSGDLATEYLQLMVYVTKTSIKIPSSHTLMKGGS TKYWSGNSEFHFYSINVGGFFKLRSGEEISIEVSNPSLLDPDQDATYFGAFK VRDID (SEQ ID NO:1).

Preferably, said dominant negative polypeptide or a fragment thereof is a peptide comprising HFYSINVGGFFK or HFYSINVGRFFK. Preferably, said dominant negative polypeptide or a fragment thereof is a peptide comprising an amino acid sequence at least 90% identical to HFYSINVGGFFK or HFYSINVGRFFK. Preferably, said peptide has between 12-100, more preferably between 12-50, most preferred between 12-30 amino acids.

As is apparent to one of skill in the art, dominant negative polypeptides useful in the methods disclosed herein also include functional fragments of said polypeptides. As used herein, “functional fragments” refers to fragments that inhibit trimerization. At a minimum, such functional fragments comprise the F beta strand residues (corresponding to amino acid residues 270-282 of human

RANKL). Preferably, said functional fragments comprise an an amino acid sequence at least 90% identical to amino acid residues 270-282 of human RANKL. Additional residues may also be present in order to provide stability or influence the pharmokinetics of said fragments. In some embodiments, the fragment is a retro-inverso analogue or a circular peptide.

In some aspects, the disclosure provides a polypeptide or a functional fragment thereof comprising an amino acid sequence having at least 80, at least 90, at least 95, or at least 99% identity to the human RANKL sequence:
MRRASRDYTKYLRGSEEMGGGPGAPHEGPLHAPPPPAPHQPPAASRSMFV
ALLGLGLGQVVCSVALFFYFRAQMDPNRISEDGTHCIYRILRLHENADFQD
TTLESQDTKLIPDSCRRIKQAFQGAVQKELQHIVGSQHIRAEKAMVDGSWL
DLAKRSKLEAQPFAHLTINATDIPSGSHKVSLSSWYHDRGWAKISNMTFSN
GKLIVNQDGFYYLYANICFRHHETSGDLATEYLQLMVYVTKTSIKIPSSHTL
MKGGSTKYWSGNSEFHFYSINVG**X**FFKLRSGEEISIEVSNPSLLDPDQDAT
YFGAFKVRDID (SEQ ID NO:2), wherein X is not glycine.

Preferably, a polypeptide or a functional fragment thereof is provided comprises an amino acid sequence having at least 80, at least 90, at least 95, or at least 99% identity to the soluble form of the human RANKL sequence:
KLEAQPFAHLTINATDIPSGSHKVSLSSWYHDRGWAKISNMTFSNGKLIVN
QDGFYYLYANICFRHHETSGDLATEYLQLMVYVTKTSIKIPSSHTLMKGGS
TKYWSGNSEFHFYSINVG**X**FFKLRSGEEISIEVSNPSLLDPDQDATYFGAFK
VRDID (SEQ ID NO:3),
wherein X is not glycine.

Said polypeptide or functional fragment thereof preferably reduces RANKL trimer assembly by at least 10, at least 20, at least 30, at least 40, at least 50, at least 60, at least 70, at least 80, or at least 90%.

In some embodiments, the fragments of TNF superfamily member polypeptides that induce a dominant negative effect are fragments of a wild-type sequence of a TNF superfamily member.

The dominant negative polypeptides may derive from any source, although mammalian polypeptides are preferred. Suitable mammals include, rodents (rats, mice, hamsters, guinea pigs, etc.), primates, farm animals (including sheep, goats, pigs, cows, horses, etc); and in the most preferred embodiment, from humans.

The mutations resulting in the dominant negative polypeptides may be generated by any number of techniques well-known to one of skill in the art. These include, for example, alanine scanning (see U.S. Pat. No. 5,506,107), gene shuffling (WO 01/25277), and site-directed PCR mutagenesis.

In addition to providing the dominant negative polypeptides as described herein, the present disclosure also provides isolated nucleic acids encoding said polypeptides, vectors containing such nucleic acids, and host cells and expression systems for transcribing and translating such nucleic acids into polypeptides.

Accordingly, one aspect of the disclosure provides nucleic acids encoding the dominant negative polypeptides as disclosed herein. Said nucleic acids may be operably linked to additional sequences such as promoter sequences, ribosomal binding sites, transcriptional start and stop sequences, translational start and stop sequences, and enhancer or activator sequences. Promoter sequences encode either constitutive or inducible promoters. The promoters may be either naturally occurring promoters or hybrid promoters. Hybrid promoters, which combine elements of more than one promoter, are also known in the art, and are useful in the present invention. In a preferred embodiment, the promoters are strong promoters, allowing high expression in cells, particularly

mammalian cells, such as the CMV promoter, particularly in combination with a Tet regulatory element.

Vectors comprising said nucleic acids are also provided. A "vector" is a recombinant nucleic acid construct, such as plasmid, phase genome, virus genome, cosmid, or artificial chromosome, to which another DNA segment may be attached. The term "vector" includes both viral and nonviral means for introducing the nucleic acid into a cell in vitro, ex vivo or in vivo. Non-viral vectors include plasmids, liposomes, electrically charged lipids (cytofectins), DNA-protein complexes, and biopolymers. Viral vectors include retrovirus, adeno-associated virus, pox, baculovirus, vaccinia, herpes simplex, Epstein-Barr and adenovirus vectors. Vector sequences may also contain one or more regulatory regions, and/or selectable markers useful in selecting, measuring, and monitoring nucleic acid transfer results (transfer to which tissues, duration of expression, etc.).

Cells comprising said nucleic acids or vectors comprising nucleic acids are also provided. The method of introduction is largely dictated by the targeted cell type include, e.g., $CaPO_4$ precipitation, liposome fusion, lipofectin, electroporation, dextran-mediated transfection, calcium phosphate precipitation, polybrene mediated transfection, protoplast fusion, , viral infection, encapsulation of the polynucleotide(s) in liposomes, and direct microinjection of the DNA into nuclei. The nucleic acids may stably integrate into the genome of the host cell (for example, with retroviral introduction, outlined below), or may exist either transiently or stably in the cytoplasm (i.e. through the use of traditional plasmids, utilizing standard regulatory sequences, selection markers, etc.).

Dominant negative polypeptides as described herein may be produced by culturing a host cell transformed with an expression vector containing nucleic

acid encoding a dominant negative polypeptide. Appropriate host cells include yeast, bacteria, archaebacteria, fungi, and insect and animal cells, including mammalian cells. Of particular interest are Drosophila melangaster cells, Saccharomyces cerevisiae and other yeasts, E. coli, Bacillus subtilis, SF9 cells, C129 cells, 293 cells, Neurospora, BHK, CHO, COS, Pichia pastoris, etc.

Preferably, said polypeptides are expressed in mammalian cells. Mammalian expression systems are also known in the art, and include retroviral systems. Suitable cell types include tumor cells, Jurkat T cells, NIH3T3 cells, CHO, and Cos, cells.

Preferably, said polypeptides are expressed in bacterial systems. Bacterial expression systems are well known in the art.

In a preferred embodiment, the nucleic acid encoding the dominant negative polypeptide may also be used in gene therapy. In gene therapy applications, genes are introduced into cells in order to achieve in vivo synthesis of a therapeutically effective genetic product, for example for replacement of a defective gene. "Gene therapy" includes both conventional gene therapy, where a lasting effect is achieved by a single treatment, and the administration of gene therapeutic agents, which involves the one time or repeated administration of a therapeutically effective DNA or mRNA.

There are a variety of techniques available for introducing nucleic acids into viable cells. The techniques vary depending upon whether the nucleic acid is transferred into cultured cells in vitro, or in vivo in the cells of the intended host. Techniques suitable for the transfer of nucleic acid into mammalian cells in vitro include the use of liposomes, electroporation, microinjection, cell fusion, DEAE-dextran, the calcium phosphate precipitation method, etc. The currently preferred in vivo gene transfer techniques include transfection with

viral (typically retroviral) vectors and viral coat protein-liposome mediated transfection (Dzau et al., Trends in Biotechnology 11:205-210 (1993)).

The disclosure further provides non-human animals, preferably mammals, comprising nucleic acids encoding dominant negative polypeptides. Methods for introducing nucleic acids into animals are known to one of skill in the art and include standard transgenic techniques such as introducing said nucleic acid into an undifferentiated cell type, e.g., an embryonic stem (ES) cell. The ES cell is injected into a mammalian embryo, where it integrates into the developing embryo. Insertion of the nucleic acid construct into the ES cells can be accomplished using a variety of methods well known in the art including for example, electroporation, microinjection, and calcium phosphate treatment. The embryo is implanted into a foster mother for the duration of gestation.

Transgenic animals comprise a heterologous nucleic acid sequence present as an extrachromosomal element or stably integrated in all or a portion of its cells, especially in germ cells. During the initial construction of the animal, "chimeras" or "chimeric animals" are generated, in which only a subset of cells have the altered genome. Chimeras are primarily used for breeding purposes in order to generate the desired transgenic animal. Animals having a heterozygous alteration are generated by breeding of chimeras. Male and female heterozygotes are typically bred to generate homozygous animals.

The present disclosure also provides the generation of a novel autosomal recessive osteopetrosis model in mice (*tles*), characterized by defective tooth eruption due to a complete lack in osteoclasts. These mice carry a loss-of-function allele of *Rankl* that corresponds to a single amino acid substitution from glycine to arginine (G278R) at the extracellular inner hydrophobic F ß-strand of RANKL. Unlike previously described mice having *Rankl* null alleles [13,14], the various forms of the RANKL protein are present in the

homozygous *Rankl*$^{tles/tles}$ mutant mice. Since, no differences were detected in the skeletal phenotype between *tles* and *Rankl* null alleles, our results indicate that a single amino acid change is sufficient to cause osteopetrosis without interfering with RANKL expression.

The *tles* osteopetrotic model closely resembles RANKL-mediated human ARO as in both cases the RANKL protein is produced but is inactive due to mutations at the extracellular bioactive region. Three RANKL mutations have been identified in ARO, M199K, del145-177AA, and V277WfX5 [27]; the single amino acid substitution M199K is located within a highly conserved domain, the deletion 145-177 removes a region essential for osteoclastogenesis whereas the frameshift deletion V277WfX5 is predicted to lack the trimerization domain. Notably, the *Rankl*$^{tles/tles}$ mice constitute a unique animal model useful in the validation of new therapeutic approaches in ARO.

The disclosure further provides pharmaceutical preparations comprising a trimerization inhibitor as disclosed herein and a pharmaceutically acceptable carrier, filler, preservative, adjuvant, solubilizer, diluent and/or excipient is also provided. Such pharmaceutically acceptable carrier, filler, preservative, adjuvant, solubilizer, diluent and/or excipient may for instance be found in Remington: The Science and Practice of Pharmacy, 20th Edition. Baltimore, MD: Lippincott Williams & Wilkins, 2000.

When administering the pharmaceutical preparations thereof to an individual, it is preferred that the compound is dissolved in a solution that is compatible with the delivery method. For intravenous, subcutaneous, intramuscular, intrathecal and/or intraventricular administration it is preferred that the solution is a physiological salt solution. Preferred are excipients capable of forming complexes, vesicles and/or liposomes that deliver such a compound as defined herein in a vesicle or liposome through a cell membrane. Many of these excipients are known in the art. Suitable excipients comprise polyethylenimine

(PEI) or similar cationic polymers, including polypropyleneimine or polyethylenimine copolymers (PECs) and derivatives, ExGen 500, synthetic amphiphils (SAINT-18), lipofectin™, DOTAP and/or viral capsid proteins that are capable of self assembly into particles that can deliver such compounds, to a cell.

Active ingredients of the invention can be administered by controlled release means or by delivery devices that are well known to those of ordinary skill in the art. Examples include, but are not limited to, those described in U.S. Pat. Nos. 3,845,770; 3,916,899; 3,536,809; 3,598,123; and 4,008,719, 5,674,533, 5,059,595, 5,591,767, 5,120,548, 5,073,543, 5,639,476, 5,354,556, and 5,733,566, each of which is incorporated herein by reference. Such dosage forms can be used to provide slow or controlled-release of one or more active ingredients using, for example, hydropropylmethyl cellulose, other polymer matrices, gels, permeable membranes, osmotic systems, multilayer coatings, microparticles, liposomes, microspheres, or a combination thereof to provide the desired release profile in varying proportions. Suitable controlled-release formulations known to those of ordinary skill in the art, including those described herein, can be readily selected for use with the active ingredients of the invention. The invention thus encompasses single unit dosage forms suitable for oral administration such as, but not limited to, tablets, capsules, gelcaps, and caplets that are adapted for controlled-release.

Actual dosage levels of the pharmaceutical preparations described herein may be varied so as to obtain an amount of the active ingredient which is effective to achieve the desired therapeutic response for a particular patient, composition, and mode of administration, without being toxic to the patient. The selected dosage level will depend upon a variety of factors including the activity of the particular compound, the route of administration, the time of administration, the rate of excretion of the particular compound being

employed, the duration of the treatment, other drugs, compounds and/or materials used in combination, the age, sex, weight, condition, general health and prior medical history of the patient being treated, and like factors well known in the medical arts.

A physician or veterinarian having ordinary skill in the art can readily determine and prescribe the effective amount of the pharmaceutical composition required. For example, the physician or veterinarian could start with doses of the compounds described herein at levels lower than that required in order to achieve the desired therapeutic effect and gradually increase the dosage until the desired effect is achieved.

A trimerization inhibitor can be administered alone or in combination with other treatments, therapeutics or agents, either simultaneously or sequentially dependent upon the condition to be treated. Additional agents or therapeutics include, e.g., as , anti-RANKL agents or antibodies, immune modulators, or anti-resorptive agents, such as progestins, polyphosphonates, bisphosphonate(s), estrogen agonists/antagonists, estrogen, estrogen/progestin combinations, and estrogen derivatives or therapeutics, hormones. Those skilled in the art will recognize that other bone anabolic agents, also referred to as bone mass augmenting agents, may be used in conjunction with a trimerization inhibitor. A bone mass augmenting agent is a compound that augments bone mass to a level which is above the bone fracture threshold as detailed in the World Health Organization Study World Health Organization, "Assessment of Fracture Risk and its Application to Screening for Postmenopausal Osteoporosis (1994). Report of a WHO Study Group. World Health Organization Technical Series 843." Any prostaglandin, or prostaglandin agonist/antagonist may be used in combination with the compounds of this invention. Those skilled in the art will recognize that IGF-1,

sodium fluoride, parathyroid hormone (PTH), active fragments of parathyroid hormone, growth hormone or growth hormone secretagogues may also be used.

As used herein, "to comprise" and its conjugations is used in its non-limiting sense to mean that items following the word are included, but items not specifically mentioned are not excluded. In addition the verb "to consist" may be replaced by "to consist essentially of" meaning that a compound or adjunct compound as defined herein may comprise additional component(s) than the ones specifically identified, said additional component(s) not altering the unique characteristic of the invention.

The articles "a" and "an" are used herein to refer to one or to more than one (i.e., to at least one) of the grammatical object of the article. By way of example, "an element" means one element or more than one element.
The word "approximately" or "about" when used in association with a numerical value (approximately 10, about 10) preferably means that the value may be the given value of 10 more or less 1% of the value.

The term "treating" includes prophylactic and/or therapeutic treatments. The term "prophylactic or therapeutic" treatment is art-recognized and includes administration to the host of one or more of the subject compositions. If it is administered prior to clinical manifestation of the unwanted condition (e.g., disease or other unwanted state of the host animal) then the treatment is prophylactic (i.e., it protects the host against developing the unwanted condition), whereas if it is administered after manifestation of the unwanted condition, the treatment is therapeutic, (i.e., it is intended to diminish, ameliorate, or stabilize the existing unwanted condition or side effects thereof).

All patent and literature references cited in the present specification are hereby incorporated by reference in their entirety.

The invention is further explained in the following examples. These examples do not limit the scope of the invention, but merely serve to clarify the invention.

EXAMPLES

Example 1. Generation of a novel ENU-induced mouse model of severe osteopetrosis

The toothless (*tles*) phenotype was identified as a recessive trait in which complete failure of tooth eruption was detected in *N*-ethyl-*N*-nitrosourea (ENU)-mutagenized G3 mice in both sexes (Figure 8A). Mutant mice displayed also growth retardation, and lymphoid aberrations characterized by thymic hypoplasia, enlarged spleens, and absence of lymph nodes. Additionally, these mice displayed early lethality, where 60% of the *tles/tles* mice died by the 7th week of age (Figure 8B). Since failure of tooth eruption is a typical finding in osteopetrosis, we performed extensive histological analysis of the tibiae and femurs in 4-6 week-old *tles/tles* mice and WT control littermates. Staining of long bones with von Kossa (Figure 1A), as well as with hematoxylin/eosin (Figure 1B) revealed severe osteopetrosis in mutant mice whereas staining with tartrate-resistant acid phosphatase (TRAP), an enzyme that is highly expressed in osteoclasts, showed that *tles/tles* mice completely lacked TRAP-positive (TRAP+) multinucleated osteoclasts (Figure 1B).

Failure of osteoclast formation can result either from an intrinsic defect in osteoclast differentiation or an impaired crosstalk between osteoclasts and osteoblasts/stromal cells [28,29]. To discriminate these possibilities we performed *ex vivo* osteoclastogenesis assays using hematopoietic progenitor cells isolated from bone marrow (BM) or spleens that can differentiate into TRAP+ mature multinucleated osteoclasts in the presence of macrophage colony-stimulating factor (M-CSF) and RANKL [13]. Cultures of BM cells and

splenocytes from either WT or *tles/tles* mice differentiated into TRAP+ multinucleated osteoclasts (Figures 1C, 9A), indicating that the intrinsic osteoclast differentiation process is not defective in the *tles/tles* mice. To determine whether osteoblasts isolated from the *tles/tles* mice can support osteoclastogenesis, we established *ex vivo* co-culture assays between primary osteoblast cultures and hematopoietic progenitors from BM or spleens in the presence of $1,25(OH)_2$ vitamin D3 and prostaglandin E2 (PGE2) [30]. Osteoblasts from WT mice supported osteoclast formation in progenitors isolated either from WT or *tles/tles* mice, whereas osteoblasts derived from *tles/tles* mice were inadequate to crosstalk with hematopoietic progenitors and direct their differentiation towards osteoclasts (Figures 1D, 9B). These results demonstrate a defective crosstalk between osteoclast precursors and osteoblasts that could be possibly caused by a critical factor missing from the osteoblasts of *tles/tles* mice.

Example 2. *tles* is a missense mutation in the *Rankl* gene

The entire genome of 124 F2 animals (62 affected and 62 normal control siblings) was scanned with a collection of 71 polymorphic markers. Initial screening of 20 animals (10 affected and 10 normal siblings) established linkage to distal chromosome 14. Fine mapping of the locus based on 248 meioses, confirmed linkage to 14qD3 at 44cM, between single nucleotide polymorphisms rs13482262 and rs30965774, with a logarithm of odds (LOD) score of 33,8 and a *p* value equal to $8,80912e^{-42}$ (Figure 2A) .

Screening of the region for candidate genes indicated the presence of the *Rankl* gene and sequencing of its coding region identified within exon 5 a single base transition of guanine to adenine (GenBank NM_011613.3), resulting in a glycine (G) to arginine (R) substitution at position 278 (G278R) (NP_035743) (Figure 2B). G278 is located at the hydrophobic F ß-strand of the monomer that is part of the inner A'AHCF ß-sheet involved in intersubunit association and trimer assembly [6]. Thus, the G278R substitution is likely to interupt trimerization of the RANKL monomers due to steric clashes and positive

charge introduction (Figure 2C-D). G278 residue is highly conserved among various TNF superfamily members, including TNF, CD40L, TRAIL, BAFF and APRIL (Figure 2E).

Example 3. Genetic confirmation of the RANKL G278R mutation

To confirm that the RANKL G278R substitution causes the osteopetrotic phenotype developed in the *tles/tles* (*Rankl*$^{tles/tles}$) mice, we performed genetic complementation by generating *Rankl*$^{-/tles}$ compound heterozygous mice through intercrosses between heterozygous *Rankl*$^{tles/+}$ mice and heterozygous *Rankl* null mice (*Rankl*$^{+/-}$) [13]. *Rankl*$^{-/tles}$ mice (n=6) exhibited severe osteopetrosis characterized by failure of tooth eruption, high bone mass and absence of osteoclasts comparable with the phenotype developed in *Rankl*$^{tles/tles}$ and *Rankl*$^{-/-}$ mice (Figure 3A). These results verify that the G to A transition is a loss-of-function mutation that results in severe osteopetrosis in the *Rankl*$^{tles/tles}$ mice.

Three-dimensional microstructural analyses using high-resolution microcomputed tomography confirmed severe osteopetrosis in *Rankl*$^{tles/tles}$ mice (Figure 3B) which was further validated using bone histomorphometric analysis (Figure 3C). *Rankl*$^{tles/tles}$ mice develop severe osteopetrosis similarly to *Rankl*$^{-/-}$ mice, also indicating that the mutant protein is inactive. Interestingly, *Rankl*$^{tles/+}$ mice are not osteopetrotic and exhibit similar bone parameters, to those of WT control mice and *Rankl*$^{+/-}$ mice (Figure 3C).

To verify whether administration of recombinant RANKL restores osteoclast formation *in vivo*, *Rankl*$^{tles/tles}$ mice were treated from day 13 of age for a period of 14 days with daily subcutaneous injections of recombinant murine RANKL at 150 µg/kg. A massive formation of TRAP+ cells was identified both in trabecular and cortical bones of RANKL-treated *Rankl*$^{tles/tles}$ mice indicating that exogenous RANKL efficiently restores osteoclast formation *in vivo* (Figure

3D). These results confirm that administration of recombinant RANKL might be considered for the therapy of human RANKL-mediated ARO [27].

Example 4. G278R impairs RANKL trimerization and binding to RANK

G278R substitution allows normal RANKL gene expression and protein production (Figure 10). Since G278 resides at the subunit interfaces in the trimer, it may alter trimer formation. To determine whether G278R affects trimer assembly, recombinant soluble WT RANKL and RANKL^{G278R} fused at the N terminus with Glutathione S-Transferase (GST) were produced and characterized biochemically. Previous studies have shown that the GST moiety doesn't impact on RANKL function [31,32], whereas it enhances the formation of multimers due to the natural tendency of GST to dimerize. RANKL multimers were detected in WT GST-RANKL, but not in GST-RANKL^{G278R}, using both monoclonal and polyclonal antibodies against murine RANKL or polyclonal antibodies against GST in native polyacrylamide gels (Figure 4A). Instead, a lower molecular weight band (LB) was detected exclusively in GST-RANKL^{G278R} using polyclonal antibodies against RANKL or GST, which corresponds most probable to GST-RANKL^{G278R} monomers. In addition, both antibodies immunoreacted with high molecular weight GST-RANKL^{G278R} complexes, indicating protein aggregation. The failure of GST-RANKL^{G278R} detection by the monoclonal antibody in native conditions could be explained by the modification of the RANKL^{G278R} structure so that the specific epitopes were either destroyed or masked. However, both GST-RANKL and GST-RANKL^{G278R} were identified by both monoclonal and polyclonal antibodies against RANKL in SDS reduced conditions (Figure 4A).

The inability of the soluble RANKL^{G278R} protein to form trimers was then verified using chemical cross-linking (Figure 4B). GST was removed from the RANKL protein with proteolytic cleavage of GST-RANKL bound on

glutathione-beads. Even though, soluble WT RANKL was released efficiently from the beads, the majority of the soluble RANKL^{G278R} protein remained bound on the beads after digestion (data not shown). This phenomenon indicates increased hydrophobicity of the RANKL^{G278R} protein due to the formation of hydrophobic protein-protein interactions. Chemical crosslinking of soluble WT RANKL showed a trimer form in addition to a dimer and a monomer form, while without cross-linker only monomers were detected (Figure 4B) [33]. In contrast, crosslinking of the released soluble RANKL^{G278R} protein revealed only the monomer form and a high molecular weight "aggregate" form.

To verify that RANKL^{G278R} cannot form trimers in eukaryotic cells, HEK 293FT cells were transiently transfected with expression vectors of the full-length WT or RANKL^{G278R} fused to FLAG or Myc tag at the C terminus (Figure 4C). Similar to the analysis of recombinant RANKL proteins, trimer formation was detected only in WT RANKL-Myc but not in RANKL^{G278R}-Myc. Co-transfection of WT RANKL-FLAG with either WT RANKL-Myc or RANKL^{G278R}-Myc revealed the presence of trimer formation only in cells coexpressing both WT forms (Figure 4C). These results indicate that RANKL^{G278R} not only fails to form trimers but also inhibits WT RANKL trimerization.

Soluble RANKL [8,9] was detected in supernatants of HEK 293FT cells transfected with WT RANKL-FLAG, WT RANKL-Myc or co-transfected with both WT forms but not in supernatants of cells transfected with RANKL^{G278R}-Myc or co-transfected with WT RANKL-FLAG (Figure 4D). These results support the failure of trimer assembly in cells expressing RANKL^{G278R} or coexpressing RANKL^{G278R} and WT RANKL, as the specific antibodies recognize epitopes on RANKL trimers which are not formed in the latter cases.

To investigate whether RANKL^{G278R} interacts with WT RANKL, immunoprecipitation was performed. Lysates of HEK 293FT cells transfected with WT RANKL-FLAG in the presence of either WT RANKL-Myc or RANKL^{G278R}-Myc, were immunoprecipitated with an anti-Myc antibody and the immunoprecipitates were assayed for the presence of the FLAG epitope by immunoblot (Figure 4E). WT RANKL-FLAG coimmunoprecipitated with either WT RANKL-Myc or RANKL^{G278R}-Myc, indicating that WT RANKL interacts with RANKL^{G278R}.

To examine whether RANKL^{G278R} binds to the RANK receptor, serial dilutions of murine RANK-Fc were incubated with immobilized WT GST-RANKL, GST-RANKL^{G278R} or GST (Figure 4F). RANK-Fc interacted with GST-RANKL in a dose-dependent manner, but not with GST-RANKL^{G278R} or GST. This result shows that the binding affinity of GST-RANKL^{G278R} for RANK-Fc was completely abolished, as a result of its inability to form trimers. Collectively, these results indicate that G278R substitution is critically involved in the abrogation of RANKL trimer formation and subsequently receptor binding.

Example 5. RANKL^{G278R} lacks biological activity and possesses a dominant negative effect

To confirm that RANKL^{G278R} is inactive and to test whether it interferes with the ability of WT RANKL to induce *ex vivo* osteoclast formation, BM cells were treated with 25ng/ml M-CSF and 50ng/ml GST-RANKL for 5 days in the presence or absence of GST-RANKL^{G278R} at different concentrations from 12.5-100ng/ml. It is prominent that RANKL^{G278R} lacks biological activity as GST-RANKL^{G278R} failed to induce formation of TRAP+ cells (ratio 0:1) (Figure 5A-C). Instead, WT GST-RANKL (ratio 1:0) induced formation of TRAP+ giant osteoclasts (Figure 5A-C). Complete inhibition in the formation of multinucleated TRAP+ osteoclasts was noticed when the concentration of WT GST-RANKL was half of that of GST-RANKL^{G278R} (ratio 1:2). Incubation of

WT GST-RANKL with GST-RANKL^{G278R} at equal molar 1:1 concentrations completely impaired the formation of TRAP+ giant multinucleated cells, whereas small size TRAP+ cells with low numbers of nuclei were still formed (Figure 5A-C). However, a small number of TRAP+ giant multinucleated cells was formed at a 2:1 ratio, which were morphologically smaller and exhibited less multinucleation as compared to osteoclasts formed in the presence of WT GST-RANKL exclusively (ratio 1:0). Formation of giant osteoclast-like-cells appeared when WT GST-RANKL was mixed with GST-RANKL^{G278R} at a ratio of 4:1 or higher. Incubation of WT GST-RANKL with GST at similar concentrations (12.5-100ng/ml), didn't affect the formation of osteoclasts. These results indicate that the RANKL^{G278R} variant lacks biological activity and possesses a dominant negative effect on WT RANKL function.

Example 6. G122R substitution abrogates TNF activity

The G278 residue of RANKL is highly conserved among various members of the TNF superfamily (Figure 2E). Thus, we investigated whether a similar substitution in soluble human TNF, which corresponds to a replacement of glycine with arginine at position 122 (G122R), modifies TNF trimerization and function. TNF multimers were detected in recombinant WT GST-TNF but not in GST-TNF^{G122R} indicating failure of spontaneous trimer assembly (Figure S4). This result was also confirmed by chemical cross-linking (Figure 6A) of soluble WT TNF or TNF^{G122R} after removal of GST. Similarly to the RANKL^{G278R} variant, G122R substitution in TNF abrogated trimer formation whereas monomers and mainly aggregates were formed instead of trimers, dimers and monomers detected in WT TNF (Figure 6A) [34].

To examine whether TNF^{G122R} binds to TNF receptor, serial dilutions of human p75TNFR-Fc were incubated with immobilized soluble TNF or TNF^{G122R} (Figure 6B). p75TNFR-Fc interacted with TNF in a dose-dependent manner, but not with TNF^{G122R}, indicating that TNF^{G122R} cannot bind to its receptor. The biological activity of the GST-TNF^{G122R} variant was tested using *in vitro* cytotoxicity assays. Although recombinant WT GST-TNF induced dose dependent cytotoxicity in L929 cells, GST-TNF^{G122R} was inefficient to induce cytotoxicity not only at similar doses (0.03-4ng/ml) (Figure 6C) but also at doses 60 times more concentrated (240ng/ml). These results indicate that a similar residue substitution in TNF, G122R, is critically involved in the abrogation of TNF trimer assembly, receptor binding and biological activity.

Example 7. Small molecule SPD304 inhibits RANKL-induced osteoclastogenesis

A novel small molecule inhibitor of TNF trimerization, named SPD304, has been recently reported [35] to interact with glycine 122 (G122) that corresponds to G278 in RANKL. To investigate whether SPD304 can also

inhibit RANKL-induced osteoclast formation, BM cells were treated with 25ng/ml M-CSF and 80ng/ml GST-RANKL in the presence of SPD304 at different concentrations ranging from 0.25 to 2 μM. SPD304 at 1 μM attenuated both the number and the size of TRAP+ multinucleated cells, whereas at 2 μM the formation of multinuclear TRAP+ osteoclast was completely inhibited (Figure 7A-C).

Experimental evidence on the TNF analogue and *in silico* binding studies on mouse RANKL confirm that the optimal binding position of SPD304, causing trimer inhibition, is located very close (<4Å) to the G278 mutation position in the structure (Figure 13A). To experimentally confirm the interference of the SPD304 with the RANKL structure, soluble mouse RANKL was preincubated with increasing concentrations of SPD304 (6-200 μM) and analyzed in native gels showing the natural conformation of RANKL protein (Figure 13B). In the absence of SPD304, soluble RANKL was detected as a single main band whereas a second band of lower molecular weight was also evident in the presence of SPD304. This change of the RANKL conformation appeared even in the lower concentration of SPD304 tested (6μM) and was more noticeable at 200 μM, indicating a possible release of RANKL dimers and monomers by SPD304. To confirm this, chemical cross-linking experiments were performed in soluble RANKL preincubated with SPD304 at similar concentrations. Indeed, in the presence of SPD304, a dramatic increase of RANKL dimers and monomers was detected indicating disruption of the trimeric RANKL structure (Figure 13C). Intriguingly, a significant increase in the intensity of the band corresponding to RANKL trimers was also noticed. This could reflect a possible conformational alteration in the structure of RANKL trimers complexed with SPD304 that lowers the threshold required for the detection of RANKL trimeric molecules by the polyclonal anti-RANKL antibody enabling the detection of more RANKL molecules.

Example 8. Inhibition of RANKL trimerization and activity by small molecules

SDP304 at 2 μM is effective in inhibiting human RANKL function (Figure 14A). However, SPD304 contains a potentially toxic 3-substituted indole moiety that produces reactive intermediates which possibly cause toxicities by covalently binding to nucleophilic residues of protein and/or DNA. In order to evaluate the toxicity induced by SPD304 we established a MTT survival assay in osteoclast precursors and observed that the SPD304 is toxic in concentrations above 5μM (IC50=3.4 μM) as shown in Figure 14A. Therefore, we investigated the potential of testing SPD304 derivatives designed to be less toxic with higher specificity for human RANKL. We present here results for the SPD304 derivatives PRA123, PRA224, PRA333, PRA738, and PRA828, that effectively inhibited RANKL activity in osteoclastogenesis assays (Figure 14B). These small molecules have been also tested as regards their effect on cell toxicity (Figure 14C). Notably, all these compounds are less toxic compared to SPD304 (IC50>3.4 μM). Among them PRA828 does not affect the survival of osteoclast precursors (IC50>20 μM) and specifically inhibits RANKL-mediated osteoclastogenesis. In addition, the small molecule T23 predicted to interact with the trimerization region also inhibited human RANK activity (Figure 14B) with IC50=8μM in cell toxicity (Figure 14C).

In order to study the effectiveness of these small molecules at the molecular levels, we initially examined the effect of PRA224 and T23 on RANKL trimerization in cross linking assays and western blot (Figure 15). Various molar ratios (from 1:1 to 100:1) between PRA224 and the trimeric form of human RANKL were tested. A gradual increase at the levels of human RANKL monomers was observed at ratios 1:1, 3:1 and 10:1, indicating disruption of the RANKL functional trimers. Similarly, T23 induced an increase of RANKL inactive monomers at the ratios of 3:1 and 10:1. Interestingly, such increase was not observed at higher concentrations of small molecule (50:1, 100:1), indicating that the ratio between the small molecules and the RANKL trimer

is critical for the inhibition of trimerization. Collectively, we have identified small molecules targeting the trimerization region of RANKL, which inhibit human RANKL function and display less toxicity compared to SPD304.

Example 9. Inhibition of RANKL trimerization and activity by peptides

In order to examine whether RANKL trimerization and function is also inhibited by RANKL peptides, we tested the efficacy of 12mer peptides that correspond to the F ß-strand of RANKL. Peptide 1 consists of the wild-type sequence (HFYSINVGGFFK), whereas peptide 2 contains the glycine to agrinine substitution (HFYSINVGRFFK). Both peptides inhibited the function of RANKL as detected in RANKL-dependent osteoclastogenesis assays (Figure 16A). However, the effect of such peptides was not possible to be examined in concentrations higher than 50 μM as in such case there was interference by the increased amounts of DMSO in culture. The effect of the peptide 1 on human RANKL trimerization was tested after cross linking in western blotting. A dramatic decrease of the RANKL trimers with a concomitant increase of RANKL inactive monomers was observed at the ratio 50:1 between peptide 1 and RANKL trimers, indicating disruption of RANKL trimers (Figure 16B). Both peptides were also found to inhibit the binding of human RANKL to its receptor RANK (Figure 16C).

Example 10. Inhibition of TNF-induced death

In order to test the ability of the two classes of small molecules to inhibit the function of TNF, one of the most frequently used assays of TNF activity was employed. This exploits the ability of TNF to induce death in the murine fibrosarcoma cell line L929 following sensitisation by the transcription inhibitor actinomycin D. If the compounds truly obstruct the activity of TNF at a functional level, they should also prevent it from being cytotoxic in this setting.

As can be seen in Figure 17A and B, both T23 (compound 1) and PRA224 (compound 2) were able to inhibit TNF-driven toxicity in L929 cells. The IC_{50} values from the respective dose-response experiments were estimated to be less than 10 μM for both compounds. Considering that the read-out of this assay is protection of death, it can also give an indication of the toxicity of the compounds; if they be more toxic than protective, no inhibition would be detected. However, in order to further test any toxicity, the compounds were used in the same concentrations as in the above experiments but with the omission of TNF in order to ascertain whether they exhibit any toxic effects. As is evident in Figure 17B and C, both compounds were found to be minimally toxic at least up to a concentration of 20 μM.

Example 11. Inhibition of the TNF/TNF-R1 interaction

Having established that both compounds (T23 and PRA224) can obstruct the function of TNF, and given that TNF exerts its functions primarily through interacting with the receptor, TNF-R1, a further test was devised to test any effects on this interaction. This test was approached using the ELISA method. Compound 1 (T23) was not found to inhibit the TNF/TNF-R1 interaction in this experimental setting (data not shown). Compound 2 (PRA224) exhibited a pronounced obstruction of this interaction (Figure 18) with an estimated IC_{50} of 10 μM.

Example 12. Reduction of TNF-induced MMP release

A further line of evidence for the inhibitory capacity of T23 and PRA224 came from taking advantage of the ability of TNF to induce the release of matrix metalloproteinases. It is known that the cellular pathogenic determinant in rheumatoid arthritis, the synovial fibroblast, releases the arthritogenic MMP9 upon stimulation with TNF. It is also known that the human TNF-expressing synovial fibroblast (i.e. isolated from the Tg197 model) releases this MMP naively. As can be seen in Figure 19A, both compounds exhibited a dose-

dependent reduction in the release of MMP9 in wild-type synovial fibroblasts stimulated by TNF. Notably, a reduction can also be observed in the TNF over-expressing synovial fibroblasts (Fig. 19B).

Example 13. Obstruction of TNF trimerisation

Given that the basis of design of these inhibitors lies in the fact that the functional species of TNF is a trimer, it is anticipated that the most likely mechanism of inhibition characterising these compounds is a disruption of this trimerisation. In order to test this hypothesis, cross-linking experiments were performed so as to detect the various TNF multimers after interaction with the compounds. Preliminary but strong evidence from these experiments indicates that specific molar ratios between inhibitor and TNF can obstruct the formation of trimers, thus resulting in TNF molecules in an inactive, monomeric state (Fig. 20).

Example 14. G249R substitution abrogates BAFF activity

Glycine at codon 278 of mouse RANKL is highly conserved among various members of the TNF superfamily. In order to investigate whether this glycine to arginine substitution is also critical for trimerization in other TNF superfamily members, we reproduced this mutation in human BAFF ($BAFF^{G249R}$), a cytokine that activates B lymphocytes. Thus, we produced recombinant GST-BAFF in *E coli* and subsequently the soluble BAFF was released from GST by proteolytic cleavage. Chemical crosslinking of various ammounts of soluble BAFF and analysis in western blot showed the presence of trimers, dimers and monomers in wild-type BAFF but not in $BAFF^{G249R}$ indicating failure of spontaneous trimer assembly in mutant BAFF (Figure 21A). To examine whether soluble $BAFF^{G249R}$ binds to BAFF receptor (BAFFR), serial dilutions of human BAFFR-Fc were incubated with immobilized soluble BAFF or $BAFF^{G249R}$ (Figure 21B). BAFFR-Fc interacted with BAFF in a dose-dependent manner, but not with $BAFF^{G249R}$, indicating

that BAFF^{G249R} cannot bind to its receptor. These results indicate that a similar residue substitution in soluble human BAFF, G249R, is critically involved in the abrogation of BAFF trimer assembly, and receptor binding. Thus, substitution of this conserved glycine abrogates trimerization not only in RANKL but also in other TNF superfamily members such as TNF, BAFF and possibly in many more.

Materials and Methods

Mouse Husbandry

The *Rankl*$^{-/-}$ mice have been previously reported [13]. DBA/2J mice were purchased from the Jackson Laboratories. Mice were maintained and bred under specific pathogen-free conditions in the animal facility of Biomedical Sciences Research Center (B.S.R.C.) "Alexander Fleming". All animal procedures were approved and carried out in strict accordance with the guidelines of the Institutional Animal Care and Use Committee of B.S.R.C. "Alexander Fleming" and in accordance to the Hellenic License for Animal Experimentation at the BSRC" Alexander Fleming" (Prot. No. 3249/18-06-07).

ENU Mutagenesis

G0 males of a mixed C57BL/6Jx129S6 background were treated with ENU (Sigma-Aldrich, Inc.) administered in three weekly doses at 100mg/kg of body weight [42]. Each G0 mouse was crossed to WT C57BL/6Jx129S6 females to produce G1 males which were further mated with WT females to produce G2 daughters that were subsequently backcrossed with the G1 parent to generate G3 progeny [43]. ENU mutagenesis was performed at B.S.R.C. "Alexander Fleming".

Mapping and Sequencing

Heterozygous *tles*/+ animals were outcrossed with DBA/2J mice and the F1 offspring were intercrossed to generate the F2 progeny harboring the recessive

tles mutation. F2 progeny were screened for osteopetrosis, and used for genetic analysis. A total of 71 polymorphic markers, including simple sequence length polymorphisms (SSLPs)and single nucleotide polymorphisms (SNPs), were used for genome-wide linkage analysis. SSLPs were resolved on 4% agarose gels whereas SNPs were identified by pyrosequencing using the Pyromark ID instrument (Biotage AB). A standard genome scan was conducted using R/qtl (The R Foundation for Statistical Computing, version 2.8.0) [44]. Log likelihood linkage for single-trait analysis was established by non-parametric interval mapping of a binary model (diseased versus healthy control siblings), on 124 F2 animals in total, computed at 1cM increments over the entire genome. Sequencing was carried out as a service by MWG Biotech AG.

Crystal Structure and Molecular Modeling

The RANKL homotrimer structure was obtained from the Protein Data Bank (PDB) (www.rcsb.org/pdb/) code 1S55. Molecular models for the G278R mutant homo and heterotrimers were built using Modeller v9.4 [45] and tested for packing inconsistencies and atomic clashes using the program QUANTA-CHARM (Molecular Simulations Inc., San Diego, California, USA) [46].

Histopathological Analysis

Femurs and tibiae were fixed in 4% PFA for 6 hours, decalcified in 13% EDTA and embedded in paraffin. Sections of 5-µm thickness were stained with hematoxylin/eosin. Osteoclasts were stained for TRAP activity using a leukocyte acid phosphatase (TRAP) kit (Sigma-Aldrich).

Ex vivo Osteoclast Formation

BM cells were collected after flushing out of femurs and tibiae, subjected to gradient purification using ficoll-paque (GE Healthcare), plated in 24-well plates at a density of $5x10^5$ cells per well and cultured in αMEM medium (GIBCO) containing 10% fetal bovine serum supplemented with 40ng/ml

RANKL (R&D Systems) and 25ng/ml M-CSF (R&D Systems) for 5 days. Similarly, splenocytes were collected, plated in 24-well plates at a density of 10^6 cells per well and cultured in the presence of recombinant RANKL and M-CSF for 6 days. GST-RANKL^{G278R} was pre-incubated with WT GST-RANKL at room temperature for 20 min, prior to the stimulation of the BM cell cultures, in order to enable exchange of the RANKL variants and heterotrimer formation. Small molecule SPD304 (Sigma-Aldrich) was pre-incubated with 80ng/ml GST-RANKL at various concentrations from 0.25 to 2 µM in αMEM medium for 1 hour at room temperature and then added to culture.

Osteoclasts were stained for TRAP activity.

Osteoblasts were isolated from calvariae of 10-day-old mice using a sequential collagenase/dispase digestion procedure, were plated in 24-well plates at a density of $4x10^4$ cells per well and cultured overnight in αMEM medium with 10% FBS. BM cells or splenocytes were collected, cultured with 10ng/ml M-CSF overnight, subjected to gradient centrifugation and co-cultured with osteoblasts at a density of $5x10^5$ (BM cells) and $2x10^6$ (splenocytes) in αMEM medium supplemented with $1,25(OH)_2$ vitamin D3 (10nM) and PGE2 (1µM) for 6 days.

Bone Histomorphometry

Left femurs were fixed in 4% formalin and embedded in methylmethacrylate resin (Technovit; Heraeus Kulzer, Wehrheim, Germany) using standard procedures. 4 µm thick sections were prepared with a Jung microtome (Jung, Heidelberg, Germany), and stained with von Kossa stain and toluidine blue. Standard bone histomorphometric measures were analyzed using a Zeiss Axioskop 2 microscope (Zeiss, Marburg, Germany) equipped with an Osteomeasure image analysis system.

MicroCT Imaging

MicroCT images were acquired on a vivaCT40 (Scanco Medical, Bassersdorf,

Switzerland). The scanner generates a cone beam at 5-mm spot size and operates at 50 keV. Images of femurs from WT, *Rankl*$^{-/-}$, *Rank*$^{+/-}$, *Rankl*$^{tles/tles}$ and *Rankl*$^{+/tles}$ mice were acquired.

Quantification of Soluble RANKL

The levels of soluble mouse RANKL were quantitated using a commercial ELISA kit (R&D).

Expression and Purification of GST-RANKL and GST-TNF

The extracellular domains of RANKL, RANKL^{G278R}, TNF, and TNF^{G122R} were expressed in *Escherichia coli* as a GST-fusion protein. Briefly, a cDNA encoding the core ectodomain of murine RANKL residues 158–316, with or without the G278R substitution, was cloned into pGEX-6P-1 (GE Healthcare Life Sciences) downstream of GST. For the generation of recombinant GST-TNF, a cDNA encoding the extracellular domain of human TNF from valine 77 to leucine 233 was also cloned into pGEX-6P-1. The G122R substitution was introduced by a two step overlapping PCR approach. Following IPTG-mediated (100μM) induction of protein expression, BL21cells were lysed by sonication, and incubated with glutathione-sepharose beads. The GST-fused proteins were released from the affinity matrix by competitive elution with 50mM glutathione (Sigma-Aldrich).

Purification of soluble RANKL and TNF

After capture of GST-RANKL or GST-TNF on glutathione beads, soluble RANKL or TNF were eluted by cleavage of beads with PreScission Protease (GE healthcare) for overnight at 4°C.

Protein cross-linking assay

The chemical cross-linking reagent disuccinimidyl suberate (DSS, Sigma) was used to examine the trimeric property of RANKL and TNF [33]. 50mM of DSS

was prepared as a stock solution in dimethyl sulfoxide (DMSO). RANKL or TNF proteins at a final concentration of 0.1mM in PBS buffer (pH 7.5) were mixed with 1mM DSS (the molar ratio of DSS is 10:1). The cross linking reactions were carried out for 1 hour at room temperature and terminated with 50mM Tris (pH 7.5) for 30 min. Proteins from reaction mixtures were separated on 12% SDS-PAGE, followed by staining with Coomassie blue R-250 or proceeded in western blot.

Generation of C-terminus Tagged Full-Length WT and RANKL^{G278R}

The full-length mouse WT or RANKL^{G278R} cDNA constructs encoded residues 1-316 without stop codon. A Myc-tagged RANKL expression vector was constructed by inserting full-length RANKL into the pcDNA3.1/myc-His A MCS vector (Invitrogen). FLAG-tagged RANKL was created by subcloning full-length RANKL into the p3XFLAG-CMV-14 expression vector (Sigma-Aldrich).

Transient 293 Transfection Assays

HEK 293FT cells were transfected with 1 μg plasmid DNA using TransIt-293 transfection reagent (Mirus, Madison, WI). After 48 h, transfected cells were harvested in PBS and the half quantity was diluted in equal volume of 2X Laemmli sample buffer, and analyzed in 12% acrylamide denatured gels. The remaining cells were lysed by sonication, centrifuged, and analyzed in 8% native acrylamide gels.

Western Blot

Recombinant proteins or lysates were resolved either on 8% native acrylamide gels or 12% SDS denatured acrylamide gels. RANKL was detected by western blotting using either a monoclonal (clone IK22/5, eBioscience) or a polyclonal (R&D Systems) anti-RANKL antibody, whereas for GST detection a rabbit polyclonal anti-GST antibody was used. Human TNF was detected using a

rabbit polyclonal anti-TNF antibody provided by Prof. Wim Buurman (Maastricht University). Moreover, antibodies against Myc (rabbit polyclonal, Santa Cruz Biotechnology), FLAG (M2, Sigma) and actin (goat polyclonal, Santa Cruz Biotechnology) were also used.

Immunoprecipitation

HEK 293FT cells were harvested 48 h after transient transfection, lysed and incubated with an anti-Myc antibody. Anti-Myc immunocomplexes were precipitated with protein A/G Sepharose (Santa Cruz Biotechnology). Protein complexes were resolved by SDS–PAGE, and immunoblotted with an anti-FLAG antibody as described previously.

Binding Assay of GST-RANKL^{G278R} to RANK

Nunc plates were coated with recombinant WT GST-RANKL, GST-RANKL^{G278R} or GST at 3µg/ml and after blocking with 1%BSA, were incubated with increasing amount of recombinant mouse RANK-Fc (R&D systems). RANK binding was detected with a phycoerythrin (PE) conjugated goat anti-human IgG (Fc) (SouthernBiotech, Birmingham, USA) that was measured (539-573nm) with the fluorescent plate reader TECAN infinite M200.

Binding Assay of TNF^{G122R} to TNFR

Nunc plates were coated with recombinant soluble TNF or TNF^{G122R} at 3µg/ml and incubated with increasing amount of recombinant human p75TNFR-Fc (Wyeth). TNFR binding was detected with a horseradish peroxidise (HRP) conjugated goat anti-human IgG (Fc) (SouthernBiotech, Birmingham, USA) using o-phenylenediamine (OPD) substrate (Thermo Scientific Pierce) that was measured at 490nm.

In vivo Administration of Soluble RANKL

Recombinant soluble RANKL was produced after digest of the GST-RANKL protein with prescission protease (GE Healthcare) for the removal of GST. Mice were treated from day 13 of age for a period of 14 days with subcutaneous injections of 150 µg/kg soluble RANKL.

Statistical Analysis

Statistical analysis was performed on Prism software, using one-way ANOVA with Tukey's Multiple Comparison Test. All values are reported as the mean ± standard error of the mean (SEM). All *P* values below 0.05 were considered significant.

Small molecules

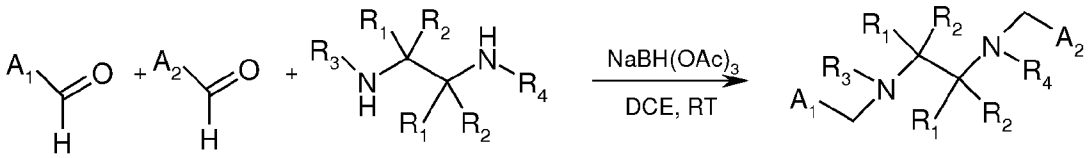
All compounds were dissolved and stored in DMSO. All pre-incubations with recombinant human TNF were carried out for 30 min at room temperature, whereas for human RANKL preincubations were performed at 37°C for 1 hour.

Based on the crystal structure of RANKL and its predicted interactions with SPD304, novel SPD304 derivatives such as PRA123, PRA224, PRA333, PRA738, and PRA828 were designed to inhibit RANKL activity by targeting its trimerization.

The synthesis of these novel compounds was performed using standard methods known to one of skill in the art. In an exemplary embodiment, the SPD304 derivatives can be prepared as described below. It is clear to a skilled person that other methods may also be used. It will also be appreciated by persons skilled in the art that within certain of the processes described herein, the order of the synthetic steps employed can be varied and will depend inter alia on factors such as the nature of functional groups present in a particular substrate and the protecting group strategy (if any) to be adopted. Clearly, such factors will also influence the choice of reagent to be used in the synthetic steps.

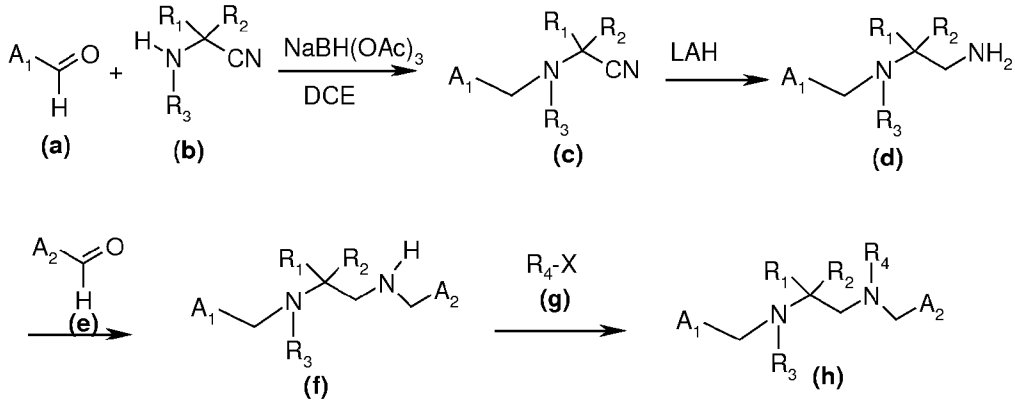
The method of preparation includes reacting aldehydes or acids, which can be same or different, containing saturated or unsaturated ring systems, optionally substituted and optionally containing heteroatoms, with substituted or unsubstituted diamines to form amines or amides respectively. This can be accomplished in a single reaction or in several steps including, but not limited to, steps such as Schiff's base formation, reduction, and reductive amination, as shown in the schemes below.

Scheme 1a :



wherein: A1 and A2 are independently a substituted or unsubstituted phenyl group or a substituted or unsubstituted heterocyclic system, as defined herein above; R1 and R2 are independently, hydrogen or (C_1-C_4)-alkyl group;

R3 and R4 are independently, hydrogen or (C_1-C_4)-alkyl group; and R3 and R4 can optionally form a ring system. The process of Scheme 1 a is analogous to the process disclosed in U.S. Patent No. 6,344,334 and Tetrahedron Lett. 37:7193-7196 (1996). Scheme 1 b :



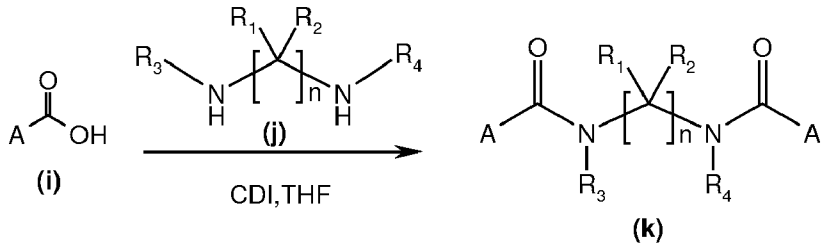
wherein:

A1 and A2 are independently a substituted or unsubstituted phenyl group or a substituted or unsubstituted heterocyclic system, as defined herein above; R1 and R2 are independently, hydrogen or (C_1-C_4)-alkyl group;

R3 and R4 are independently, hydrogen or (C_1-C_4)-alkyl group; and R3 and R4 can optionally form a ring system.

In Scheme 1 b, reductive amination of an aromatic aldehyde (a) with amino nitrile (b) compound provides a substituted nitrile intermediate (c). The reducing agent used can be selected from, for example, sodium triacetoxy borohydride and sodium cyanoborohydride in solvents such as DCE, THF, acetonitrile and dioxane. In an embodiment, sodium triacetoxy borohydride is used as reducing agent in THF as solvent. The temperature used is 20-40 <0>C, for example, ambient temperature (25 <0>C). 1 .0 equivalent of the intermediate (c) is taken in a suitable solvent such as ether, THF or dioxane at O <0>C and treated with LAH (Lithium aluminium hydride) (0.5 to 2.5 equivalent) to obtain an amino intermediate (d). In an embodiment, the solvent used is THF. The amino intermediate (d) is then reacted with an aldehyde (e) to give a compound (f) (intermediate/product) by reductive amination, which can be N-alkylated using suitable alkyl halide (g) in solvent such as DMF or acetone, in presence of a base such as pyridine, triethylamine, sodium hydride, sodium carbonate or potassium carbonate to give the desired product (h).

Scheme 2 :



wherein:

A1 and A2 are independently a substituted or unsubstituted phenyl group or a substituted or unsubstituted heterocyclic system, as defined herein above; n is an integer from 2-4;

R1 and R2 are independently, hydrogen or (C_1-C_4)-alkyl group; R3 and R4 are independently, hydrogen or (C_1-C_4)-alkyl group; and R3 and R4 can optionally form a ring system. In Scheme 2, an aromatic acid (i) is treated with a diamine (j) in presence of a coupling agent in a suitable solvent to obtain compound (k). The coupling agent used can be, for example, CDI (1 ,1 '-Carbonyldiimidazole), DCC (1 ,3- Dicyclohexylcarbodiimide), EDC (1 -(3-Dimethylaminopropyl)-3-ethylcarbodiimide hydrochloride), chloro-dipyrrolidinocarbenium tetrafluoroborate, PyBOP (Benzotriazol-1 -yl-oxy-thspyrrolidinophosphonium hexafluorophosphate), HOBT (1 - Hydroxybenzotriazole), or DIPEA (N,N-Diisopropylethylamine). In an embodiment, CDI is used as the coupling agent. The solvent used can be, for example, THF, ether, dioxane, or DMF. In an embodiment, the solvent used is THF. The temperature used is 20-40 <0>C, for example, ambient temperature (25 <0>C). The time required for the completion of the reaction is 3-10 h. In an embodiment, the reaction is mostly completed in 6 h. The resulting product is purified by various methods, which optionally include free base isolation or salt formation. Normal phase or reversed phase silica gel chromatography or precipitation techniques are used wherever required.

The reagents, reactants and intermediates used in the present processes are either commercially available or can be prepared according to standard literature procedures known in the art.

Compound 1 of Figure 23 (T23) was identified in a multi-step in silico approach, including computational molecular docking studies. A chemical library of more than 14,000 small molecules was screened to identify molecules with suitable properties that are predicted to interact with the TNF-alpha dimer. T23 was identified and its ability to act as a trimerization inhibitor was confirmed in vivo. The PubChem database was used to identify chemicals having a similar 3D structure as T23. The functional derivatives listed in Figure 23 are predicted to interact with residues from TNF superfamily polypeptides. T23 and its functional derivatives are commercially available or can be prepared according to standard literature procedures known in the art.

RANKL peptides

12mer peptides corresponding to the F-beta strand of RANKL were synthesized by JPT Peptide Technologies GmbH. The sequence of the wild-type peptide (peptide 1) was HFYSINVGGFFK, whereas the sequence of the peptide containing the glycine to arginine substitution (peptide 2) was HFYSINVGRFFK. Peptides were dissolved and stored in 100% DMSO. The purity of the peptides was above 90%.

Expression and Purification of soluble human RANKL

The extracellular domain of human RANKL was expressed in *Escherichia coli* as a GST-fusion protein as previously described (Douni et al., 2012). Briefly, a cDNA encoding the core ectodomain of human RANKL residues 143–317 (20 kD), was cloned into pGEX-6P-1 (GE Healthcare Life Sciences) downstream of GST. Following IPTG-mediated (100μM) induction of protein expression, BL21cells were lysed by sonication, and incubated with glutathione-sepharose beads. After capture of GST-RANKL on

glutathione beads, soluble human RANKL were eluted by cleavage of beads with PreScission Protease (GE healthcare) for overnight at 4°C.

RANKL cross-linking and western

The chemical cross-linking reagent disuccinimidyl suberate (DSS, Sigma) was used to examine the effect of potent RANKL inhibitors (small molecules, peptides) in the trimerization of human RANKL (Douni et al., 2012). Recombinant soluble human RANKL (prepared in our laboratory) was pre-incubated with increasing amounts of inhibitors at various ratios for 1 hour at 37oC. Such complexes were mixed with 1mM DSS (the molar ratio of DSS is 10:1). The cross linking reactions were carried out for 1 hour at room temperature and terminated with 50mM Tris (pH 7.5) for 30 min. Cross linked soluble human RANKL protein was separated on 12% SDS-PAGE, and was detected using a polyclonal goat anti-RANKL antibody (R&D Systems) in western blotting

RANKL/RANK ELISA

Nunc plates were coated with 100µl of 250ng/ml recombinant soluble human RANK-Fc (R&D Systems) overnight. Recombinant soluble human RANKL at 200ng/ml was pre-incubated with increasing amounts of peptides (3-100µM) for 1 hour at 37oC and was added in the RANK-coated wells. RANKL binding was detected with a polyclonal goat anti-RANKL antibody (R&D Systems), followed by a horseradish peroxidase (HRP) conjugated horse anti-goat IgG (Vector) using o-phenylenediamine (OPD) substrate (Thermo Scientific Pierce) that was measured at 490nm.

RANKL-mediated Osteoclastogenesis assays

BM cells were collected after flushing out of femurs and tibiae, subjected to gradient purification using ficoll-paque (GE Healthcare), plated in 96-well plates at a density of $6x10^4$ cells per well and cultured in αMEM medium

(GIBCO) containing 10% fetal bovine serum supplemented with 50ng/ml human RANKL (Peprotech) and 25ng/ml M-CSF (R&D Systems) for 5 days. RANKL was pre-incubated with inhibitors at 37°C for 1 hr, prior to the stimulation of the BM cell cultures, in order to enable potent interactions. Osteoclasts were stained for TRAP activity (Sigma).

TNF-induced L929 cytotoxicity assay

L929 cells were seeded onto a 96-well plate ($3x10^4$ cells/well). On the following day, cells were treated with 0.25 ng/ml human TNF and 2 µg/ml actinomycin D. After 18-24h, dead cells were removed by washing with PBS, remaining live cells were fixed with methanol, stained with crystal violet and quantified spectrophotometrically at 570 nm after solubilisation of the stain using acetic acid.

TNF/TNF-R1 ELISA

96-well plates were coated with 0.1 µg/ml recombinant soluble human TNR-R1 in PBS over-night at 4°C. Following 4 washes with PBS containing 0.05% Tween-20, blocking was carried out using 1% BSA in PBS. 0.025 µg/ml recombinant human TNF in PBS was added and the plates were incubated for 1 h at room temperature. After another round of washes, plates were incubated with a 1:5000 dilution of an anti-TNF antibody conjugated with HRP for 1 h at room temperature. After a final round of washes, the signal was developed using TMB and measured spectrophoto-metrically at 450 nm.

Gelatin zymography

For gelatin zymography experiments, serum-free supernatants were collected from serum-starved cells usually after 24 hours of stimulation. Following non-reducing SDS-PAGE in gels containing 1 mg/ml gelatin, these were incubated for 18 hours in developing buffer (50 mM Tris-HCl, pH 7.5; 5 mM $CaCl_2$; 0.02% NaN_3; 1 µM $ZnCl_2$) at 37°C. Finally, gels were stained with 0.5% Coomassie

Brilliant Blue R250 in 45% methanol/10% acetic acid and de-stained with 50% methanol/10% acetic acid.

TNF cross-linking experiments

100 ng of recombinant human TNF was cross-linked using 4.8 mM BS3 for 45 min at room temperature. The reaction was stopped by adding 1/10th volume of 1 M Tris-HCl, pH 7.5. Samples were then subjected to SDS-PAGE and western blotting using an anti-TNF antibody.

Expression and Purification of soluble BAFF

The extracellular domains of BAFF and BAFF^{G249R} were expressed in *Escherichia coli* as a GST-fusion protein. Briefly, a cDNA encoding the core ectodomain of human BAFF residues 134–285 (17.5 kD), with or without the G249R substitution, was cloned into pGEX-6P-1 (GE Healthcare Life Sciences) downstream of GST. The G249R substitution was introduced by a two step overlapping PCR approach. Following IPTG-mediated (100µM) induction of protein expression, BL21cells were lysed by sonication, and incubated with glutathione-sepharose beads. After capture of GST-BAFF on glutathione beads, soluble BAFF was eluted by cleavage of beads with PreScission Protease (GE healthcare) for overnight at 4°C.

BAFF cross-linking and western

The chemical cross-linking reagent disuccinimidyl suberate (DSS, Sigma) was used to examine the trimeric property of BAFF as previously described (Douni et al., 2012). Various amounts of BAFF proteins in PBS buffer (pH 7.5) were mixed with 1mM DSS (the molar ratio of DSS is 10:1). The cross linking reactions were carried out for 1 hour at room temperature and terminated with 50mM Tris (pH 7.5) for 30 min. Proteins from reaction mixtures were separated on 12% SDS-PAGE and proceeded in western blot using a polyclonal anti- BAFF antibody (PeproTech).

BAFF/BAFF receptor ELISA

Nunc plates were coated with 3µg/ml recombinant soluble human BAFF or $BAFF^{G249R}$ and incubated with increasing amount of recombinant human BAFFR-Fc (R&D Systems). BAFFR binding was detected with a horseradish peroxidase (HRP) conjugated goat anti-human IgG (Fc) (SouthernBiotech, Birmingham, USA) using o-phenylenediamine (OPD) substrate (Thermo Scientific Pierce) that was measured at 490nm.

MTT viability assay

Bone marrow (BM) cells were plated in 96-well plates at a density of 10^5 cells per well after gradient purification using ficoll-paque (GE Healthcare). BM cells were cultured in αMEM medium (GIBCO) containing 10% fetal bovine serum supplemented with 25ng/ml M-CSF (R&D Systems) in the presence of the tested compounds at concentrations from 1-20 µM for 2 days (0.1% DMSO). Serum free a-MEM medium containing 0.5mg/ml MTT [3-(4,5-Dimethylthiazol-2-yl)-2,5-diphenyltetrazolium bromide] was added for 2 hours in a 37°C CO_2 incubator. After removal of the MTT solution, DMSO was added to extract the dye from the cells and cell viability was accessed at 550nm.

References

1. Karsenty G, Wagner EF (2002) Reaching a genetic and molecular understanding of skeletal development. Dev Cell 2: 389-406.

2. Boyle WJ, Simonet WS, Lacey DL (2003) Osteoclast differentiation and activation. Nature 423: 337-342.

3. Fuller K, Wong B, Fox S, Choi Y, Chambers TJ (1998) TRANCE is necessary and sufficient for osteoblast-mediated activation of bone resorption in osteoclasts. J Exp Med 188: 997-1001.

4. Anderson DM, Maraskovsky E, Billingsley WL, Dougall WC, Tometsko ME, et al. (1997) A homologue of the TNF receptor and its ligand enhance T-cell growth and dendritic-cell function. Nature 390: 175-179.

5. Wong BR, Rho J, Arron J, Robinson E, Orlinick J, et al. (1997) TRANCE is a novel ligand of the tumor necrosis factor receptor family that activates c-Jun N-terminal kinase in T cells. J Biol Chem 272: 25190-25194.

6. Lam J, Nelson CA, Ross FP, Teitelbaum SL, Fremont DH (2001) Crystal structure of the TRANCE/RANKL cytokine reveals determinants of receptor-ligand specificity. J Clin Invest 108: 971-979.

7. Ito S, Wakabayashi K, Ubukata O, Hayashi S, Okada F, et al. (2002) Crystal structure of the extracellular domain of mouse RANK ligand at 2.2-A resolution. J Biol Chem 277: 6631-6636.

8. Hikita A, Yana I, Wakeyama H, Nakamura M, Kadono Y, et al. (2006) Negative regulation of osteoclastogenesis by ectodomain shedding of receptor activator of NF-kappaB ligand. J Biol Chem 281: 36846-36855.

9. Ikeda T, Kasai M, Utsuyama M, Hirokawa K (2001) Determination of three isoforms of the receptor activator of nuclear factor-kappaB ligand and their differential expression in bone and thymus. Endocrinology 142: 1419-1426.

10. Lacey DL, Timms E, Tan HL, Kelley MJ, Dunstan CR, et al. (1998) Osteoprotegerin ligand is a cytokine that regulates osteoclast differentiation and activation. Cell 93: 165-176.

11. Yasuda H, Shima N, Nakagawa N, Yamaguchi K, Kinosaki M, et al. (1998) Osteoclast differentiation factor is a ligand for osteoprotegerin/osteoclastogenesis-inhibitory factor and is identical to TRANCE/RANKL. Proc Natl Acad Sci U S A 95: 3597-3602.

12. Lacey DL, Tan HL, Lu J, Kaufman S, Van G, et al. (2000) Osteoprotegerin ligand modulates murine osteoclast survival in vitro and in vivo. Am J Pathol 157: 435-448.

13. Kong YY, Yoshida H, Sarosi I, Tan HL, Timms E, et al. (1999) OPGL is a key regulator of osteoclastogenesis, lymphocyte development and lymph-node organogenesis. Nature 397: 315-323.

14. Kim N, Odgren PR, Kim DK, Marks SC, Jr., Choi Y (2000) Diverse roles of the tumor necrosis factor family member TRANCE in skeletal physiology revealed by TRANCE deficiency and partial rescue by a lymphocyte-expressed TRANCE transgene. Proc Natl Acad Sci U S A 97: 10905-10910.

15. Dougall WC, Glaccum M, Charrier K, Rohrbach K, Brasel K, et al. (1999) RANK is essential for osteoclast and lymph node development. Genes Dev 13: 2412-2424.

16. Li J, Sarosi I, Yan XQ, Morony S, Capparelli C, et al. (2000) RANK is the intrinsic hematopoietic cell surface receptor that controls osteoclastogenesis and regulation of bone mass and calcium metabolism. Proc Natl Acad Sci U S A 97: 1566-1571.

17. Bucay N, Sarosi I, Dunstan CR, Morony S, Tarpley J, et al. (1998) osteoprotegerin-deficient mice develop early onset osteoporosis and arterial calcification. Genes Dev 12: 1260-1268.

18. Rossi SW, Kim MY, Leibbrandt A, Parnell SM, Jenkinson WE, et al. (2007) RANK signals from CD4(+)3(-) inducer cells regulate development of Aire-expressing epithelial cells in the thymic medulla. J Exp Med 204: 1267-1272.

19. Takayanagi H (2007) Osteoimmunology: shared mechanisms and crosstalk between the immune and bone systems. Nat Rev Immunol 7: 292-304.

20. Fata JE, Kong YY, Li J, Sasaki T, Irie-Sasaki J, et al. (2000) The osteoclast differentiation factor osteoprotegerin-ligand is essential for mammary gland development. Cell 103: 41-50.

21. Hanada R, Leibbrandt A, Hanada T, Kitaoka S, Furuyashiki T, et al. (2009) Central control of fever and female body temperature by RANKL/RANK. Nature 462: 505-509.

22. Jones DH, Nakashima T, Sanchez OH, Kozieradzki I, Komarova SV, et al. (2006) Regulation of cancer cell migration and bone metastasis by RANKL. Nature 440: 692-696.

23. Schramek D, Leibbrandt A, Sigl V, Kenner L, Pospisilik JA, et al. (2010) Osteoclast differentiation factor RANKL controls development of progestin-driven mammary cancer. Nature 468: 98-102.

24. Leibbrandt A, Penninger JM (2009) RANK(L) as a key target for controlling bone loss. Adv Exp Med Biol 647: 130-145.

25. Cummings SR, San Martin J, McClung MR, Siris ES, Eastell R, et al. (2009) Denosumab for prevention of fractures in postmenopausal women with osteoporosis. N Engl J Med 361: 756-765.

26. Smith MR, Egerdie B, Hernandez Toriz N, Feldman R, Tammela TL, et al. (2009) Denosumab in men receiving androgen-deprivation therapy for prostate cancer. N Engl J Med 361: 745-755.

27. Sobacchi C, Frattini A, Guerrini MM, Abinun M, Pangrazio A, et al. (2007) Osteoclast-poor human osteopetrosis due to mutations in the gene encoding RANKL. Nat Genet 39: 960-962.

28. Grigoriadis AE, Wang ZQ, Cecchini MG, Hofstetter W, Felix R, et al. (1994) c-Fos: a key regulator of osteoclast-macrophage lineage determination and bone remodeling. Science 266: 443-448.

29. Yoshida H, Hayashi S, Kunisada T, Ogawa M, Nishikawa S, et al. (1990) The murine mutation osteopetrosis is in the coding region of the macrophage colony stimulating factor gene. Nature 345: 442-444.

30. Suda T, Ueno Y, Fujii K, Shinki T (2003) Vitamin D and bone. J Cell Biochem 88: 259-266.

31. Xu J, Tan JW, Huang L, Gao XH, Laird R, et al. (2000) Cloning, sequencing, and functional characterization of the rat homologue of receptor activator of NF-kappaB ligand. J Bone Miner Res 15: 2178-2186.

32. Cheng T, Pavlos NJ, Wang C, Tan JW, Lin JM, et al. (2009) Mutations within the TNF-like core domain of RANKL impair osteoclast differentiation and activation. Mol Endocrinol 23: 35-46.

33. Zhang S, Liu C, Huang P, Zhou S, Ren J, et al. (2009) The affinity of human RANK binding to its ligand RANKL. Arch Biochem Biophys 487: 49-53.

34. Zhang XM, Weber I, Chen MJ (1992) Site-directed mutational analysis of human tumor necrosis factor-alpha receptor binding site and structure-functional relationship. J Biol Chem 267: 24069-24075.

35. He MM, Smith AS, Oslob JD, Flanagan WM, Braisted AC, et al. (2005) Small-molecule inhibition of TNF-alpha. Science 310: 1022-1025.

36. Liu C, Walter TS, Huang P, Zhang S, Zhu X, et al. (2010) Structural and functional insights of RANKL-RANK interaction and signaling. J Immunol 184: 6910-6919.

37. Aoki K, Saito H, Itzstein C, Ishiguro M, Shibata T, et al. (2006) A TNF receptor loop peptide mimic blocks RANK ligand-induced signaling, bone resorption, and bone loss. J Clin Invest 116: 1525-1534.

38. Ta HM, Nguyen GT, Jin HM, Choi J, Park H, et al. (2010) Structure-based development of a receptor activator of nuclear factor-kappaB ligand (RANKL) inhibitor peptide and molecular basis for osteopetrosis. Proc Natl Acad Sci U S A 107: 20281-20286.

39. Poblenz AT, Jacoby JJ, Singh S, Darnay BG (2007) Inhibition of RANKL-mediated osteoclast differentiation by selective TRAF6 decoy peptides. Biochem Biophys Res Commun 359: 510-515.

40. Ameloot P, Declercq W, Fiers W, Vandenabeele P, Brouckaert P (2001) Heterotrimers formed by tumor necrosis factors of different species or muteins. J Biol Chem 276: 27098-27103.

41. Douni E, Armaka M, Kontoyiannis DL, Kollias G (2007) Functional genetic and genomic analysis of modeled arthritis. Adv Exp Med Biol 602: 33-42.

42. Justice MJ, Carpenter DA, Favor J, Neuhauser-Klaus A, Hrabe de Angelis M, et al. (2000) Effects of ENU dosage on mouse strains. Mamm Genome 11: 484-488.

43. Nelms KA, Goodnow CC (2001) Genome-wide ENU mutagenesis to reveal immune regulators. Immunity 15: 409-418.

44. Broman KW, Wu H, Sen S, Churchill GA (2003) R/qtl: QTL mapping in experimental crosses. Bioinformatics 19: 889-890.

45. Sali A, Blundell TL (1993) Comparative protein modelling by satisfaction of spatial restraints. J Mol Biol 234: 779-815.

46. Brooks BR, Brooks CL, 3rd, Mackerell AD, Jr., Nilsson L, Petrella RJ, et al. (2009) CHARMM: the biomolecular simulation program. J Comput Chem 30: 1545-1614.

Douni E, Rinotas V, Makrinou E, Zwerina J, Penninger JM, Eliopoulos E, Schett G, Kollias G. (2012). A RANKL G278R mutation causing osteopetrosis identifies a functional amino acid essential for trimer assembly in RANKL and TNF. *Hum Mol Genet.*; 21(4):784-98.

Claims

1. A method for inhibiting trimerization of a TNF superfamily member polypeptide comprising contacting said polypeptide with a trimerization inhibitor selected from

a) a compound that binds to said TNF superfamily member polypeptide in the F beta-strand of said polypeptide, preferably at the glycine residue that corresponds to position 279 in human RANKL, provided that when the trimerization inhibitor is 6,7-Dimethyl-3-[[methyl[2-[methyl[[1-[3-(trifluoromethyl)phenyl]-1H-indol-3-yl]methyl]amino]ethyl]amino]methyl]-(4H-1-Benzopyran-4-one), said TNF superfamily member polypeptide is not TNF-alpha, and

b) a dominant negative TNF superfamily member polypeptide or fragment thereof, preferably having a dominant negative mutation in the trimerization domain.

2. The method according to claim 1, wherein said compound that binds to said TNF superfamily member polypeptide is selected from PRA224, PRA828, PRA123, PRA333, PRA738, and T23.

3. A method for inhibiting osteoclast formation or decreasing bone loss in an individual, comprising administering to an individual in need thereof a therapeutically effective amount of a compound that inhibits trimerization of RANKL selected from,

- a) a compound that binds to said TNF superfamily member polypeptide in the F beta-strand of said polypeptide, preferably at the glycine residue that corresponds to position 279 in human RANKL, and

-b) a dominant negative RANKL polypeptide or fragment thereof, preferably having a dominant negative mutation in the trimerization domain.

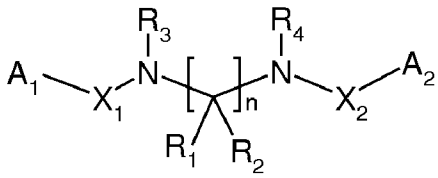
4. A method for preventing, treating, or reducing symptoms in an individual afflicted with osteoporosis, rheumatoid arthritis, multiple myeloma, bone metastasis, juvenile osteoporosis, osteogenesis imperfecta, hypercalcemia, hyperparathyroidism, osteomalacia, osteohalisteresis, osteolytic bone disease, osteonecrosis, Paget's disease of bone, bone loss due to rheumatoid arthritis, inflammatory arthritis, osteomyelitis, periodontal bone loss, bone loss due to cancer, age-related loss of bone mass, osteopenia, and inflammatory bowel syndrome,
comprising administering to a individual in need thereof a therapeutically effective amount of a compound that inhibits trimerization of RANKL selected from

- a) a compound that binds to said TNF superfamily member polypeptide in the F beta-strand of said polypeptide, preferably at the glycine residue that corresponds to position 279 in human RANKL, and

-b) a dominant negative RANKL polypeptide or fragment thereof, preferably having a dominant negative mutation in the trimerization domain.

5. The method according to claims 3 or 4, wherein said RANKL polypeptide or fragment thereof comprises a mutation in the F beta-strand, preferably at the glycine residue that corresponds to position 279 in human RANKL.

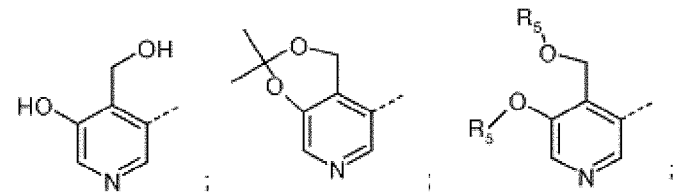
6. The method according to any one of claims 1, 3, or 4, wherein said compound that binds to said TNF superfamily member polypeptide is a compound of formula 1, or a stereoisomer thereof, tautomer thereof, or mixture thereof in any ratio; a pharmaceutically acceptable salt, pharmaceutically acceptable solvate, or pharmaceutically acceptable polymorph thereof;

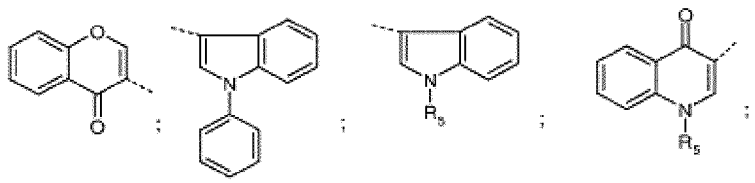


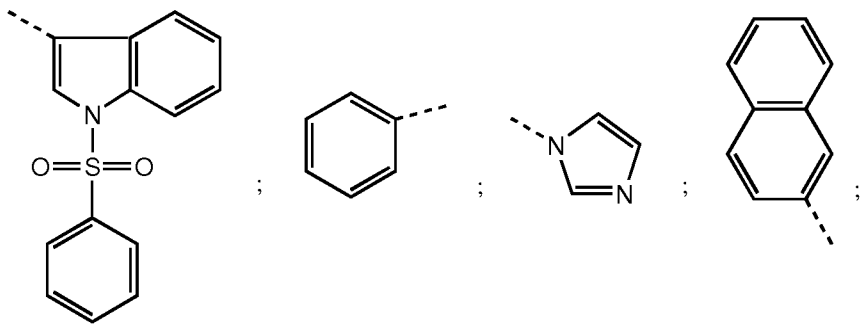
Formula 1

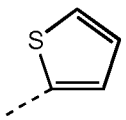
wherein:

A_1 and A_2 are independently a substituted or unsubstituted heterocyclic system selected from;









10

wherein the dotted line indicates the point of attachment, R_5 is hydrogen or (C_1-C_4)- alkyl group and the rings of the heterocyclic systems herein above are unsubstituted or substituted with one or more groups selected from (C_1-C_4)-alkyl, (C_1-C_4)-alkoxy, hydroxyl, hydroxy-(C_1-C_4)-alkyl (e.g., hydroxymethyl or 1-hydroxyethyl or 2-hydroxyethyl), fluoroalkyl (e.g., CF_3), halide (e.g. fluoro); nitro (NO_2) and amino (NH_2);

X_1 and X_2 are independently a carbonyl group or a methylene (-CH_2-) group; n is an integer from 2-4;

R_1 and R_2 are independently, hydrogen or (C_1-C_4)-alkyl group;

R_3 and R_4 are independently, hydrogen or (C_1-C_4)-alkyl group;

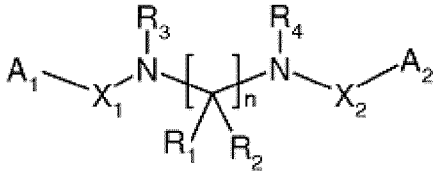
or wherein R_3 and R_4 are a single (C_1-C_8)-hydrocarbon group connecting the two nitrogen atoms of formula 1, which group may be selected from saturated hydrocarbon (*e.g.* C_2H_4) and aromatic hydrocarbon (*e.g.* phenyl).

7. The method of claim 6, wherein said compound is 6,7-Dimethyl-3-[[methyl[2-[methyl[[1-[3-(trifluoromethyl)phenyl]-1H-indol-3-yl]methyl]amino]ethyl]amino]methyl]-(4H-1-Benzopyran-4-one) or a functional derivative thereof.

8. The method according to any one of claims 1, 3, or 4, wherein said compound that binds to said TNF superfamily member polypeptide is a compound as depicted in Figure 23, preferably compound 1 of Figure 23.

9. A compound selected from PRA224, PRA828, PRA123, PRA333, and PRA738.

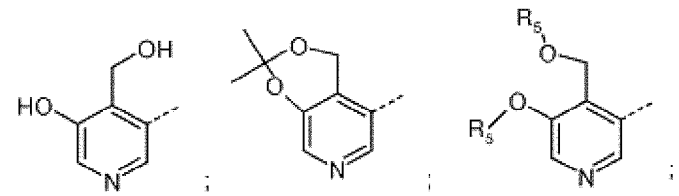
10. A compound having formula 1

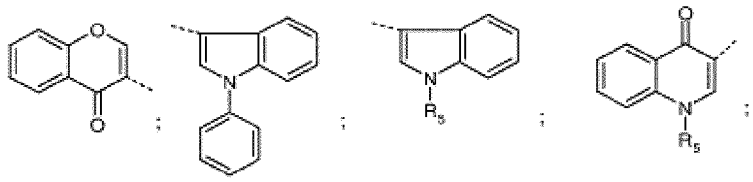


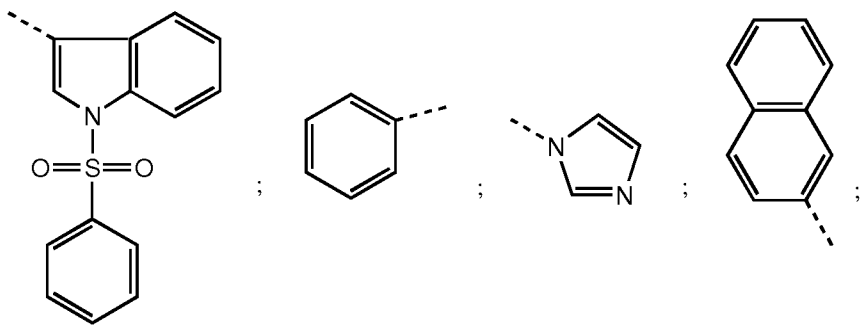
Formula 1

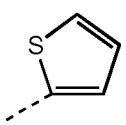
wherein:

A_1 and A_2 are independently a substituted or unsubstituted heterocyclic system selected from;









;

10

wherein the dotted line indicates the point of attachment, R_5 is hydrogen or (C_1-C_4)- alkyl group and the rings of the heterocyclic systems herein above are unsubstituted or substituted with one or more groups selected from (C_1-C_4)-alkyl, (C_1-C_4)-alkoxy, hydroxyl, hydroxy-(C_1-C_4)-alkyl (e.g., hydroxymethyl or 1-hydroxyethyl or 2-hydroxyethyl), fluoroalkyl (e.g., CF_3), halide (e.g. fluoro); nitro (NO_2) and amino (NH_2);

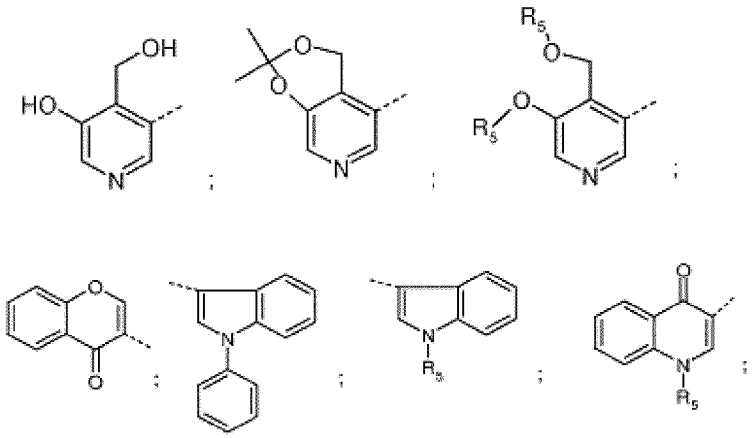
X_1 and X_2 are independently a carbonyl group or a methylene (-CH_2-) group; n is an integer from 2-4;

R_1 and R_2 are independently, hydrogen or (C_1-C_4)-alkyl group;

R_3 and R_4 are independently, hydrogen or (C_1-C_4)-alkyl group;

or wherein R_3 and R_4 are a single (C_1-C_8)-hydrocarbon group connecting the two nitrogen atoms of formula 1, which group may be selected from saturated hydrocarbon (*e.g.* C_2H_4) and aromatic hydrocarbon (*e.g.* phenyl);

with the proviso that when A_1 and A_2 are both selected from;



then at least one of the heterocyclic systems is substituted with one or more groups selected from halide (e.g. fluoro); nitro (NO_2) and amino (NH_2).

11. A compound according to claim wherein the heterocyclic systems are unsubstituted or substituted with one or more groups selected from trifluoromethyl (CF_3), fluoro (F); nitro (NO_2) and amino (NH_2).

12. A TNF superfamily member polypeptide or fragment thereof that inhibits trimerization of said TNF superfamily member, preferably said polypeptide or fragment thereof having a dominant negative mutation in the trimerization domain.

13. The TNF superfamily member polypeptide or a functional fragment thereof according to claim 12, comprising a mutation in F beta-strand, preferably in the glycine residue that corresponds to position 279 in human RANKL.

14. The TNF superfamily member polypeptide or a functional fragment thereof according to claim 13, comprising an amino acid sequence having at least 80% sequence identity to K L E A Q P F A H L T I N A T D I P S G S H K V S L S S W Y H D R G W A K I S N M T F S N G K L I V N Q D G F Y Y L Y A N I C F R H H E T S G D L A T E Y L Q L M V Y V T K T S I K I P S S H T L M K G G S T K Y W S G N S E F H F Y S I N V G X F F K L R S G E E I S I E V S N P S L L D P D Q D A T Y F G A F K V R D I D (SEQ ID NO:3), wherein X is not glycine.

15. An isolated nucleic acid encoding the TNF superfamily member polypeptide or fragment thereof according to any one of claims 12-14.

16. A non-human animal comprising a nucleic acid encoding the TNF superfamily member polypeptide or fragment thereof according to any one of claims 12-14.

17. A vector comprising the nucleic acid according to claim 15.

18. A cell comprising the vector according to claim 17.

19. A pharmaceutical composition comprising the TNF superfamily member polypeptide or fragment thereof according to any one of claims 12-14 or a compound according to any one of claims 9-11 and a pharmaceutically acceptable carrier.

20. A liposome comprising the TNF superfamily member polypeptide or fragment thereof according to claim 9-11.

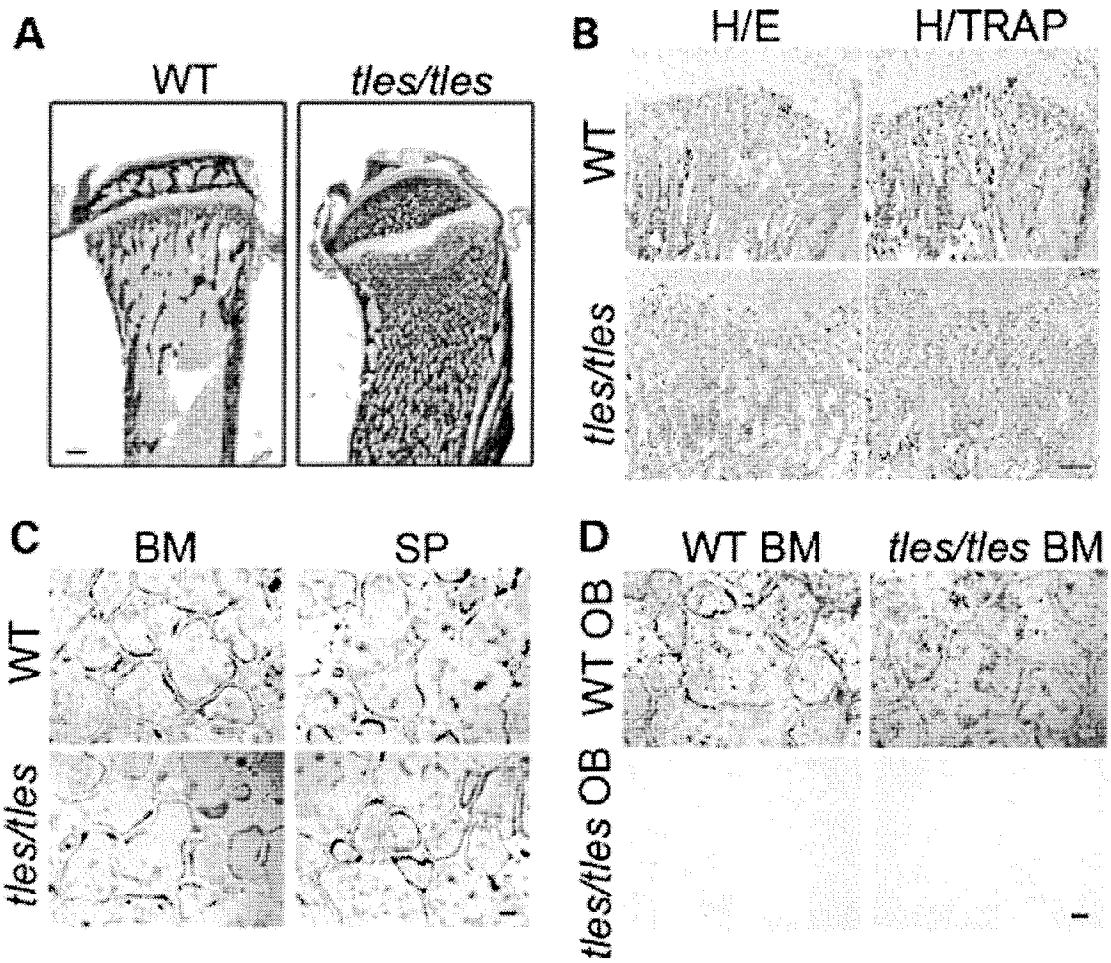

A
WT
tles/tles
B
H/E
H/TRAP
WT
tles/tles
C
BM
SP
WT
tles/tles
D
WT BM
tles/tles BM
WT OB
tles/tles OB

Fig. 1

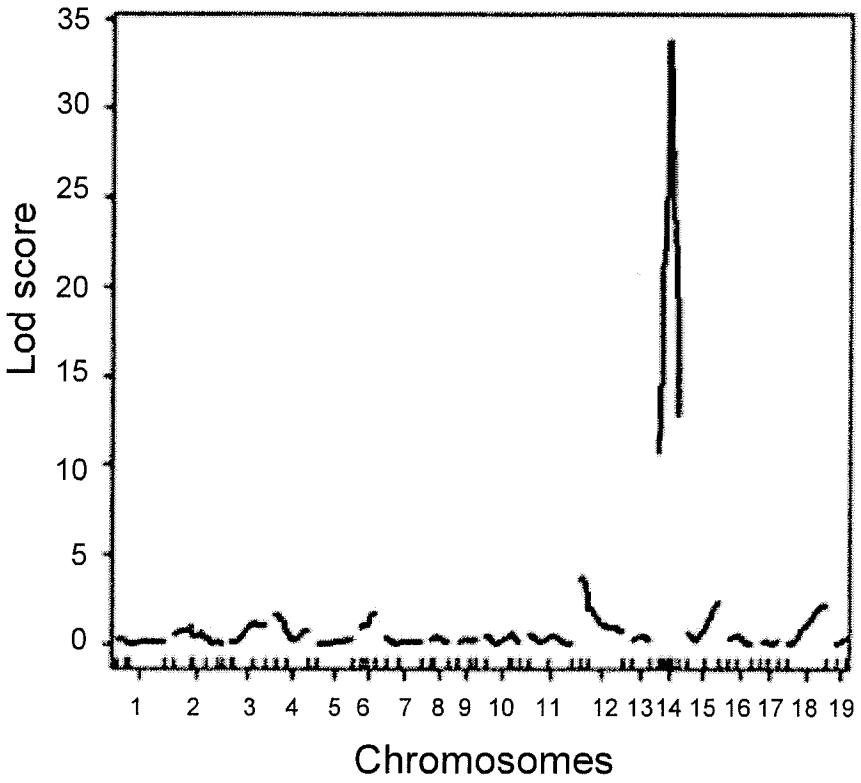

Lod score
35
30
25
20
15
10
5
0
1 2 3 4 5 6 7 8 9 10 11 12 13 14 15 16 17 18 19
Chromosomes

Fig. 2A

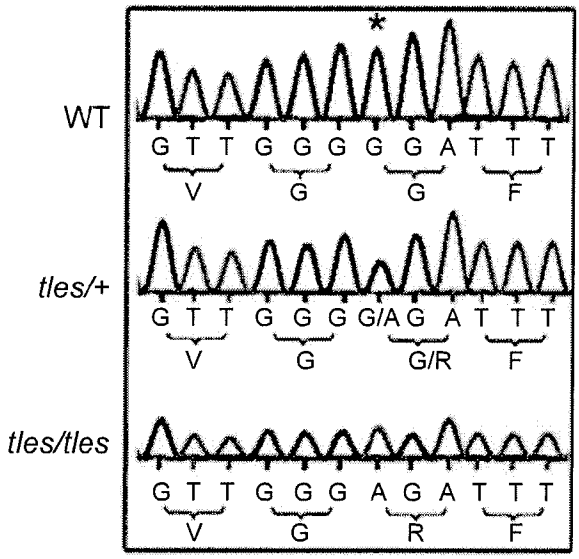

*
WT
G T T G G G G G A T T T
V G G F
tles/+
G T T G G G G/A G A T T T
V G G/R F
tles/tles
G T T G G G A G A T T T
V G R F

Fig. 2B



Fig. 2C

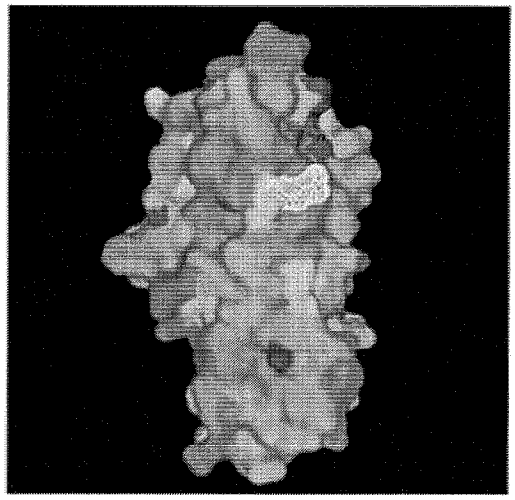


Fig. 2D

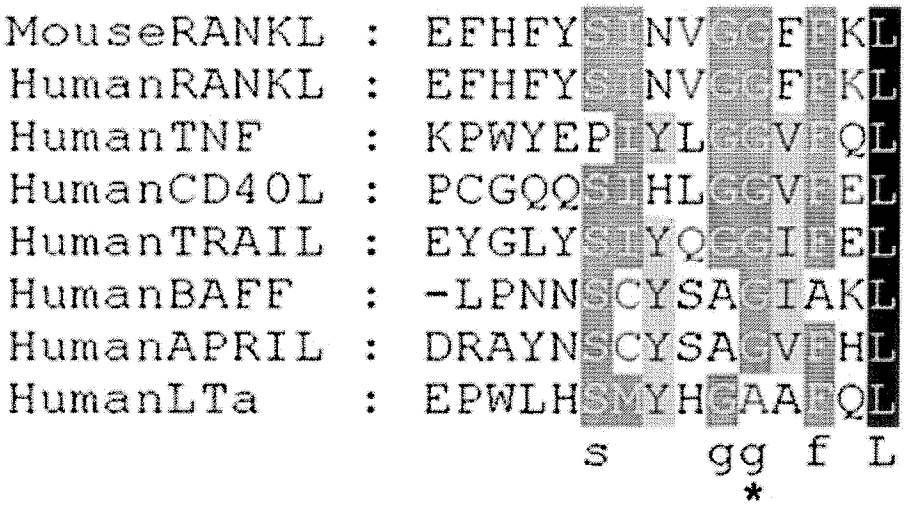


Fig. 2E

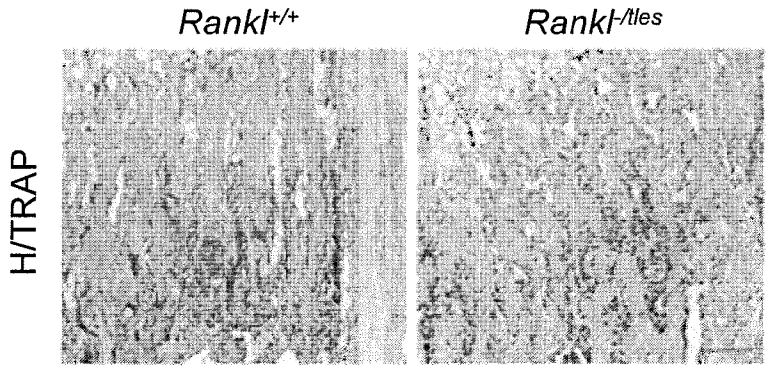


Fig. 3A

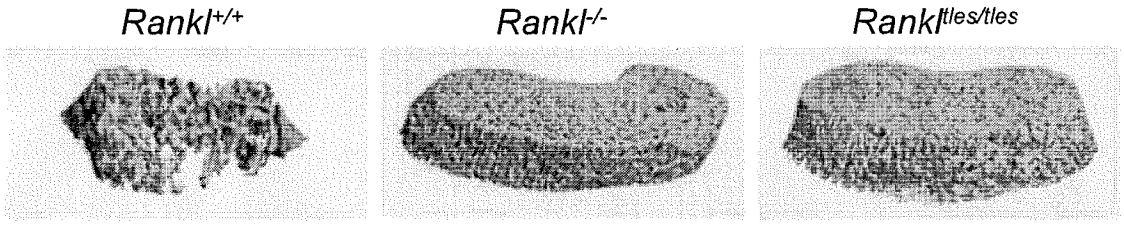


Fig. 3B

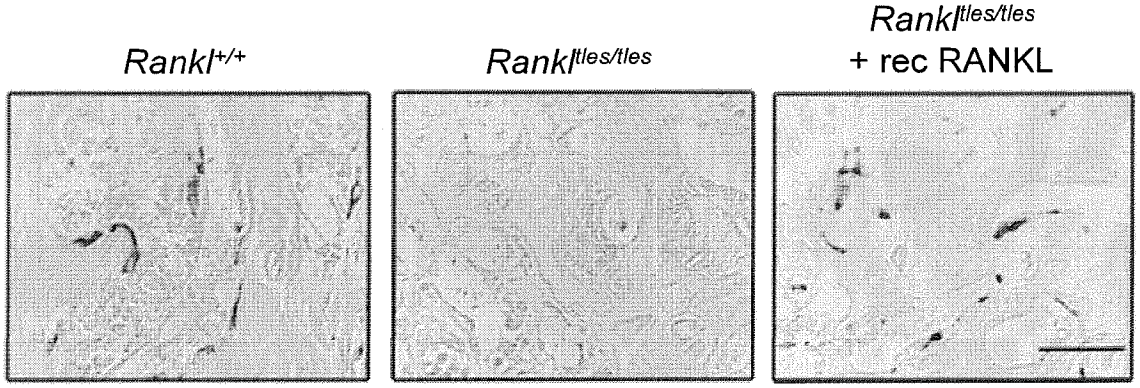


Fig. 3D

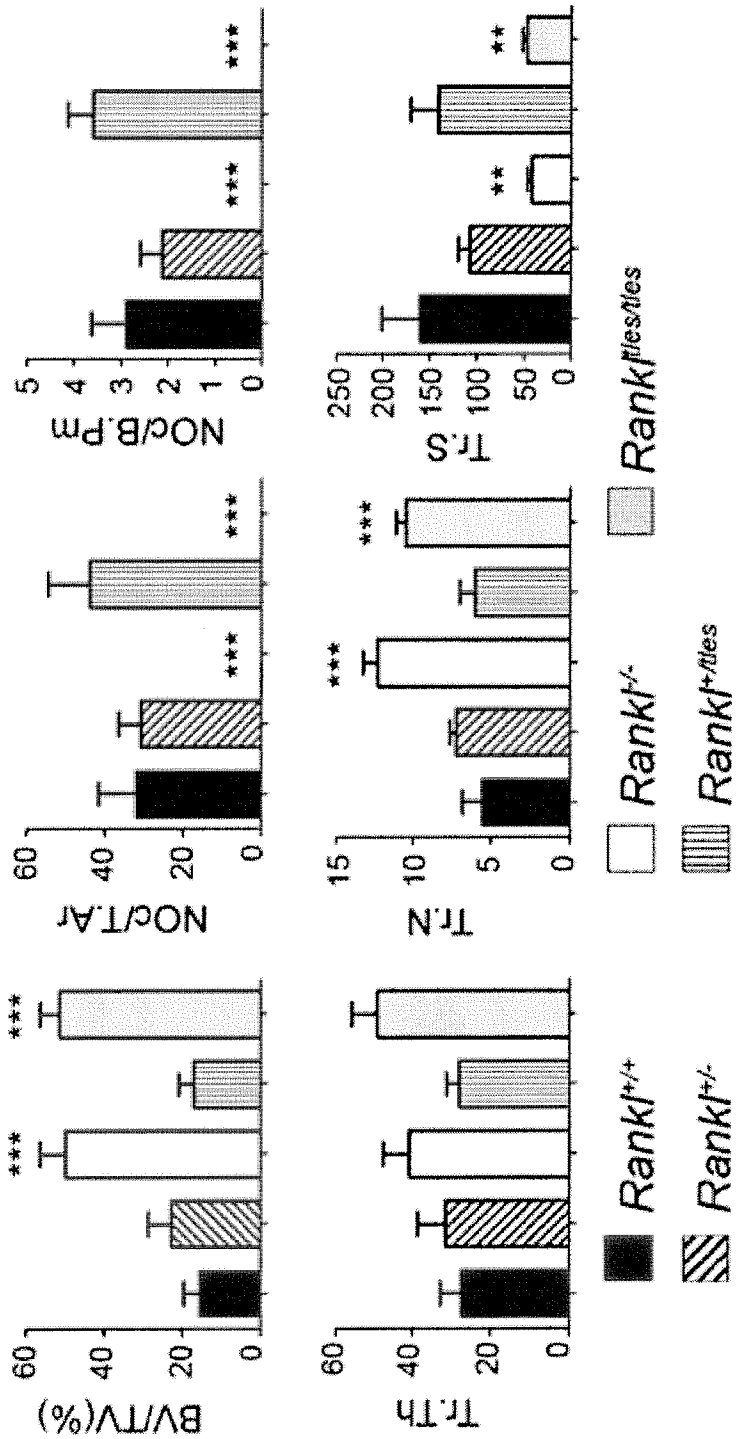

BV/TV(%)
Tr.Th
NOc/T.Ar
Tr.N
NOc/B.Pm
Tr.S
Rankl+/+
Rankl+/-
Rankl-/-
Rankltles/tles
Rankl+/tles

Fig. 3C

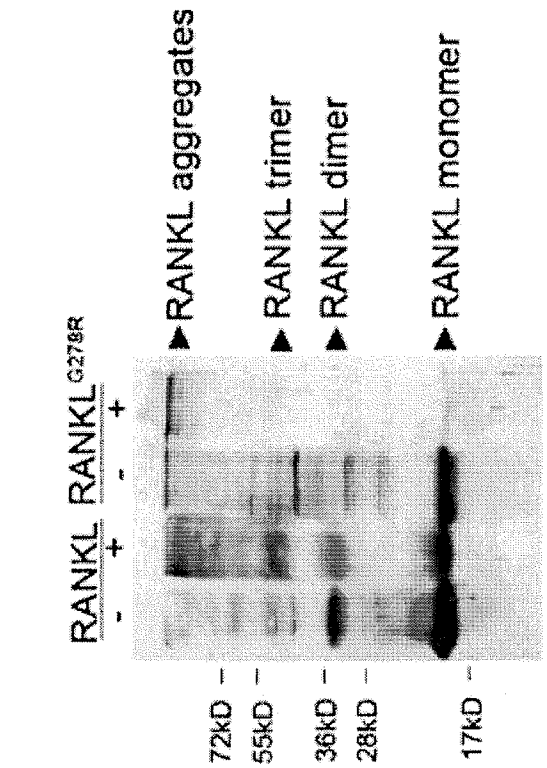

RANKL aggregates
RANKL trimer
RANKL dimer
RANKL monomer
RANKL
RANKL G278R
- + - +
72kD
55kD
36kD
28kD
17kD

Fig. 4B

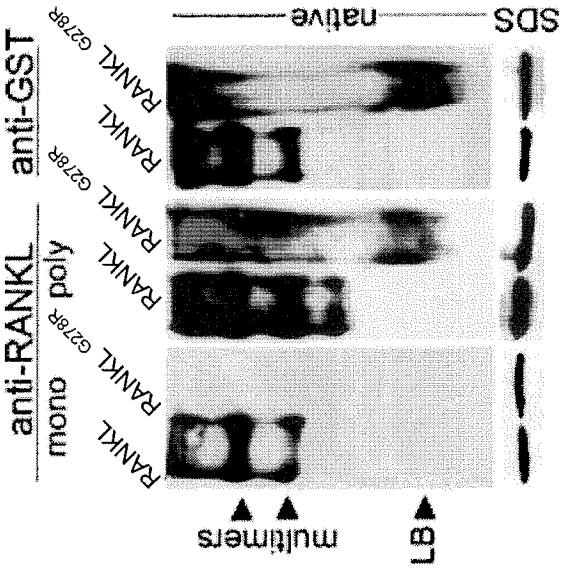

native
SDS
anti-GST
anti-RANKL
mono
poly
RANKL
RANKL G278R
multimers
LB

Fig. 4A

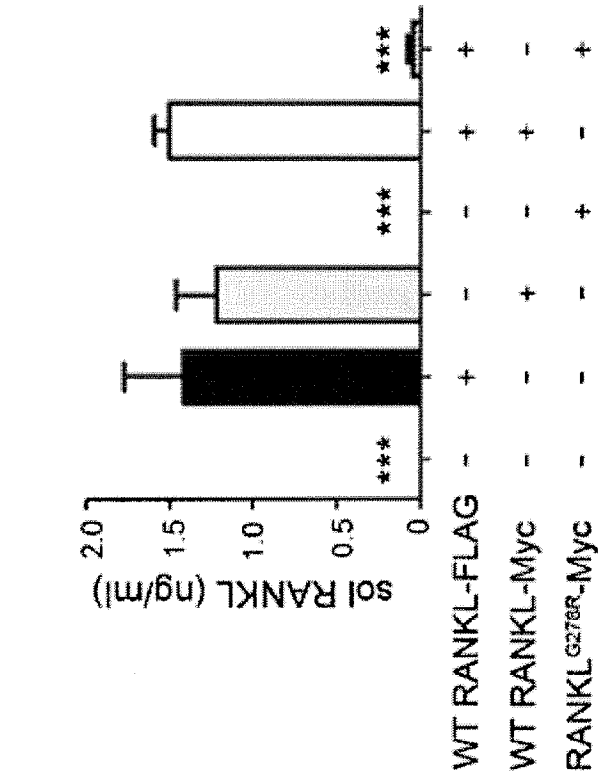

sol RANKL (ng/ml)
2.0
1.5
1.0
0.5
0
***
***
***
WT RANKL-FLAG
WT RANKL-Myc
RANKL G278R-Myc

Fig. 4D

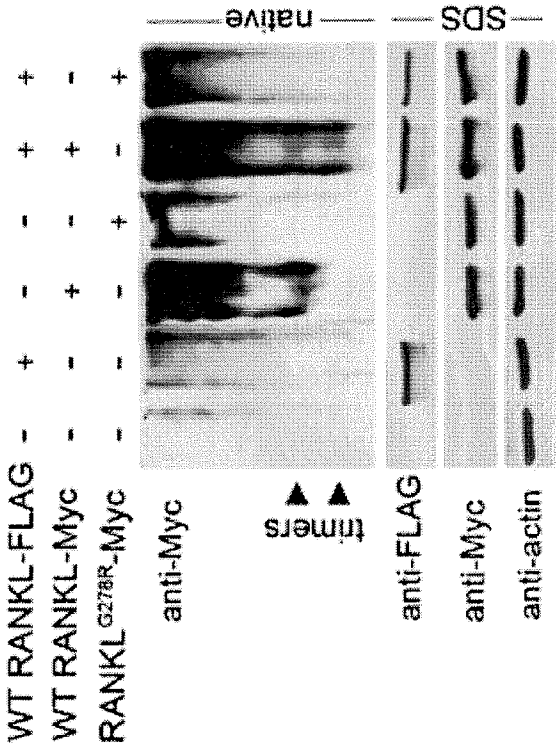

native
SDS
WT RANKL-FLAG
WT RANKL-Myc
RANKL G278R-Myc
anti-Myc
trimers
anti-FLAG
anti-Myc
anti-actin

Fig. 4C

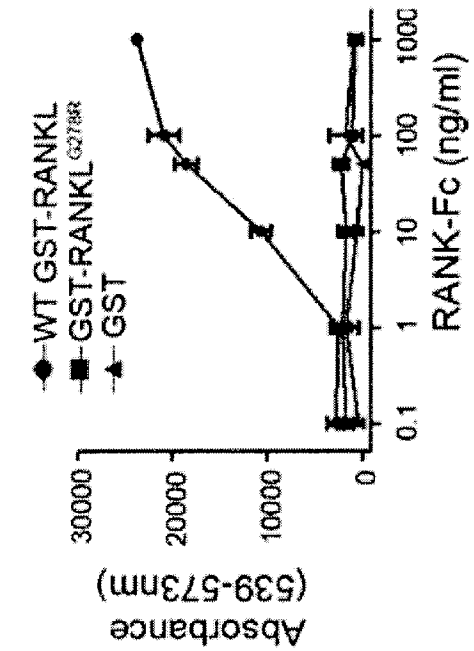

WT GST-RANKL
GST-RANKL G278R
GST
Absorbance (539-573nm)
30000
20000
10000
0
0.1
1
10
100
1000
RANK-Fc (ng/ml)

Fig. 4F

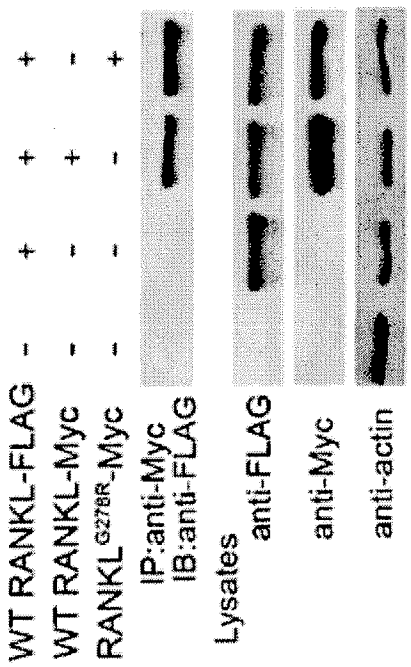

WT RANKL-FLAG
WT RANKL-Myc
RANKL G278R-Myc
IP:anti-Myc
IB:anti-FLAG
Lysates
anti-FLAG
anti-Myc
anti-actin

Fig. 4E

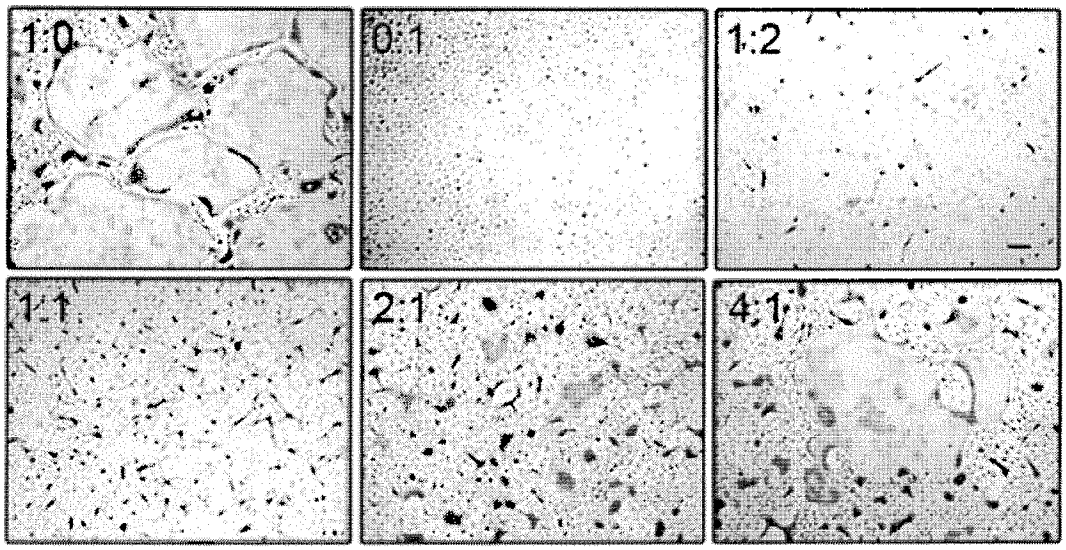


Fig. 5A

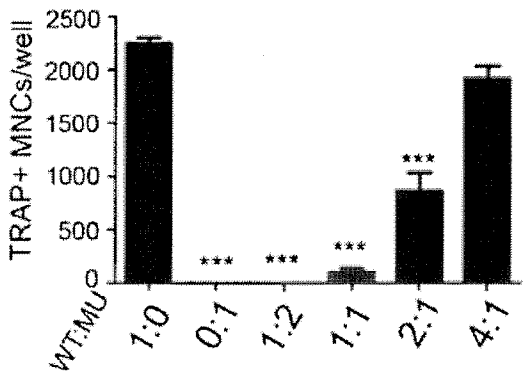


Fig. 5B

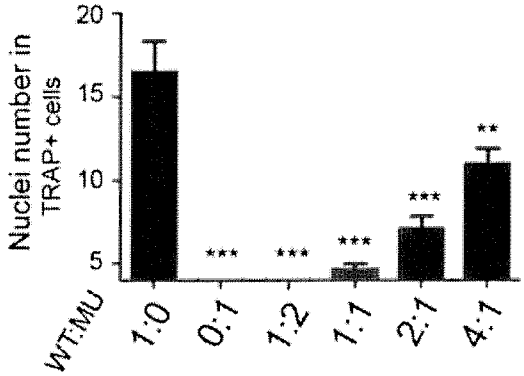


Fig. 5C

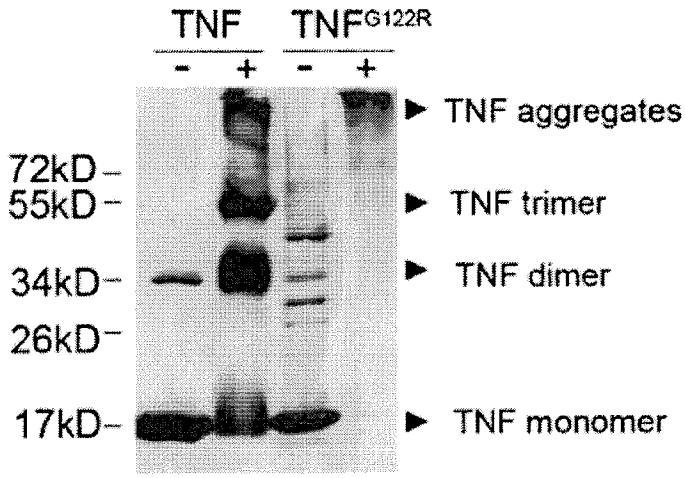


Fig. 6A

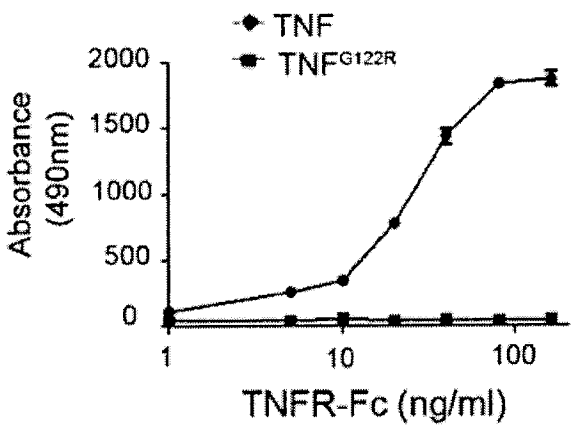


Fig. 6B

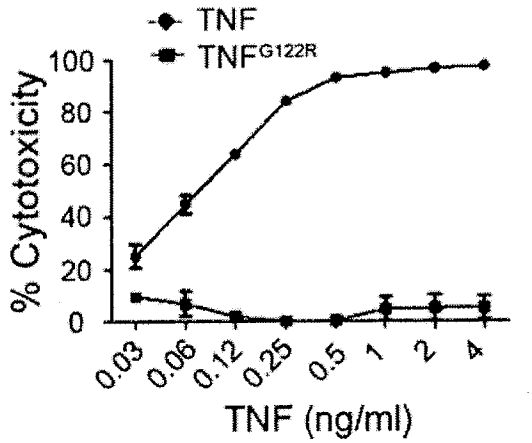


Fig. 6C

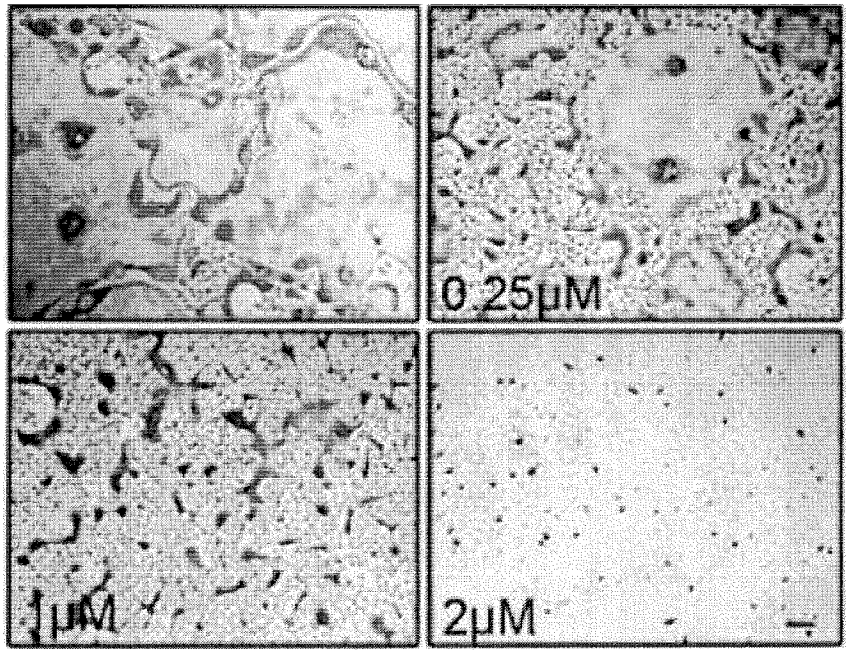


Fig. 7A

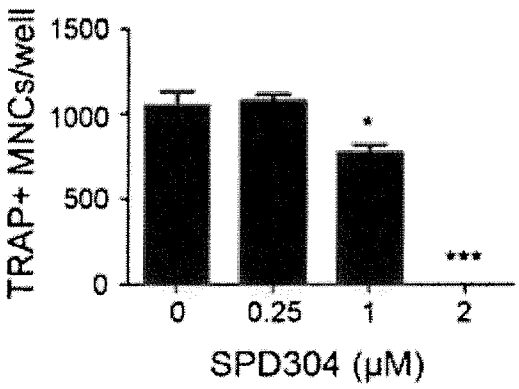


Fig. 7B

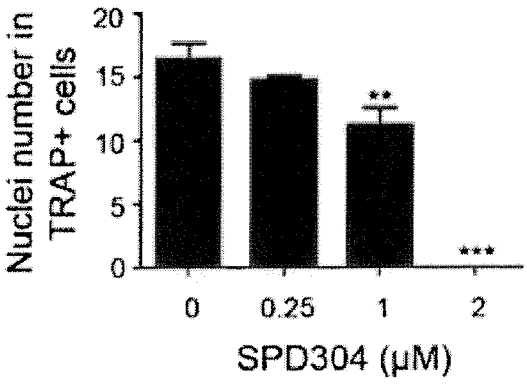


Fig. 7C

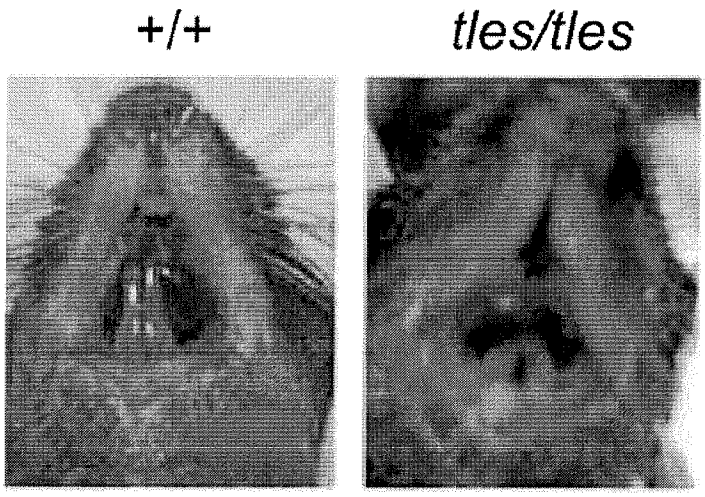

+/+
tles/tles

Fig. 8A

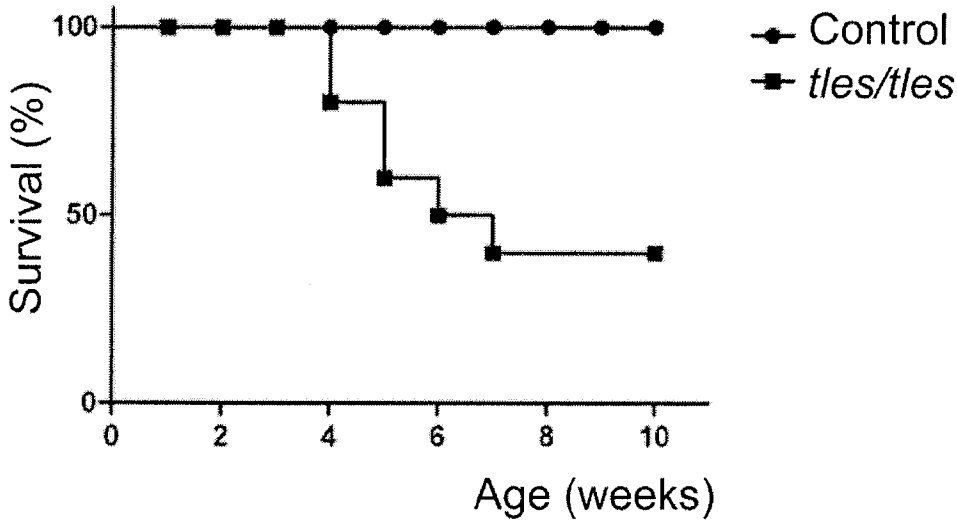

100
50
0
Survival (%)
0
2
4
6
8
10
Age (weeks)
Control
tles/tles

Fig. 8B

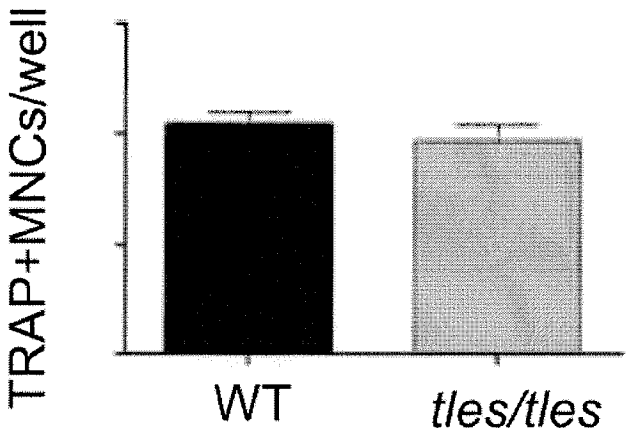

TRAP+MNCs/well
WT
tles/tles

Fig. 9A

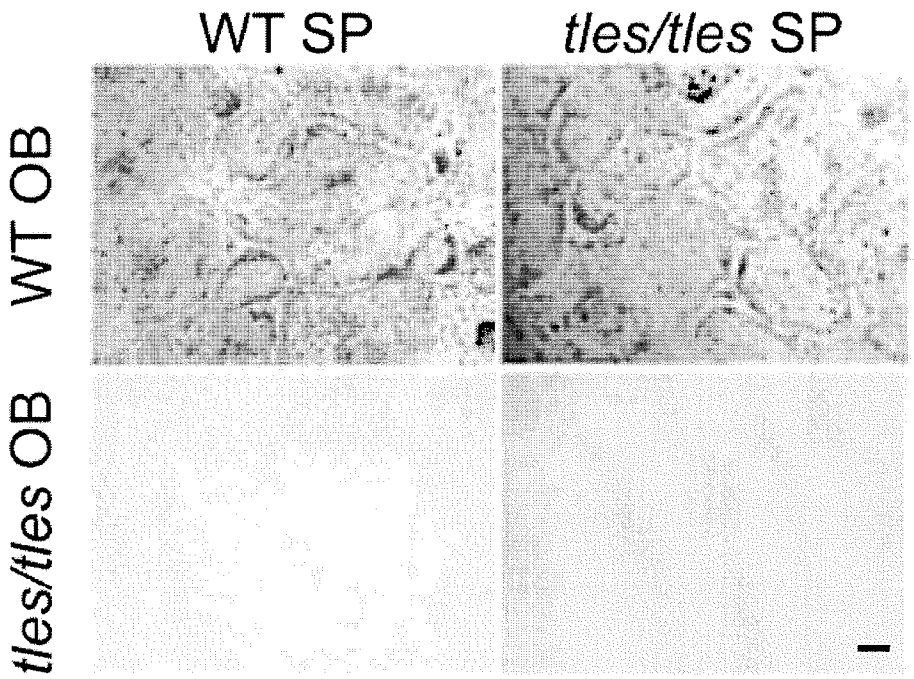

WT SP
tles/tles SP
WT OB
tles/tles OB

Fig. 9B

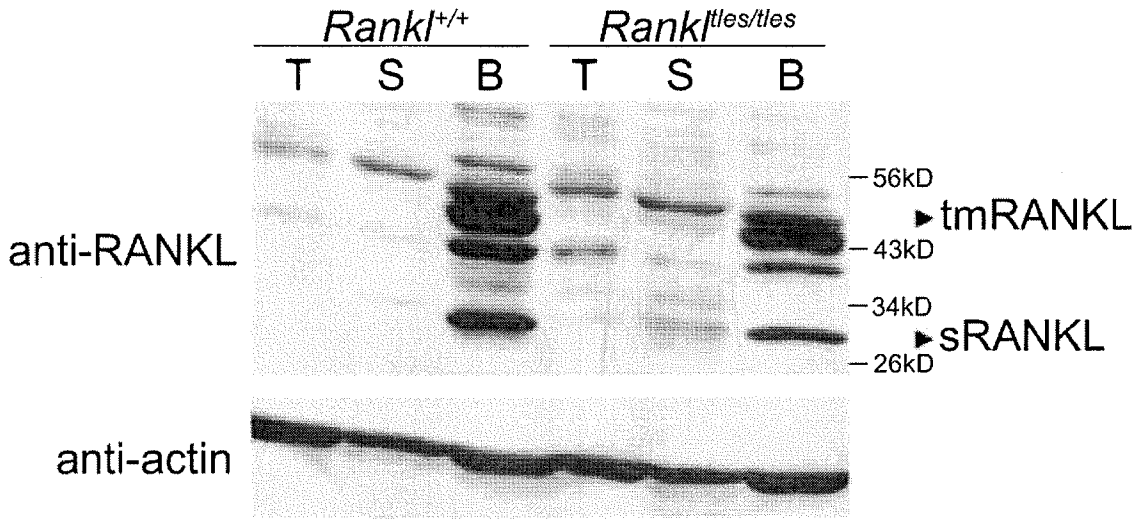

Rankl+/+
Rankltles/tles
T S B T S B
anti-RANKL
56kD
tmRANKL
43kD
34kD
sRANKL
26kD
anti-actin

Fig. 10

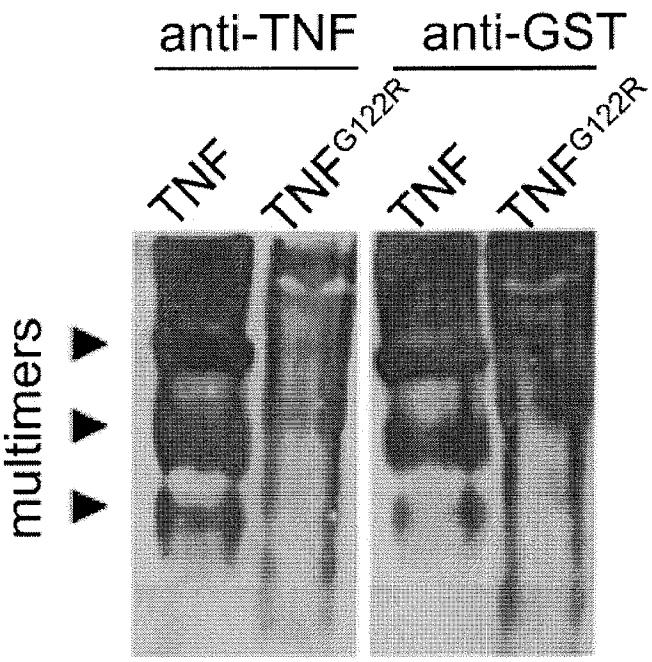

anti-TNF
anti-GST
TNF
TNFG122R
TNF
TNFG122R
multimers

Fig. 11

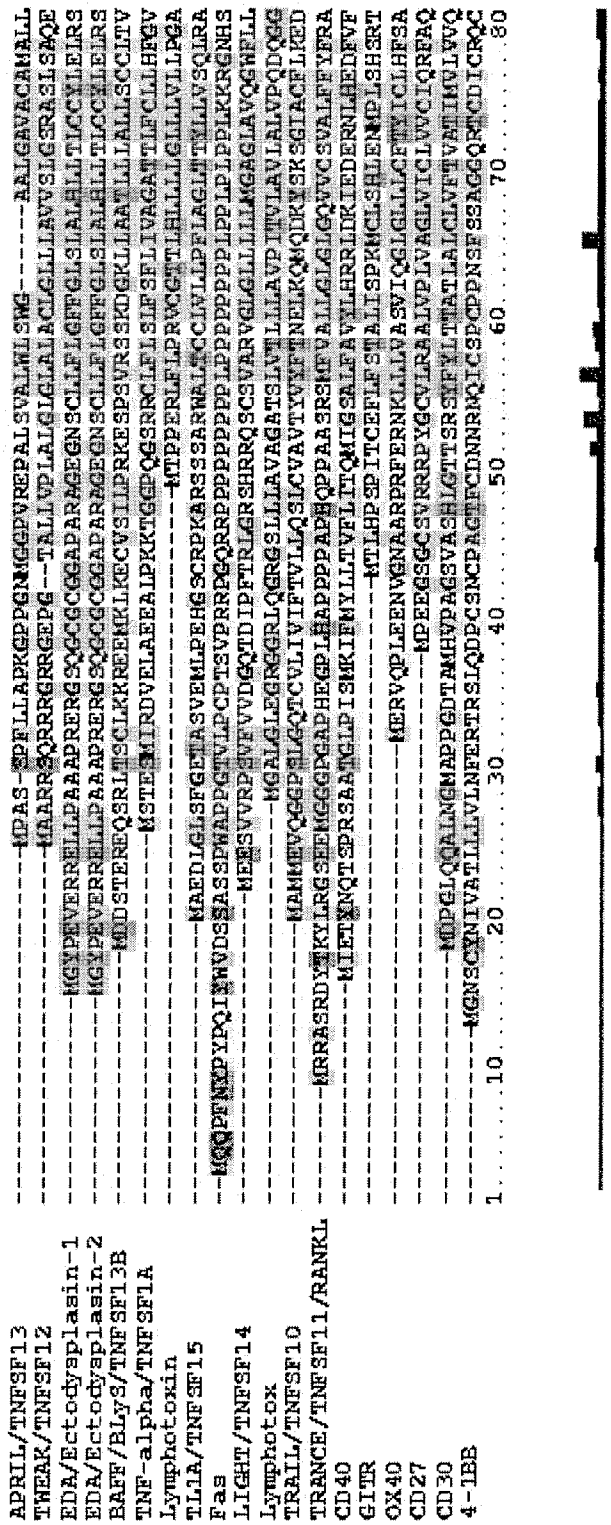


Fig. 12

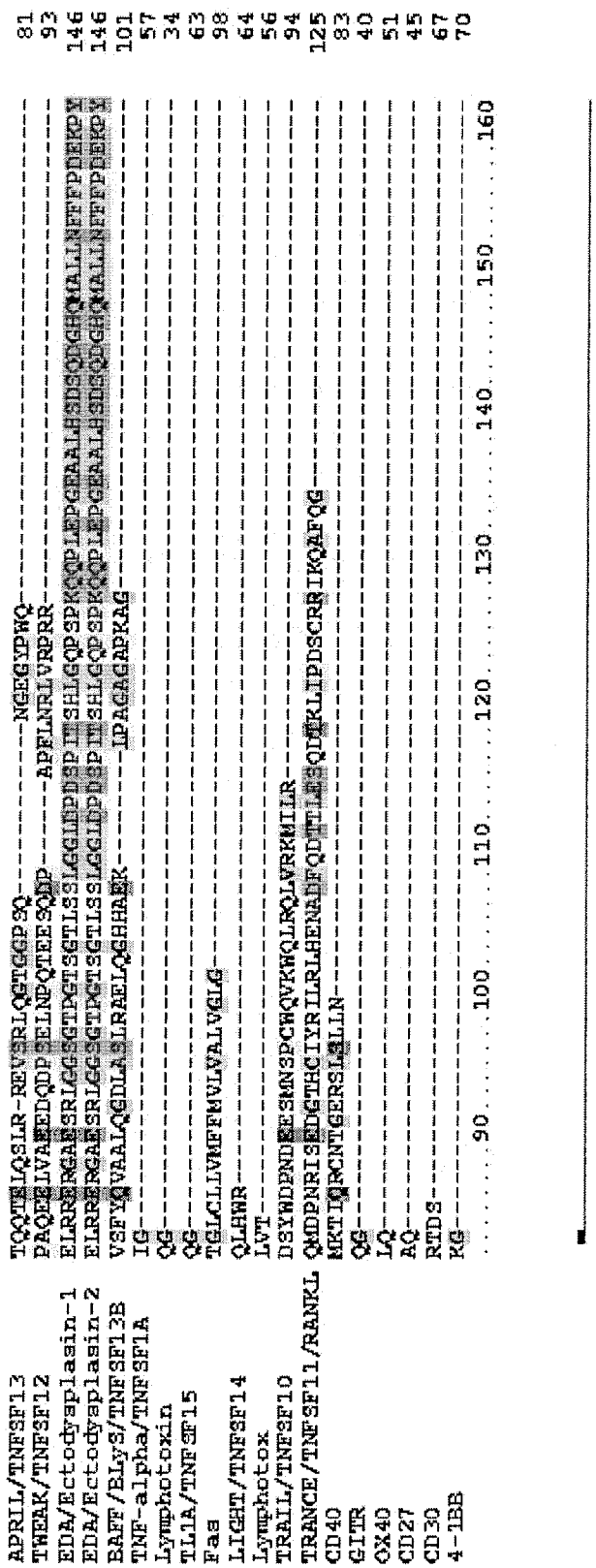

APRIL/TNFSF13
TWEAK/TNFSF12
EDA/Ectodysplasin-1
EDA/Ectodysplasin-2
BAFF/BLyS/TNFSF13B
TNF-alpha/TNFSF1A
Lymphotoxin
TL1A/TNFSF15
Fas
LIGHT/TNFSF14
Lymphotox
TRAIL/TNFSF10
TRANCE/TNFSF11/RANKL
CD40
GITR
OX40
CD27
CD30
4-1BB
81
93
146
146
101
57
34
63
98
64
56
94
125
83
40
51
45
67
70
90
100
110
120
130
140
150
160

Fig. 12, cont'd

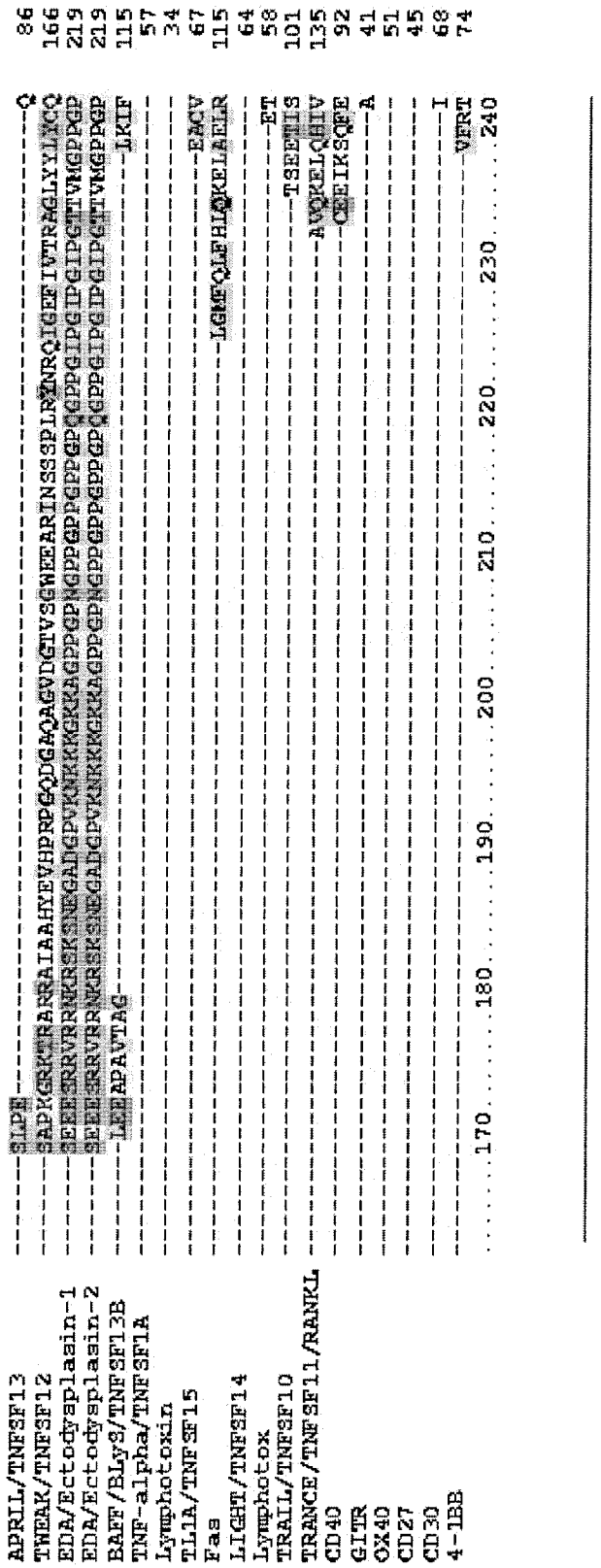

APRIL/TNFSF13
TWEAK/TNFSF12
EDA/Ectodysplasin-1
EDA/Ectodysplasin-2
BAFF/BLyS/TNFSF13B
TNF-alpha/TNFSF1A
Lymphotoxin
TL1A/TNFSF15
Fas
LIGHT/TNFSF14
Lymphotox
TRAIL/TNFSF10
TRANCE/TNFSF11/RANKL
CD40
GITR
OX40
CD27
CD30
4-1BB
170
180
190
200
210
220
230
240

Fig. 12, cont'd

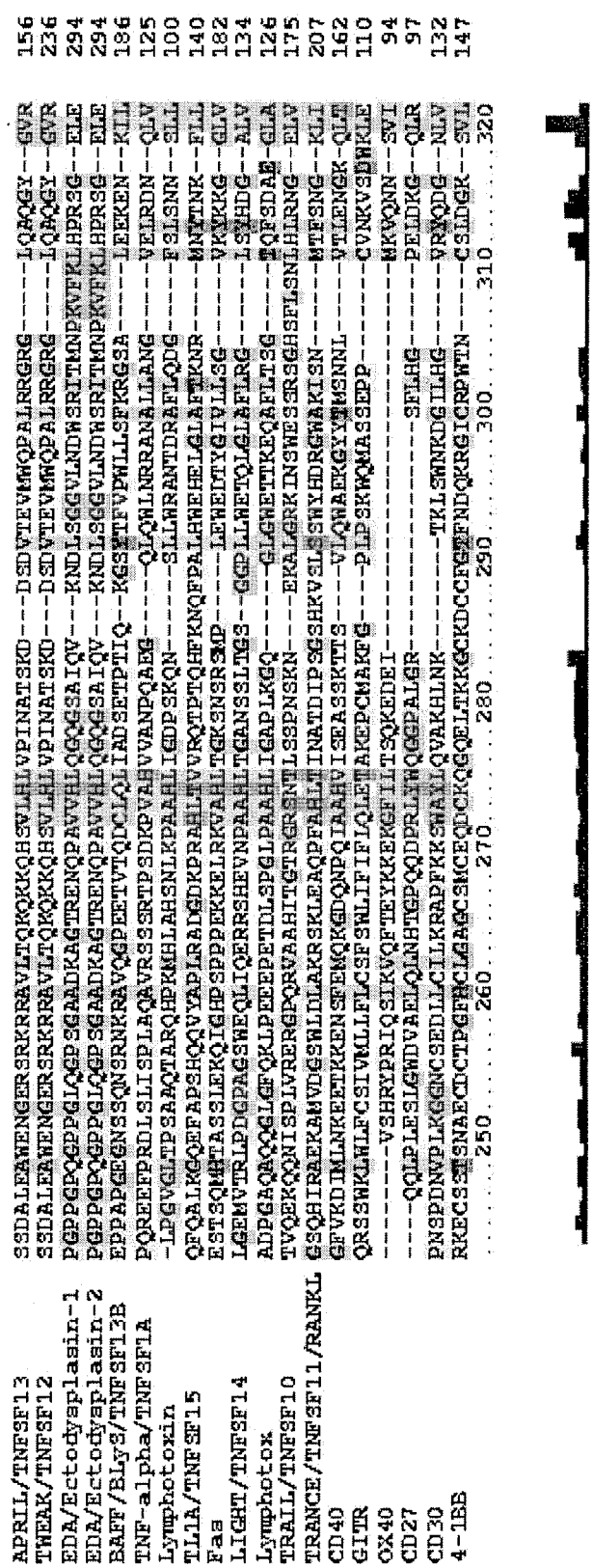


Fig. 12, cont'd

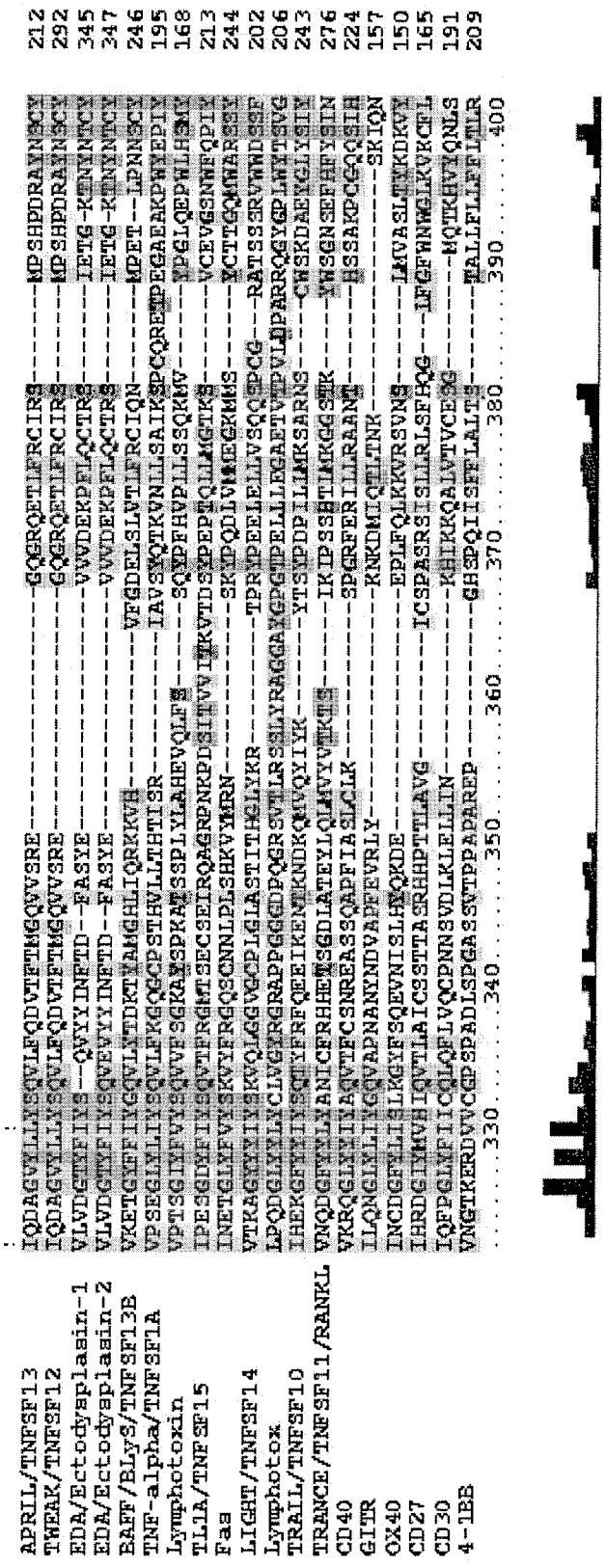


Fig. 12, cont'd

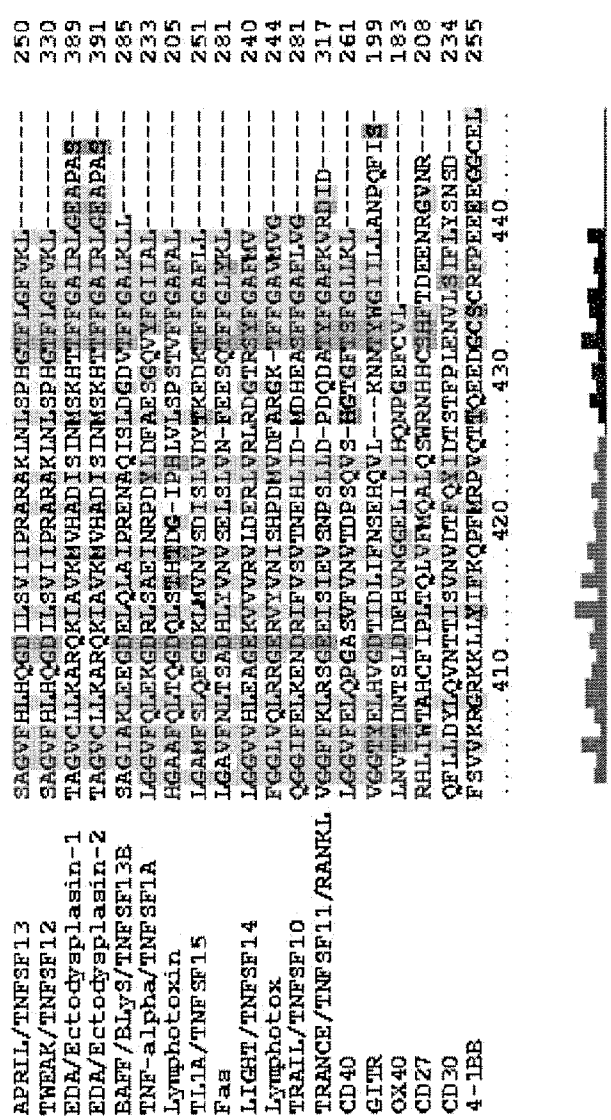


Fig. 12, cont'd

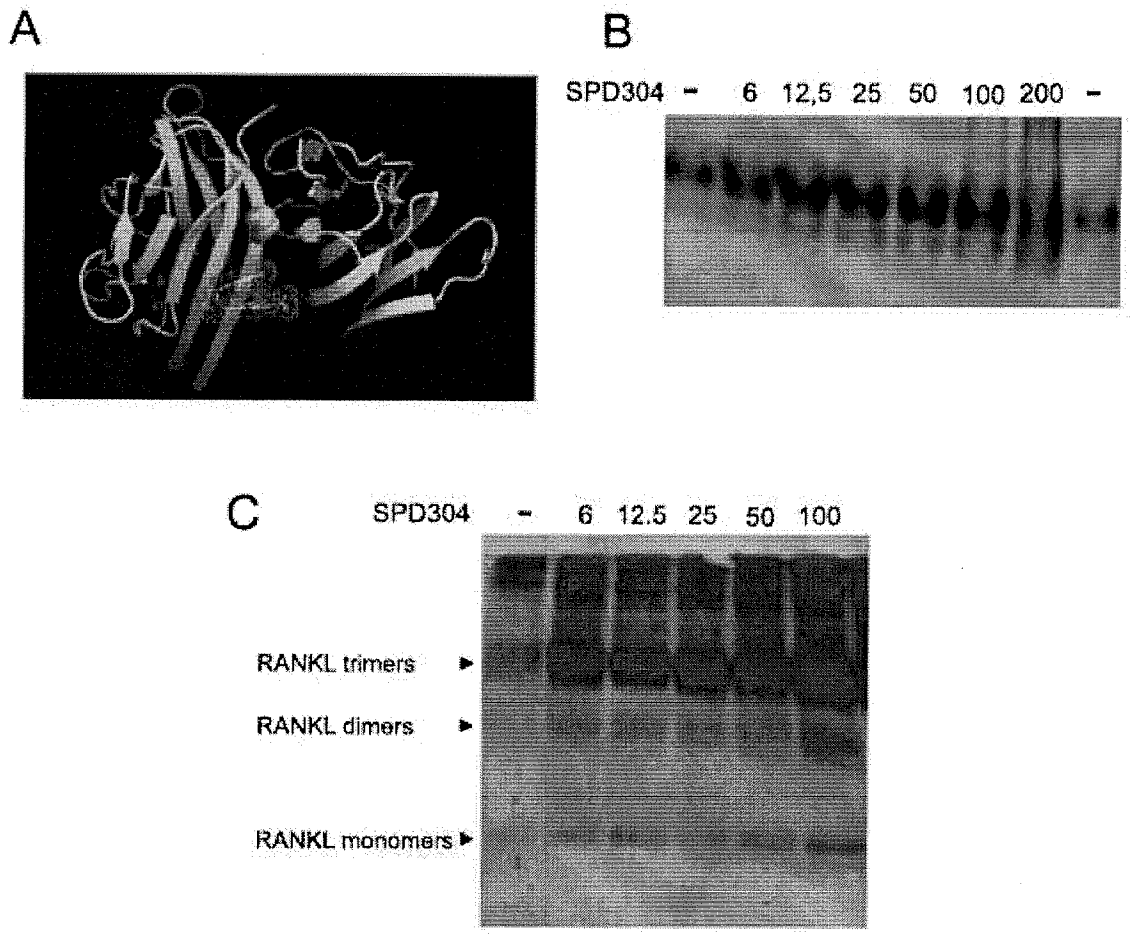

A
B
SPD304 - 6 12,5 25 50 100 200 -
C
SPD304 - 6 12.5 25 50 100
RANKL trimers
RANKL dimers
RANKL monomers

Fig. 13

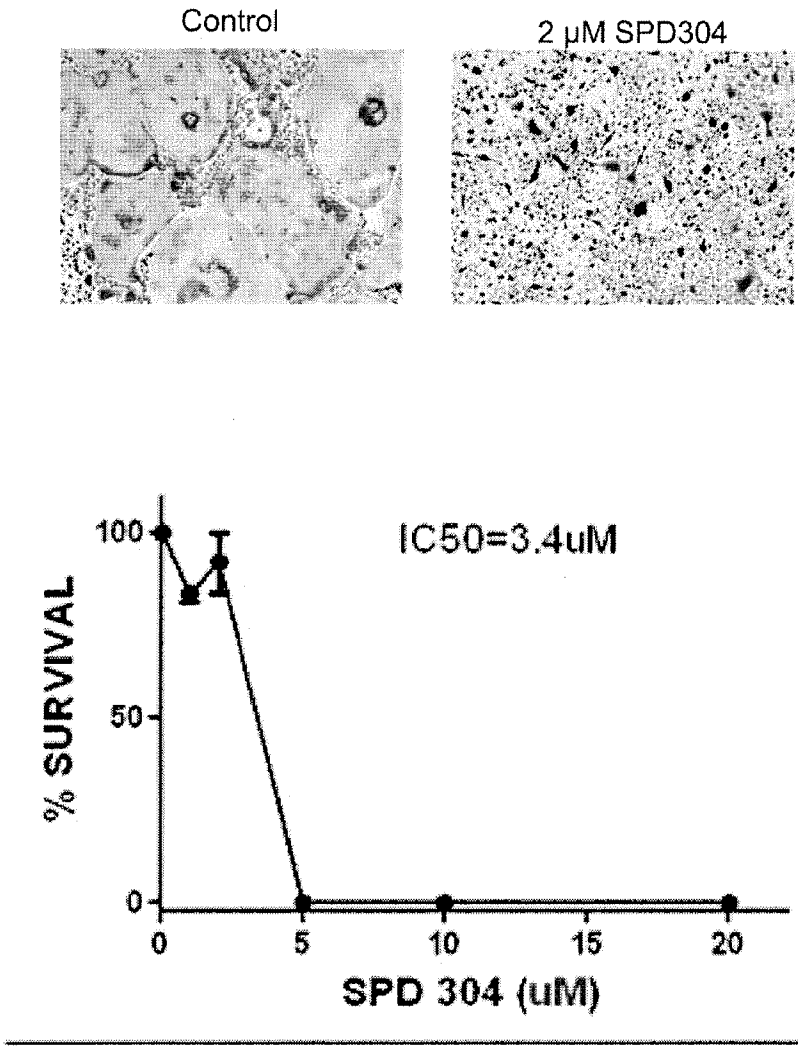

Control
2 µM SPD304
IC50=3.4uM
% SURVIVAL
100
50
0
0
5
10
15
20
SPD 304 (uM)

Fig. 14A

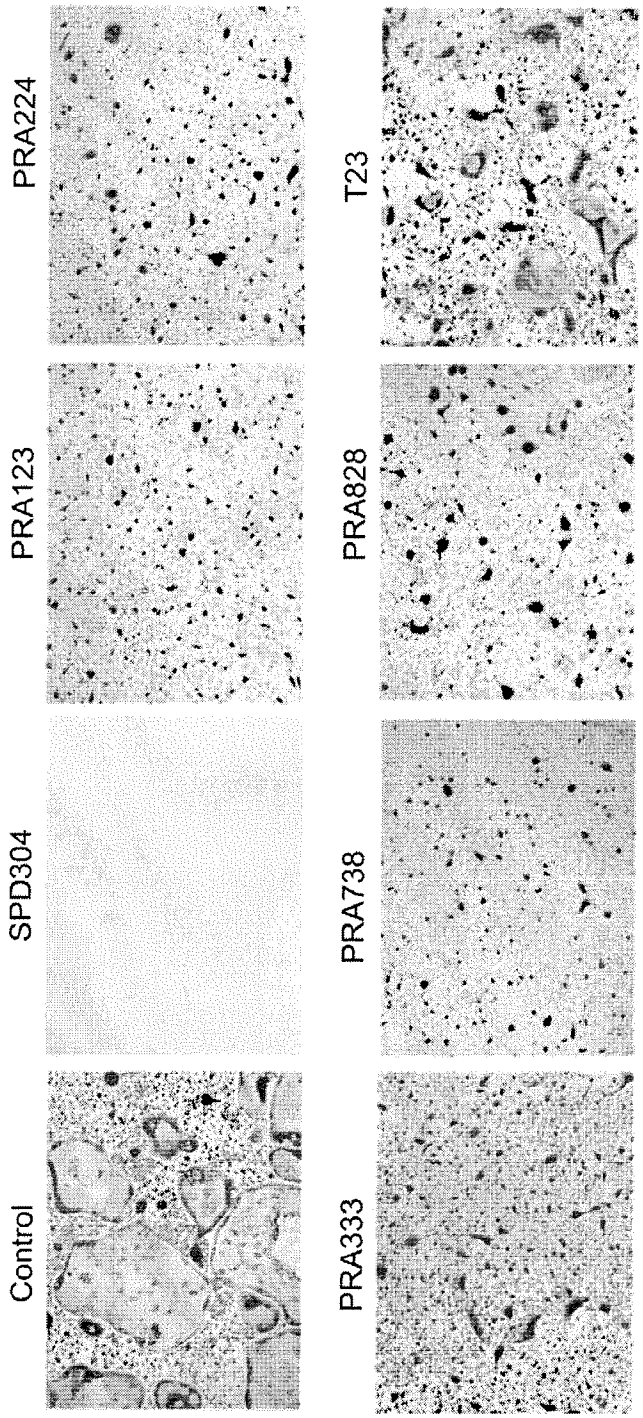


Fig. 14B

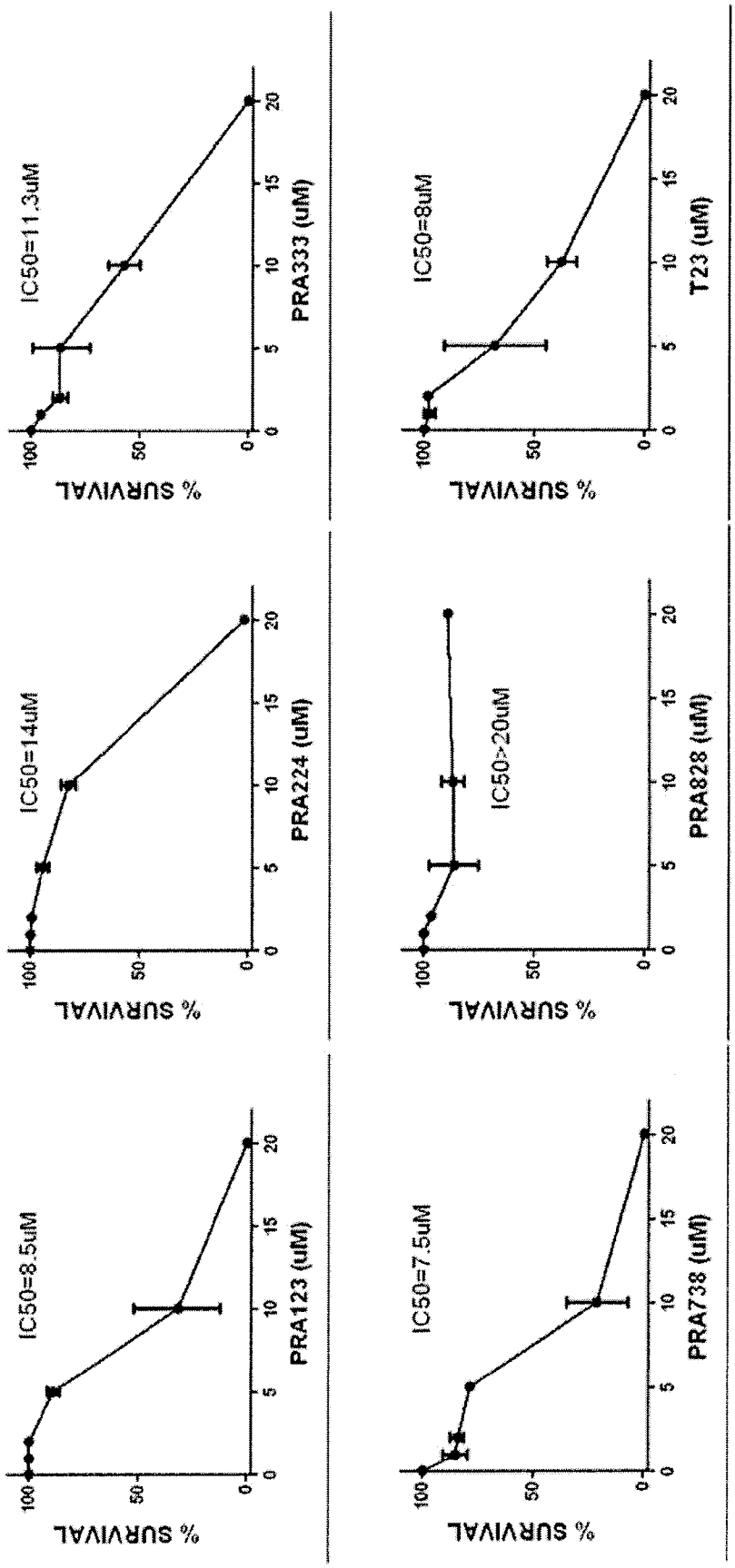

IC50=11.3uM
PRA333 (uM)
% SURVIVAL
IC50=8uM
T23 (uM)
% SURVIVAL
IC50=14uM
PRA224 (uM)
% SURVIVAL
IC50>20uM
PRA828 (uM)
% SURVIVAL
IC50=8.5uM
PRA123 (uM)
% SURVIVAL
IC50=7.5uM
PRA738 (uM)
% SURVIVAL

Fig. 14C

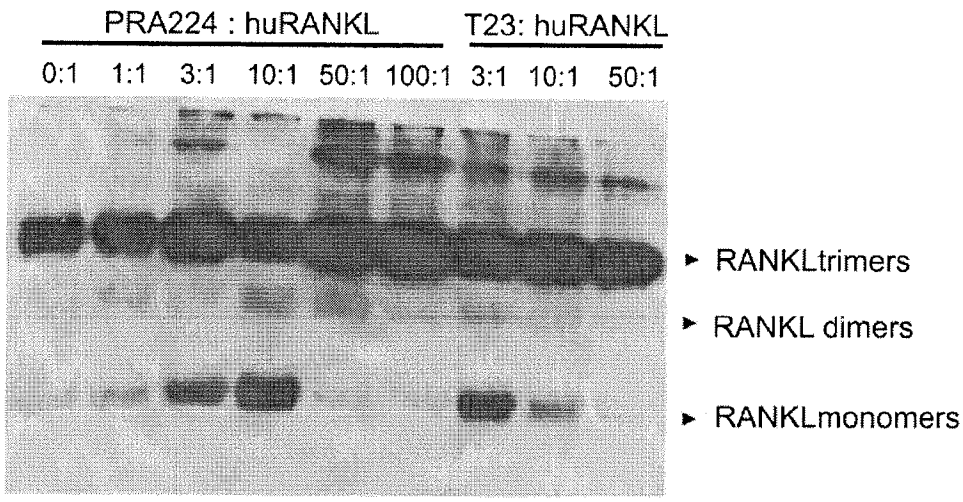

PRA224 : huRANKL
T23: huRANKL
0:1 1:1 3:1 10:1 50:1 100:1 3:1 10:1 50:1
RANKLtrimers
RANKL dimers
RANKLmonomers

Fig. 15

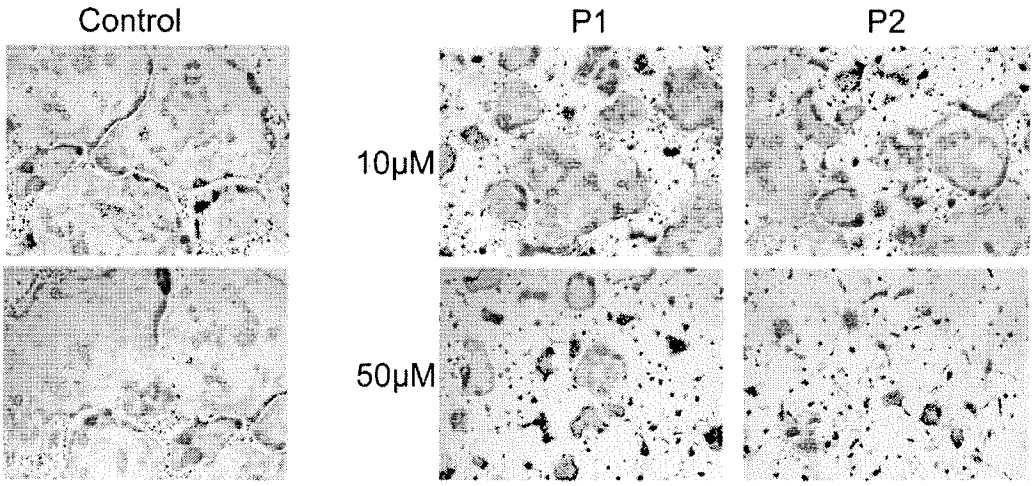


Fig. 16A

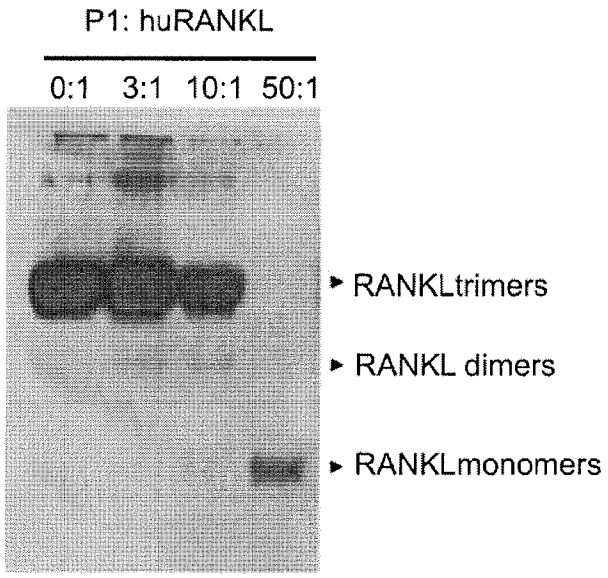


Fig. 16B

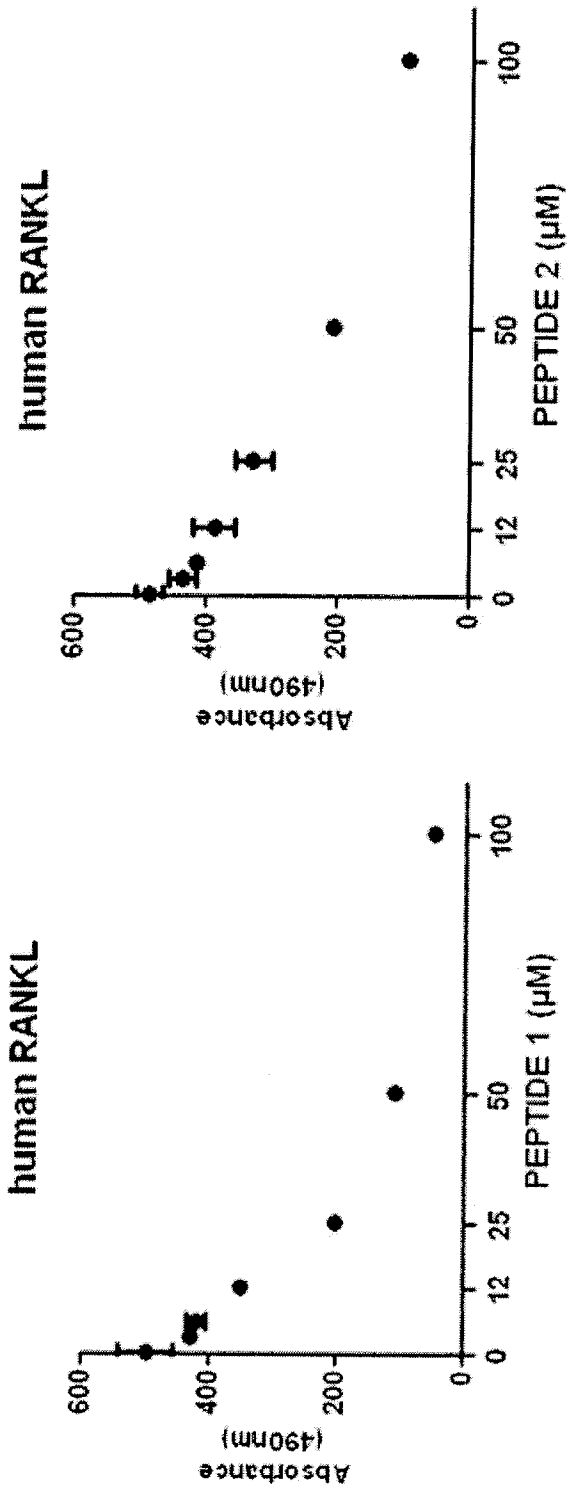

human RANKL
Absorbance (490nm)
600
400
200
0
0
12
25
50
100
PEPTIDE 1 (µM)
human RANKL
Absorbance (490nm)
600
400
200
0
0
12
25
50
100
PEPTIDE 2 (µM)

Fig. 16C

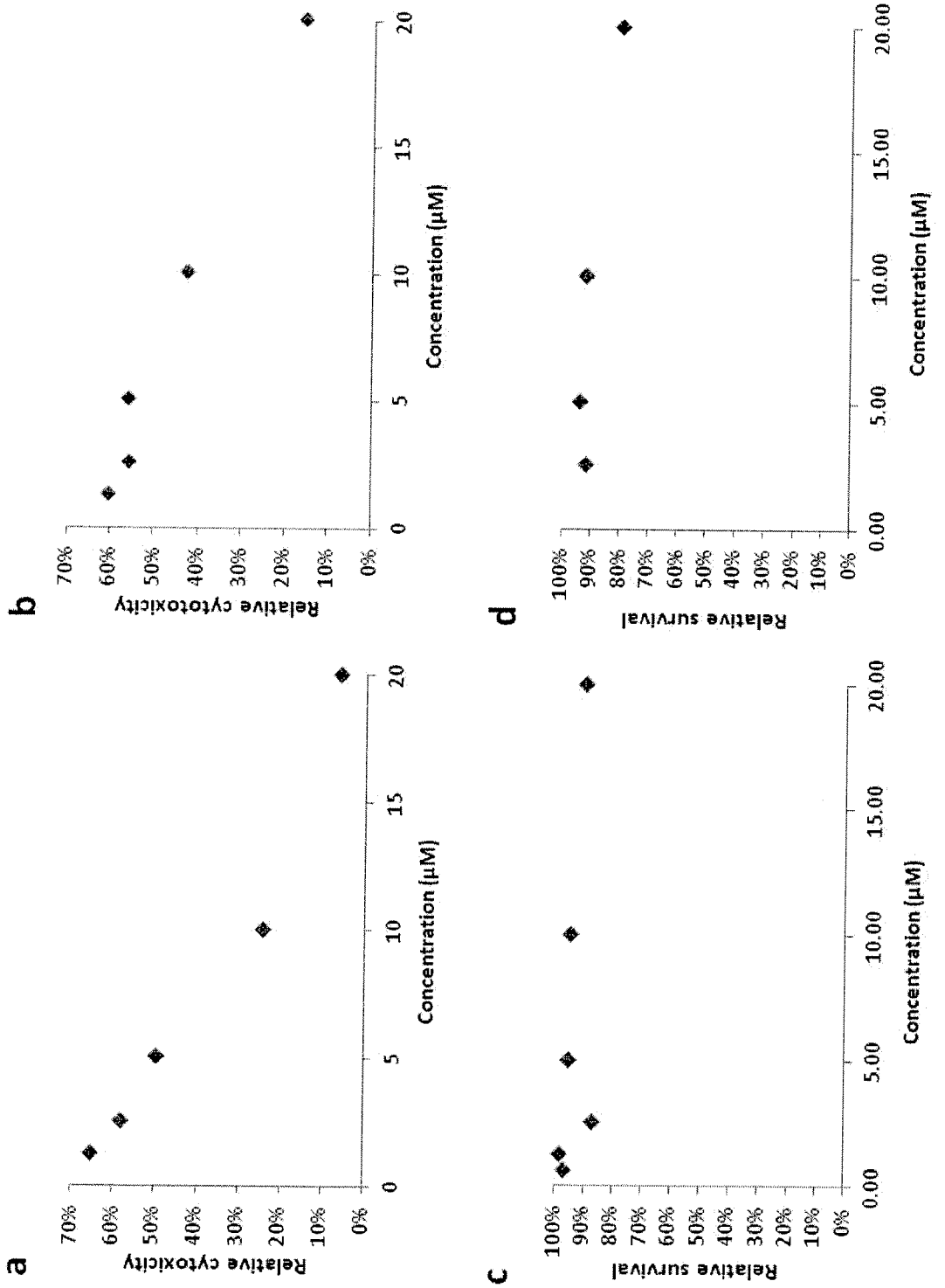

a
Relative cytotoxicity
70%
60%
50%
40%
30%
20%
10%
0%
0
5
10
15
20
Concentration (µM)
b
Relative cytotoxicity
70%
60%
50%
40%
30%
20%
10%
0%
0
5
10
15
20
Concentration (µM)
c
Relative survival
100%
90%
80%
70%
60%
50%
40%
30%
20%
10%
0%
0.00
5.00
10.00
15.00
20.00
Concentration (µM)
d
Relative survival
100%
90%
80%
70%
60%
50%
40%
30%
20%
10%
0%
0.00
5.00
10.00
15.00
20.00
Concentration (µM)

Fig. 17

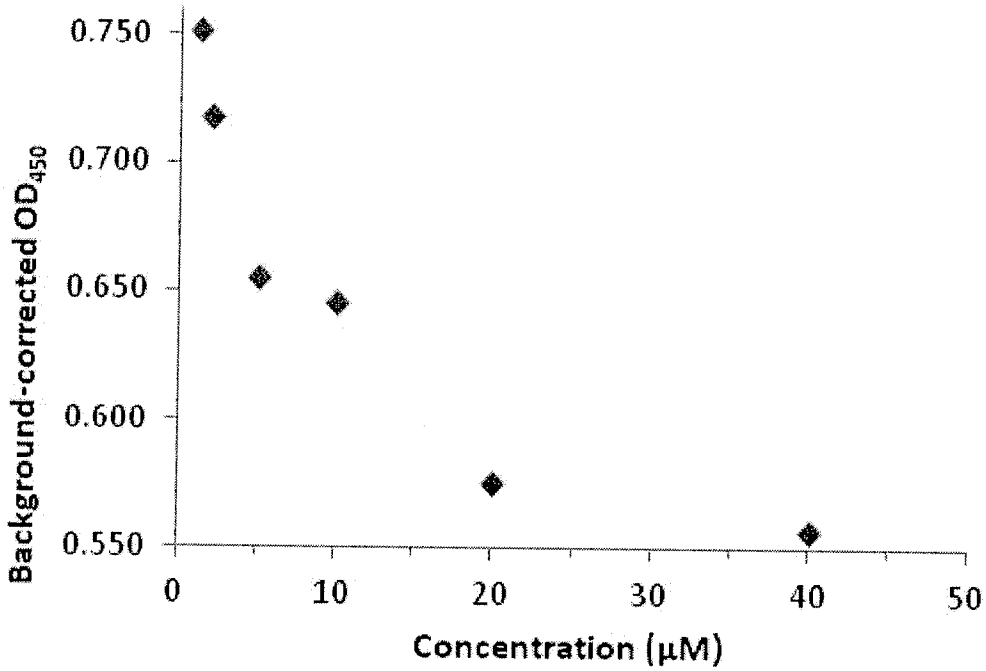

0.750
0.700
0.650
0.600
0.550
Background-corrected OD_{450}
0
10
20
30
40
50
Concentration (µM)

Fig. 18

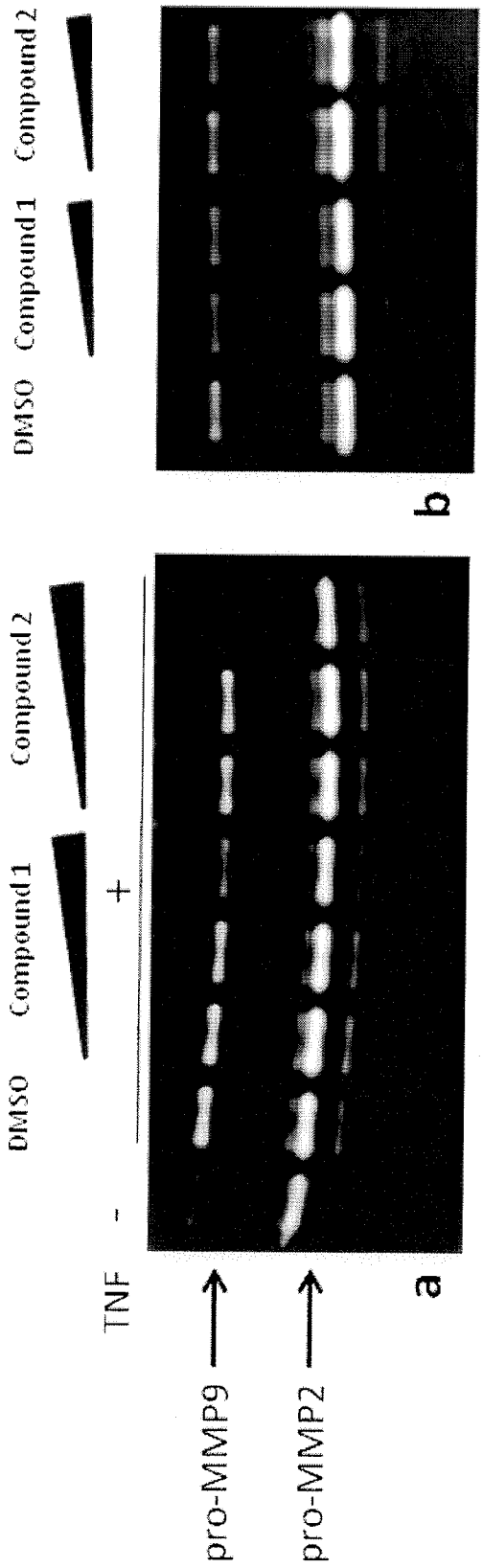

DMSO
Compound 1
Compound 2
b
TNF
-
+
DMSO
Compound 1
Compound 2
a
pro-MMP9
pro-MMP2

Fig. 19

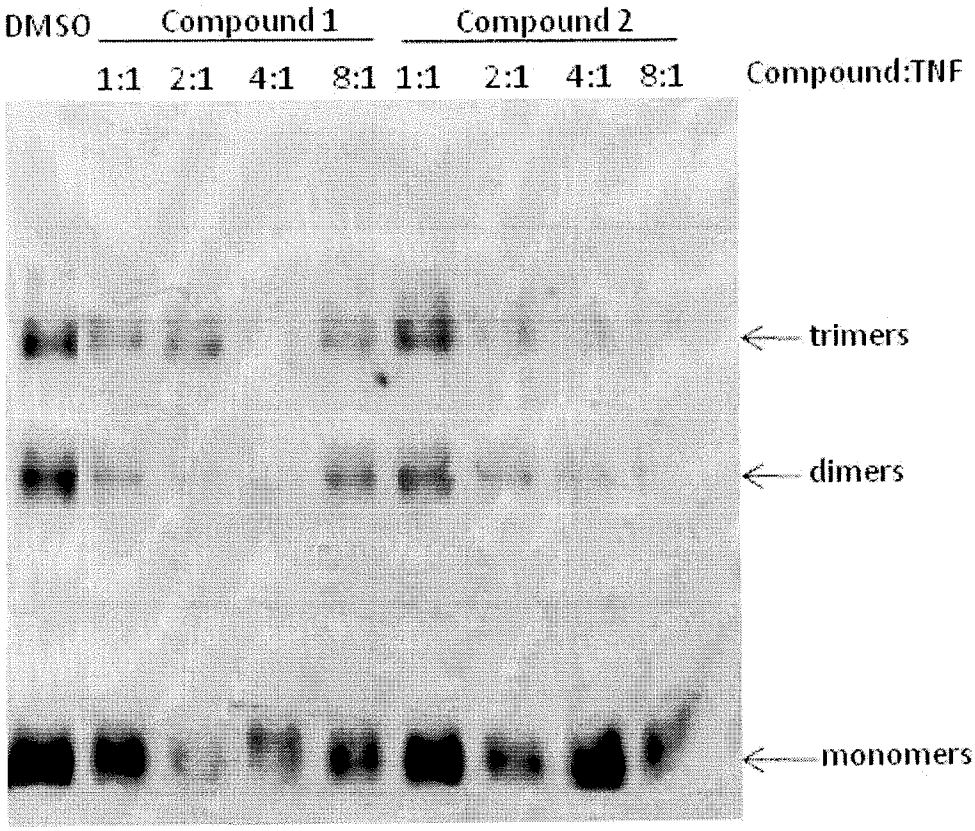

DMSO
Compound 1
Compound 2
1:1 2:1 4:1 8:1 1:1 2:1 4:1 8:1
Compound:TNF
trimers
dimers
monomers

Fig. 20

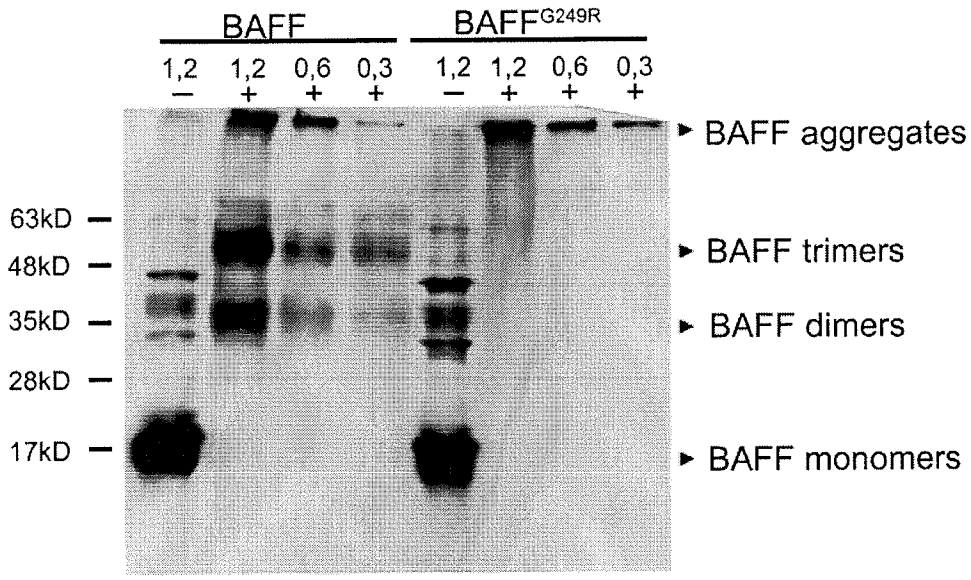


Fig. 21A

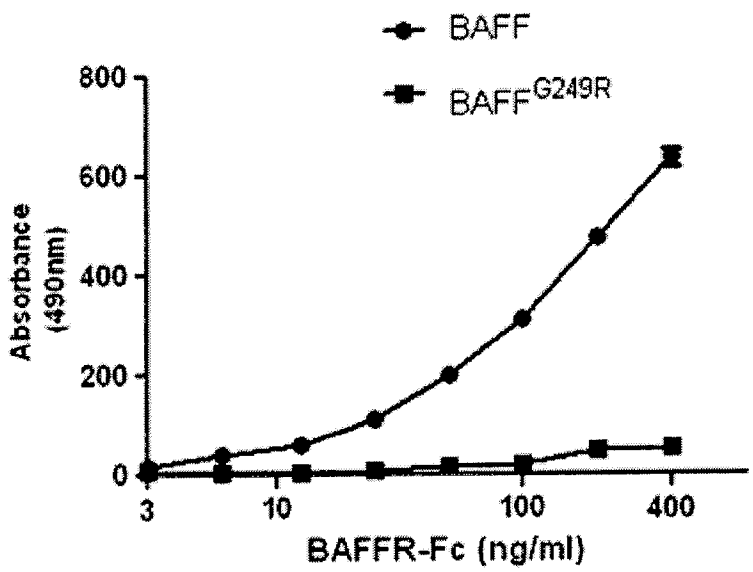


Fig. 21B

Fig. 22

SPD analogues-Map of 70 synthesized analogues

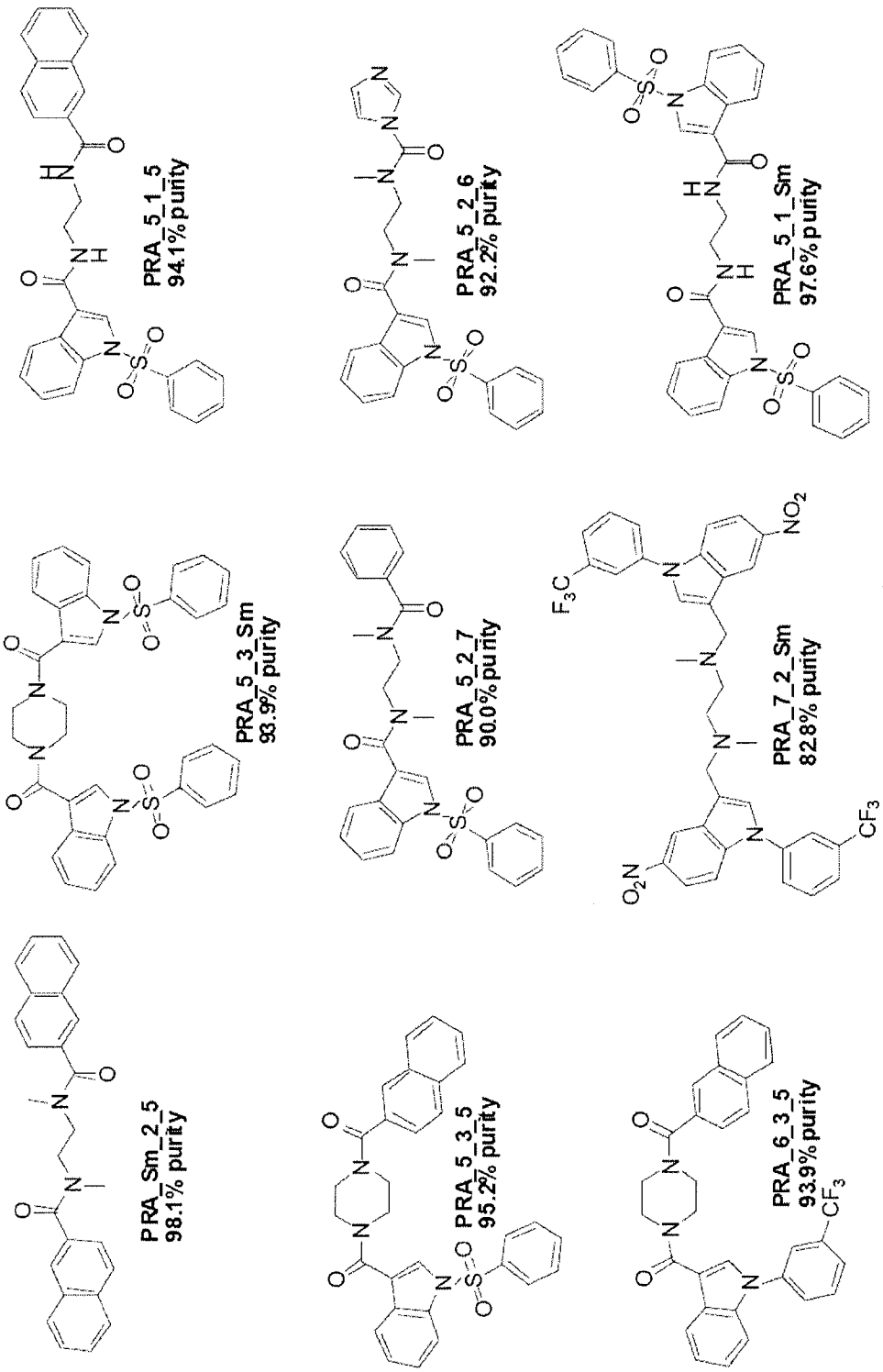


Fig. 22, cont'd

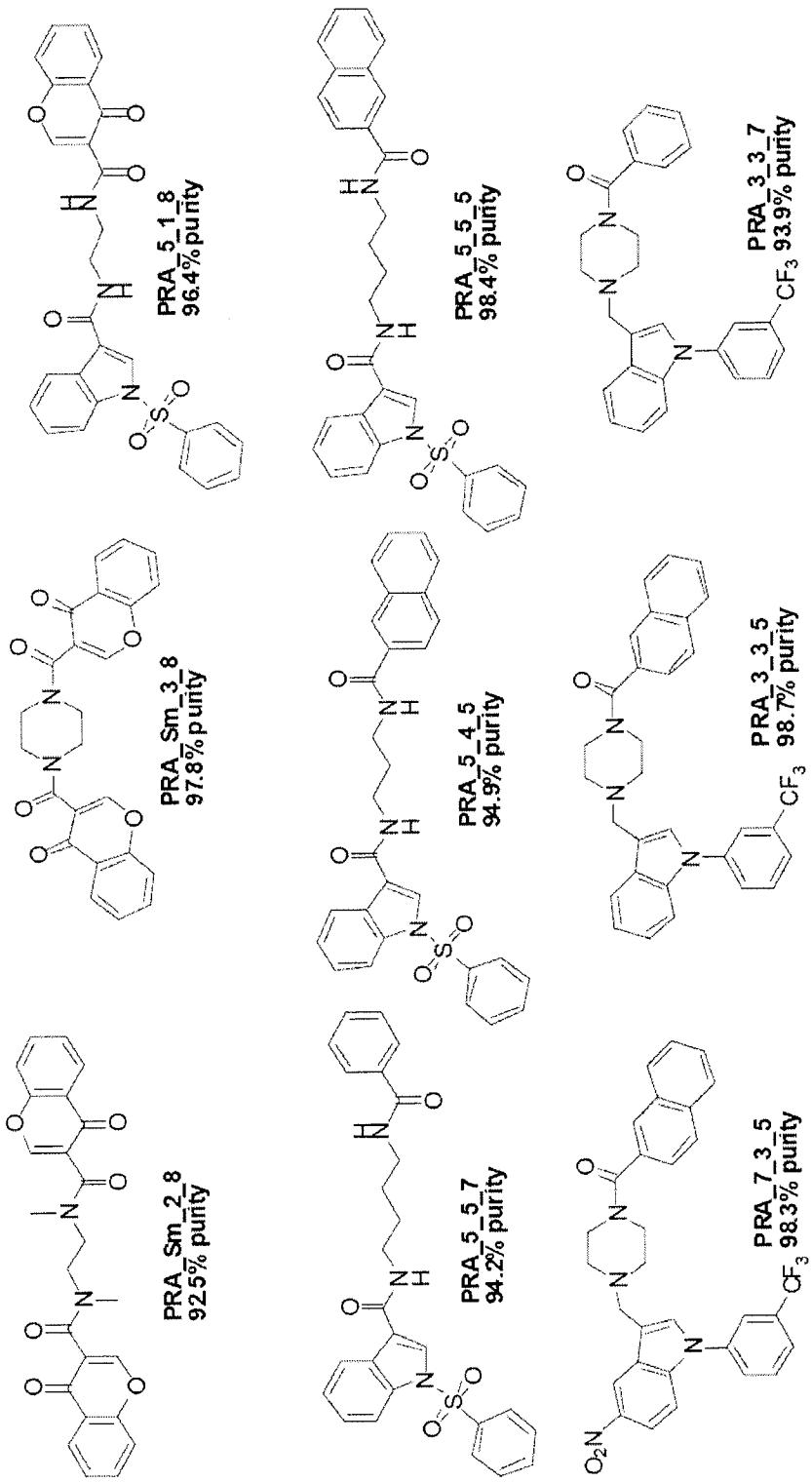

PRA_5_1_8
96.4% purity
PRA_5_5_5
98.4% purity
PRA_3_3_7
CF3 93.9% purity
PRA_Sm_3_8
97.8% purity
PRA_5_4_5
94.9% purity
PRA_3_3_5
98.7% purity
PRA_Sm_2_8
92.5% purity
PRA_5_5_7
94.2% purity
PRA_7_3_5
CF3 98.3% purity

Fig. 22, cont'd

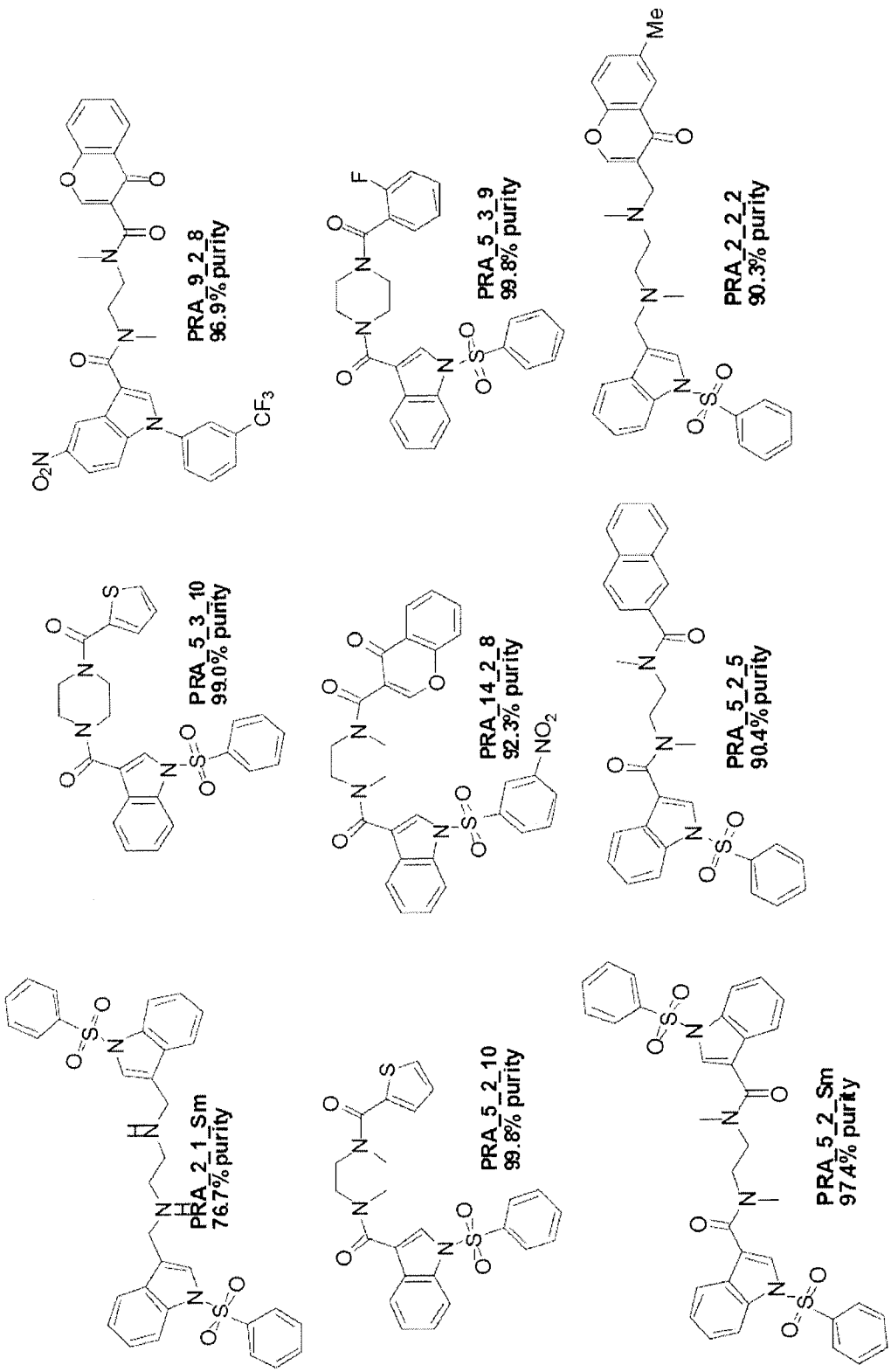

PRA_9_2_8
96.9% purity
PRA_5_3_9
99.8% purity
PRA_2_2_2
90.3% purity
PRA_5_3_10
99.0% purity
PRA_14_2_8
92.3% purity
PRA_5_2_5
90.4% purity
PRA_2_1_Sm
76.7% purity
PRA_5_2_10
99.8% purity
PRA_5_2_Sm
97.4% purity

Fig. 22, cont'd

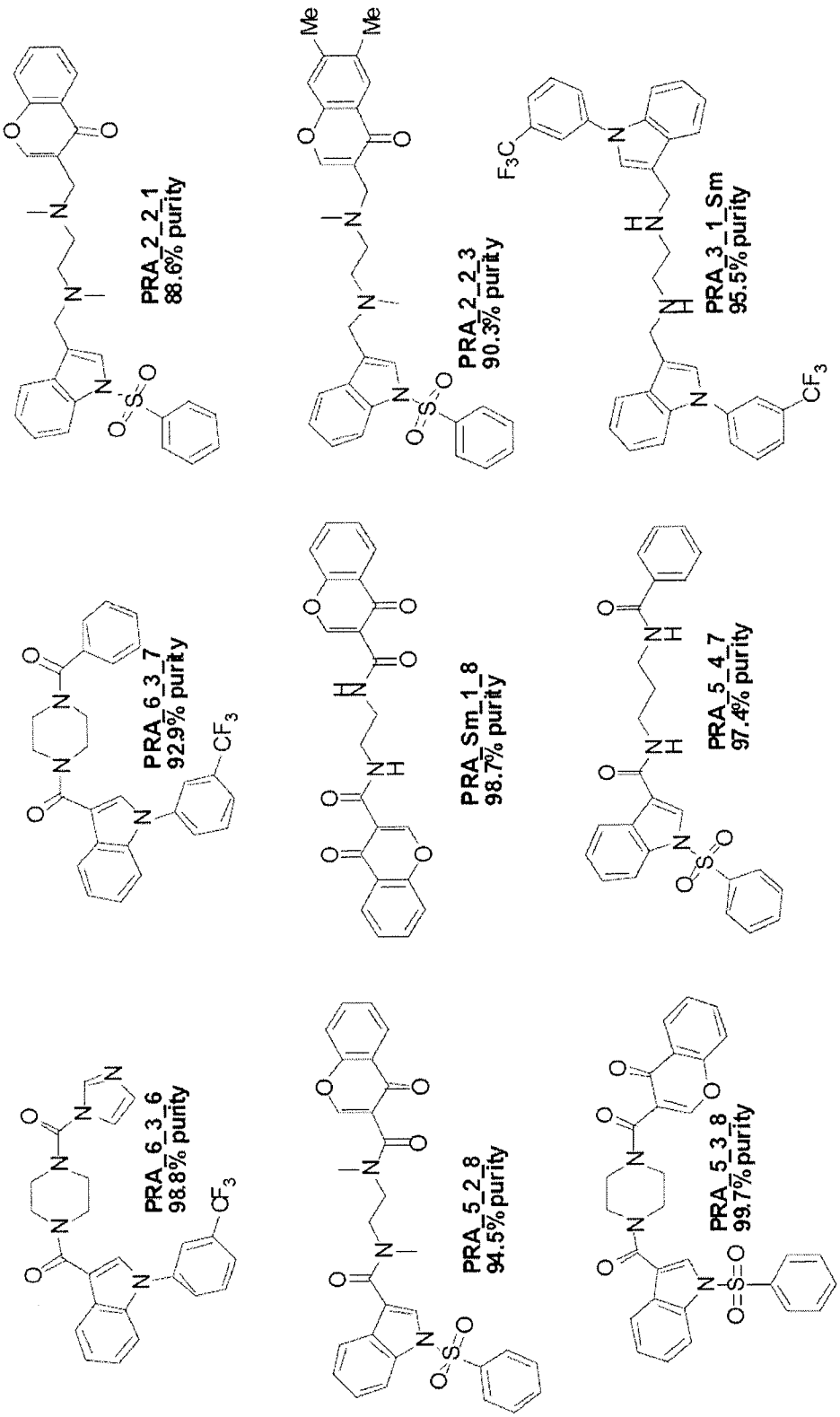

PRA_2_2_1
88.6% purity
PRA_2_2_3
90.3% purity
PRA_3_1_Sm
95.5% purity
PRA_6_3_7
92.9% purity
PRA_Sm_1_8
98.7% purity
PRA_5_4_7
97.4% purity
PRA_6_3_6
98.8% purity
PRA_5_2_8
94.5% purity
PRA_5_3_8
99.7% purity

Fig. 22, cont'd

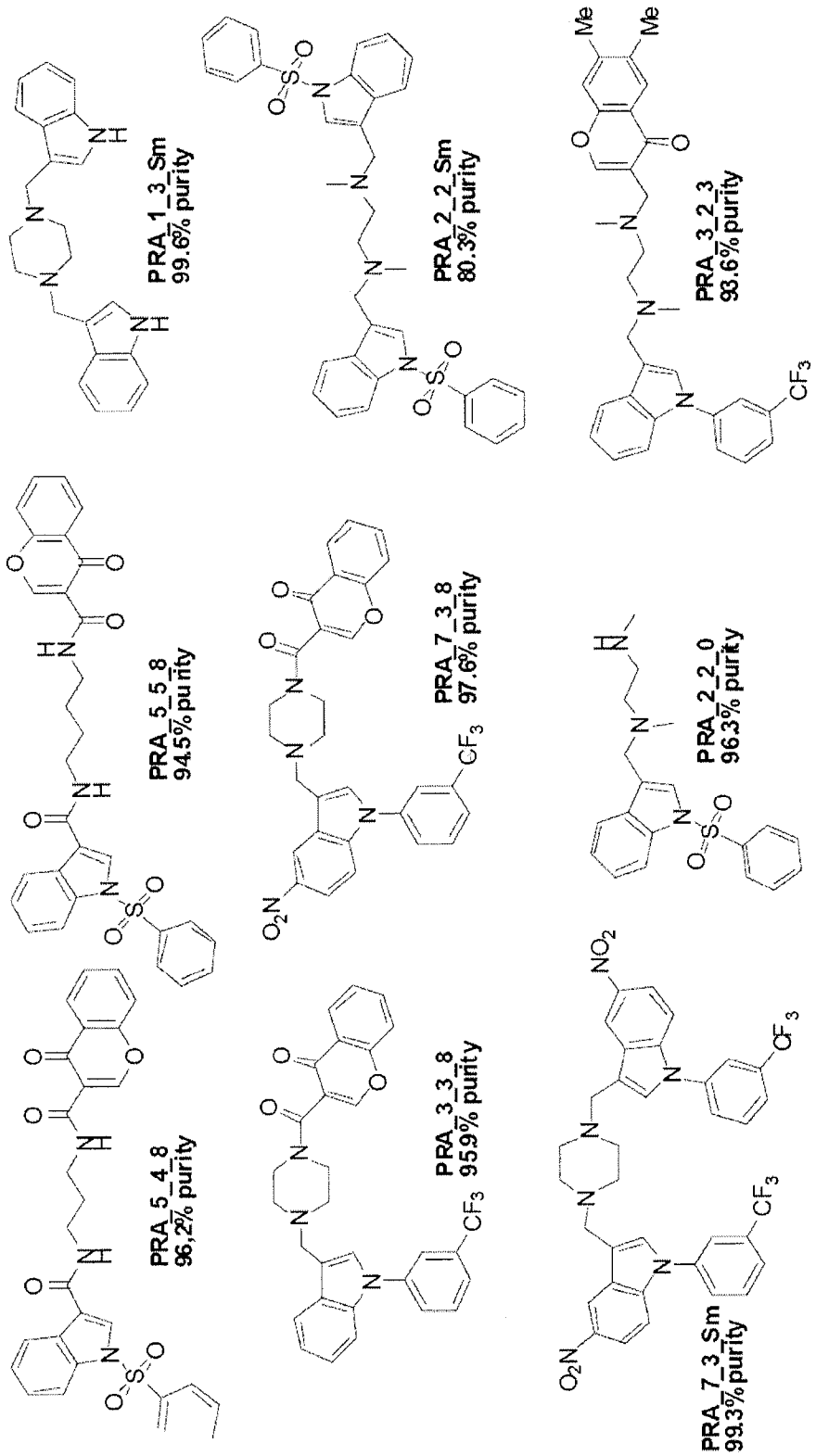

PRA_1_3_Sm
99.6% purity
PRA_2_2_Sm
80.3% purity
PRA_3_2_3
93.6% purity
PRA_5_5_8
94.5% purity
PRA_7_3_8
97.6% purity
PRA_2_2_0
96.3% purity
PRA_5_4_8
96,2% purity
PRA_3_3_8
95.9% purity
PRA_7_3_Sm
99.3% purity

Fig. 22, cont'd

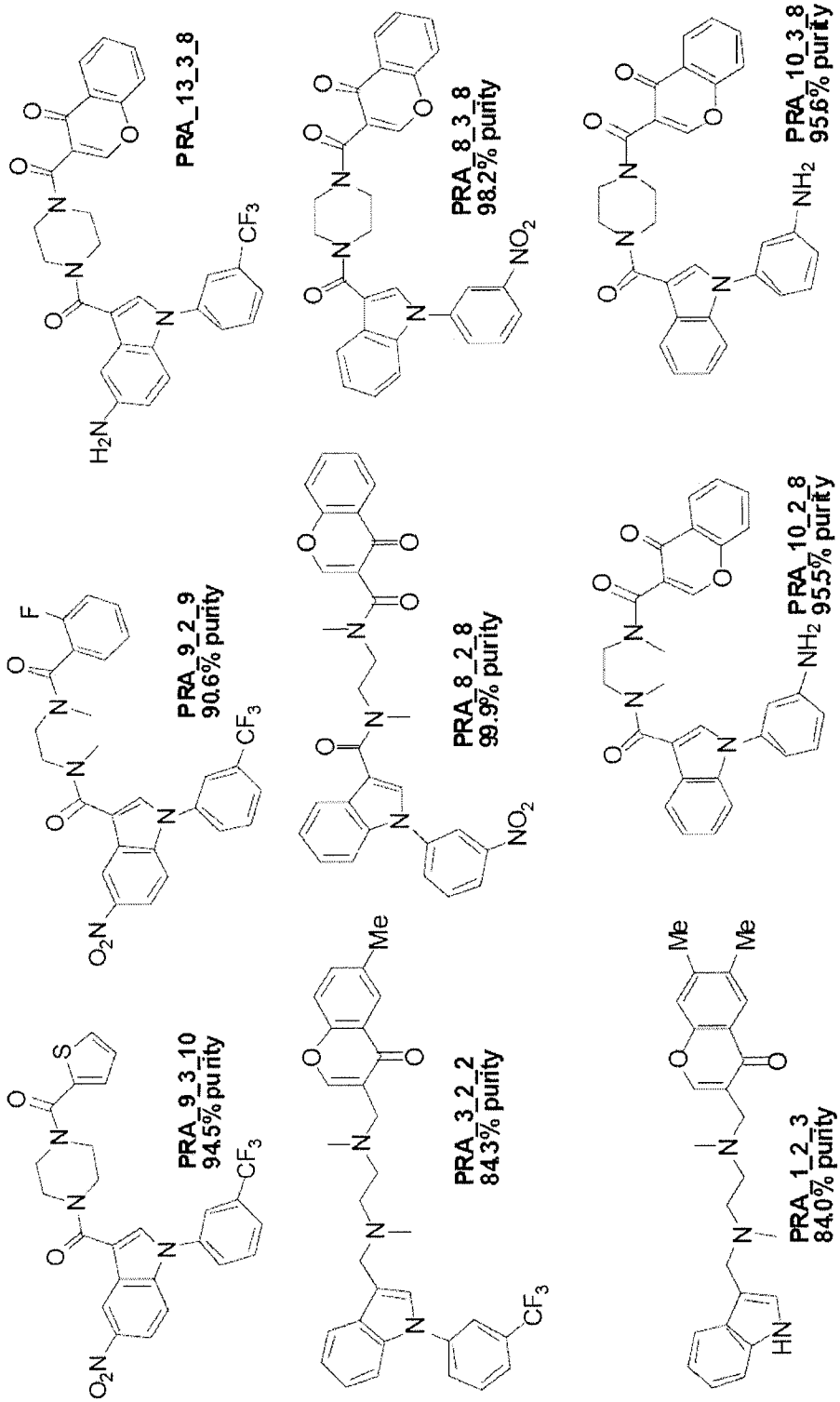

PRA_13_3_8
PRA_8_3_8
98.2% purity
PRA_10_3_8
95.6% purity
PRA_9_2_9
90.6% purity
PRA_8_2_8
99.9% purity
PRA_10_2_8
95.5% purity
PRA_9_3_10
94.5% purity
PRA_3_2_2
84.3% purity
PRA_1_2_3
84.0% purity

Fig. 22, cont'd

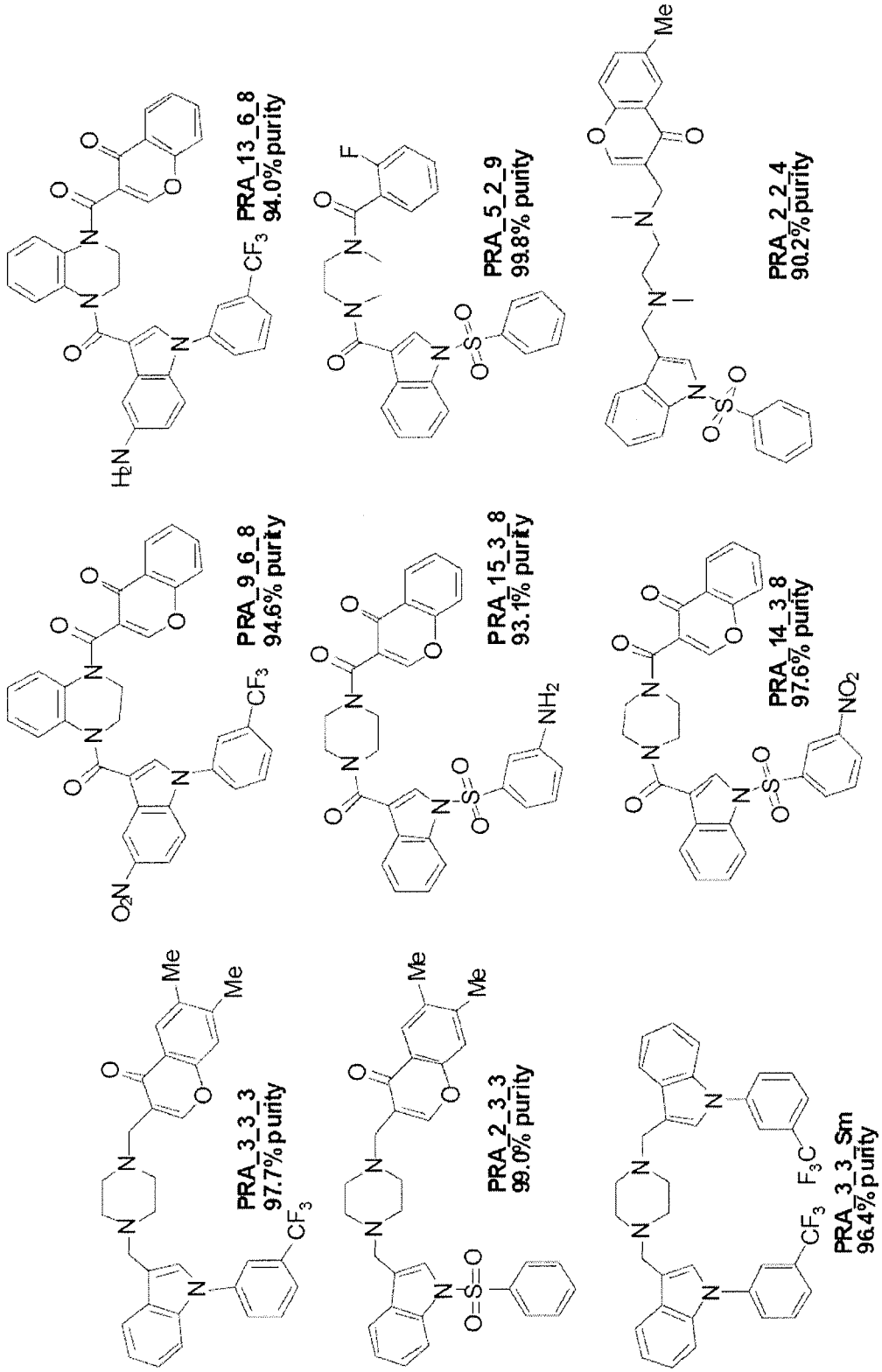

PRA_13_6_8
94.0% purity
PRA_5_2_9
99.8% purity
PRA_2_2_4
90.2% purity
PRA_9_6_8
94.6% purity
PRA_15_3_8
93.1% purity
PRA_14_3_8
97.6% purity
PRA_3_3_3
97.7% purity
PRA_2_3_3
99.0% purity
PRA_3_3_Sm
96.4% purity

Fig. 22, cont'd

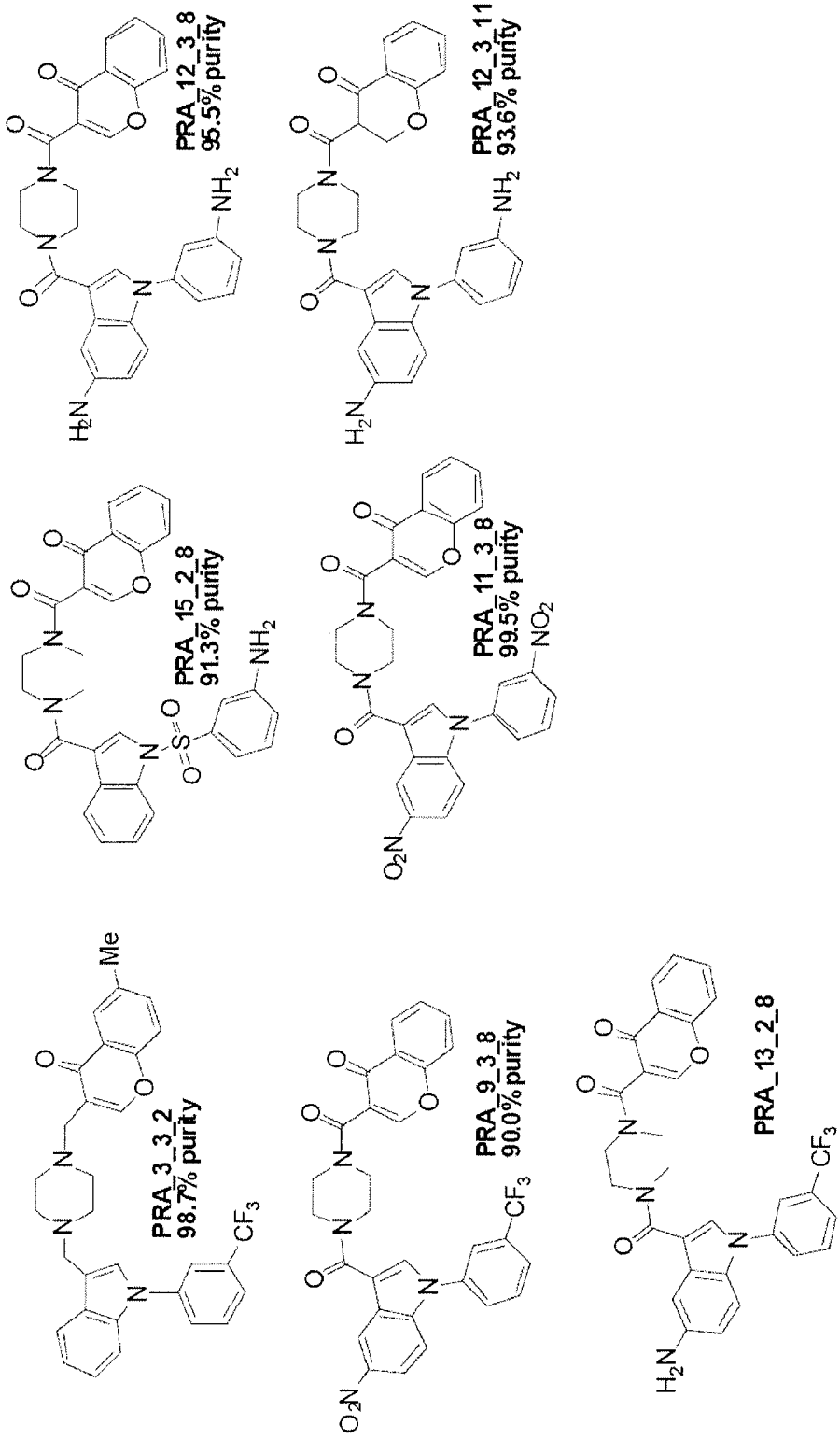

PRA_12_3_8
95.5% purity
PRA_12_3_11
93.6% purity
PRA_15_2_8
91.3% purity
PRA_11_3_8
99.5% purity
PRA_3_3_2
98.7% purity
PRA_9_3_8
90.0% purity
PRA_13_2_8

Fig. 23

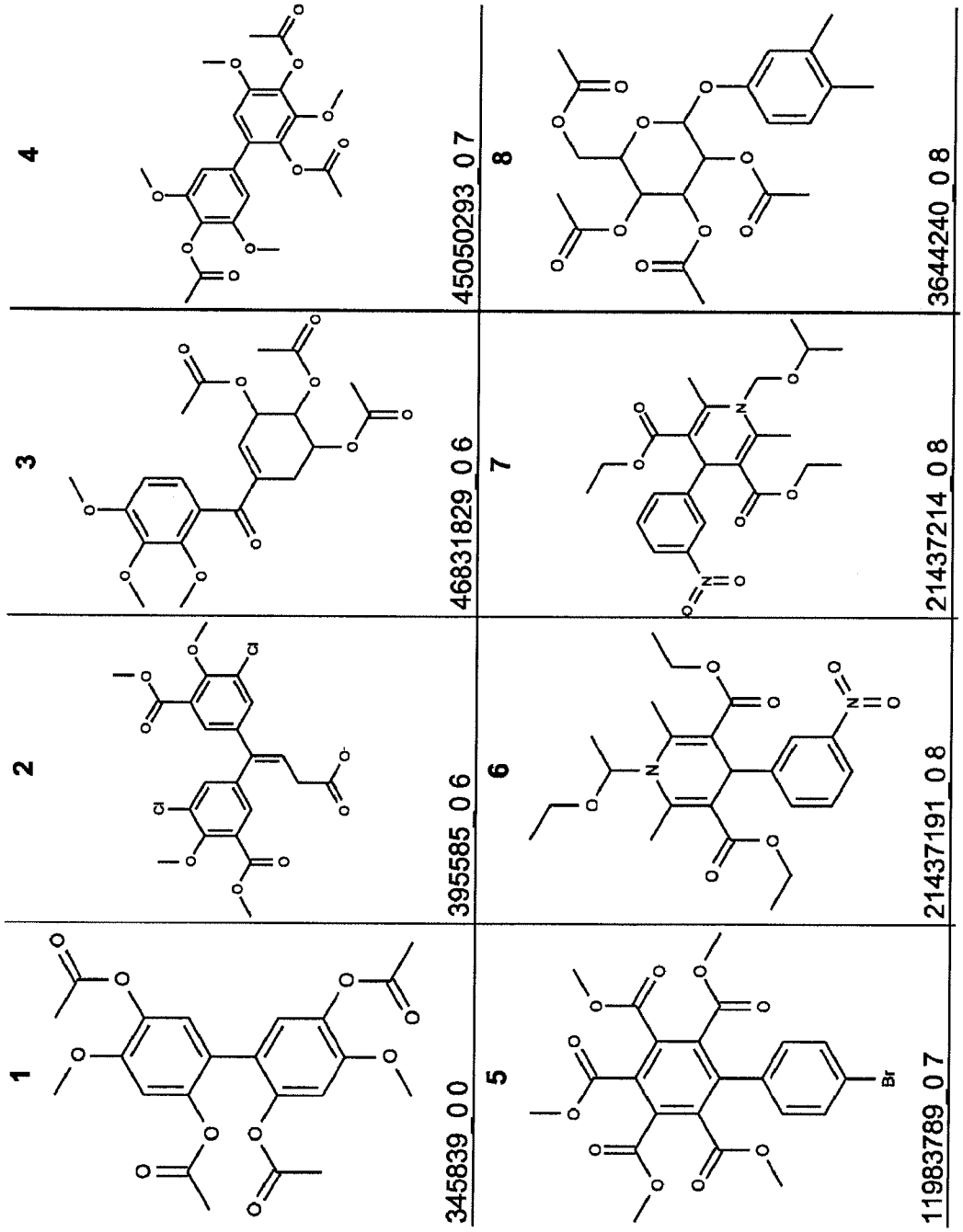

1
345839_0 0
2
395585_0 6
3
46831829_0 6
4
45050293_0 7
5
11983789_0 7
6
21437191_0 8
7
21437214_0 8
8
3644240_0 8

Fig. 23, cont'd

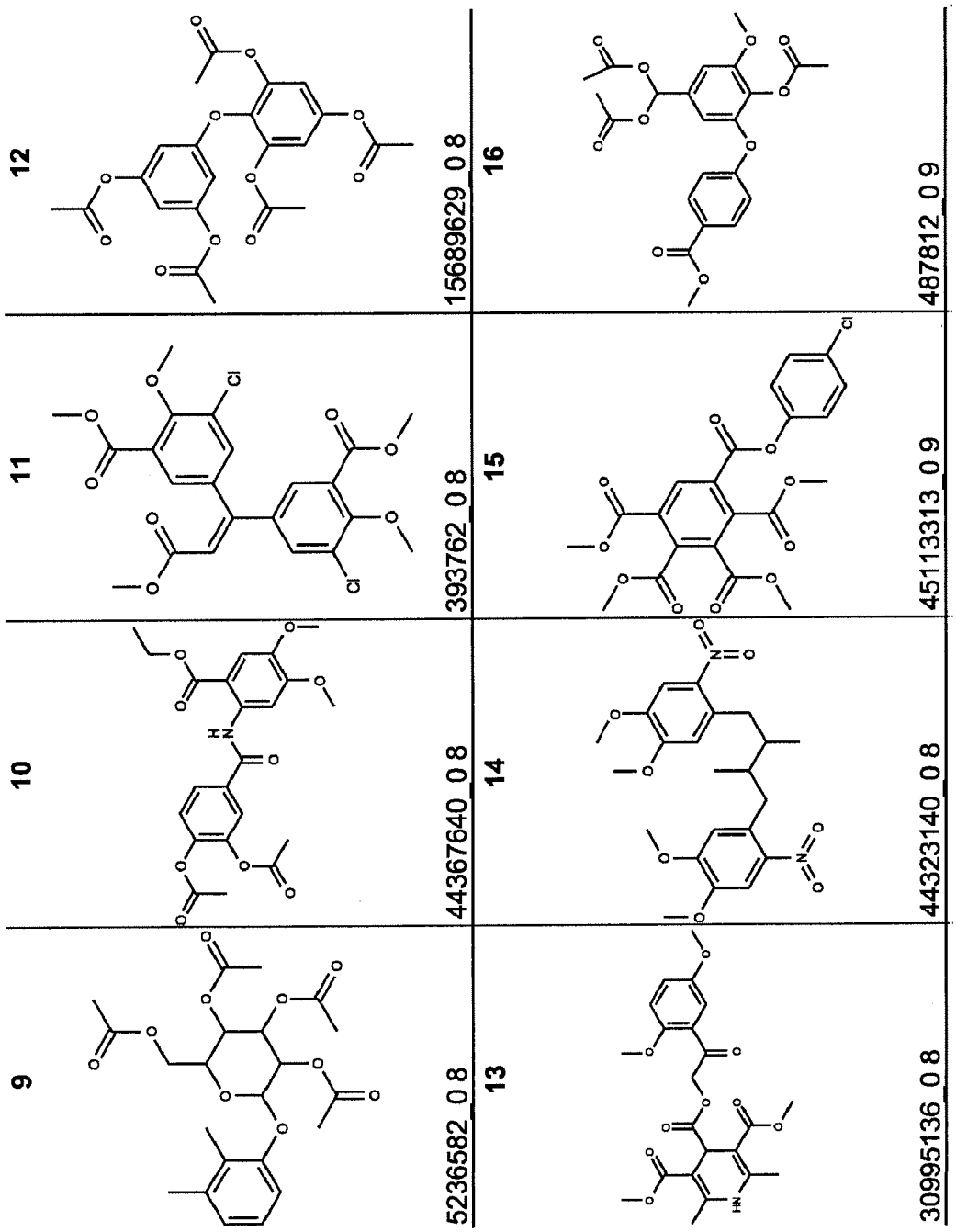

9
5236582_0 8
10
44367640_0 8
11
393762_0 8
12
15689629_0 8
13
30995136_0 8
14
44323140_0 8
15
45113313_0 9
16
487812_0 9

Fig. 23, cont'd

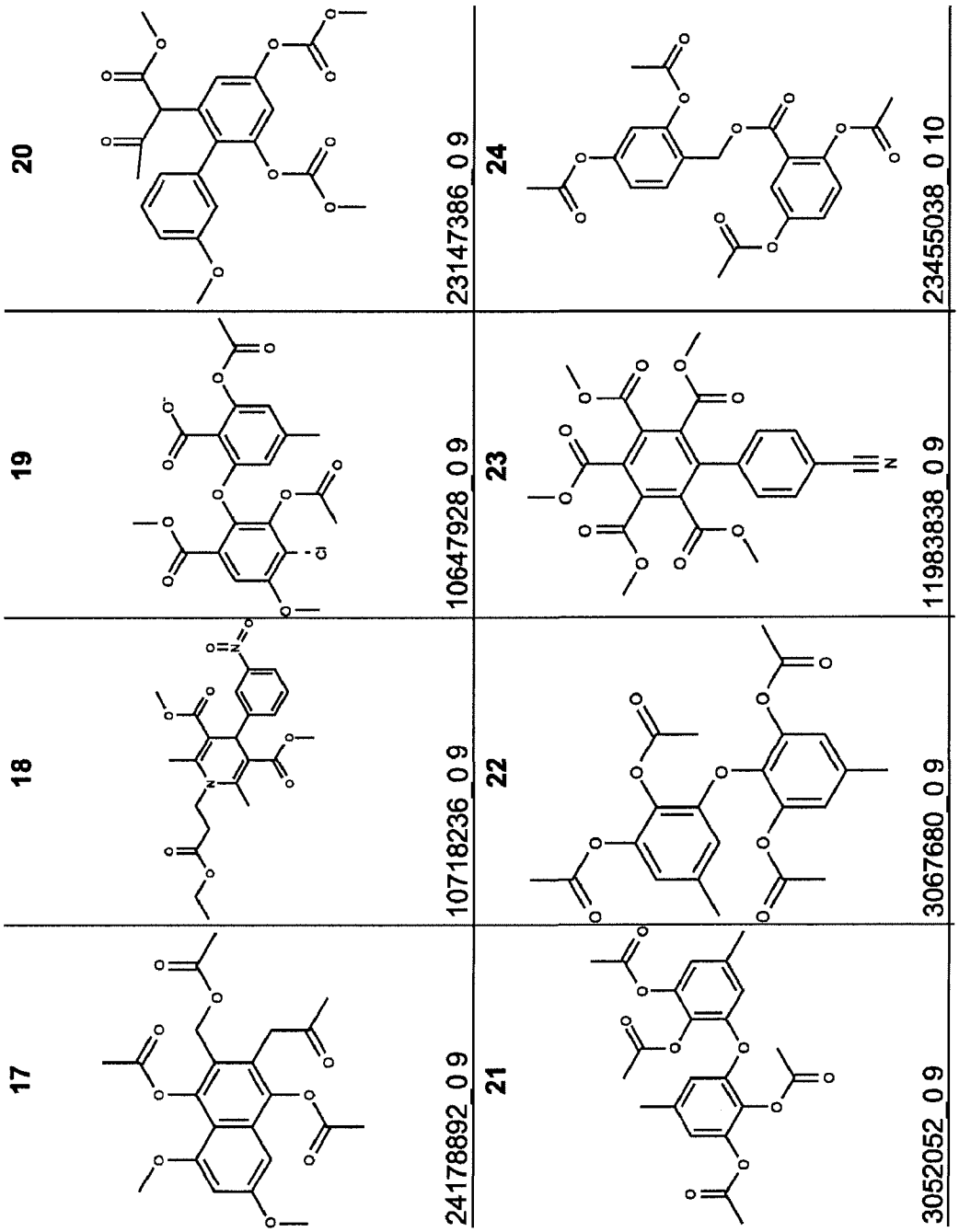

17
18
19
20
21
22
23
24
24178892_0 9
10718236_0 9
10647928_0 9
23147386_0 9
3052052_0 9
3067680_0 9
11983838_0 9
23455038_0 10

Fig. 23, cont'd

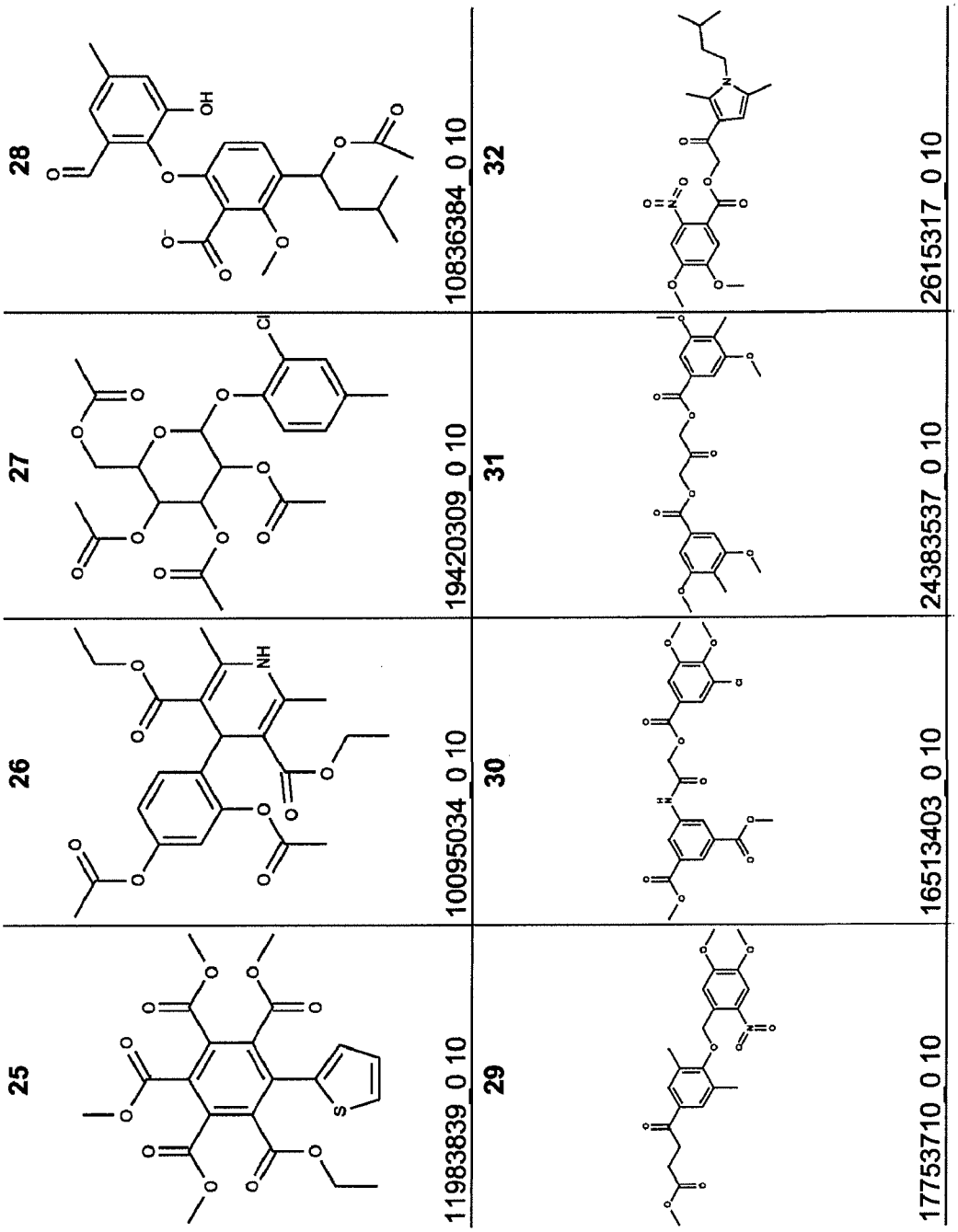

25
11983839_0 10
26
10095034_0 10
27
19420309_0 10
28
10836384_0 10
29
17753710_0 10
30
16513403_0 10
31
24383537_0 10
32
2615317_0 10

Fig. 23, cont'd

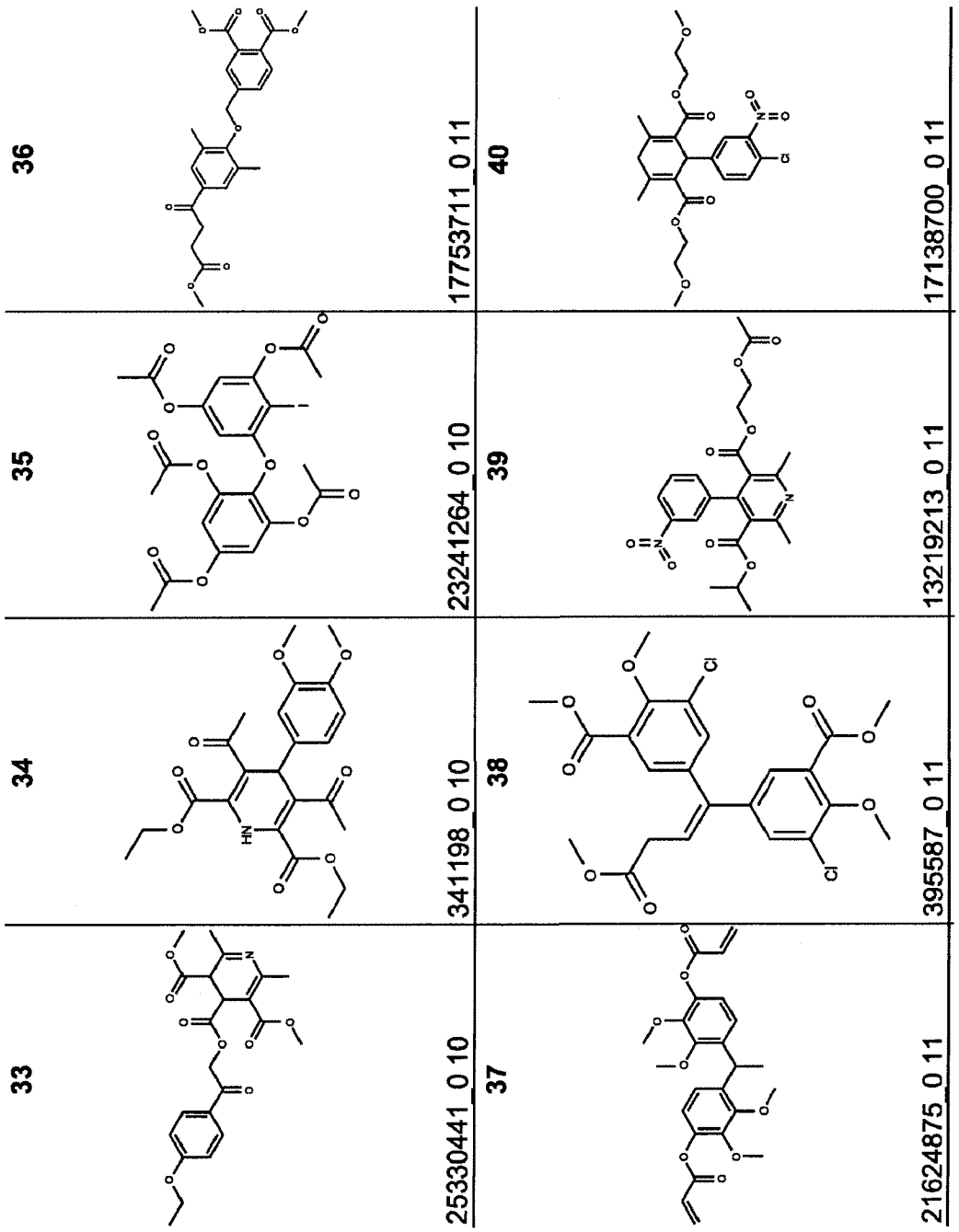

33
25330441_0 10
34
341198_0 10
35
23241264_0 10
36
17753711_0 11
37
21624875_0 11
38
395587_0 11
39
13219213_0 11
40
17138700_0 11

Fig. 23, cont'd

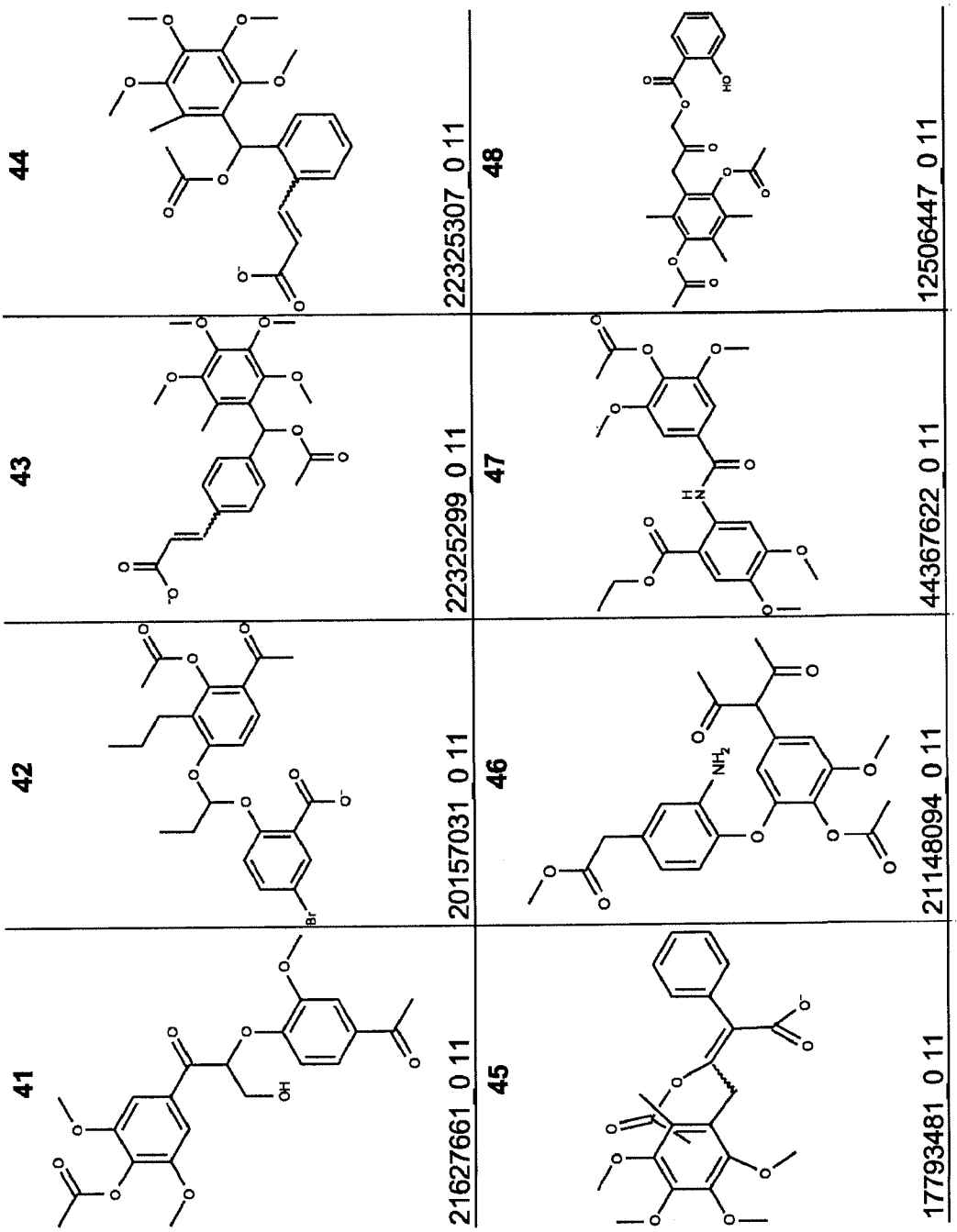

41
21627661_0 11
42
20157031_0 11
43
22325299_0 11
44
22325307_0 11
45
17793481_0 11
46
21148094_0 11
47
44367622_0 11
48
12506447_0 11

Fig. 23, cont'd

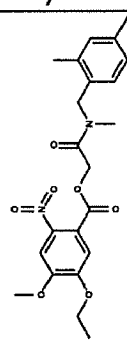
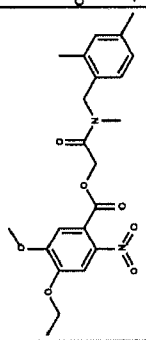
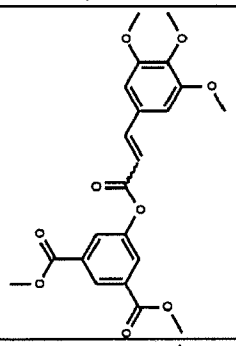
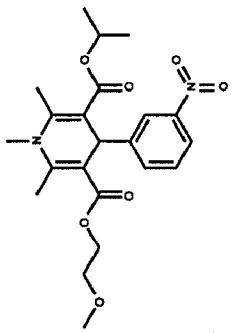
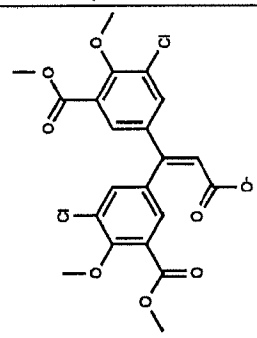
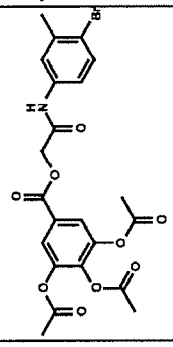
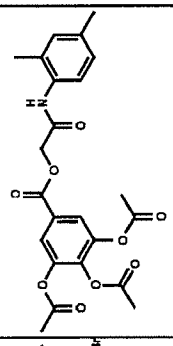
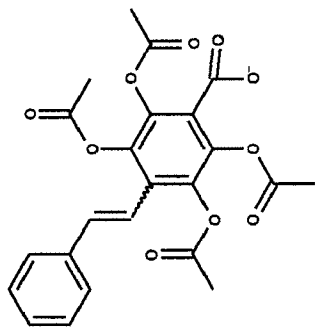
49	50	51	52
			
24483967_0 11	24485558_0 11	16229290_0 11	9867451_0 11
53	54	55	56
			
393669_0 11	2356815_0 11	2356814_0 11	18546967_0 11

Fig. 23, cont'd

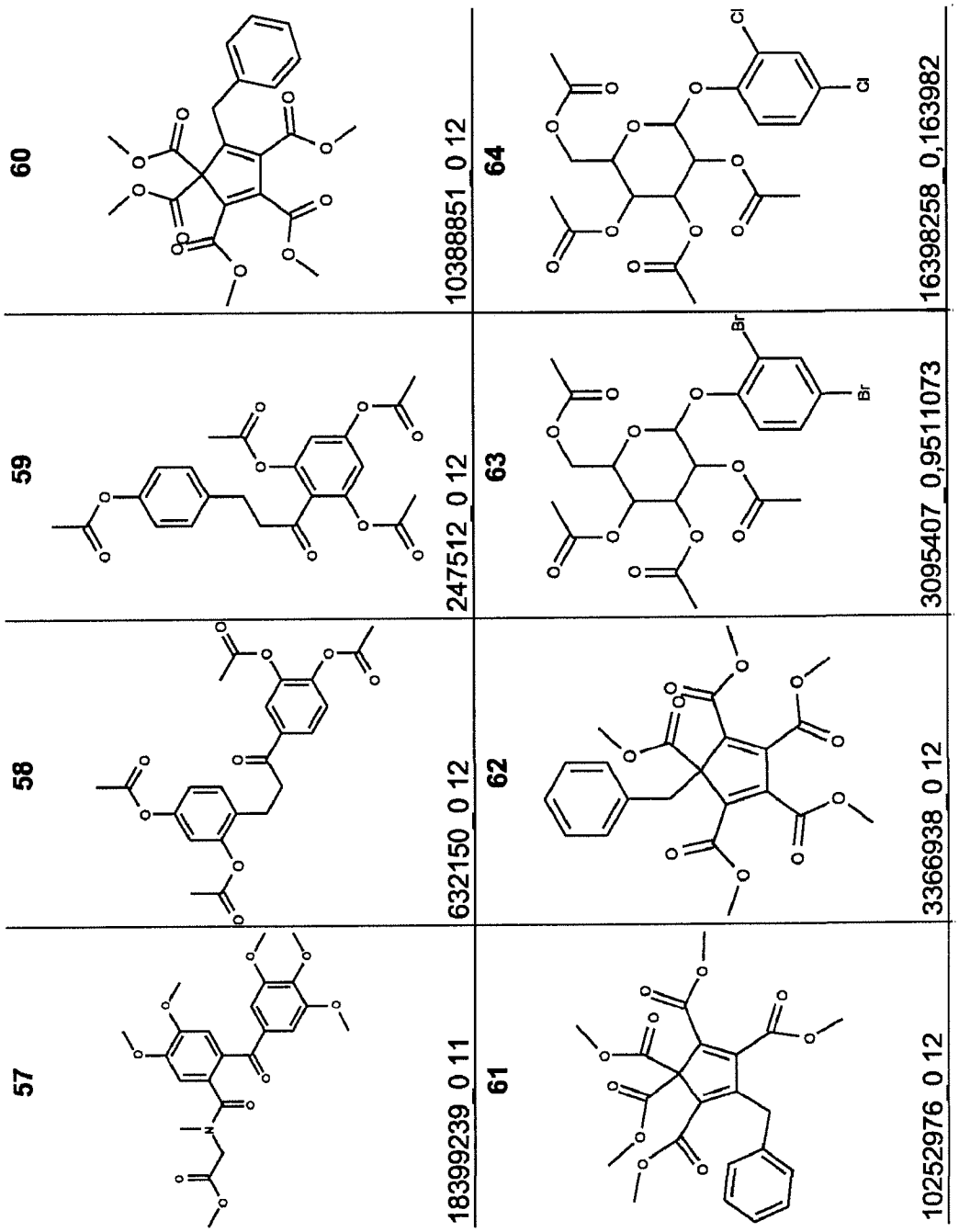

57
58
59
60
18399239_0 11
632150_0 12
247512_0 12
10388851_0 12
61
62
63
64
10252976_0 12
3366938_0 12
3095407_0,9511073
16398258_0,163982
Br
Br
Cl
Cl

Fig. 23, cont'd

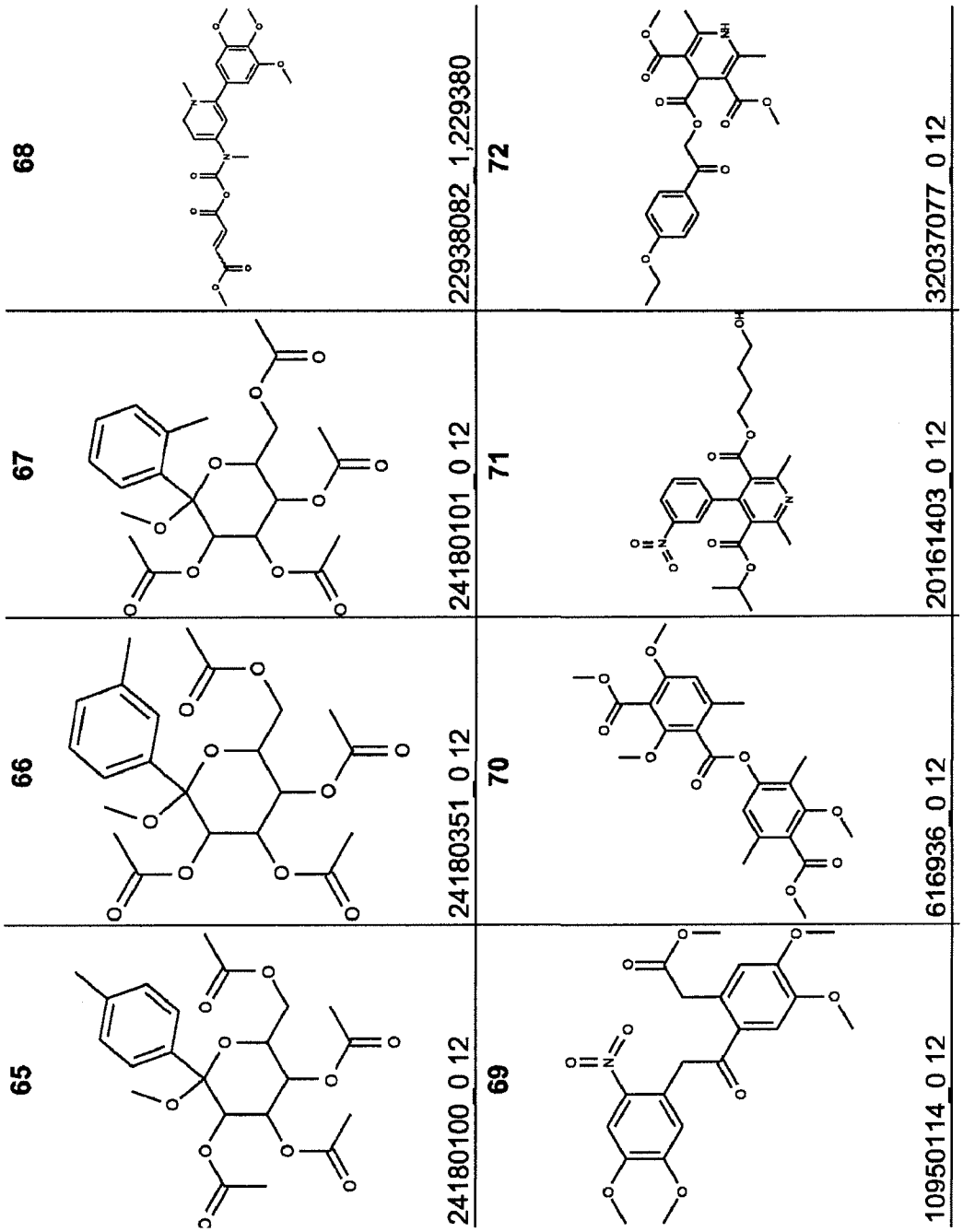

65
66
67
68
24180100_0 12
24180351_0 12
24180101_0 12
22938082_1,229380
69
70
71
72
10950114_0 12
616936_0 12
20161403_0 12
32037077_0 12

Fig. 23, cont'd

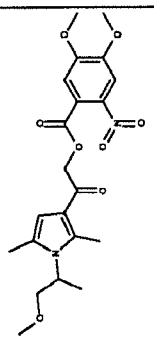
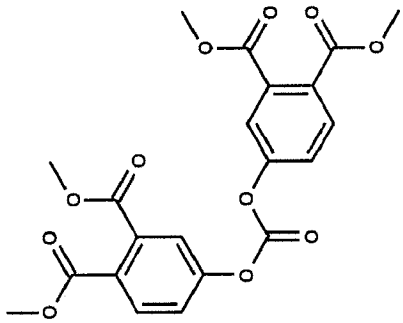
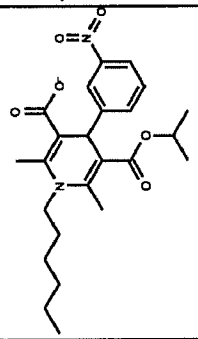
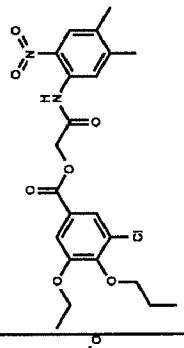
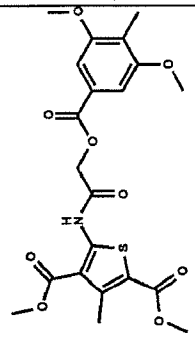
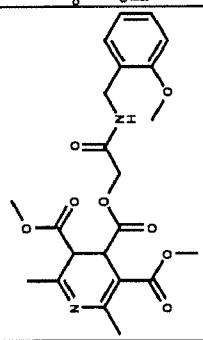
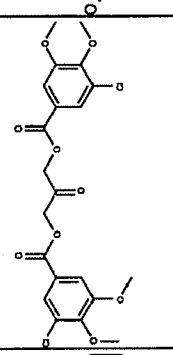
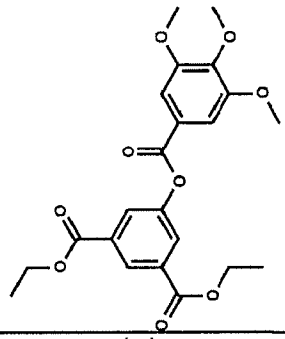
73	74	75	76
			
2519621_0,2519624	23316305_0 12	20272927_0 12	1695617_0 12
77	78	79	80
			
2505931_0 12	25330461_0 12	30547020_0 12	2462729_0 12

Fig. 23, cont'd

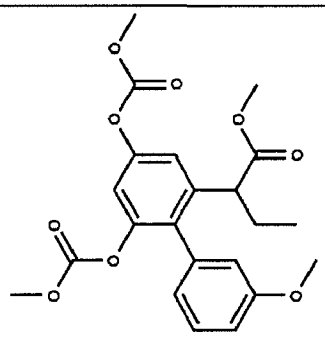
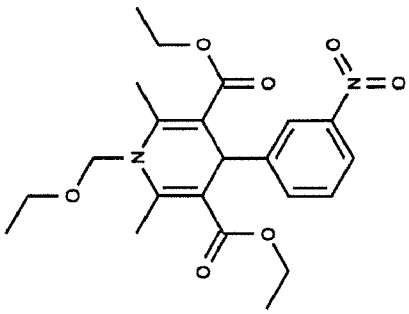
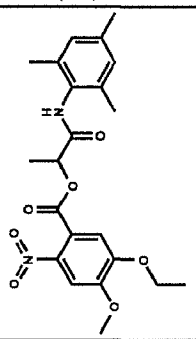
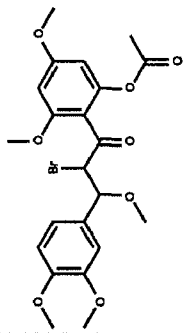
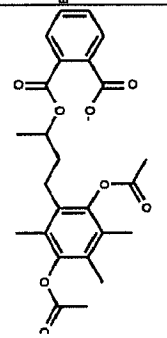
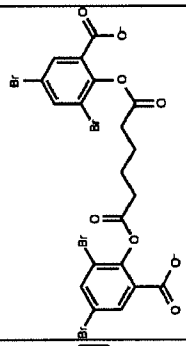
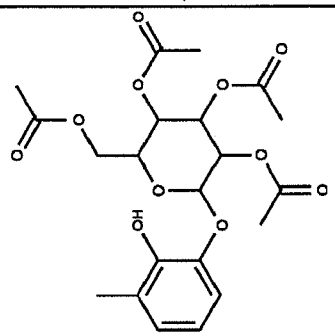
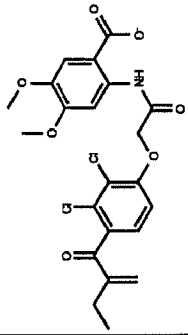
81	82	83	84
			
23147563_0 12	12529074_0 12	46609879_0 12	11466118_0 12
85	**86**	**87**	**88**
			
18637763_0,198663	4603928_0 12	10939379_0 12	44570869_0 12

Fig. 23, cont'd

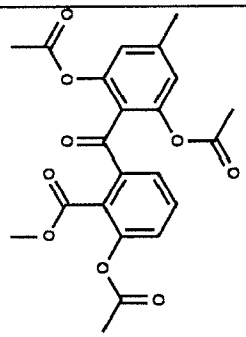
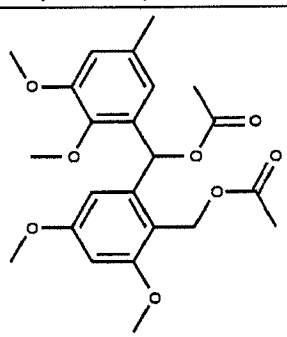
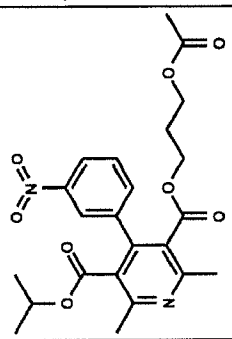
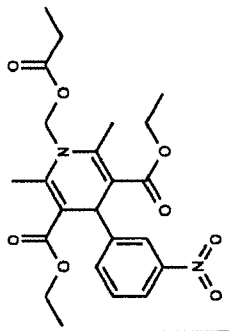
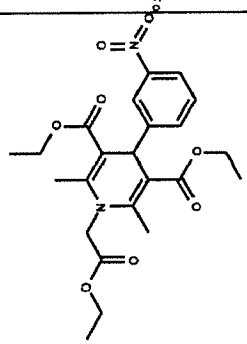
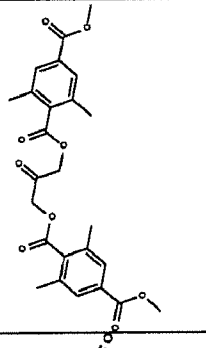
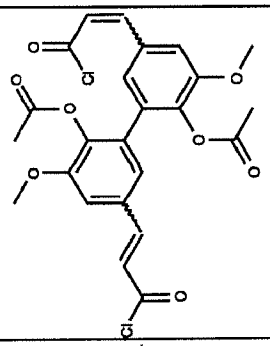
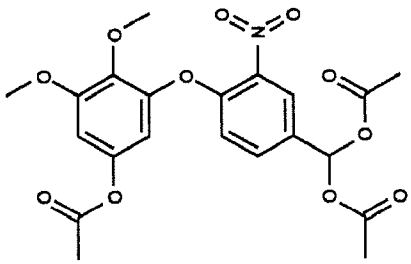
89	90	91	92
			
9979991_0 12	10432936_0 12	20161394_0 12	21437208_0 12
93	**94**	**95**	**96**
			
12529191_0 12	19812817_1,198128	10601741_0 12	487813_0 12

Fig. 23, cont'd

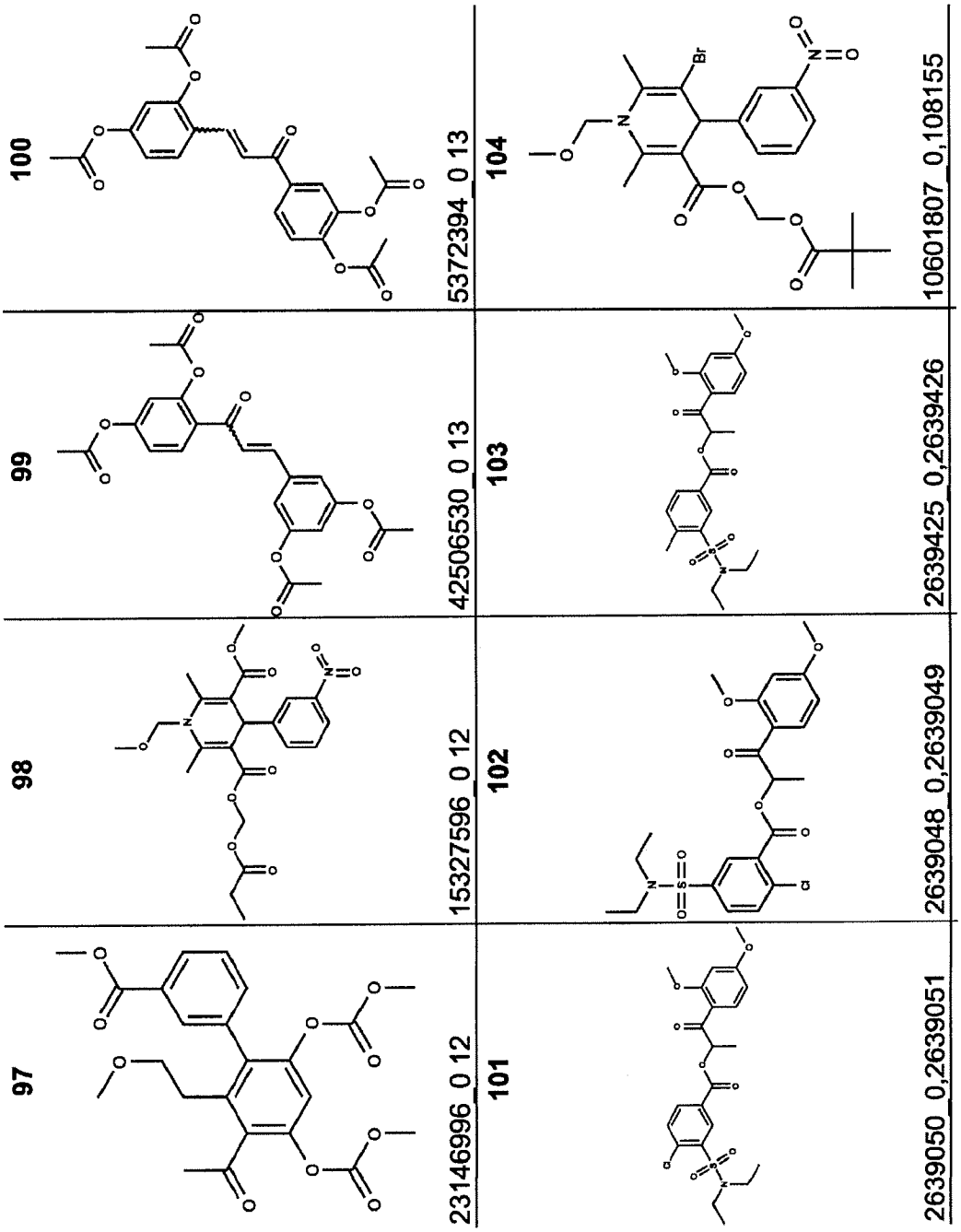

97
98
99
100
23146996_0 12
15327596_0 12
4250530_0 13
5372394_0 13
101
102
103
104
2639050_0,2639051
2639048_0,2639049
2639425_0,2639426
10601807_0,108155

Fig. 23, cont'd

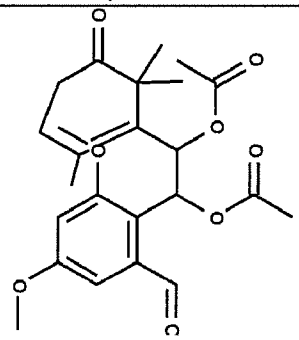
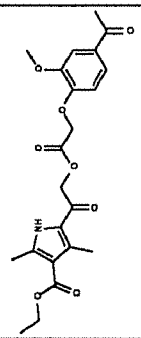
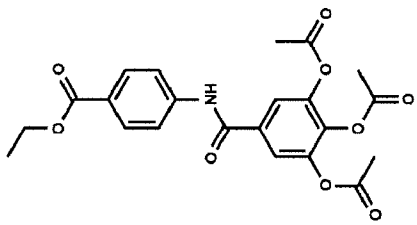
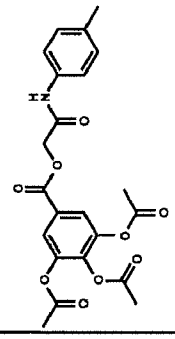
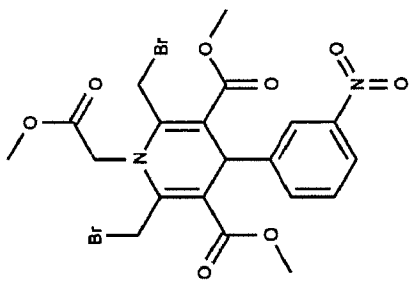
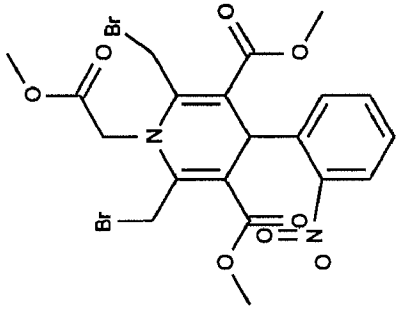
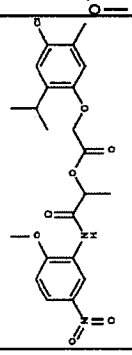
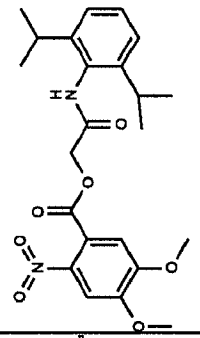
105	106	107	108
			
10765783_0 13	2395282_0 13	541111_0 13	5151597_0 13
109	110	111	112
			
10603256_0 13	10531231_0 13	16959188_0 13	2488337_0 13

Fig. 23, cont'd

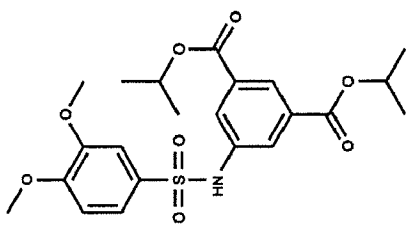
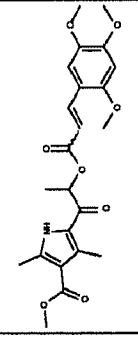
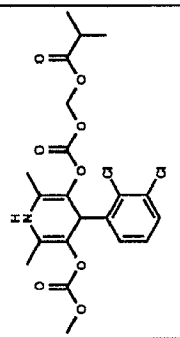
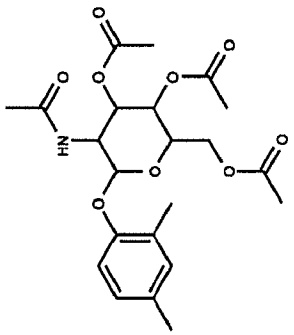
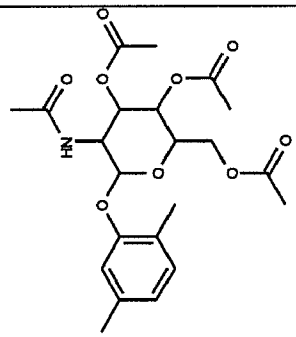
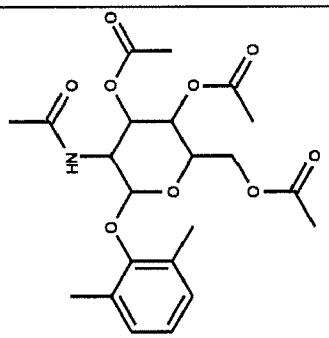
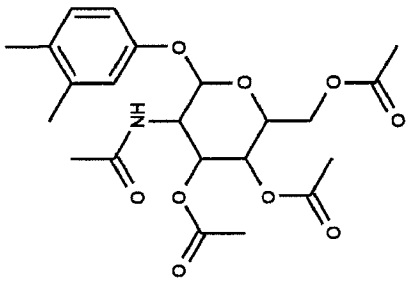
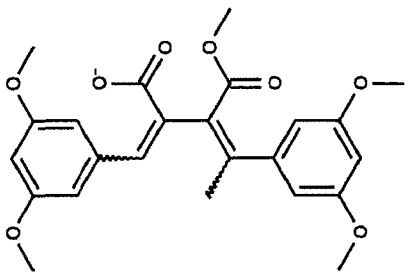
113	114	115	116
			
22773049_0 13	24379537_0,295139	23215649_0 13	25711524_0,257115
117	**118**	**119**	**120**
			
3735610_0,4258035	18805123_0,517817	18805122_0,398358	21192650_0 13

Fig. 23, cont'd

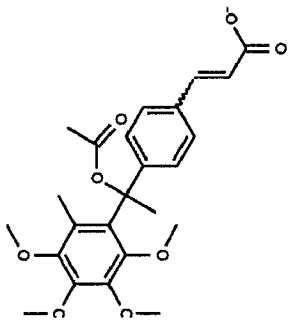
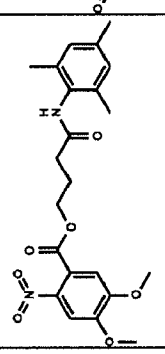
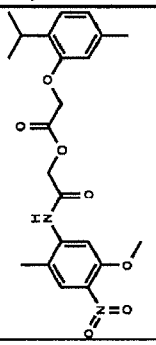
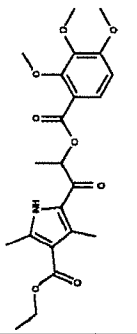
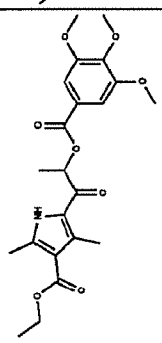
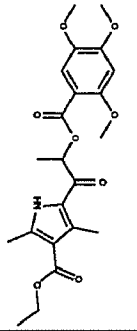
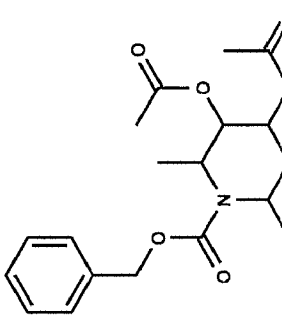
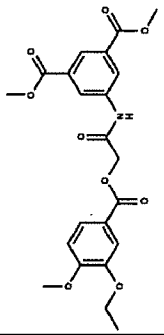
121	122	123	124
			
22743131_0 13	2469593_0 13	4598498_0 13	16523961_0 13
125	**126**	**127**	**128**
			
16522429_0 13	16528377_0 13	10983476_0,237706	29458941_0 13

Fig. 23, cont'd

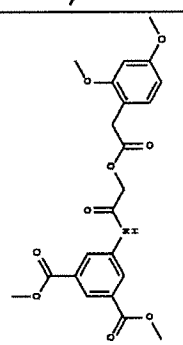
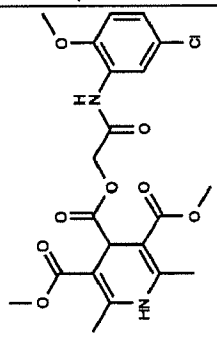
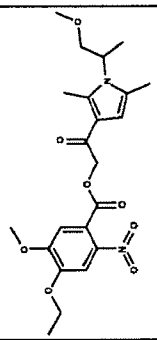
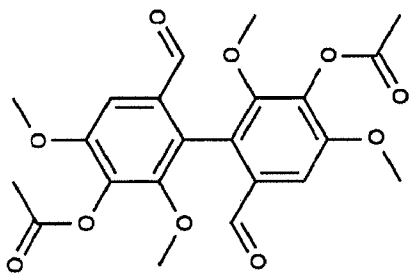
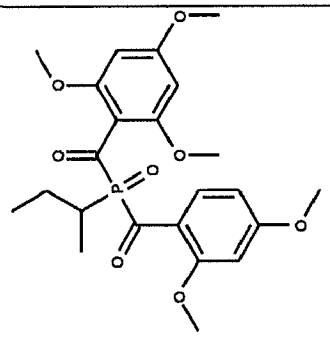
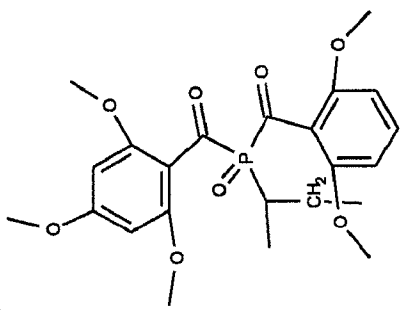
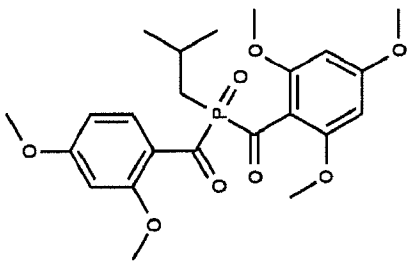
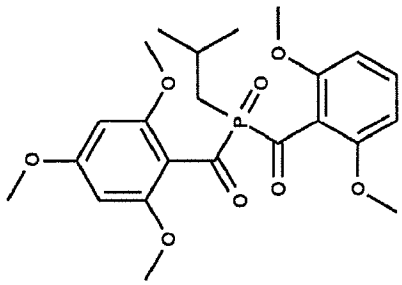
129	130	131	132
			
29622333_0 13	42964076_0 13	46611424_0 13	44242894_0 13
133	**134**	**135**	**136**
			
22184010_0 13	22183604_0 13	22183238_0 13	22183814_0 13

Fig. 23, cont'd

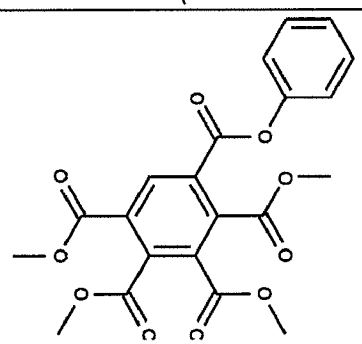
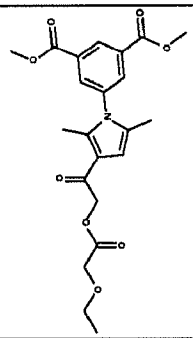
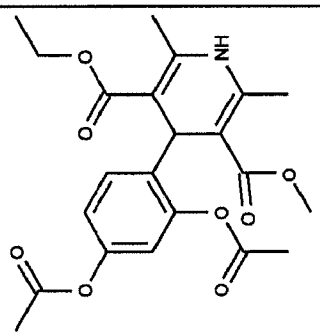
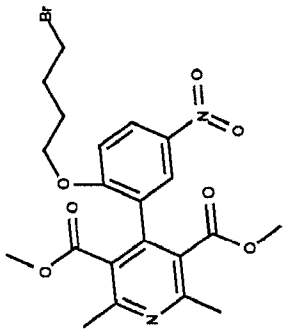
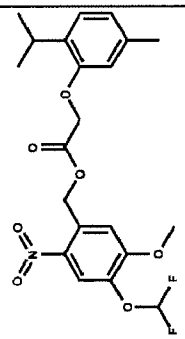
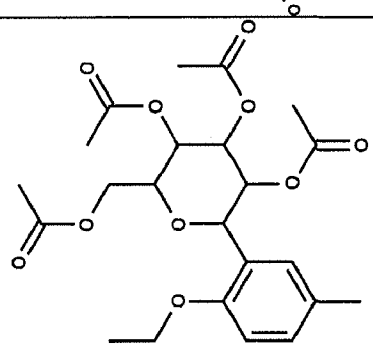
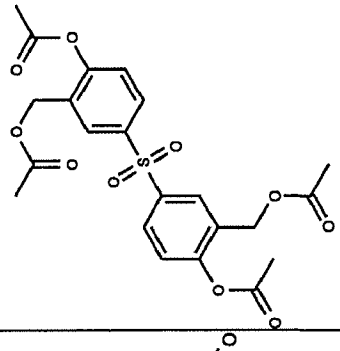
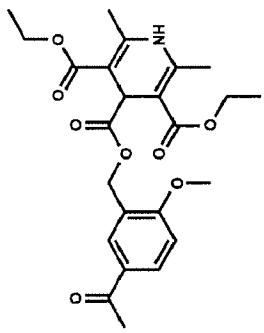
137	138	139	140
			
45113312_0 13	24355332_0 13	9980168_0 13	14580316_0 13
141	**142**	**143**	**144**
			
24557483_0 13	23080601_0 13	20293871_0 13	40146894_0 13

Fig. 23, cont'd

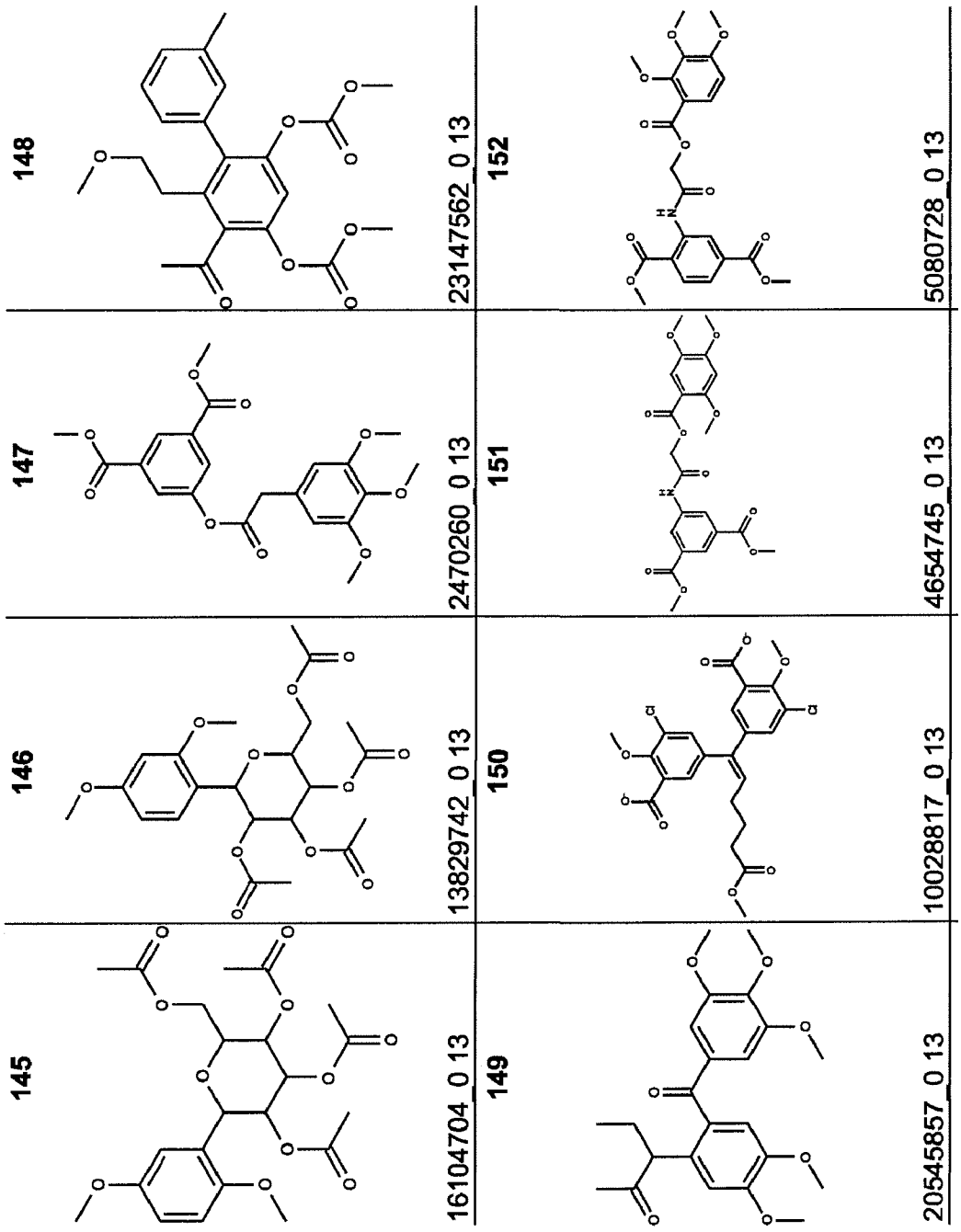

145
16104704_0 13
146
13829742_0 13
147
2470260_0 13
148
23147562_0 13
149
20545857_0 13
150
10028817_0 13
151
4654745_0 13
152
5080728_0 13

Fig. 23, cont'd

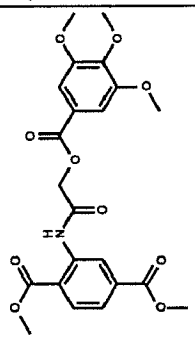
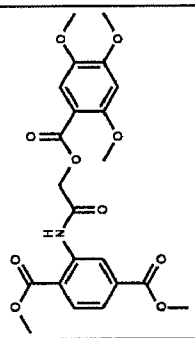
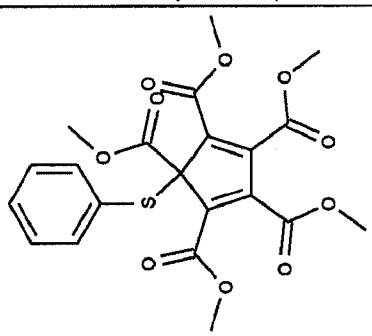
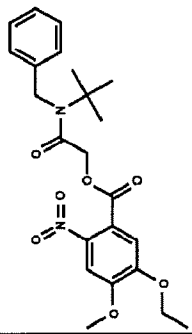
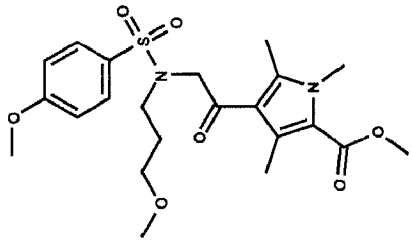
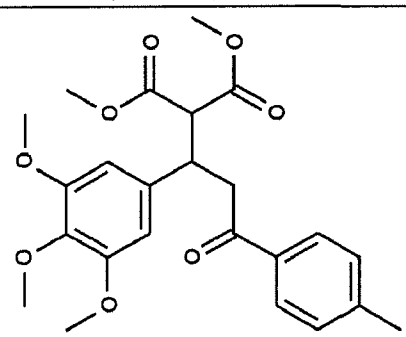
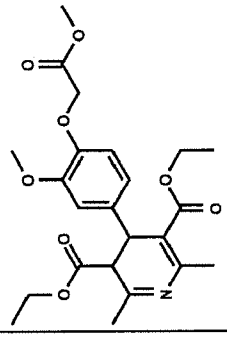
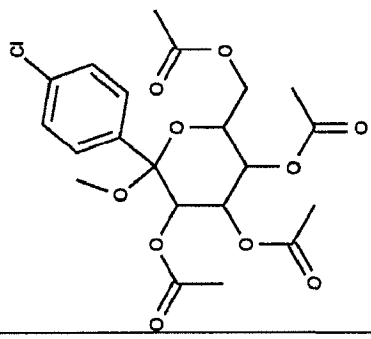
153	154	155	156
			
16251991_0 13	4348869_0 13	3368766_0 14	35350160_0 14
157	**158**	**159**	**160**
			
42823189_0 14	2768272_0,4081541	25898089_0 14	24180102_0 14

Fig. 23, cont'd

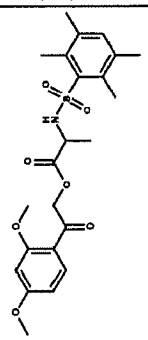
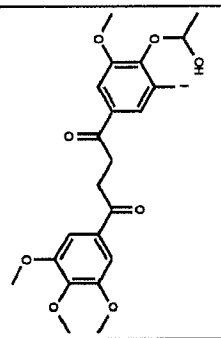
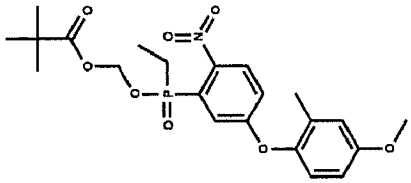
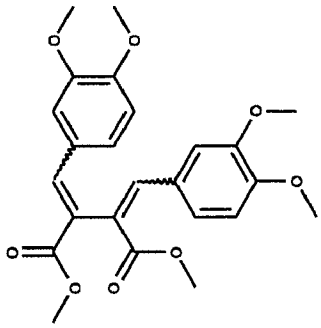
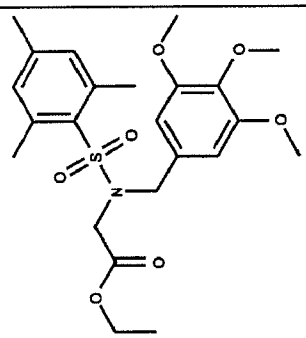
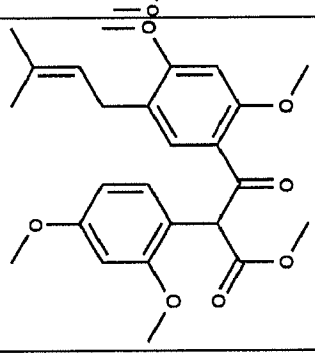
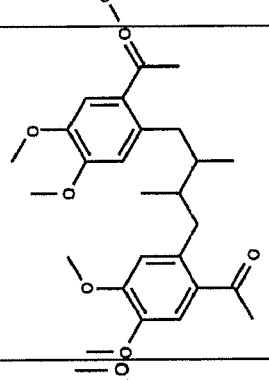
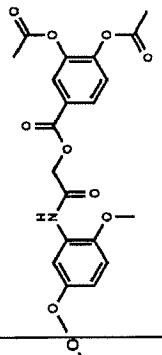
161	162	163	164
			
16279413_0,412931	18467388_0 14	20454860_0 14	16731958_0 14
165	166	167	168
			
5104009_0 14	42600506_0 14	10972262_0 14	2350747_0 14

Fig. 23, cont'd

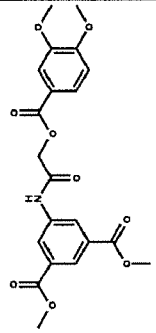
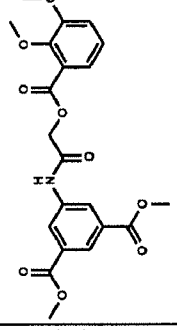
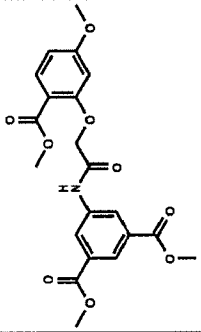
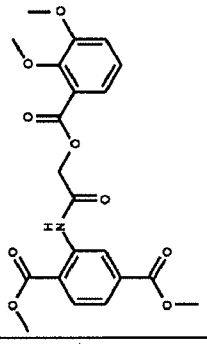
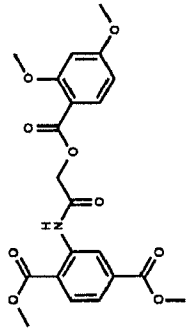
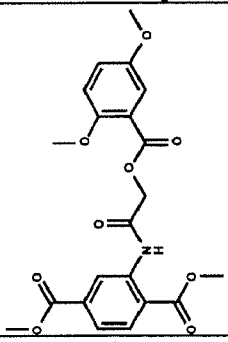
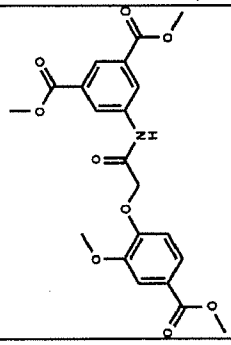
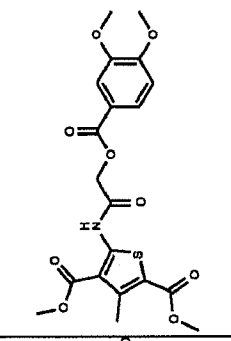
169	170	171	172
			
2591318_0 14	2528118_0 14	24390185_0 14	2503676_0 14
173	**174**	**175**	**176**
			
2505044_0 14	16232860_0 14	2627596_0 14	2591271_0 14

Fig. 23, cont'd

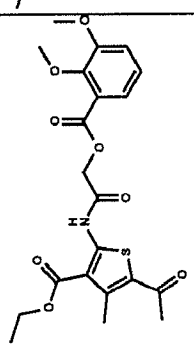
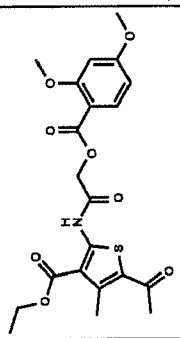
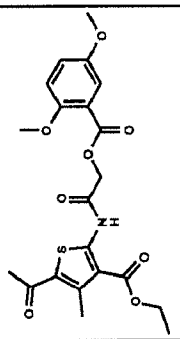
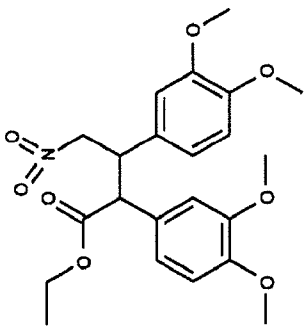
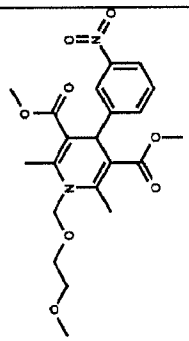
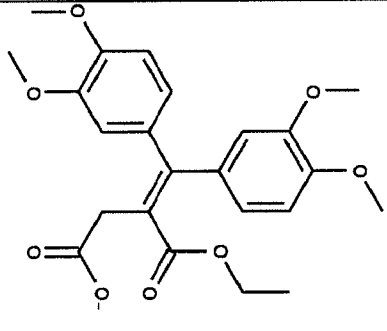
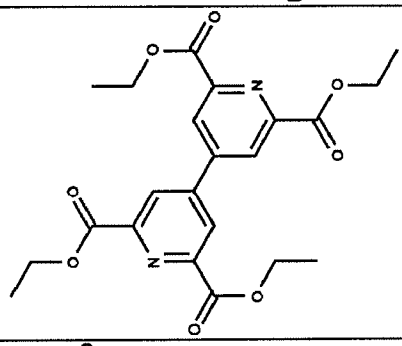
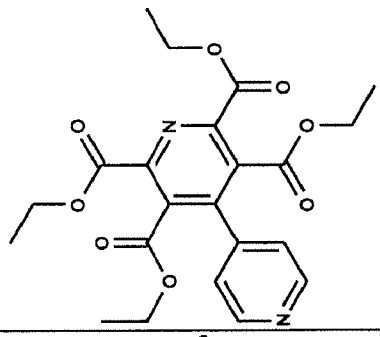
177	178	179	180
			
2528114_0 14	2504680_0 14	18775981_0 14	10025860_0,102522
181	182	183	184
			
14208793_0 14	4294879_0 14	2762457_0 14	4086243_0 14

Fig. 23, cont'd

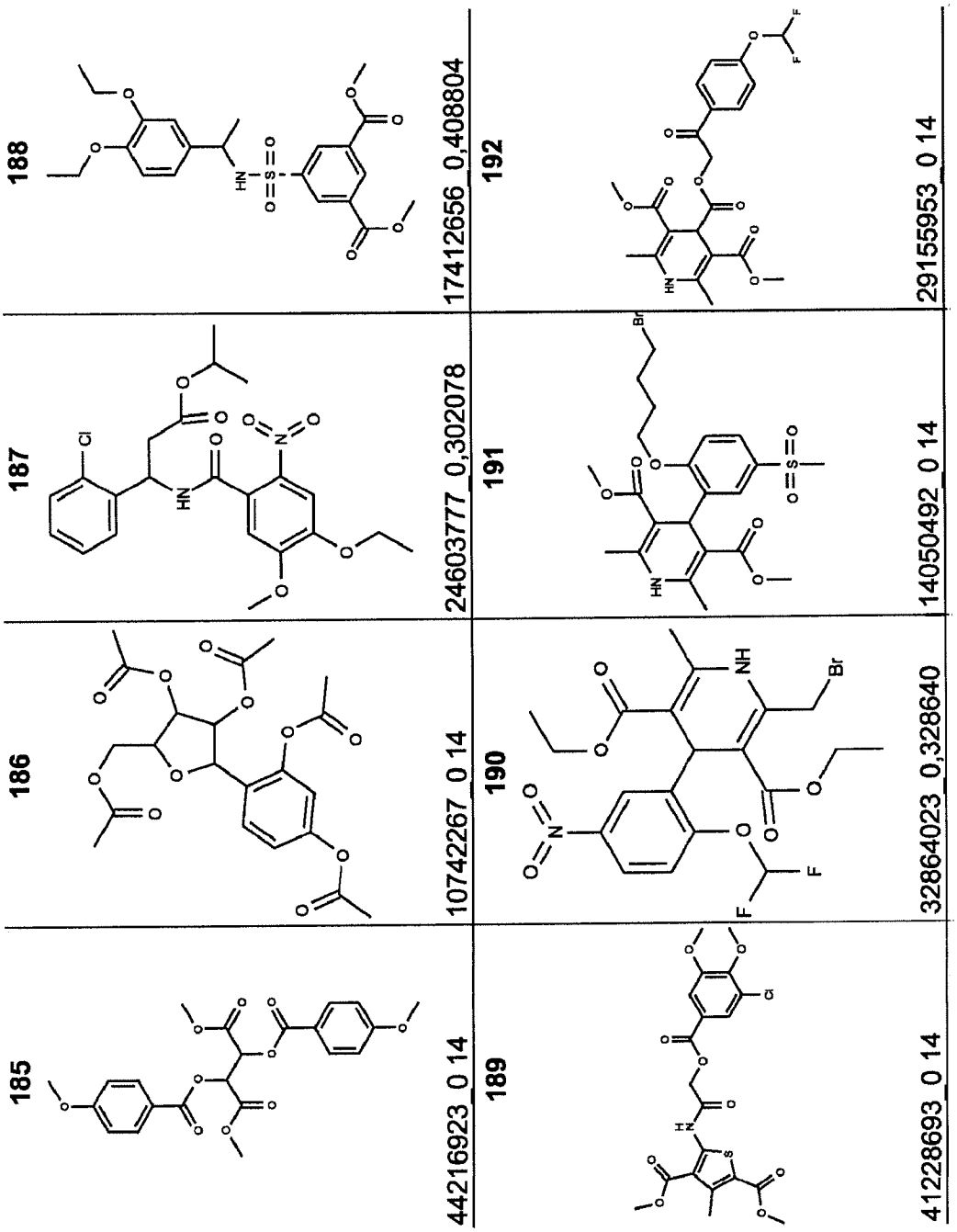

185
186
187
188
44216923_0 14
10742267_0 14
24603777_0,302078
17412656_0,408804
189
190
191
192
41228693_0 14
32864023_0,328640
14050492_0 14
29155953_0 14

Fig. 23, cont'd

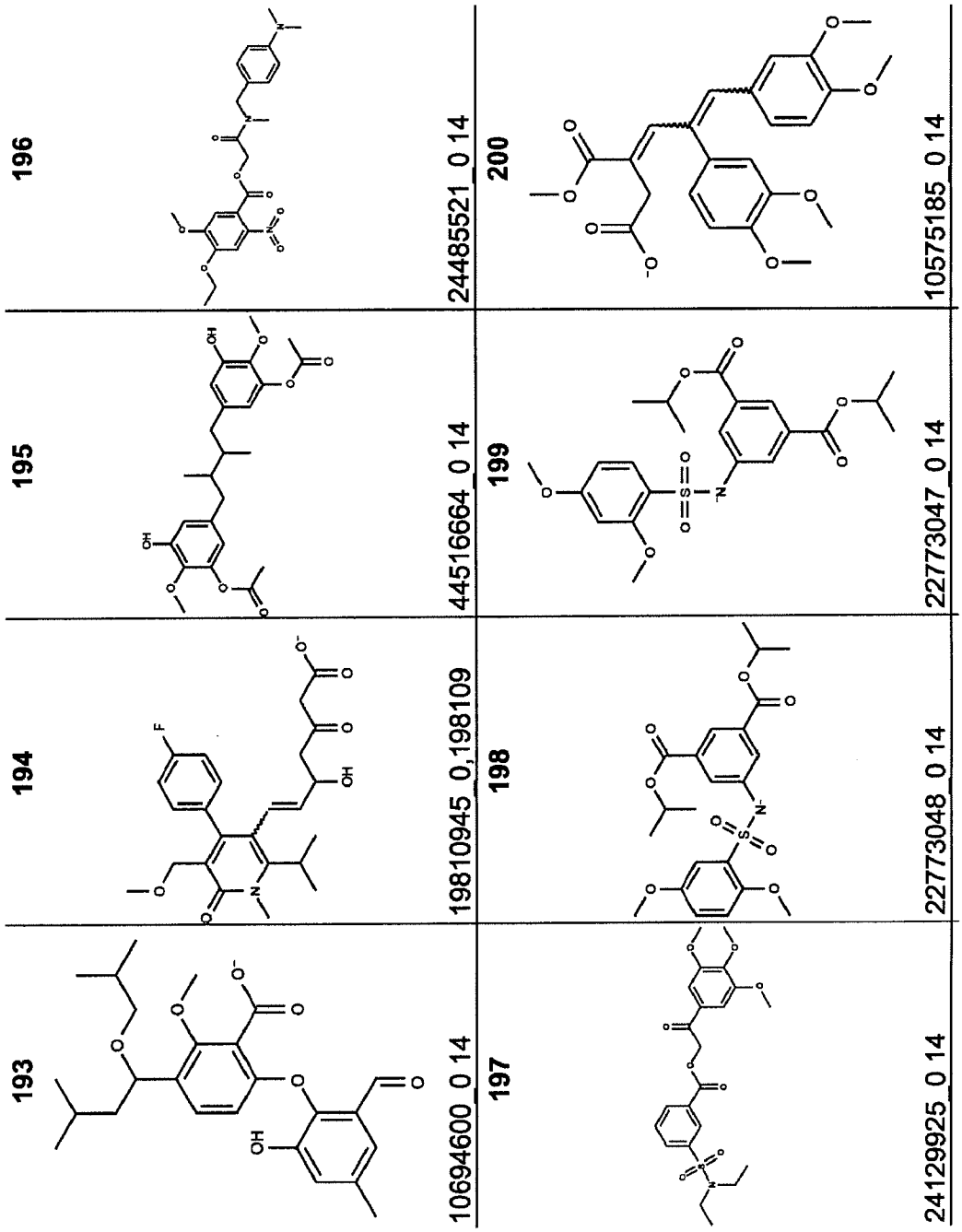

193
194
195
196
10694600_0 14
19810945_0,198109
44516664_0 14
24485521_0 14
197
198
199
200
24129925_0 14
22773048_0 14
22773047_0 14
10575185_0 14

Fig. 23, cont'd

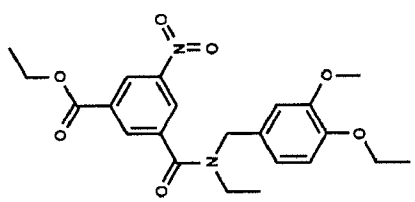
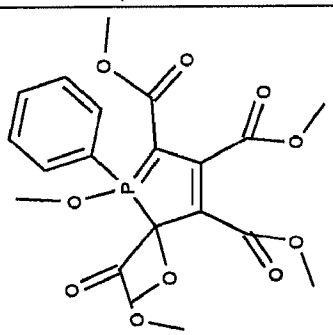
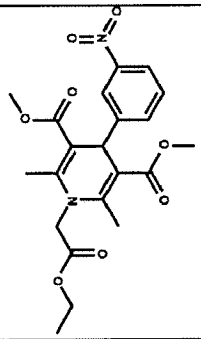
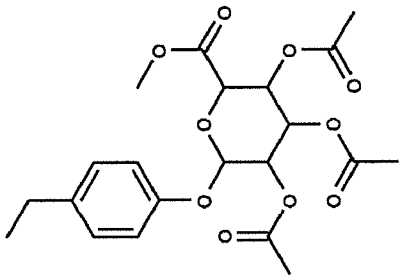
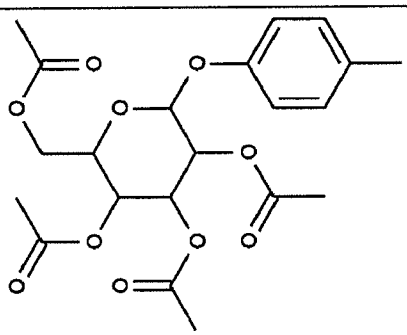
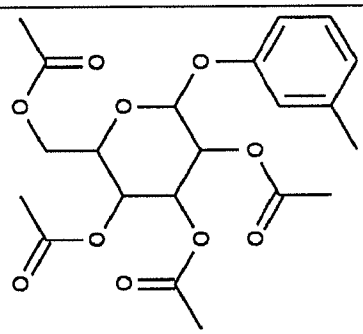
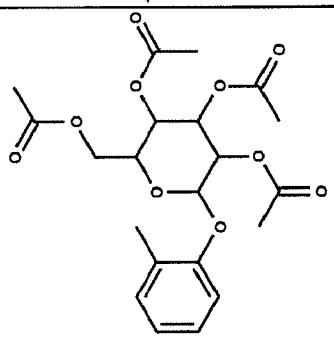
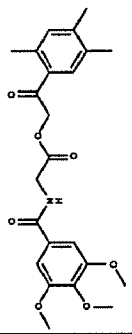
201	202	203	204
			
31338383_0 14	23416491_0 14	10598833_0 14	276318_0 14
205	**206**	**207**	**208**
			
13325752_0,256199	14370109_0,373474	10961121_0,219880	24367319_0 14

Fig. 23, cont'd

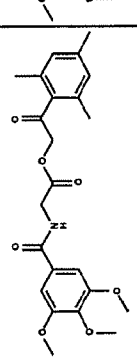
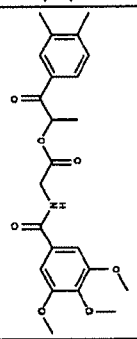
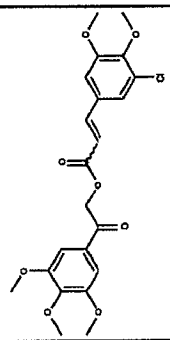
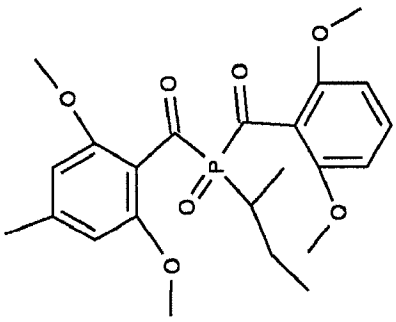
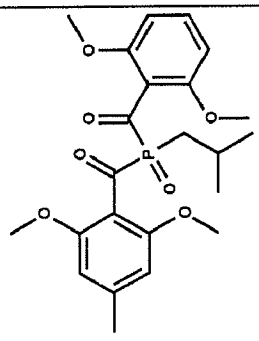
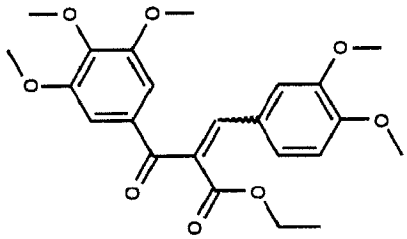
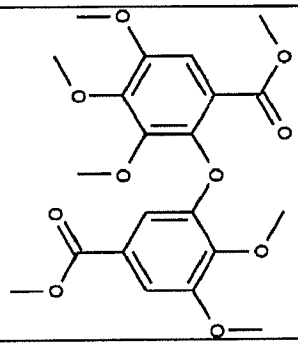
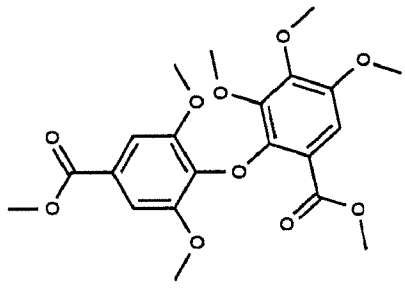
209	210	211	212
			
24367320_0 14	24367375_0,291913	25689363_0 14	22183567_0 14
213	**214**	**215**	**216**
			
22183280_0 14	44419818_0 14	10342969_0 14	10003136_0 14

Fig. 23, cont'd

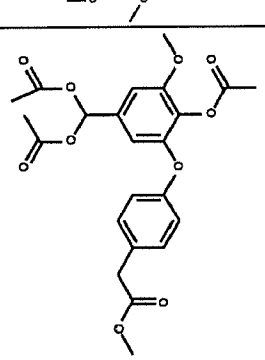
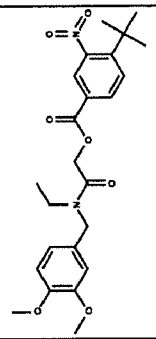
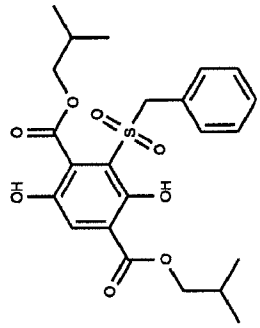
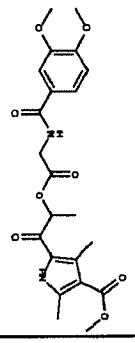
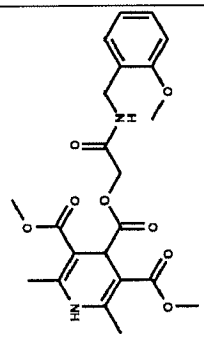
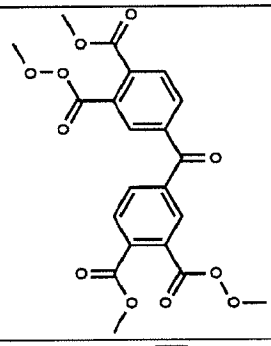
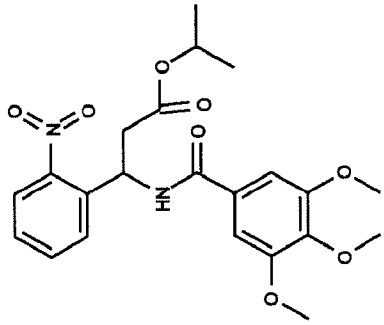
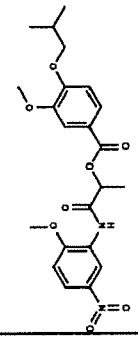
217	218	219	220
			
487797_0 14	24480122_0 14	13781843_0 14	41569085_0,415690
221	222	223	224
			
32037111_0 14	22944783_0 14	46697877_0 14	16229460_0,409419

Fig. 23, cont'd

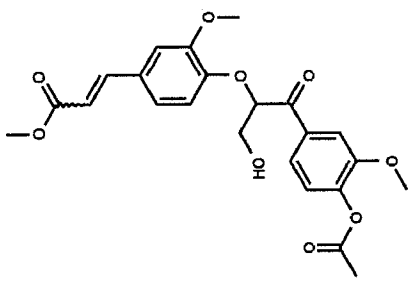
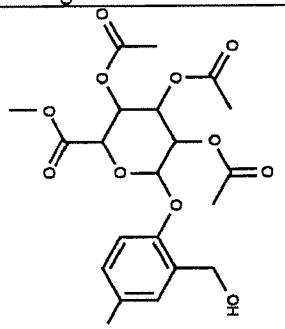
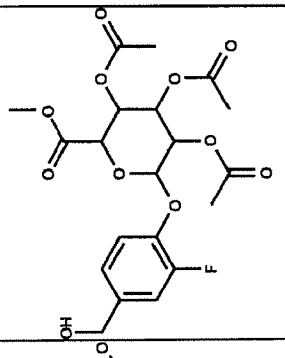
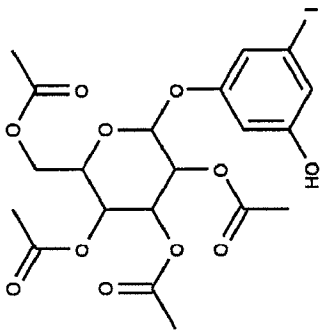
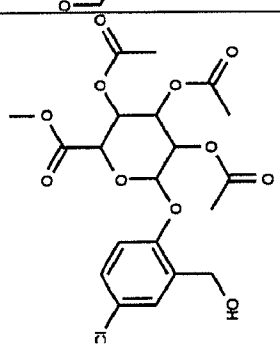
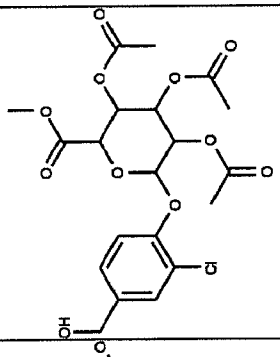
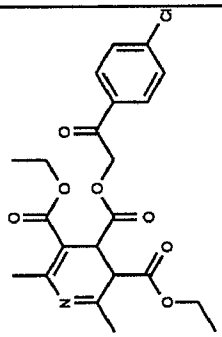
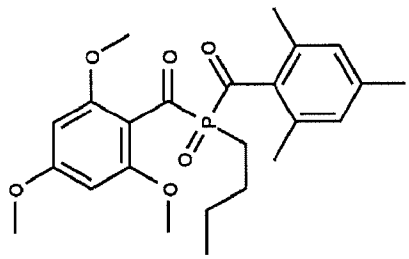
225	226	227	228
			
11026642_0 14	10790051_0 14	10575853_0 14	11410472_0 14
229	**230**	**231**	**232**
			
10576505_0 14	10790713_0 14	40933144_0 14	22183231_0 14

Fig. 23, cont'd

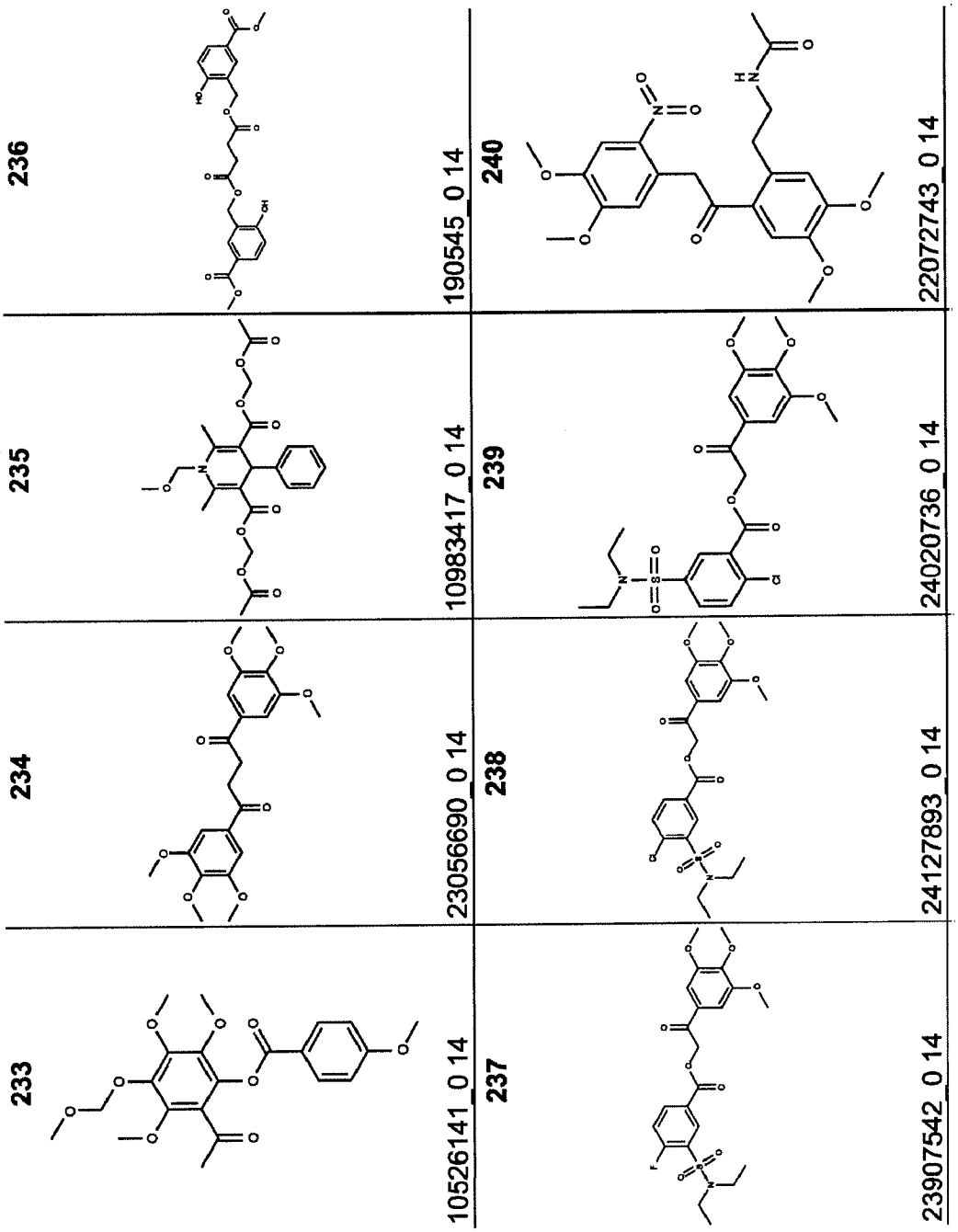

233
10526141_0 14
234
23056690_0 14
235
10983417_0 14
236
190545_0 14
237
23907542_0 14
238
24127893_0 14
239
24020736_0 14
240
22072743_0 14

Fig. 23, cont'd

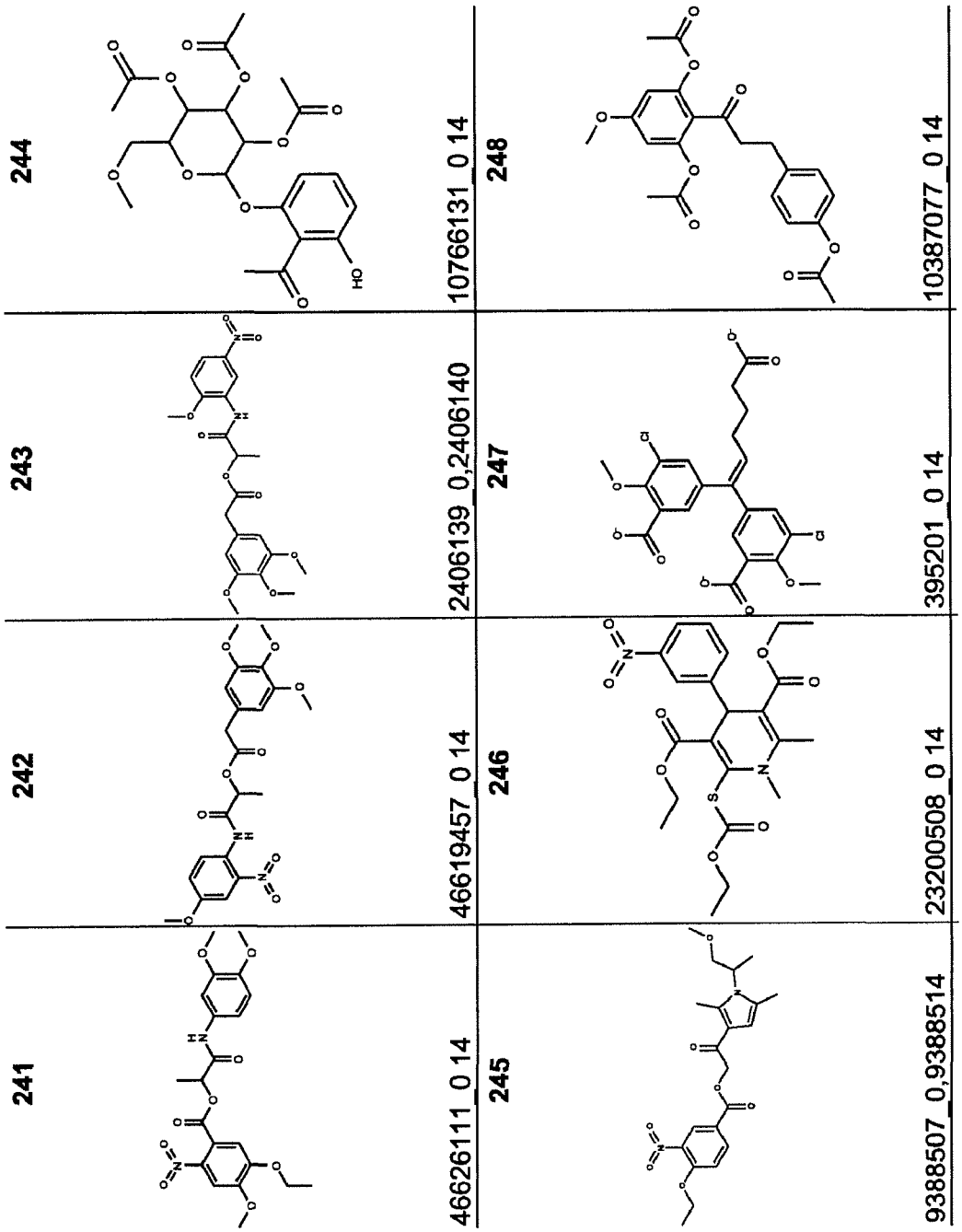

241
242
243
244
4662611_0 14
46619457_0 14
2406139_0,2406140
10766131_0 14
245
246
247
248
9388507_0,9388514
23200508_0 14
395201_0 14
10387077_0 14

Fig. 23, cont'd

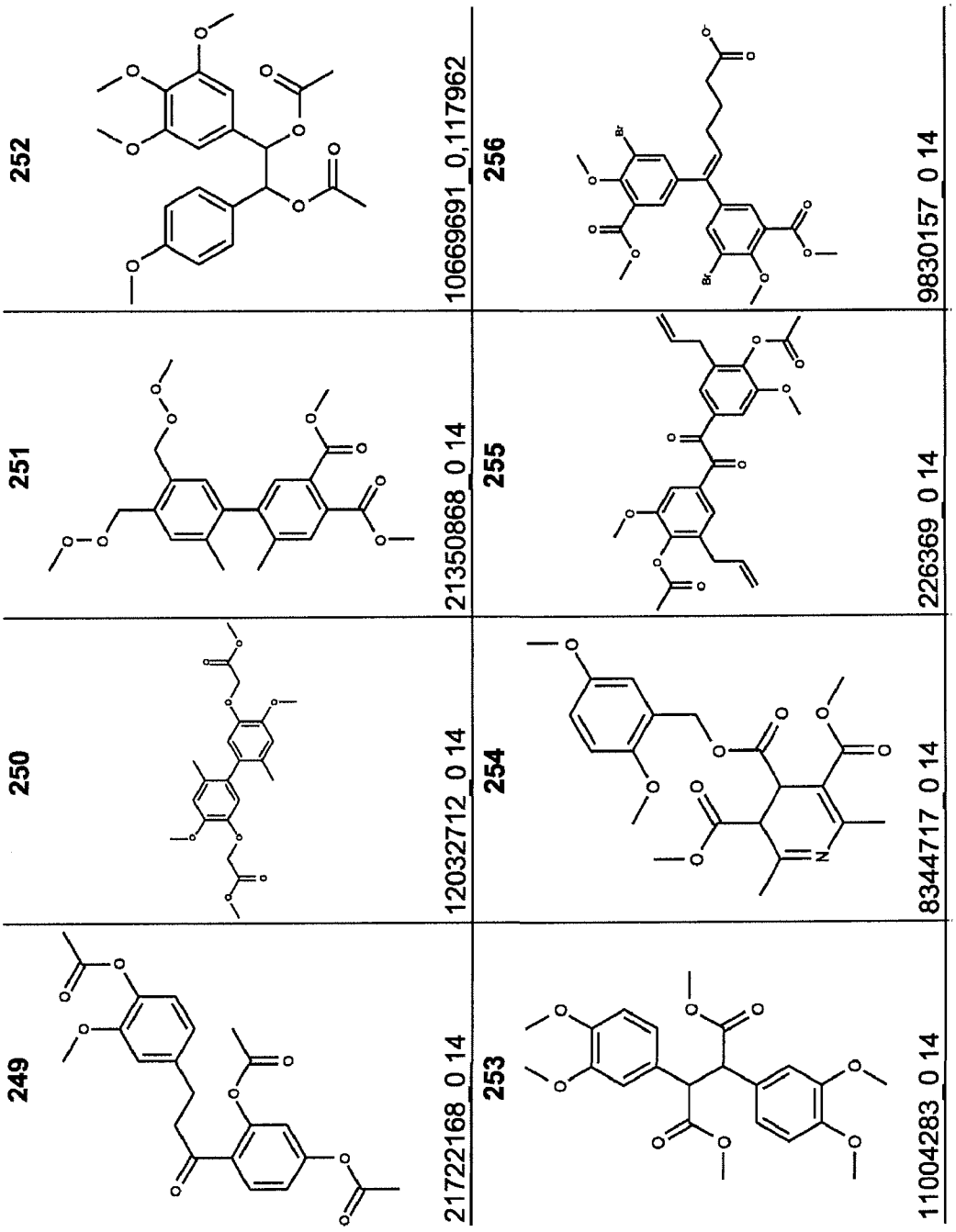

249
21722168_0 14
250
12032712_0 14
251
21350868_0 14
252
10669691_0,117962
253
11004283_0 14
254
8344717_0 14
255
226369_0 14
256
9830157_0 14

Fig. 23, cont'd

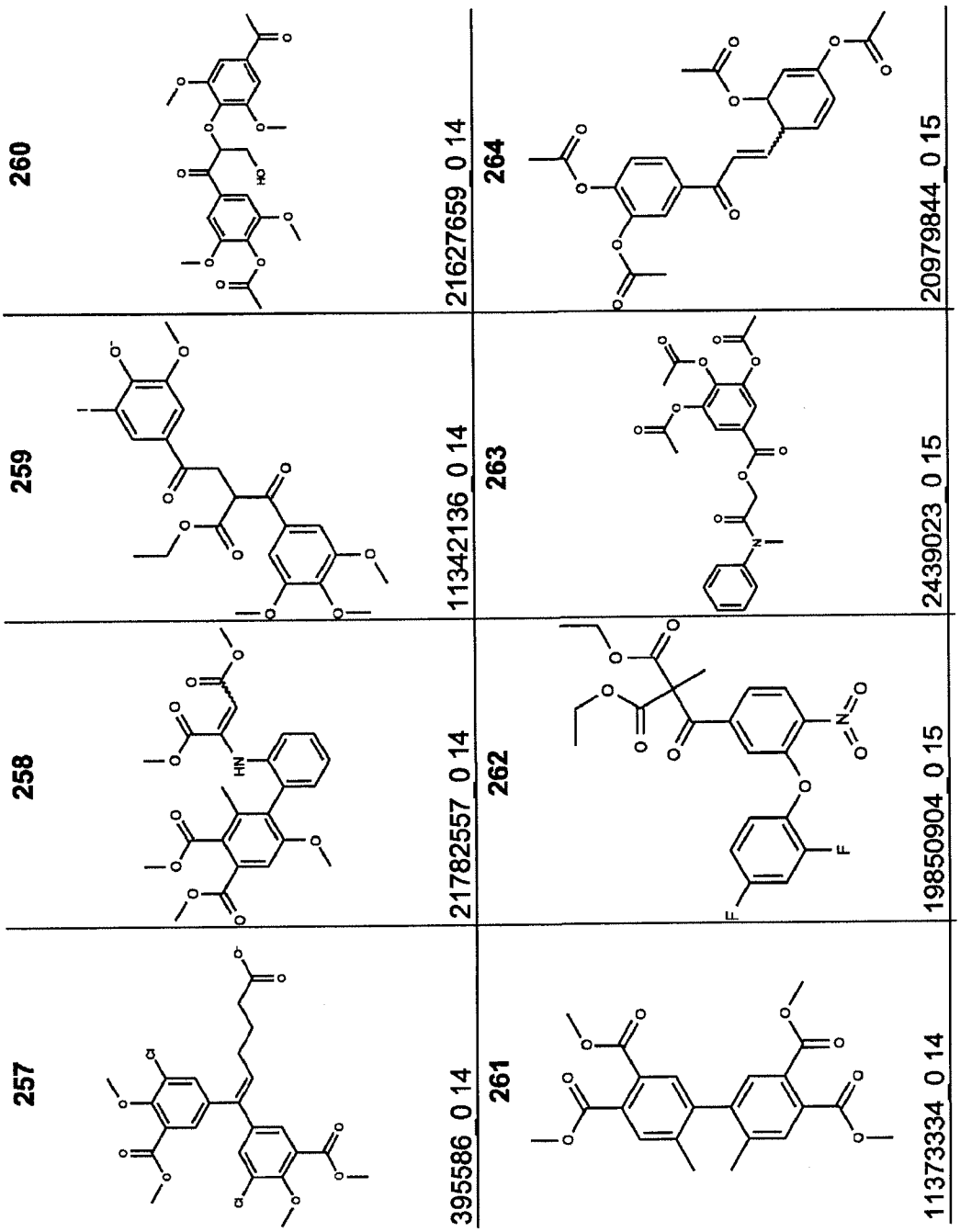

257
258
259
260
395586_0 14
21782557_0 14
11342136_0 14
21627659_0 14
261
262
263
264
11373334_0 14
19850904_0 15
2439023_0 15
20979844_0 15

Fig. 23, cont'd

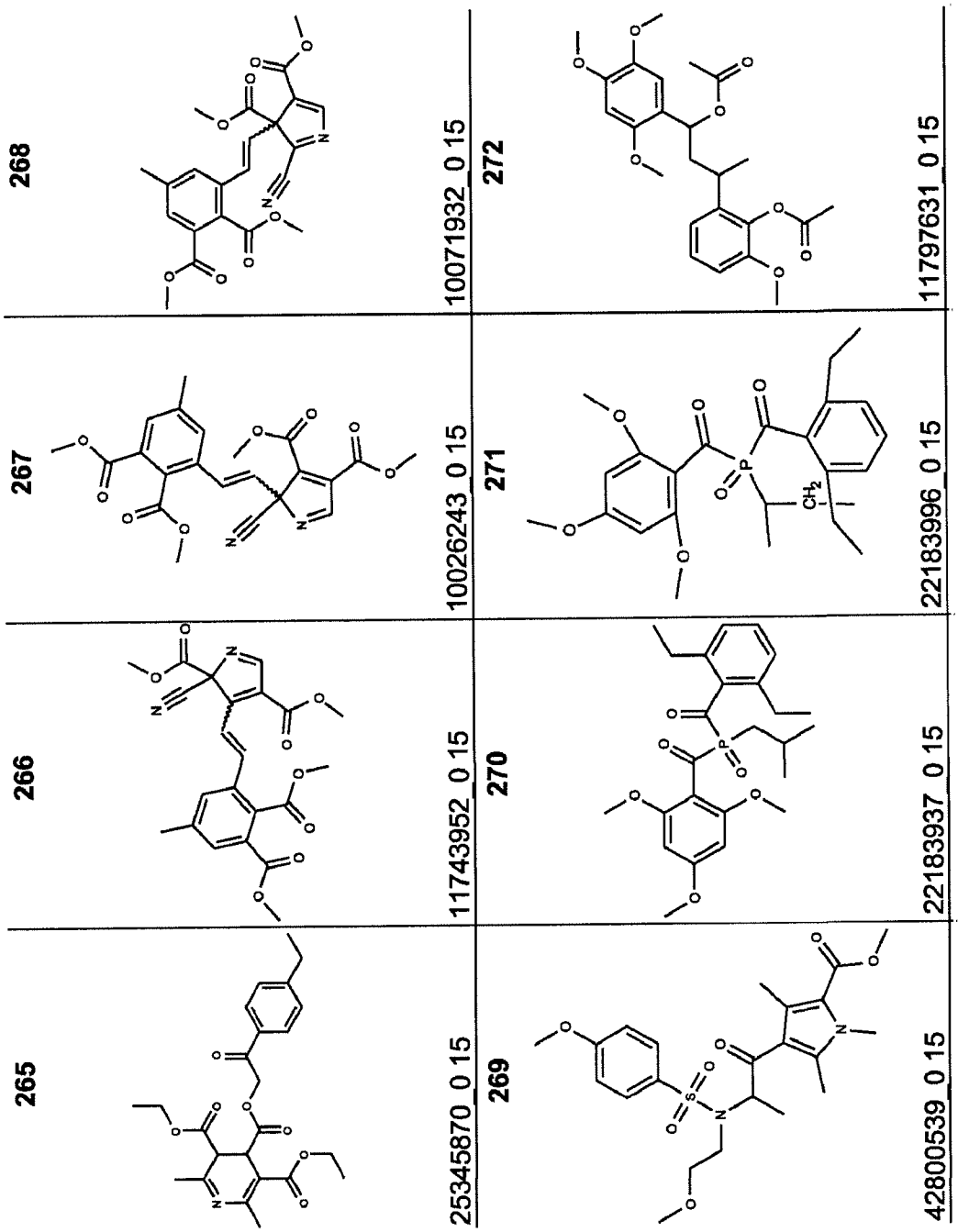

265
25345870_0 15
269
266
11743952_0 15
270
267
10026243_0 15
271
268
10071932_0 15
272
42800539_0 15
22183937_0 15
22183996_0 15
11797631_0 15

Fig. 23, cont'd

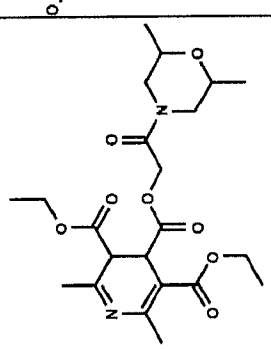
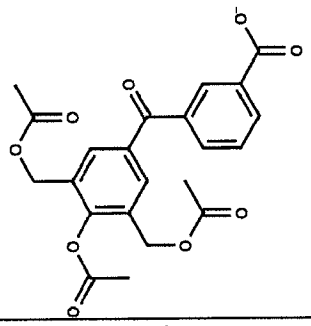
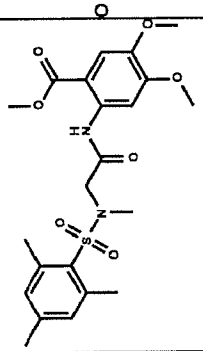
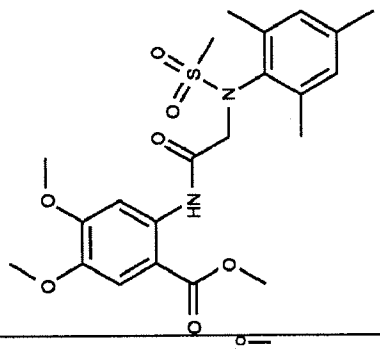
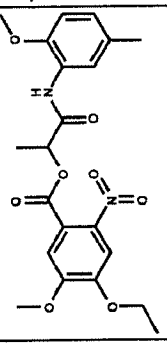
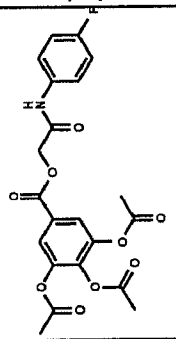
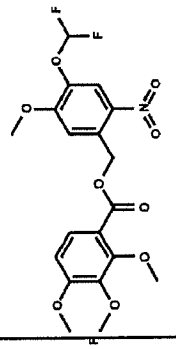
273	274	275	276
			
41039407_0,410394	14405511_0 15	45372872_0 15	30276324_0 15
277	**278**	**279**	**280**
			
45359529_0 15	46627470_0 15	17559048_0 15	24557242_0 15

Fig. 23, cont'd

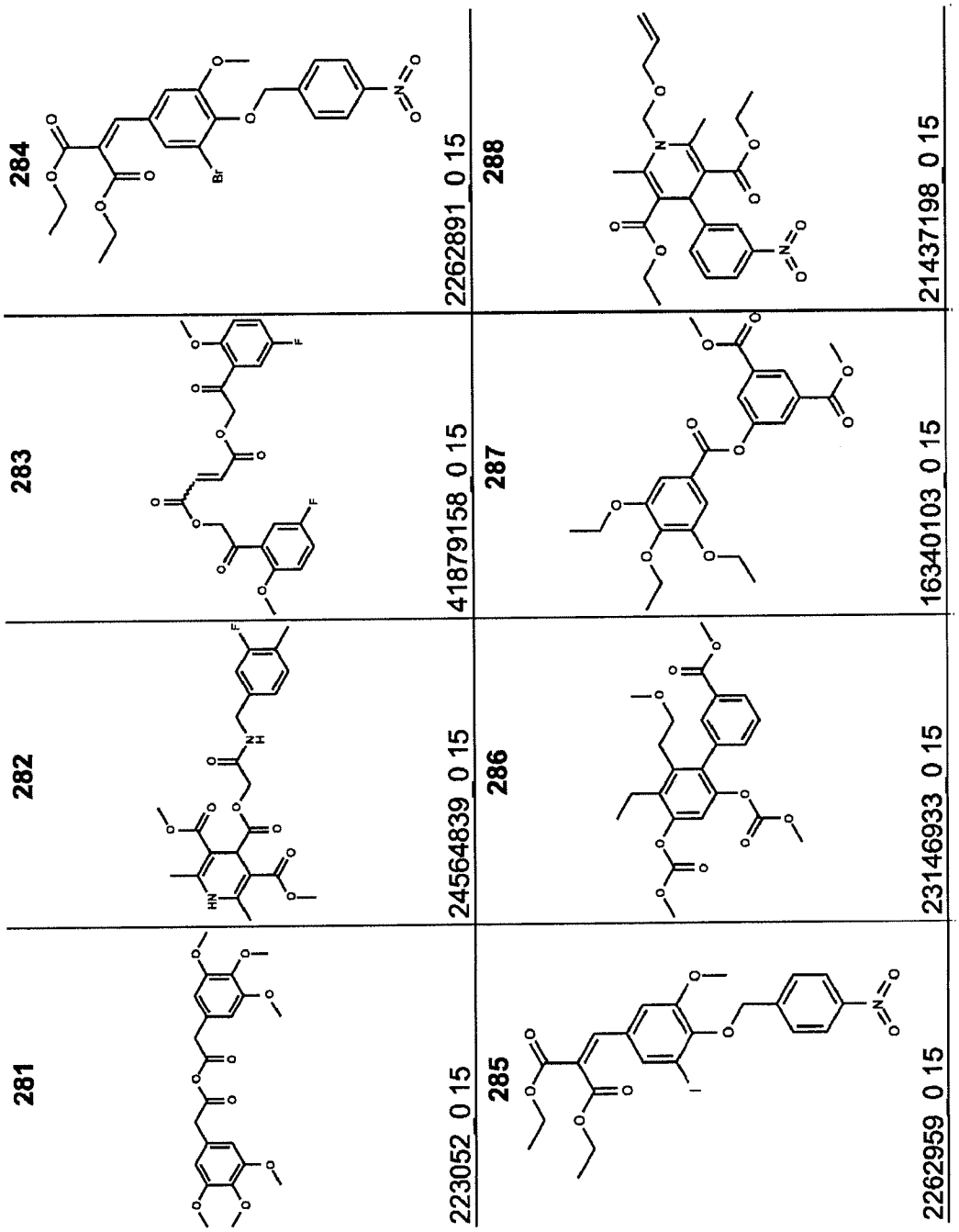

281
223052_0 15
282
2456839_0 15
283
41879158_0 15
284
2262891_0 15
285
2262959_0 15
286
23146933_0 15
287
16340103_0 15
288
21437198_0 15

Fig. 23, cont'd

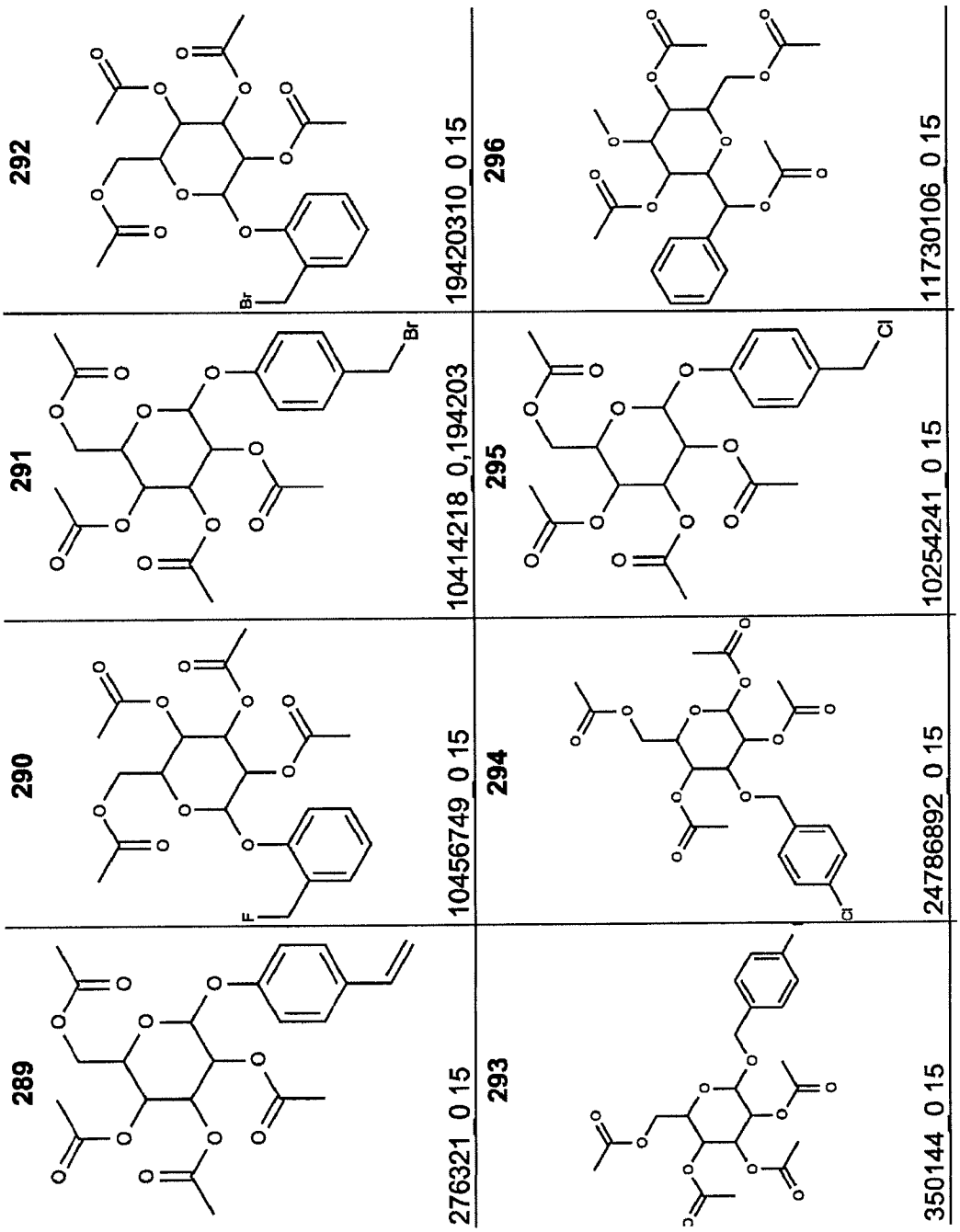

289
276321_0 15
290
10456749_0 15
291
10414218_0,194203
292
19420310_0 15
293
350144_0 15
294
24786892_0 15
295
10254241_0 15
296
11730106_0 15

Fig. 23, cont'd

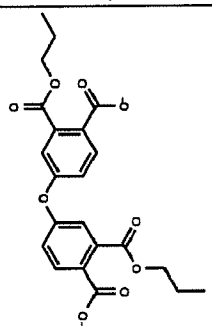
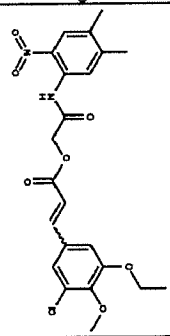
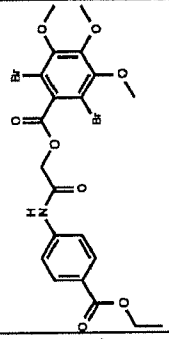
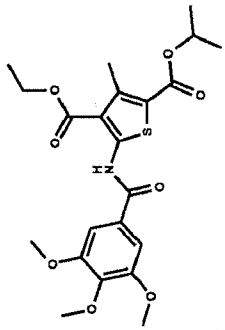
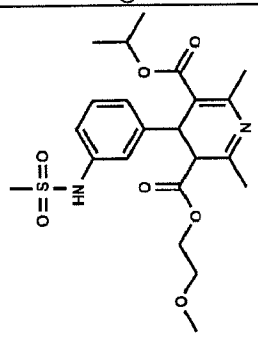
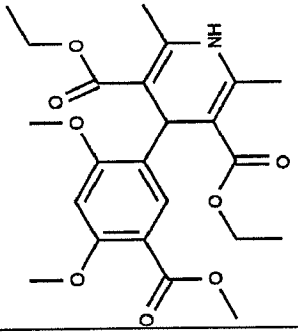
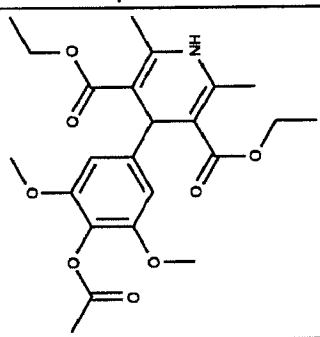
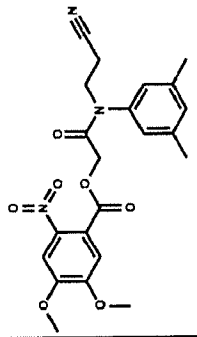
297	298	299	300
			
20321797_0 15	16280553_0 15	1682108_0 15	19182079_0 15
301	302	303	304
			
40732272_0,407322	4143811_0 15	20101061_0 15	2615156_0 15

Fig. 23, cont'd

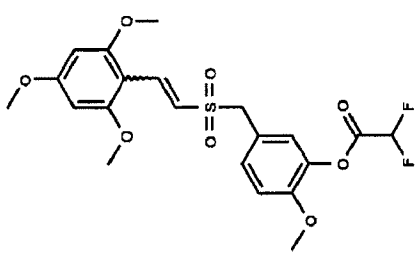
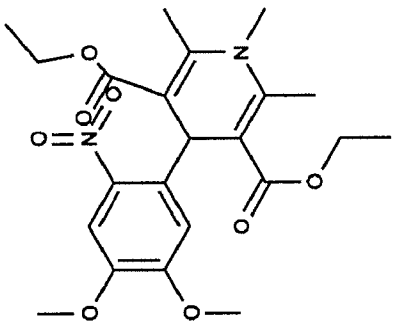
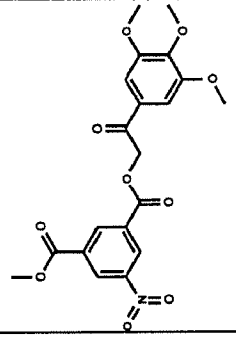
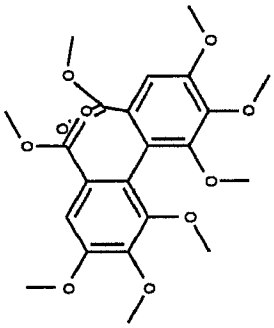
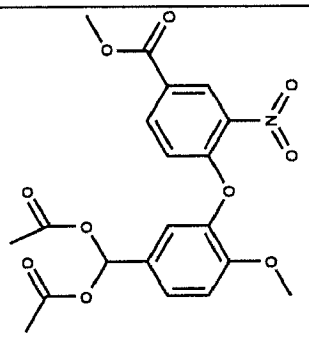
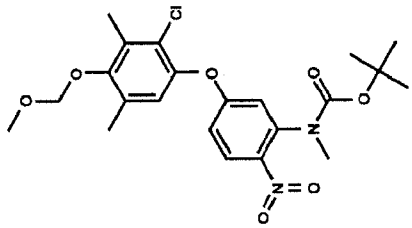
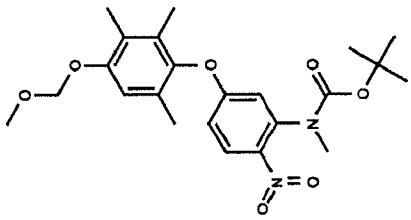
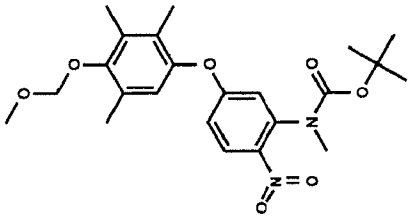
305	306	307	308
			
11751795_0 15	20766148_0 15	16796643_0 15	471114_0 15
309	**310**	**311**	**312**
			
10836528_0 15	18461339_0 15	18184930_0 15	18461411_0 15

Fig. 23, cont'd

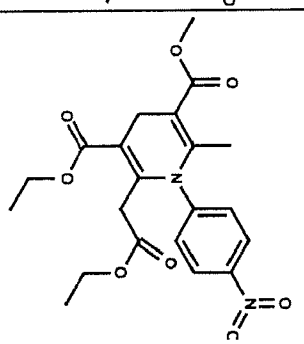
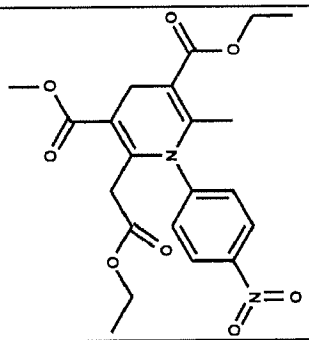
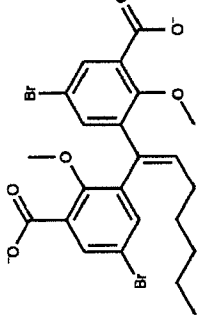
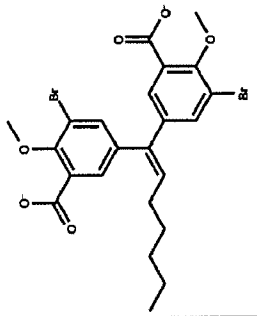
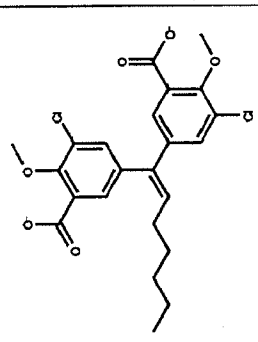
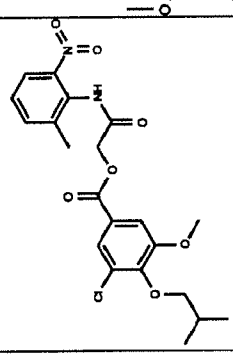
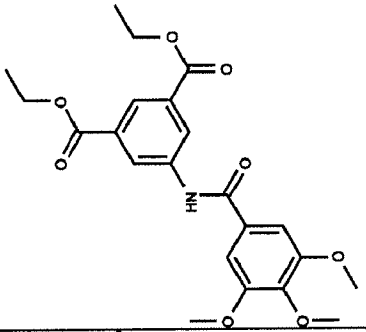
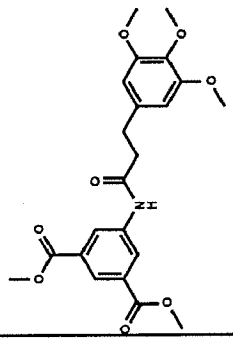
313	314	315	316
			
22009032_0 15	23004195_0 15	365177_0,365178_0	381262_0 15
317	318	319	320
			
364886_0,364887_0	41278680_0 15	4813360_0 15	24406079_0 15

Fig. 23, cont'd

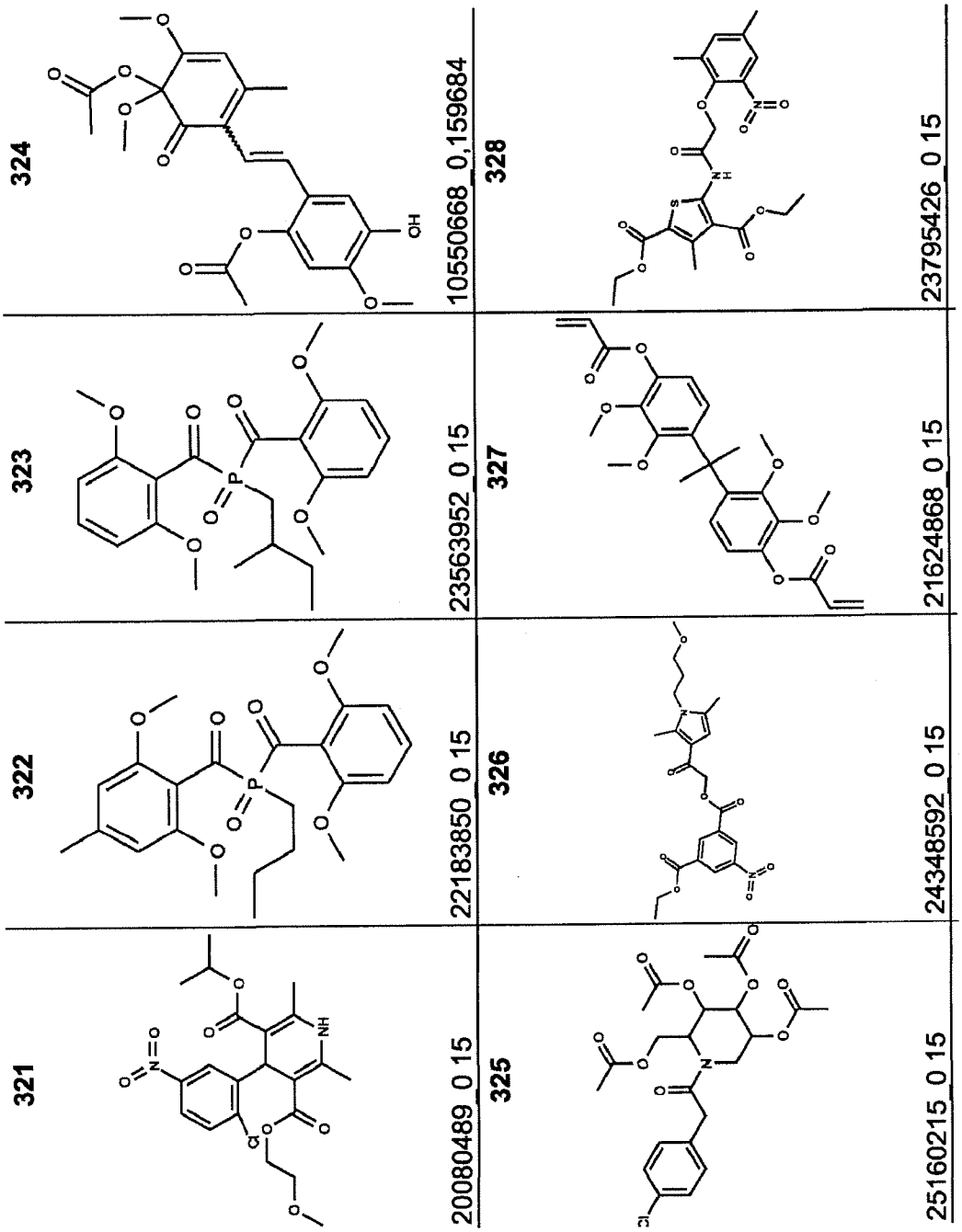

321
322
323
324
20080489_0 15
22183850_0 15
23563952_0 15
10550668_0,159684
325
326
327
328
25160215_0 15
24348592_0 15
21624868_0 15
23795426_0 15

Fig. 23, cont'd

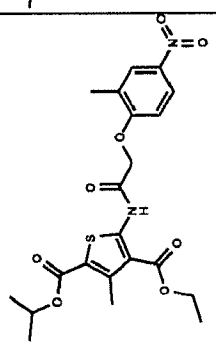
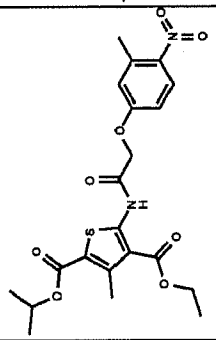
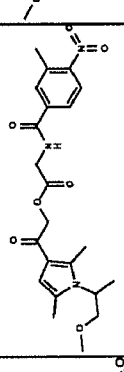
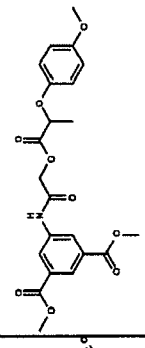
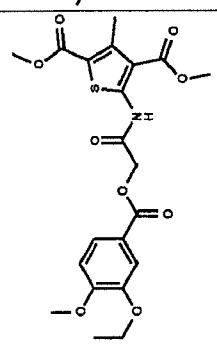
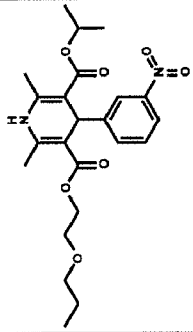
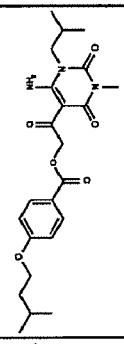
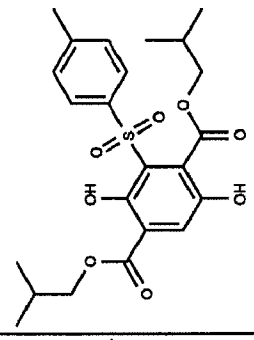
329	330	331	332
			
2072544_0 15	2072634_0 15	46787282_0 15	46509782_0 15
333	**334**	**335**	**336**
			
24370262_0 15	3017726_0 15	3975274_0 15	13781841_0 15

Fig. 23, cont'd

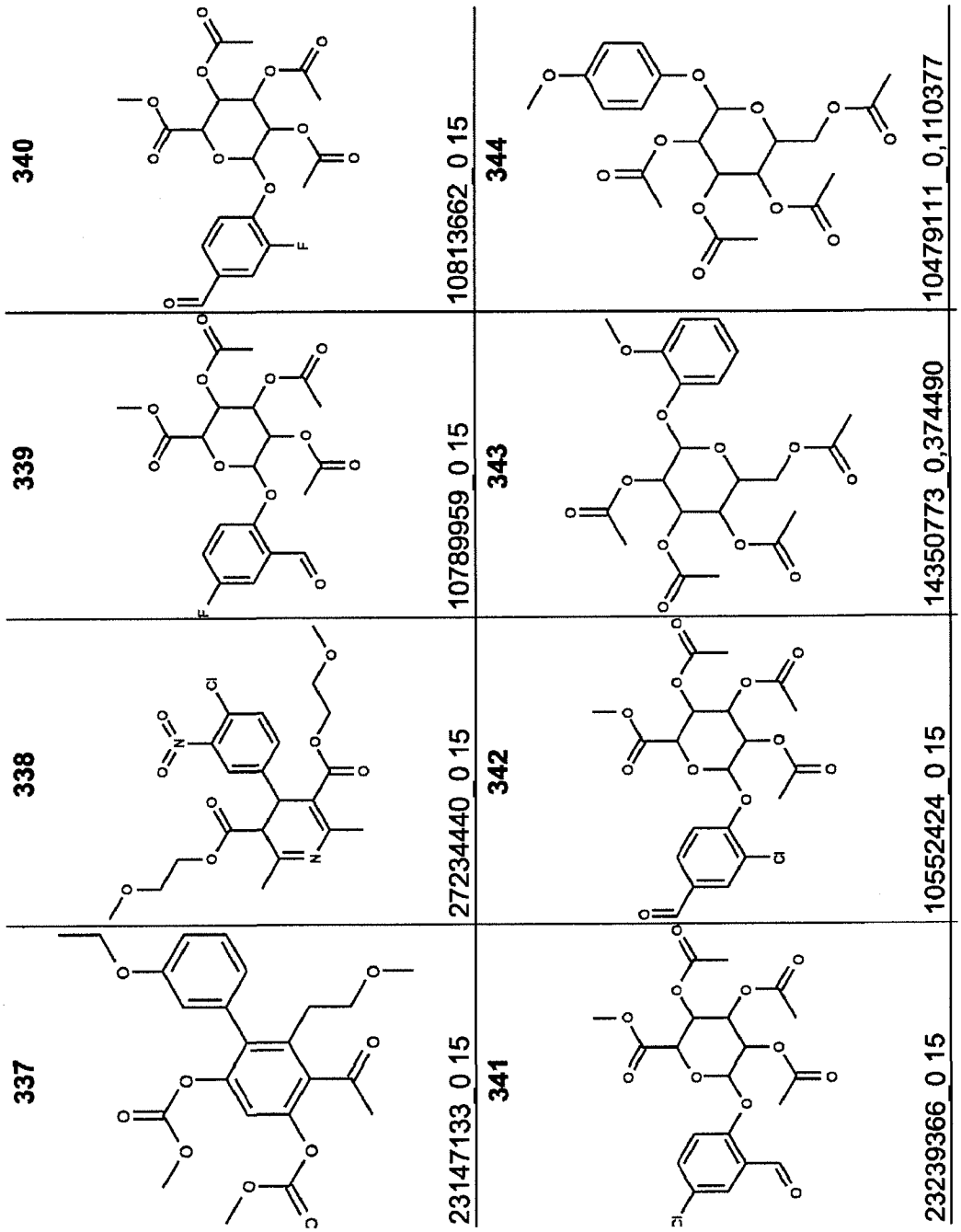

337
338
339
340
23147133_0 15
27234440_0 15
1078959_0 15
10813662_0 15
341
342
343
344
23239366_0 15
10552424_0 15
14350773_0,374490
10479111_0,110377

Fig. 23, cont'd

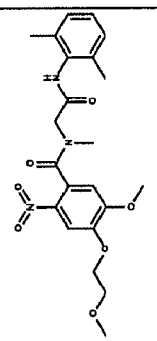
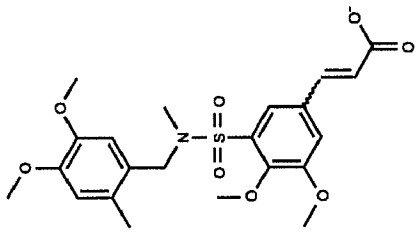
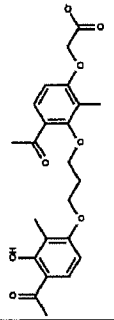
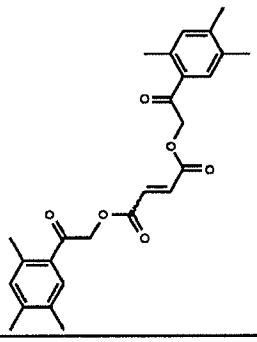
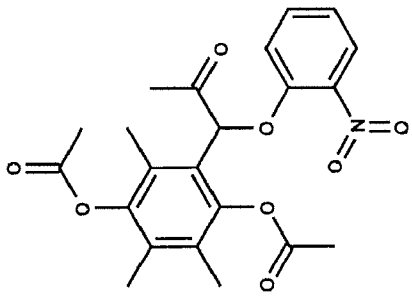
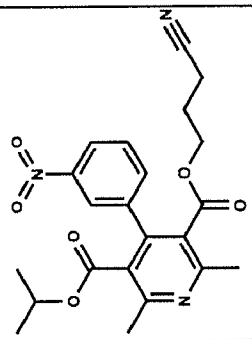
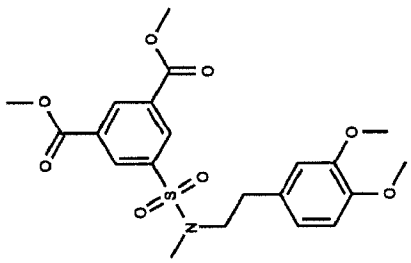
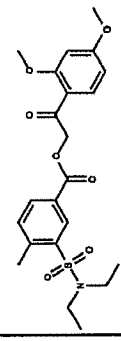
345	346	347	348
			
32116221_0 15	45439519_0 15	21286975_0 15	3892284_0 15
349	**350**	**351**	**352**
			
12506451_0 15	20161404_0 15	26949012_0 15	2545994_0 15

Fig. 23, cont'd

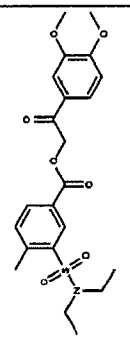
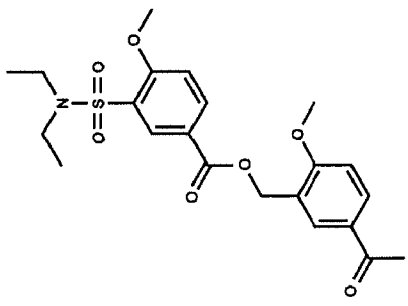
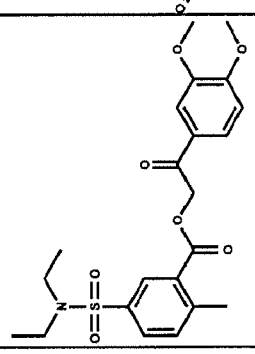
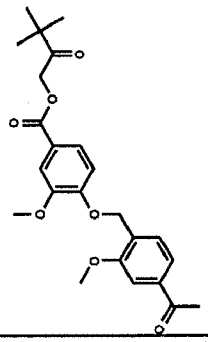
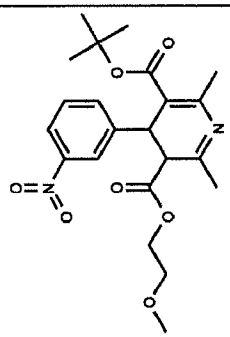
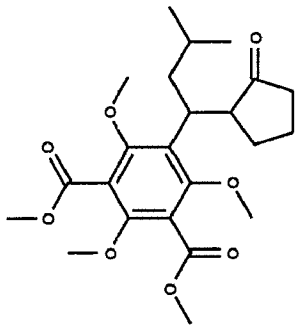
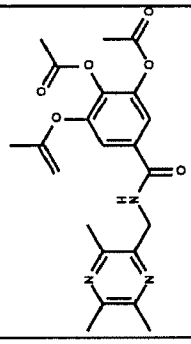
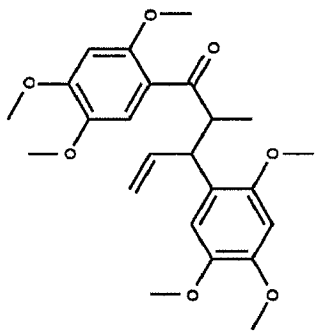
353	354	355	356
			
2545778_0 15	16512589_0 15	31725217_0 15	2128958_0 15
357	358	359	360
			
27234380_0,272343	11080611_0 15	25216622_0 15	10025706_0,103653

Fig. 23, cont'd

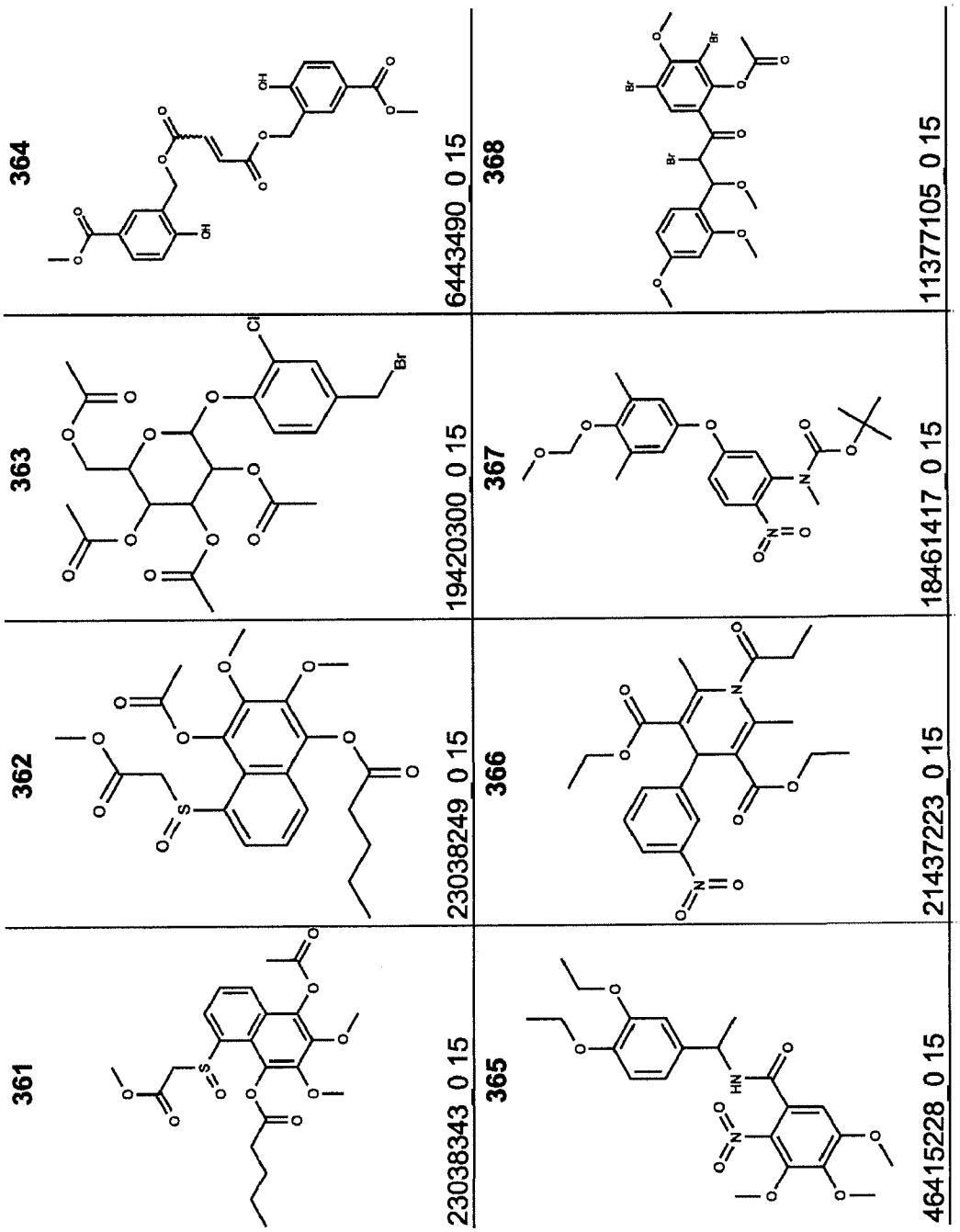

361
362
363
364
23038343_0 15
23038249_0 15
19420300_0 15
6443490_0 15
365
366
367
368
46415228_0 15
21437223_0 15
18461417_0 15
11377105_0 15

Fig. 23, cont'd

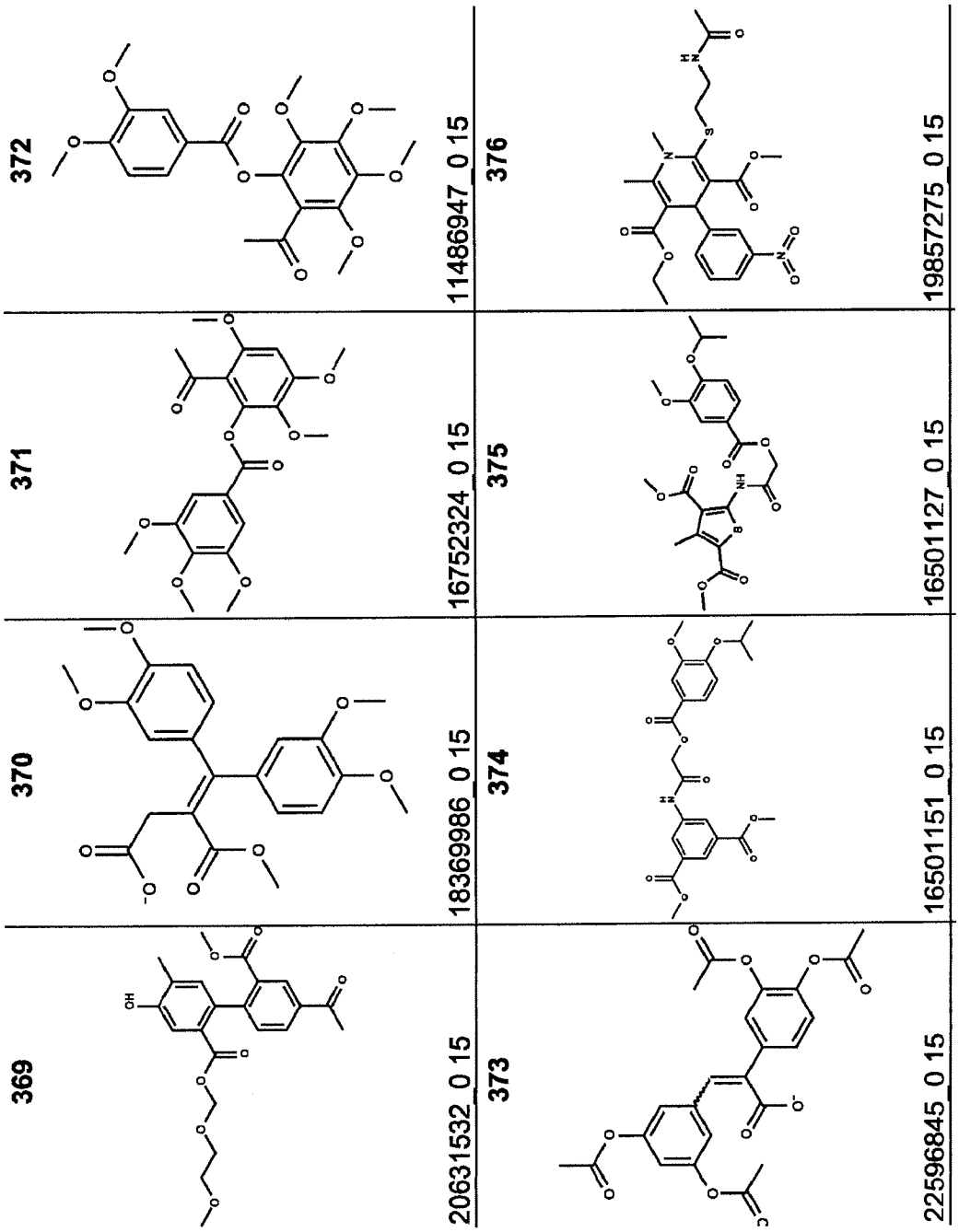

369
20631532_0 15
370
18369986_0 15
371
16752324_0 15
372
11486947_0 15
373
22596845_0 15
374
16501151_0 15
375
16501127_0 15
376
19857275_0 15

Fig. 23, cont'd

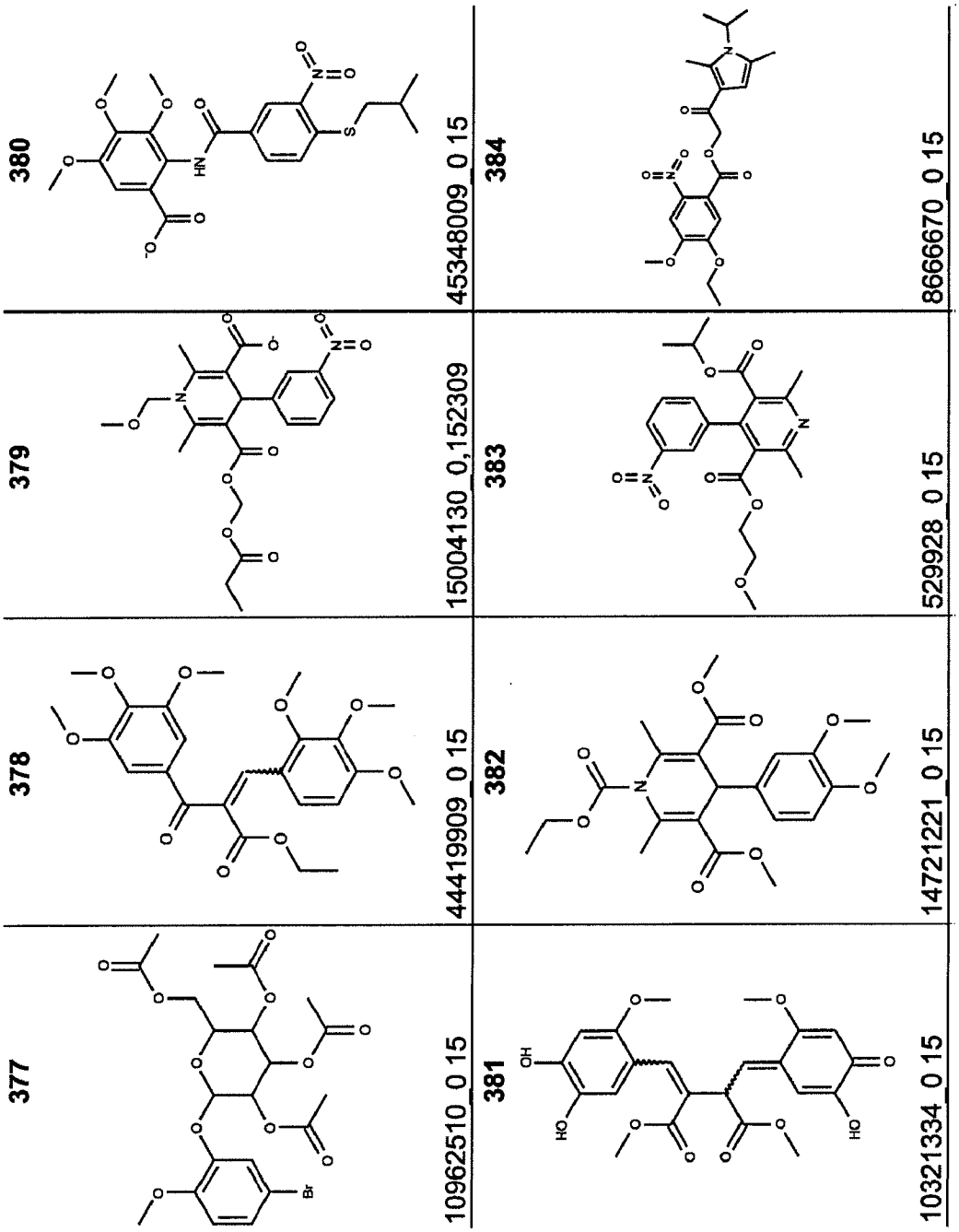

377
10962510_0 15
378
44419909_0 15
379
15004130_0,152309
380
45348009_0 15
381
10321334_0 15
382
14721221_0 15
383
529928_0 15
384
8666670_0 15

Fig. 23, cont'd

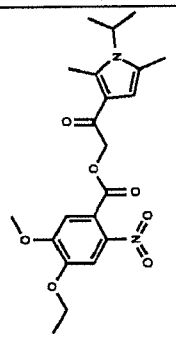
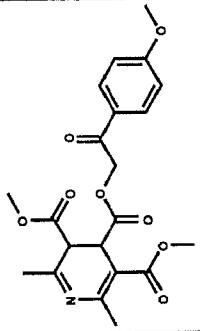
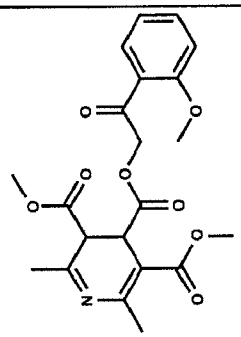
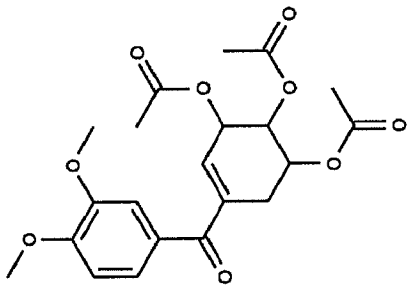
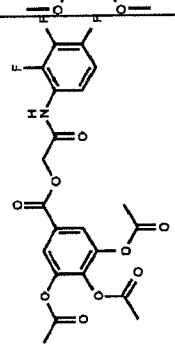
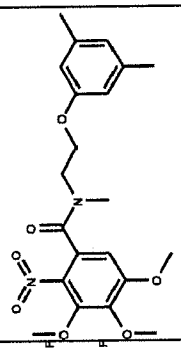
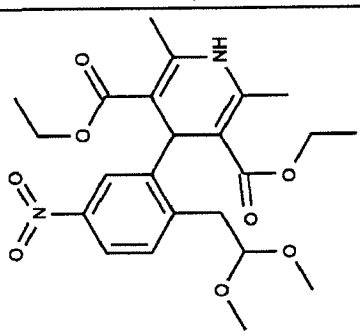
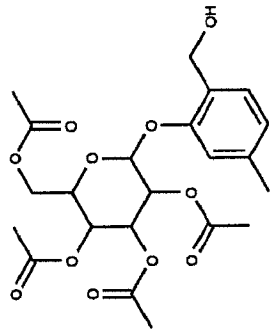
385	386	387	388
			
9125129_0 15	7587071_0 15	7586967_0 15	46831545_0 15
389	390	391	392
			
2389949_0 15	18119698_0 15	20199022_0 15	14837936_0 15

Fig. 23, cont'd

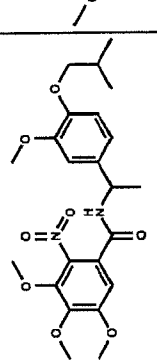
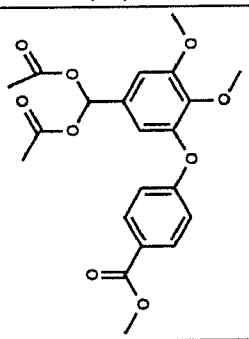
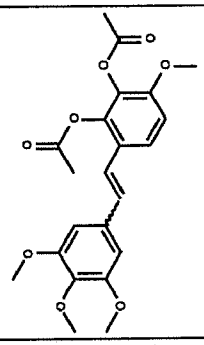
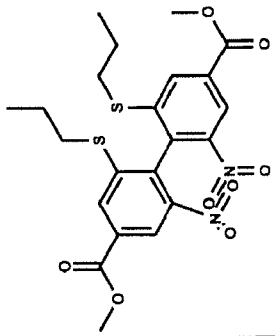
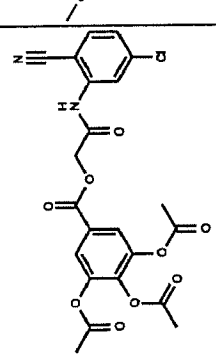
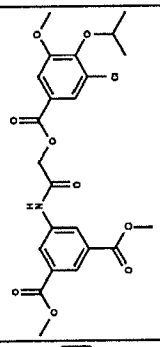
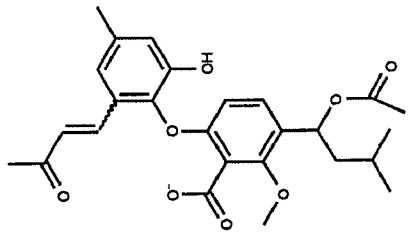
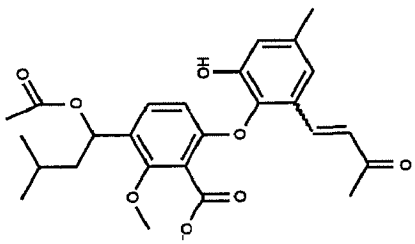
393	394	395	396
			
46418477_0 15	487804_0 15	356770_0,5386547_0	11752547_0 15
397	**398**	**399**	**400**
			
2358595_0 15	16517104_0 15	38350837_0,383508	38350838_0,383508

Fig. 23, cont'd

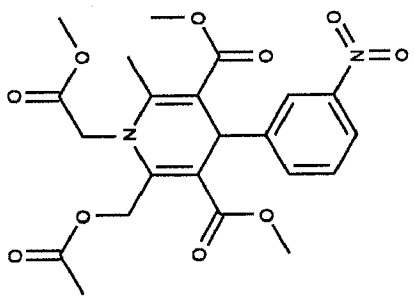
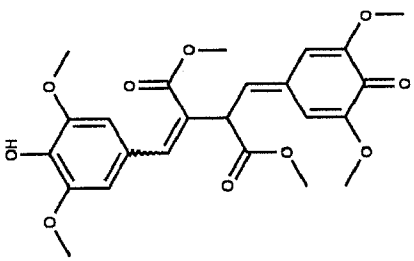
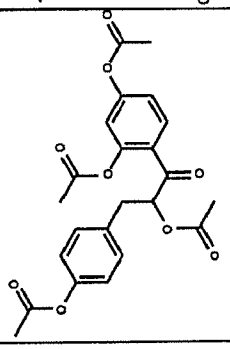
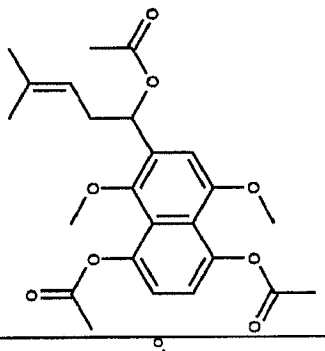
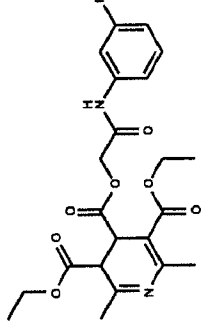
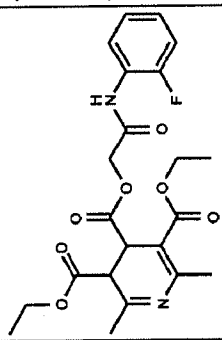
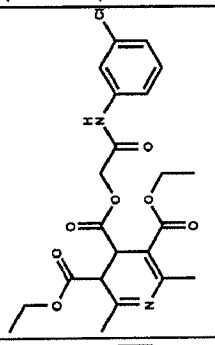
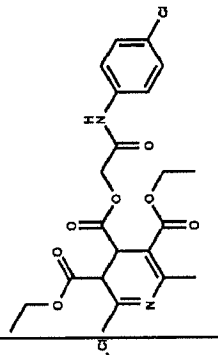
401	402	403	404
			
11798785_0 15	10073601_0 15	14632194_0 16	10917249_0 16
405	**406**	**407**	**408**
			
41101850_0 16	40950258_0 16	40950255_0 16	41101782_0 16

Fig. 23, cont'd

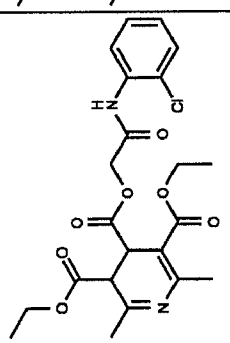
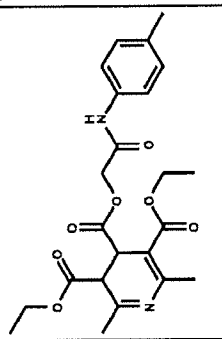
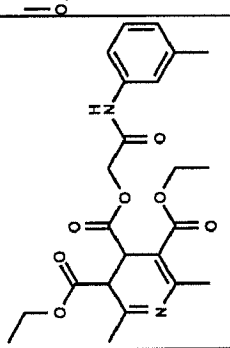
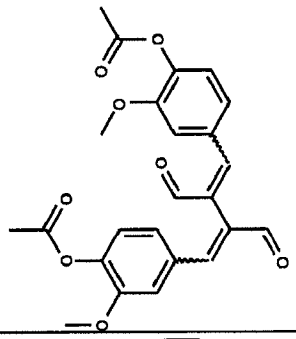
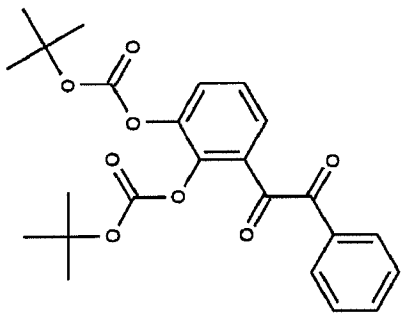
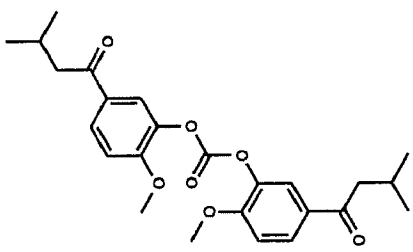
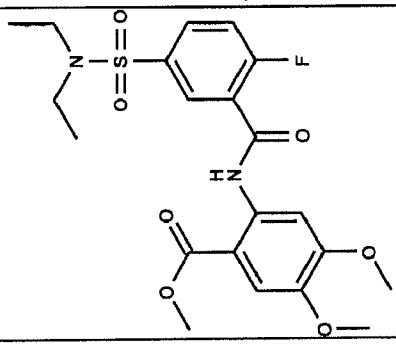
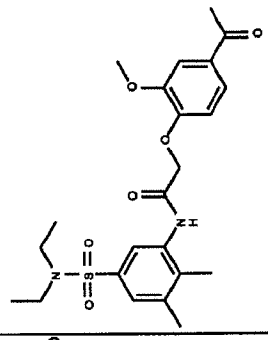
409	410	411	412
			
41101817_0 16	40956726_0 16	41022235_0 16	11189832_0 16
413	**414**	**415**	**416**
			
20277636_0 16	16101159_0 16	4800359_0 16	27832617_0 16

Fig. 23, cont'd

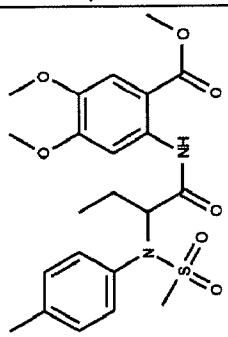
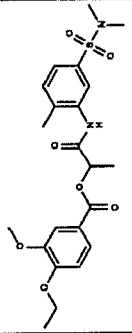
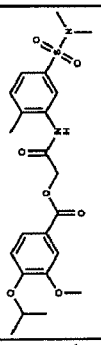
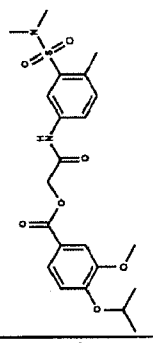
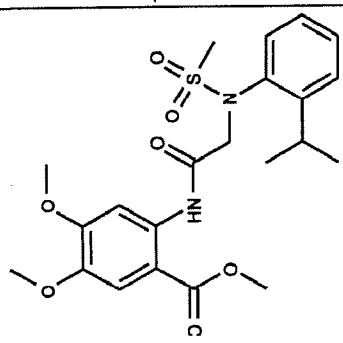
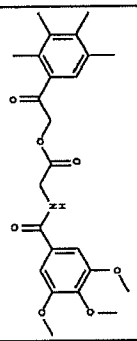
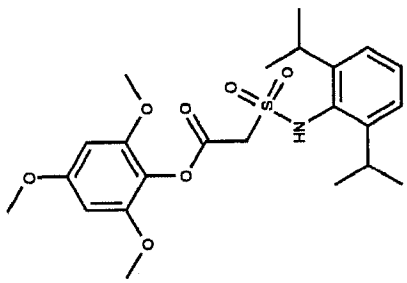
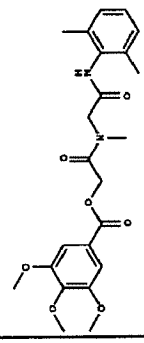
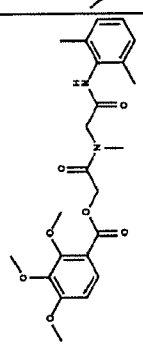
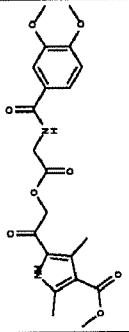
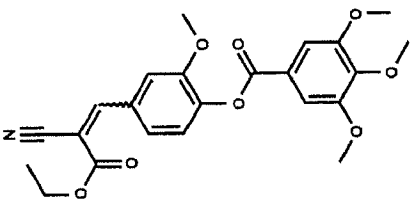
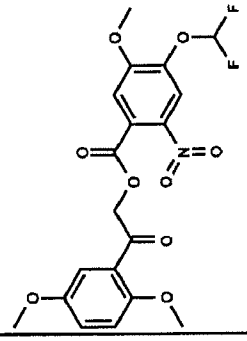
417	418	419	420
			
17651609_0 16	16516104_0 16	16501302_0 16	16501091_0 16
421	**422**	**423**	**424**
			
30276318_0 16	24367354_0 16	15341063_0 16	27890828_0 16

Fig. 23, cont'd

425	426	427	428
			
27880119_0 16	41569078_0 16	19166359_0 16	41435530_0 16

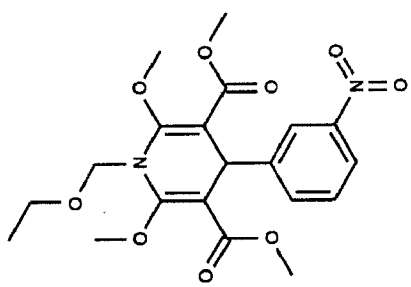
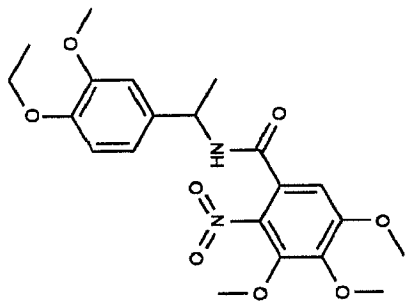
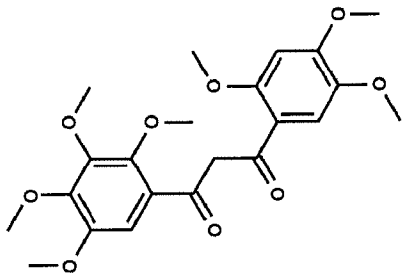
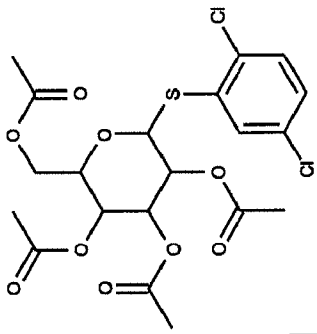
429	430	431	432
			
19009978_0 16	46414636_0 16	360323_0 16	219545_0 16

Fig. 23, cont'd

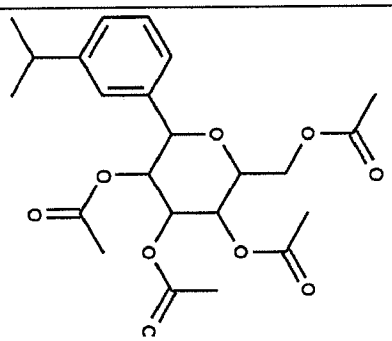
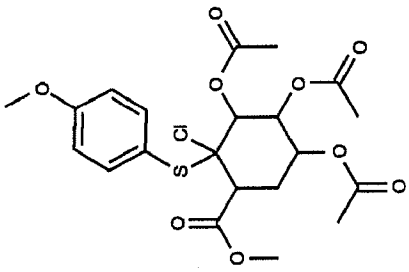
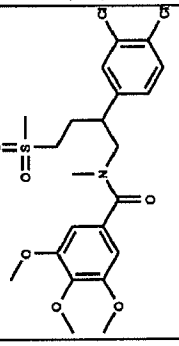
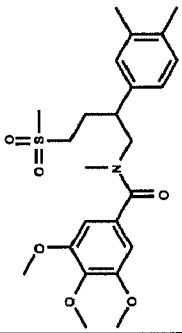
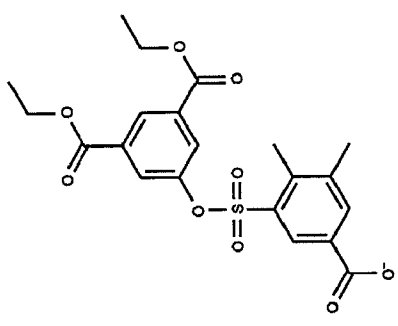
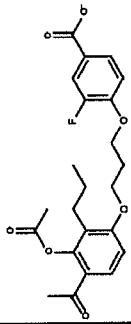
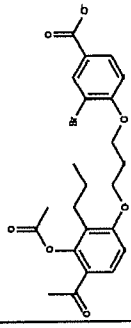
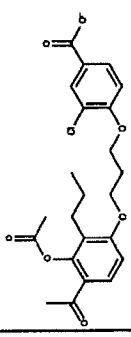
433	434	435	436
			
24178573_0 16	10435620_0 16	21697620_0 16	18354440_0 16
437	**438**	**439**	**440**
			
45420450_0 16	13745628_0 16	13745630_0 16	13745631_0 16

Fig. 23, cont'd

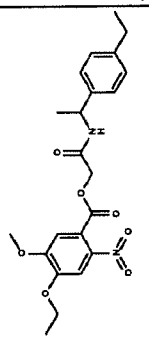
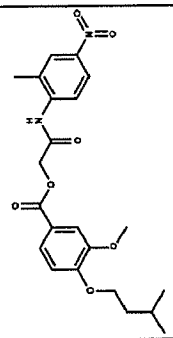
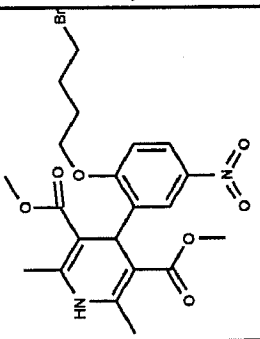
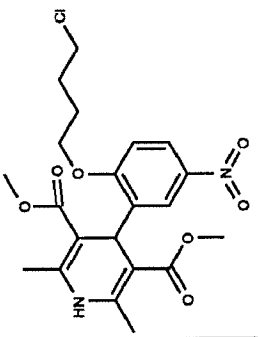
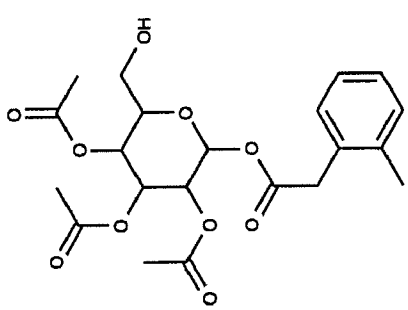
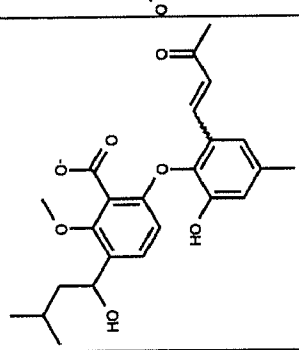
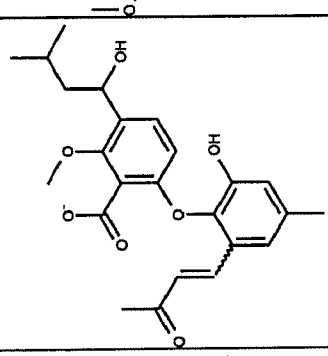
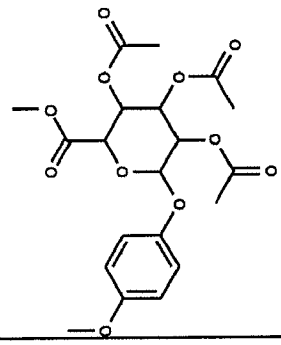
441	442	443	444
			
4611592_0 16	18291561_0 16	14554057_0 16	19846258_0 16
445	**446**	**447**	**448**
			
24838388_0 16	23815306_0,383512	38351242_0,383512	11838968_0 16

Fig. 23, cont'd

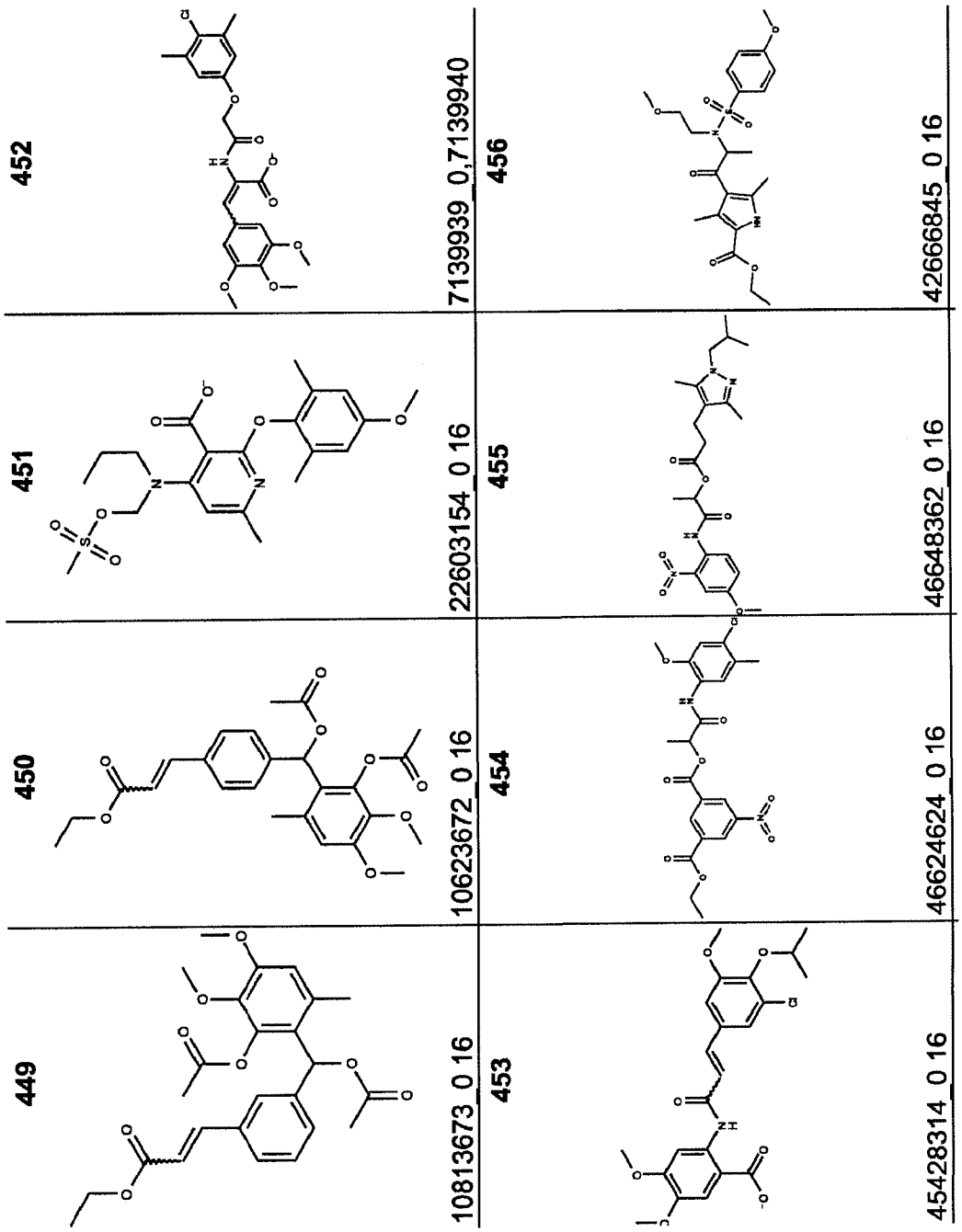

449
10813673_0 16
450
10623672_0 16
451
22603154_0 16
452
7139939_0,7139940
453
45428314_0 16
454
46624624_0 16
455
46648362_0 16
456
42666845_0 16

Fig. 23, cont'd

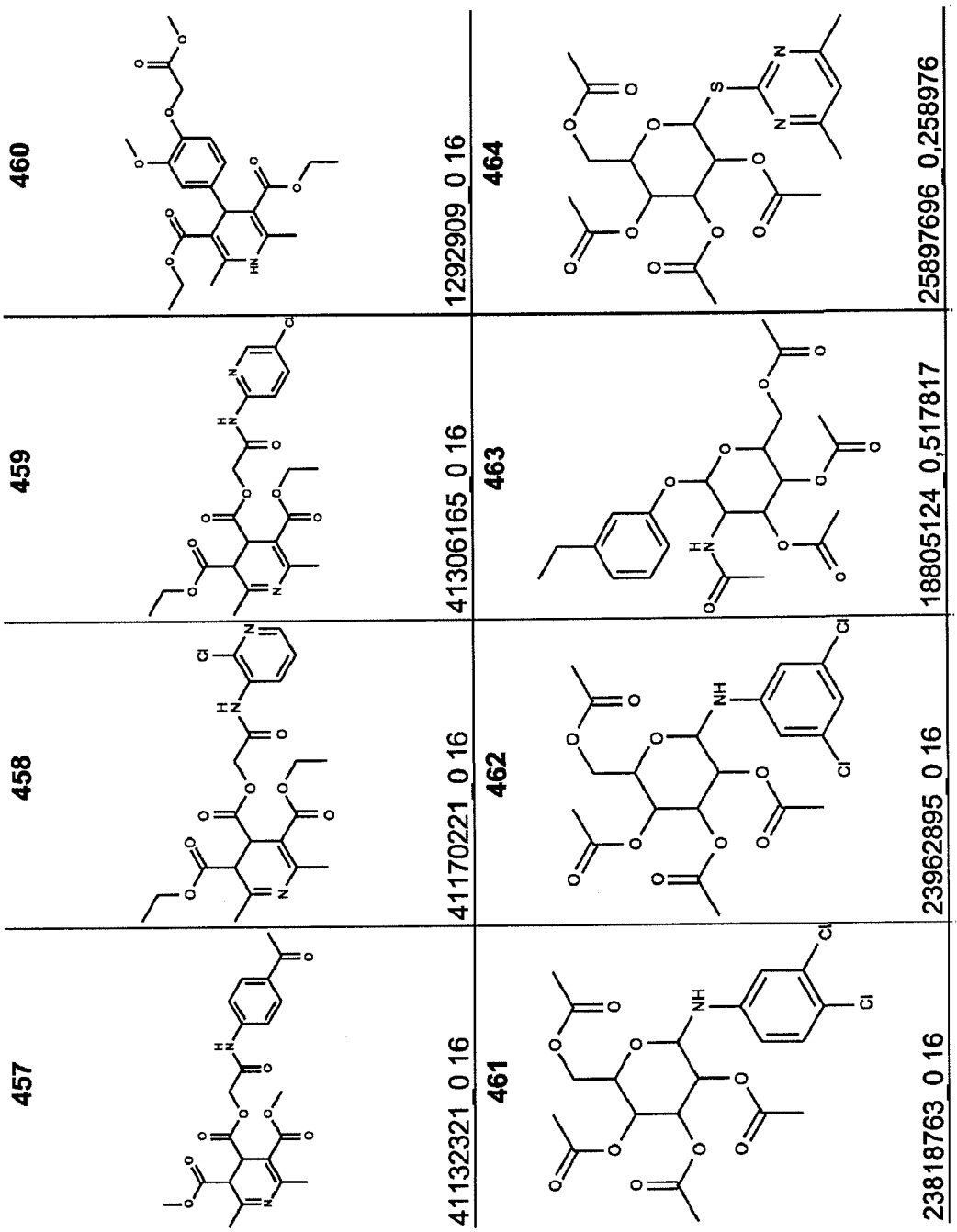

457
458
459
460
41132321_0 16
41170221_0 16
41306165_0 16
1292909_0 16
461
462
463
464
23818763_0 16
23962895_0 16
18805124_0,517817
25897696_0,258976

Fig. 23, cont'd

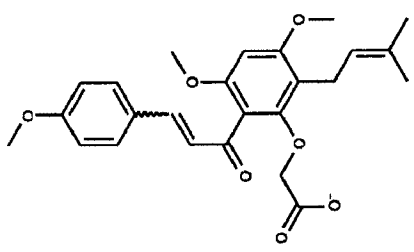
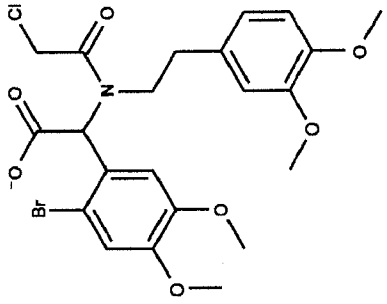
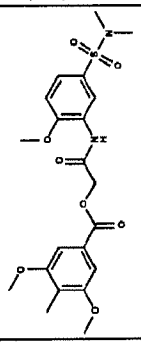
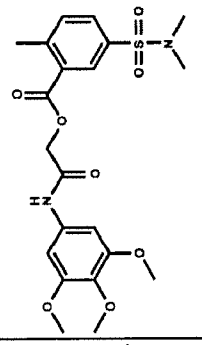
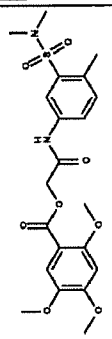
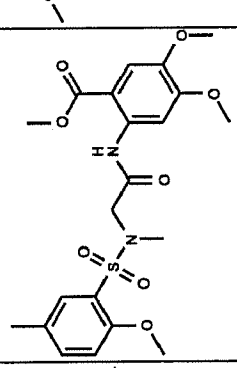
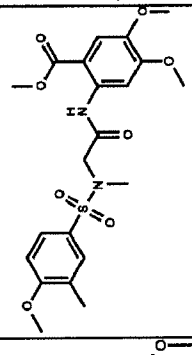
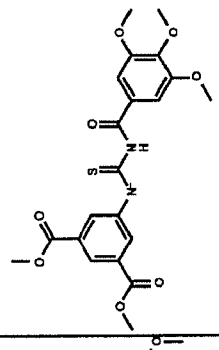
465	466	467	468
			
14368080_0 16	10346919_0 16	24383499_0 16	29512490_0 16
469	470	471	472
			
3619947_0 16	45372898_0 16	45372889_0 16	4941777_0 16

Fig. 23, cont'd

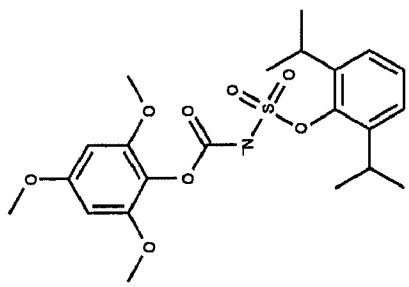
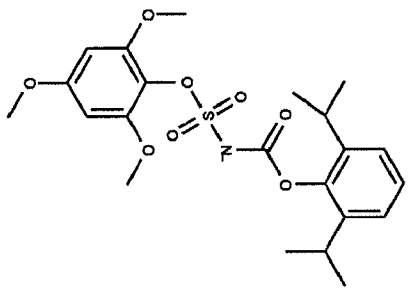
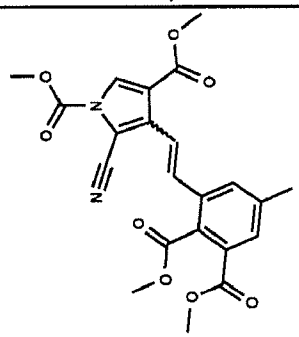
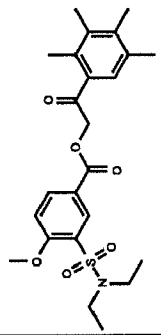
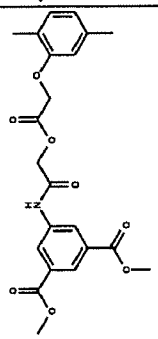
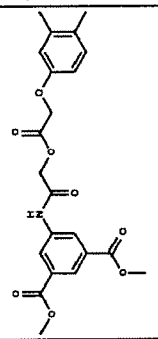
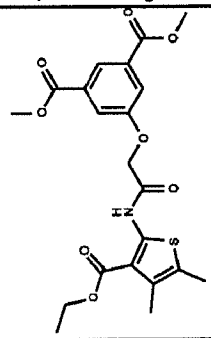
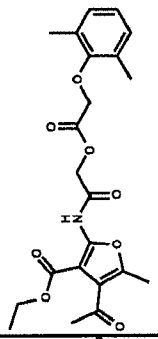
473	474	475	476
			
10695566_0 16	10695567_0 16	10003352_0 16	32040059_0 16
477	**478**	**479**	**480**
			
42966705_0 16	42966711_0 16	16499657_0 16	24470496_0 16

Fig. 23, cont'd

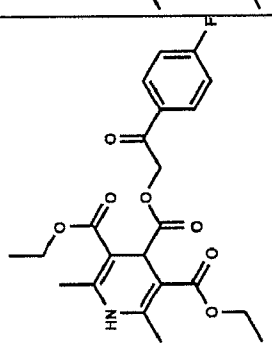
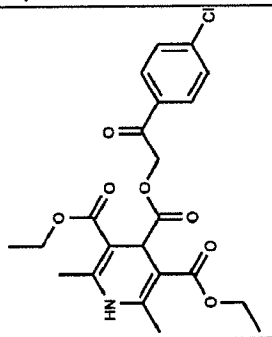
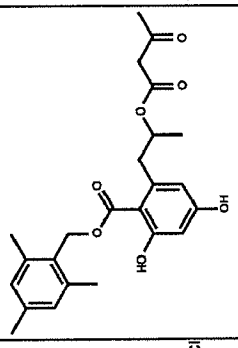
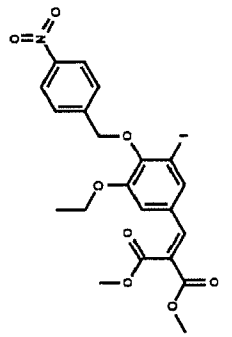
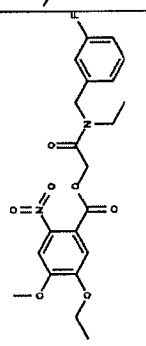
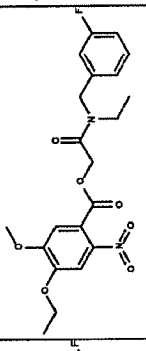
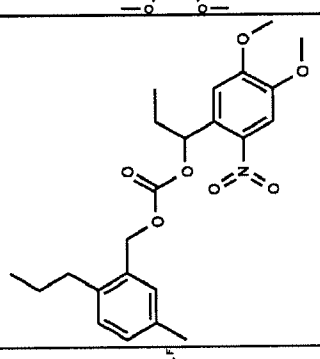
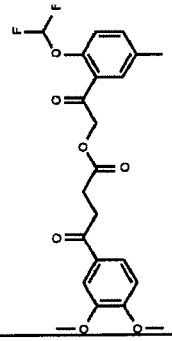
481	482	483	484
			
16531176_0 16	4224762_0 16	44520095_0 16	1363112_0 16
485	486	487	488
			
35350941_0 16	35484417_0 16	23586651_0 16	43050895_0 16

Fig. 23, cont'd

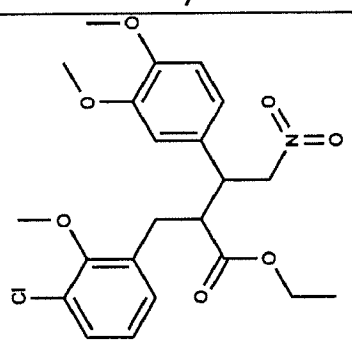
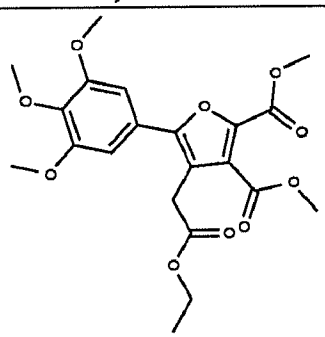
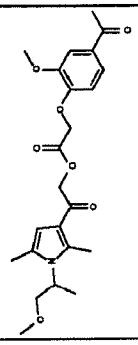
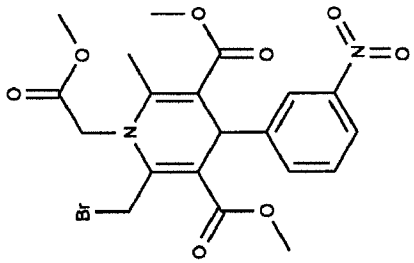
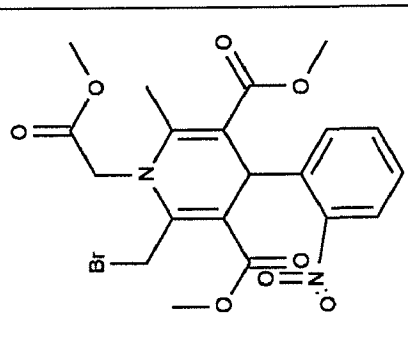
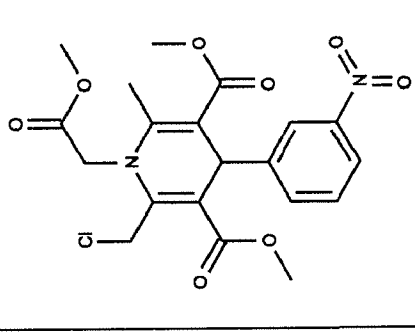
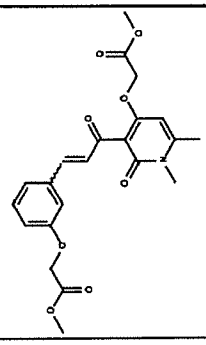
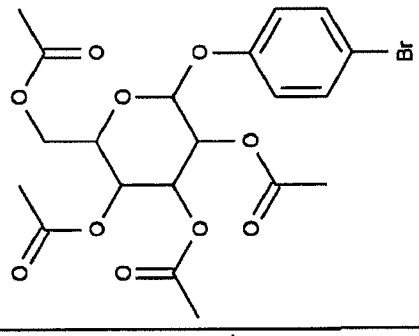
489	490	491	492
			
19390124_0 16	16094263_0 16	2107460_0,2107461	11799458_0 16
493	**494**	**495**	**496**
			
10767603_0 16	10575651_0 16	23131772_0 16	10951226_0,356851

Fig. 23, cont'd

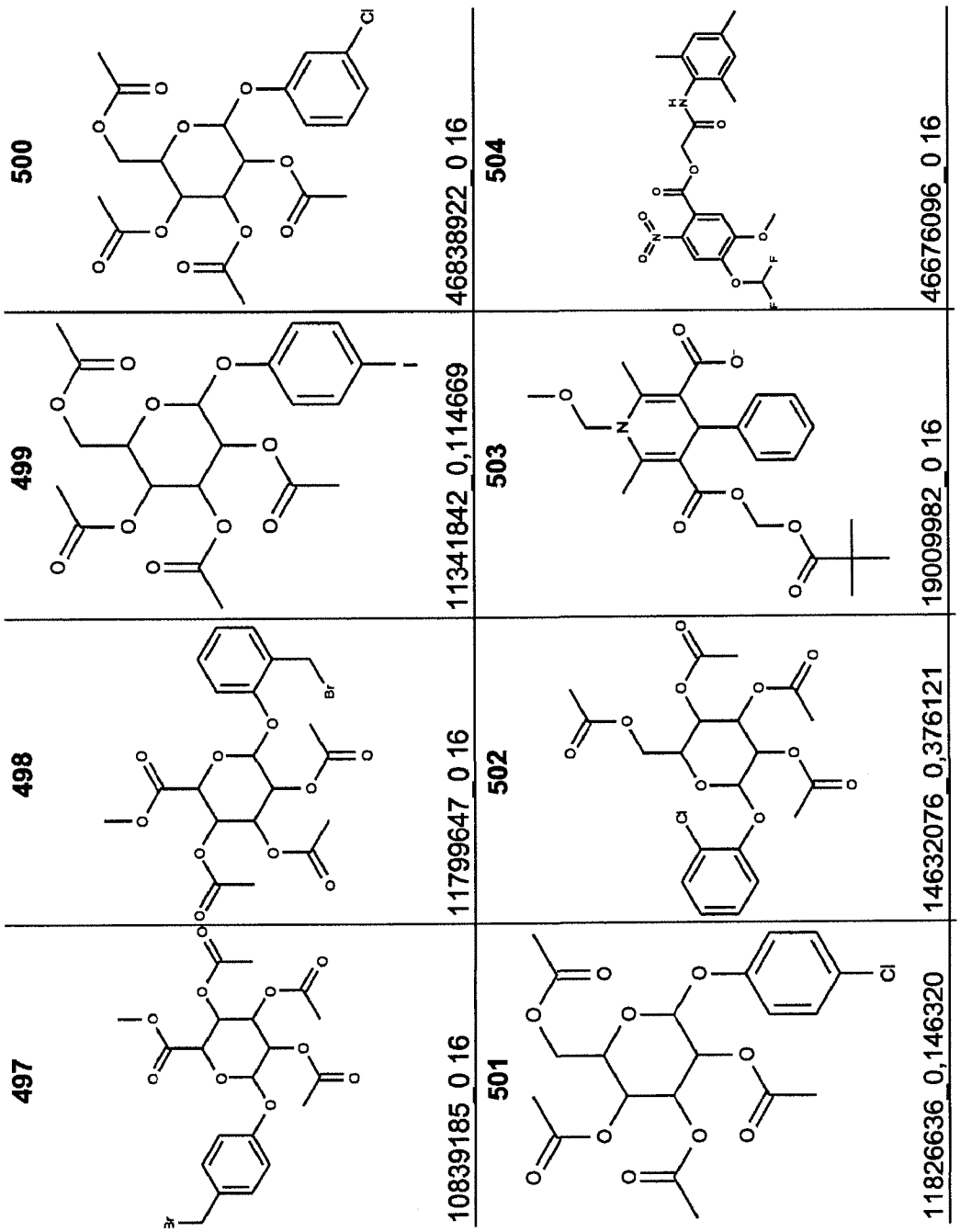

497
498
499
500
10839185_0_16
11799647_0_16
11341842_0,114669
46838922_0_16
501
502
503
504
11826636_0,146320
14632076_0,376121
19009982_0_16
46676096_0_16

Fig. 23, cont'd

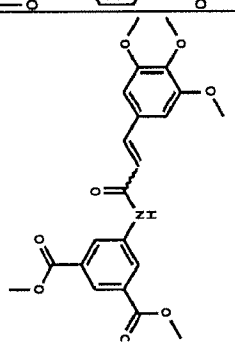
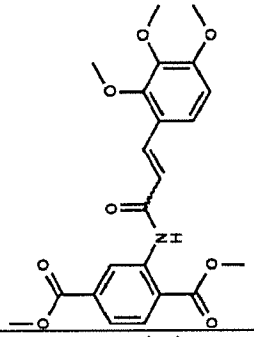
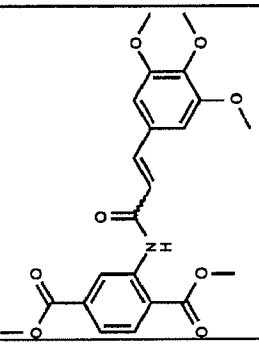
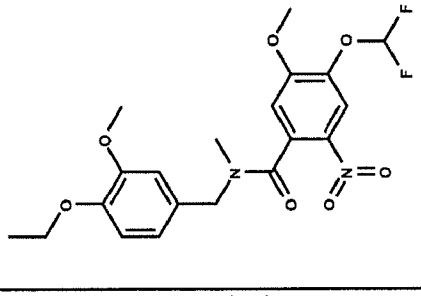
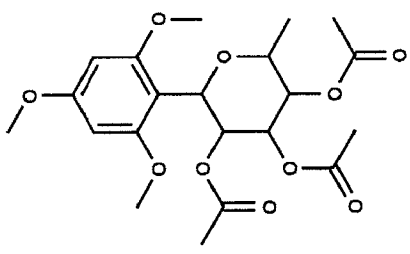
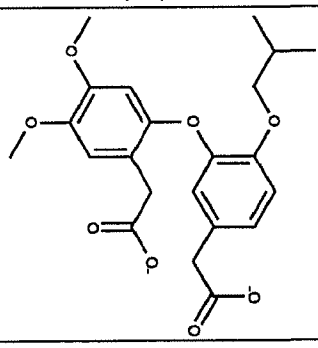
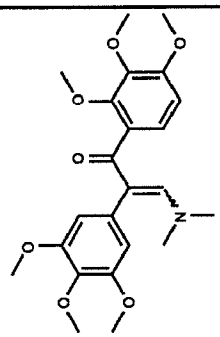
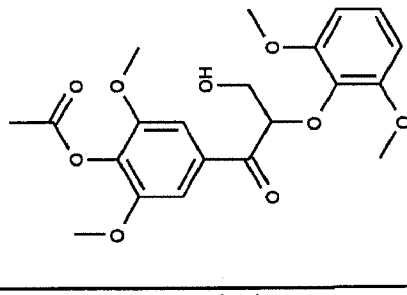
505	506	507	508
			
2290701_0,2916520	4320614_0,6068530	1320454_0,1320455	38400472_0 16
509	**510**	**511**	**512**
			
10094772_0,233539	21818018_0 16	10574707_0 16	21627771_0 16

Fig. 23, cont'd

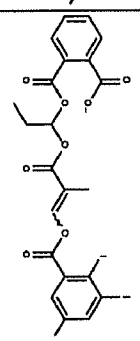
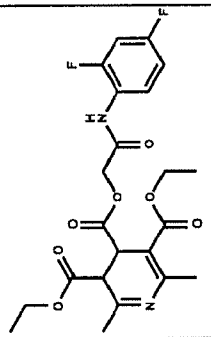
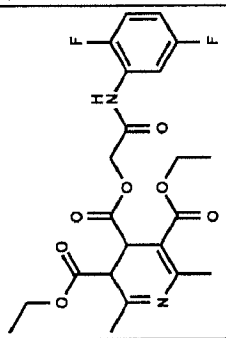
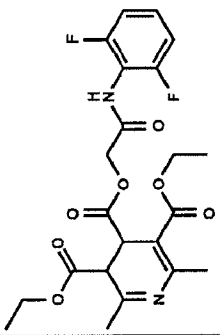
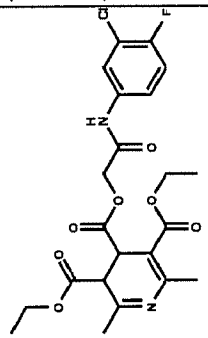
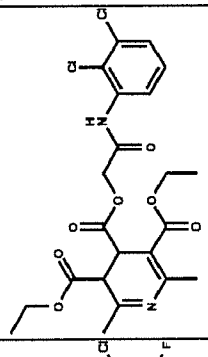
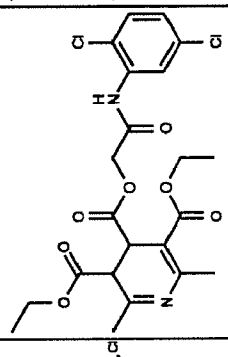
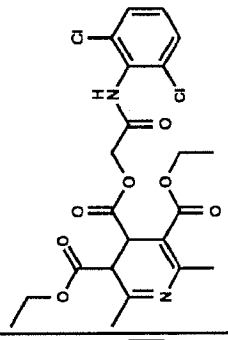
513	514	515	516
			
22370635_0,223706	41000746_0 16	41101851_0 16	41101783_0 16
517	518	519	520
			
25346158_0 16	41101799_0 16	40950263_0 16	41022209_0 16

Fig. 23, cont'd

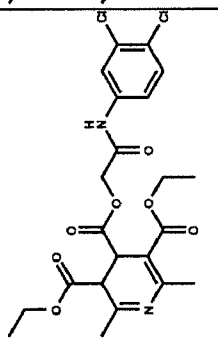
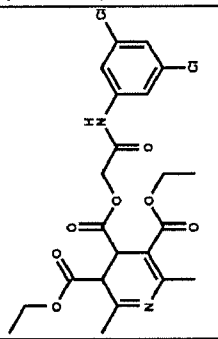
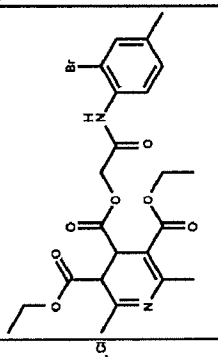
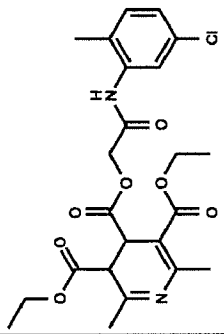
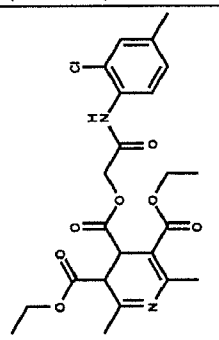
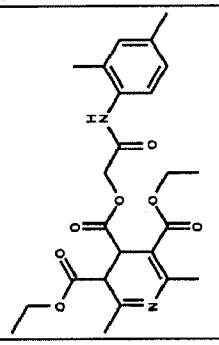
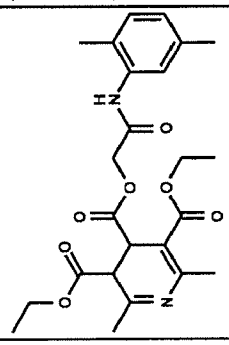
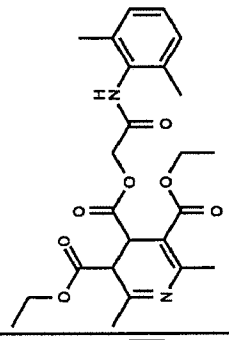
521	522	523	524
			
25372620_0 16	25346439_0 16	25387608_0 16	41101815_0 16
525	**526**	**527**	**528**
			
41101764_0 16	41101726_0 16	41101930_0 16	40950250_0 16

Fig. 23, cont'd

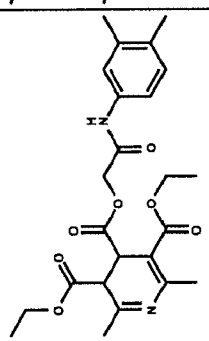
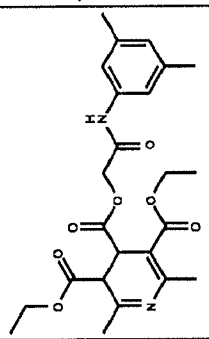
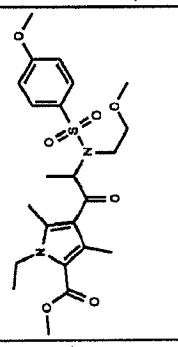
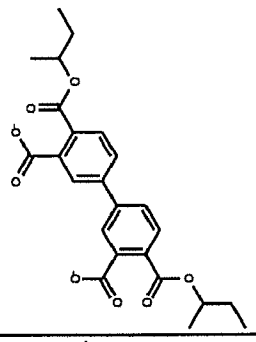
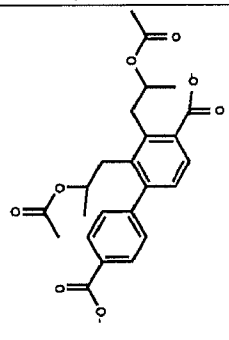
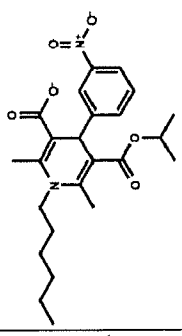
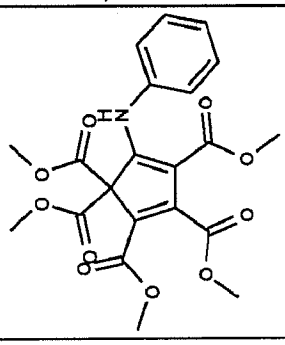
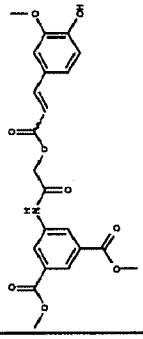
529	530	531	532
			
41101892_0 16	41101765_0 16	42679535_0 16	18324590_2,183245
533	534	535	536
			
18649832_0,186498	20272926_0 16	4779218_0 16	2551725_0 16

Fig. 23, cont'd

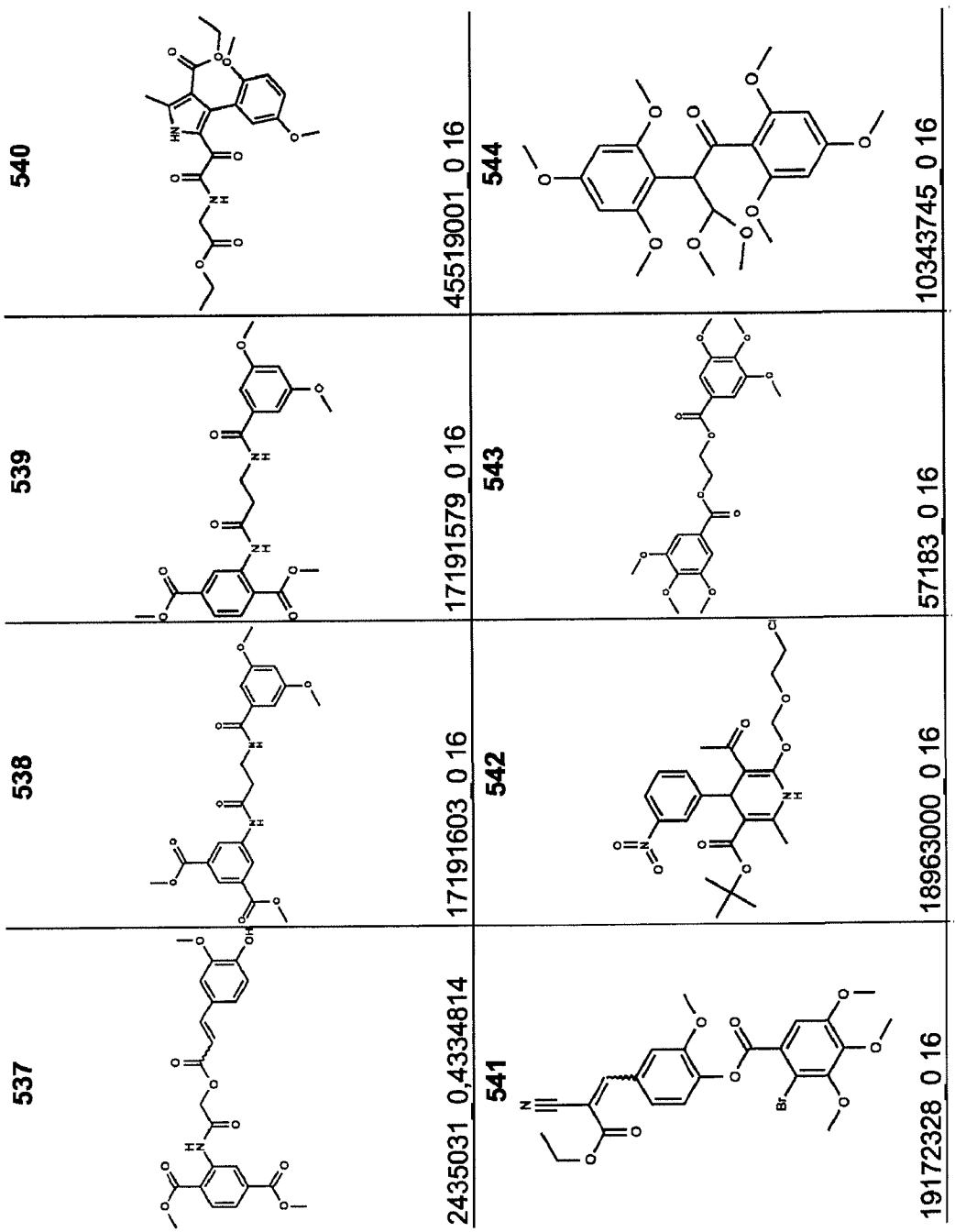

537
538
539
540
2435031_0,4334814
17191603_0 16
17191579_0 16
45519001_0 16
541
542
543
544
19172328_0 16
18963000_0 16
57183_0 16
10343745_0 16

Fig. 23, cont'd

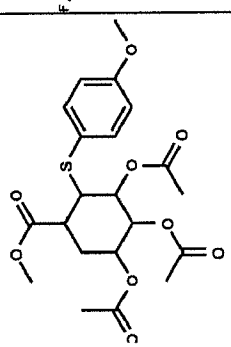
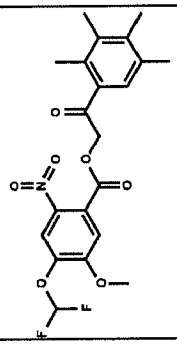
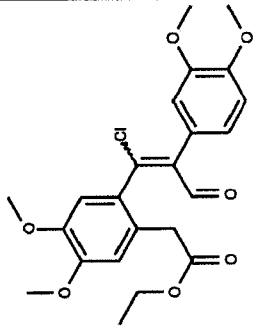
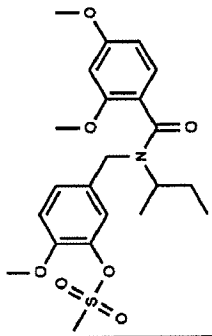
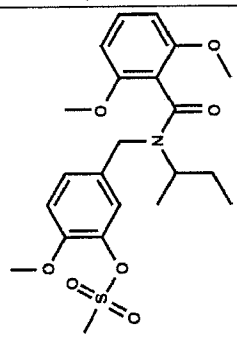
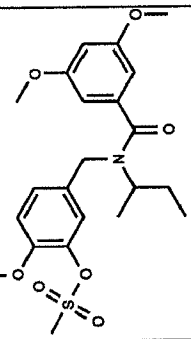
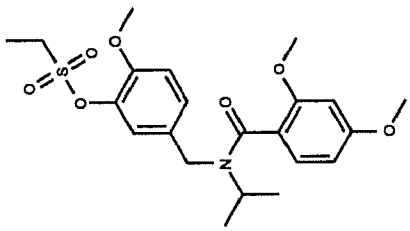
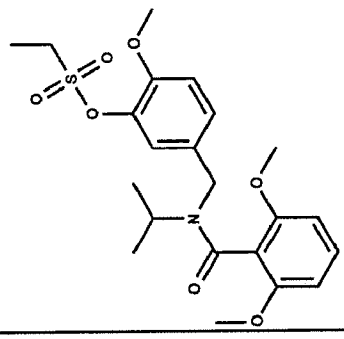
545	546	547	548
			
10049614_0 16	37228748_0 16	358222_0;5386814_0	3465261_0 16
549	550	551	552
			
4142508_0 16	3455369_0 16	42664945_0 16	42776079_0 16

Fig. 23, cont'd

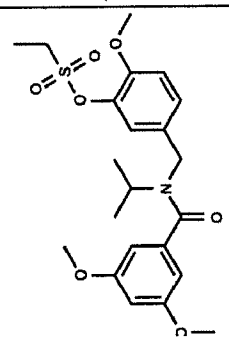
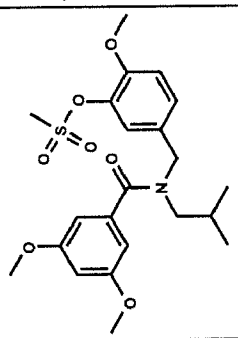
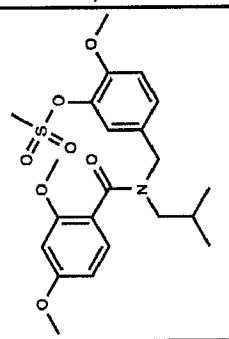
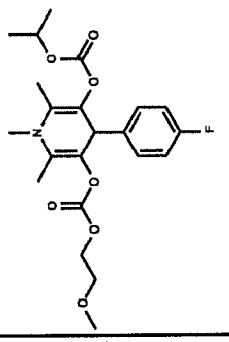
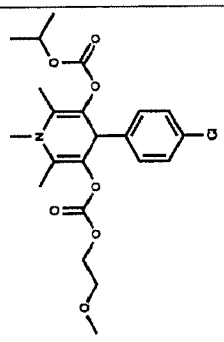
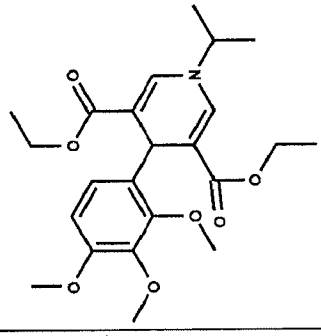
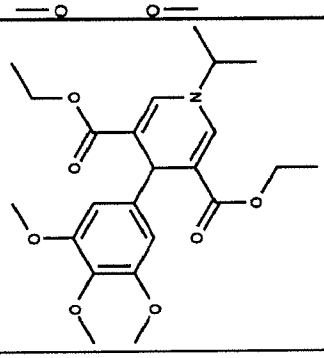
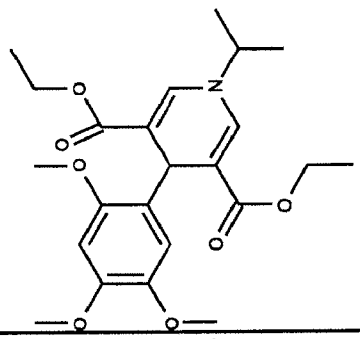
553	554	555	556
			
4055169_0 16	4034632_0 16	5038392_0 16	21803587_0 16
557	**558**	**559**	**560**
			
21803583_0 16	1530544_0 16	1530551_0 16	1531831_0 16

Fig. 23, cont'd

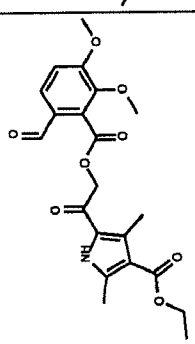
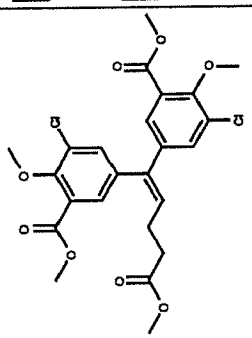
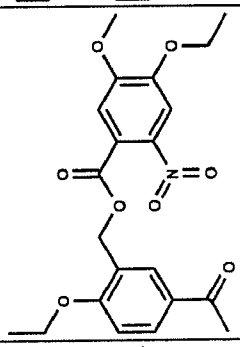
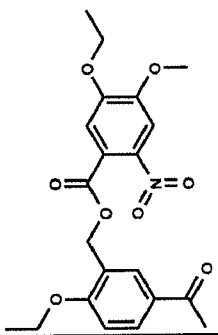
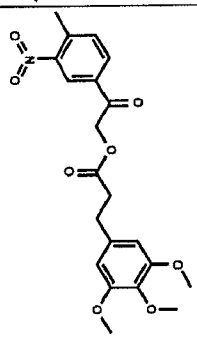
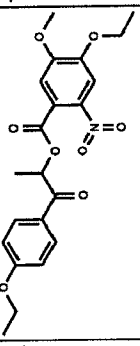
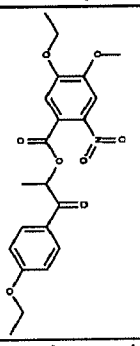
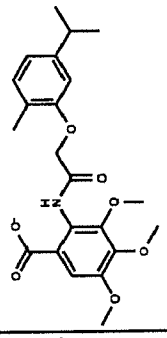
561	562	563	564
			
8370020_0 16	394180_0 16	9124873_0 16	8666463_0 16
565	566	567	568
			
8019189_0 16	9125167_0,9125168	8666698_0,8666700	45347908_0 16

Fig. 23, cont'd

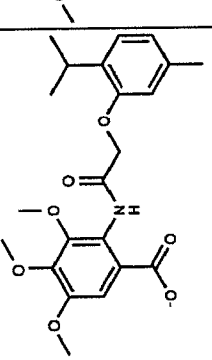
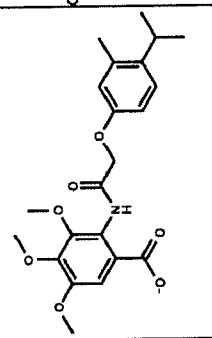
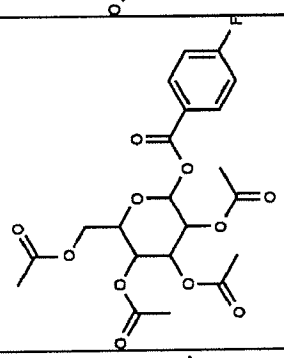
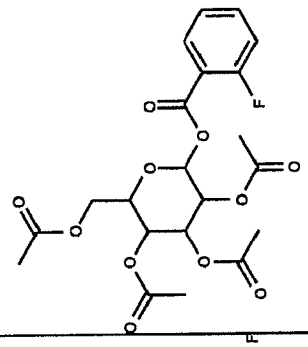
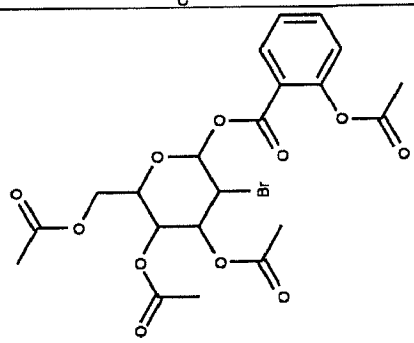
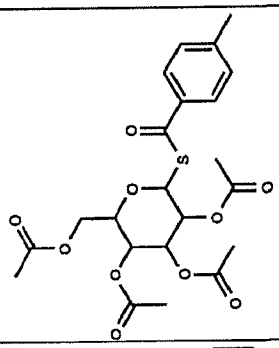
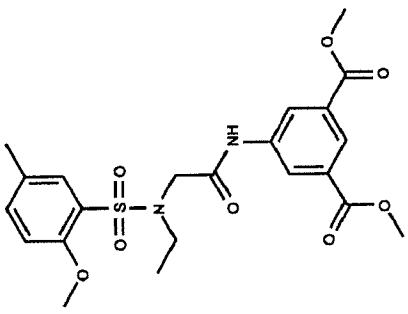
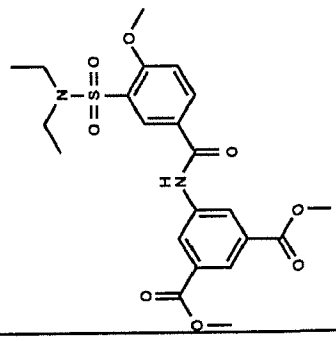
569	570	571	572
			
45348188_0 16	45347906_0 16	16080433_0,160804	15139312_0,160804
573	**574**	**575**	**576**
			
10940404_0 16	11283066_0 16	45372693_0 16	17733308_0 16

Fig. 23, cont'd

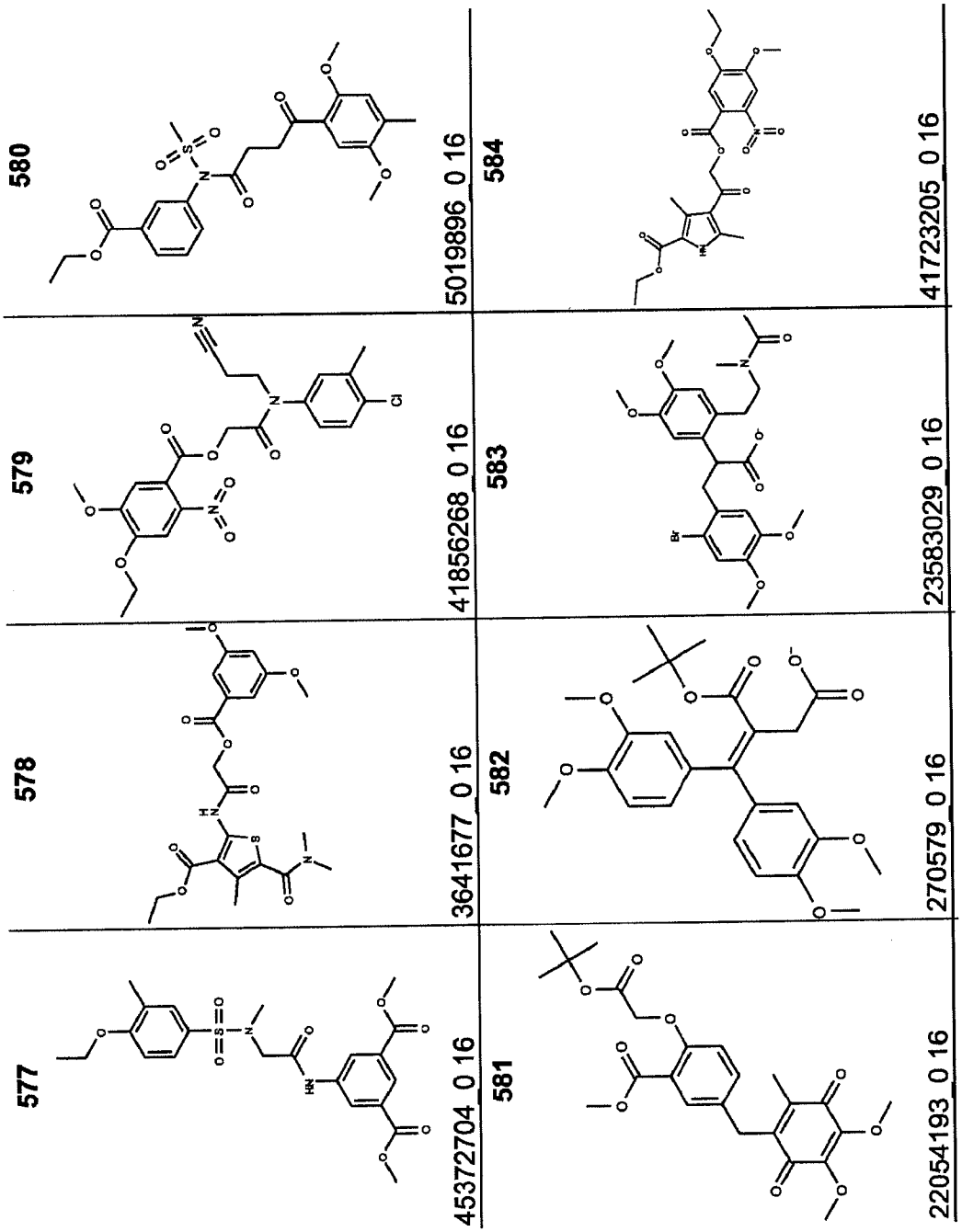

577
45372704_0 16
578
3641677_0 16
579
41856268_0 16
580
5019896_0 16
581
22054193_0 16
582
270579_0 16
583
23583029_0 16
584
41723205_0 16

Fig. 23, cont'd

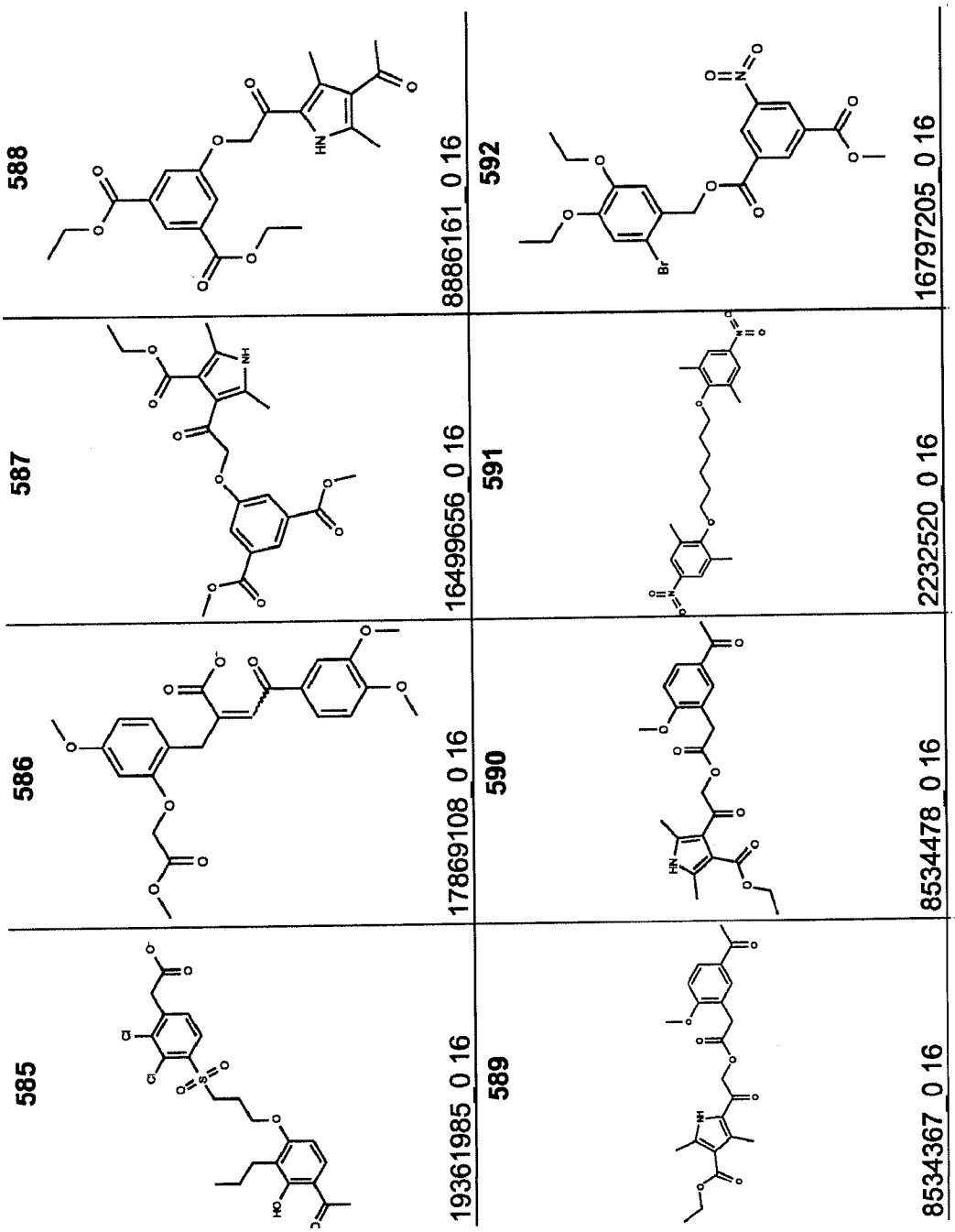

585
19361985_0 16
586
17869108_0 16
587
16499656_0 16
588
8861161_0 16
589
8534367_0 16
590
8534478_0 16
591
2232520_0 16
592
16797205_0 16

Fig. 23, cont'd

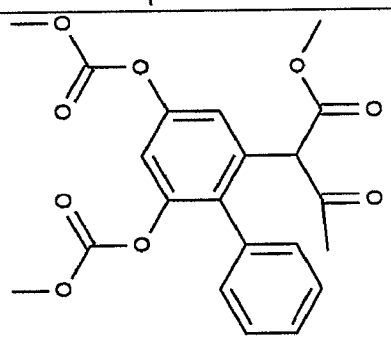
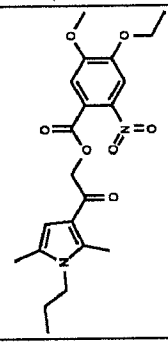
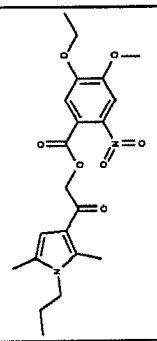
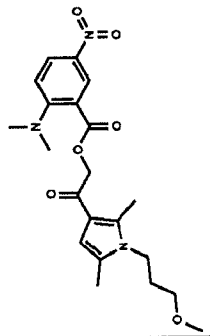
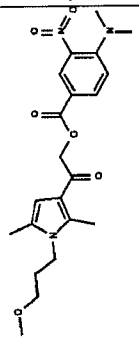
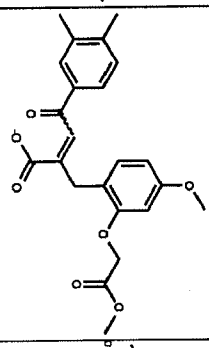
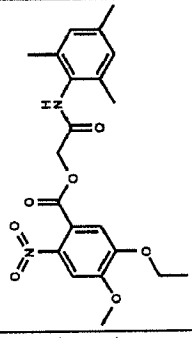
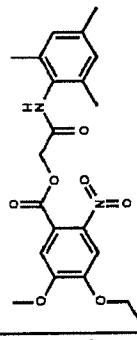
593	594	595	596
			
23147277_0 16	9125024_0 16	8666618_0 16	7684797_0 16
597	598	599	600
			
7261922_0 16	17869151_0 16	8666363_0 16	9124735_0 16

Fig. 23, cont'd

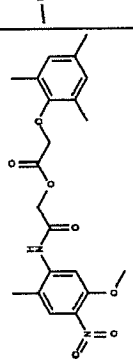
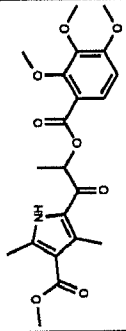
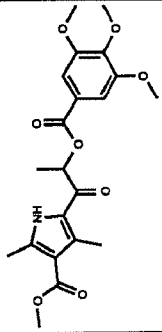
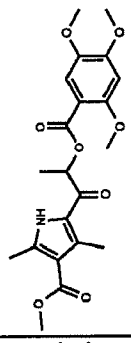
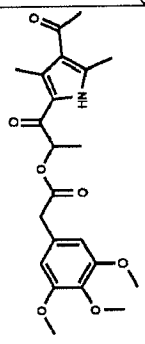
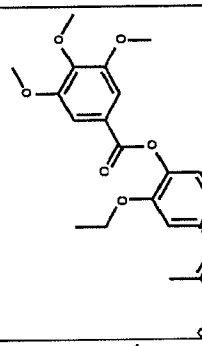
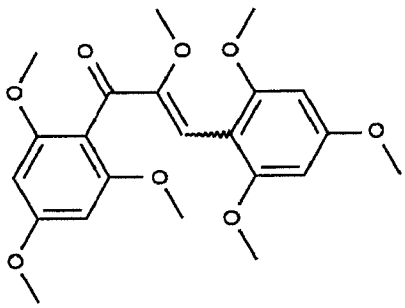
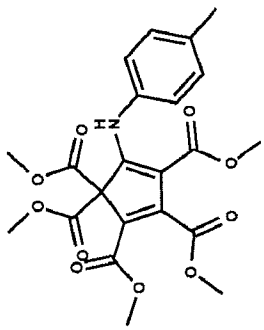
601	602	603	604
			
7997896_0 16	16523974_0,861127	16522443_0,801345	16528391_0,739497
605	**606**	**607**	**608**
			
8649253_0,8649256	4014146_0 16	16754162_0 16	4779188_0 16

Fig. 23, cont'd

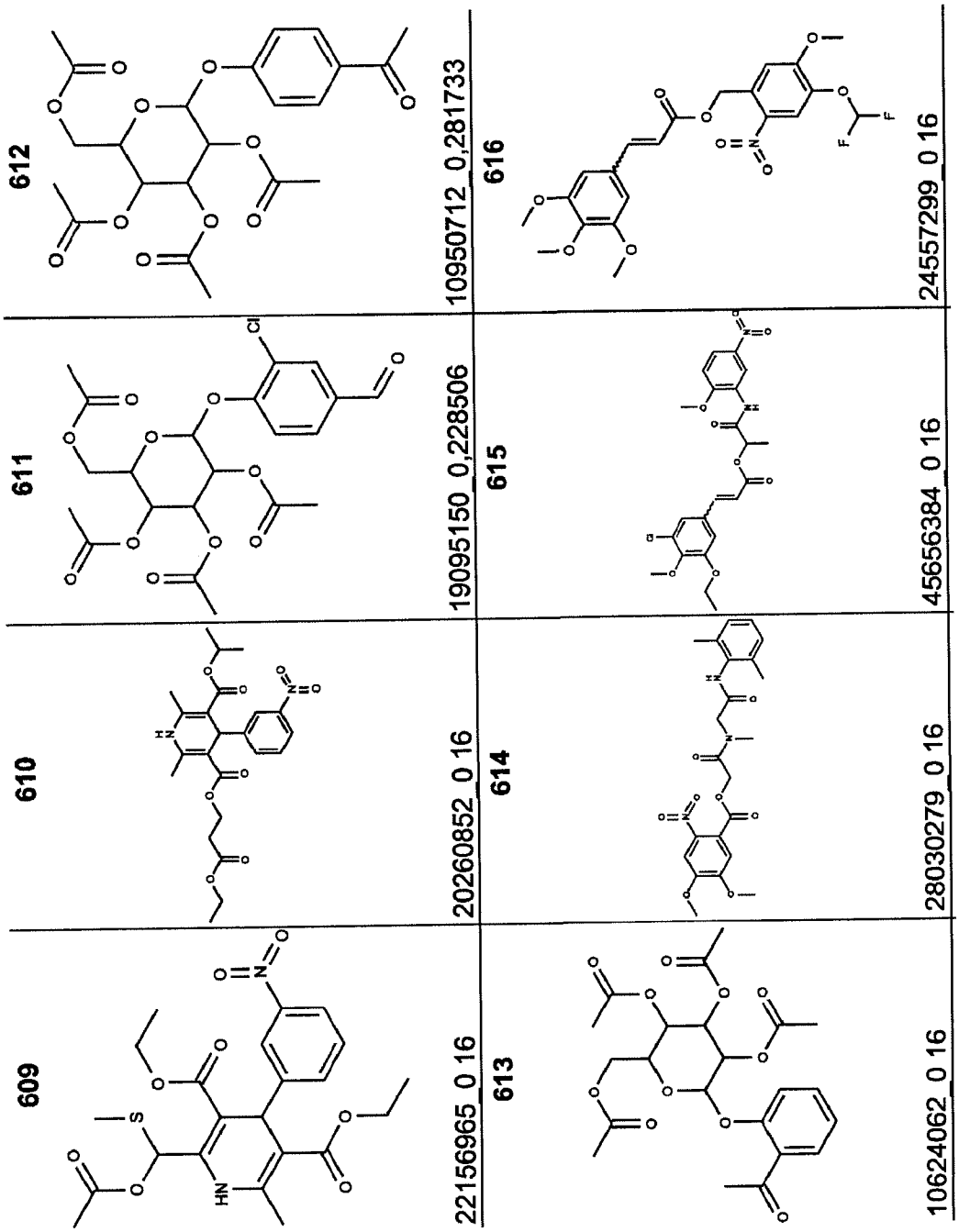

609
22156965_0 16
610
20260852_0 16
611
19095150_0,228506
612
10950712_0,281733
613
10624062_0 16
614
28030279_0 16
615
45656384_0 16
616
24557299_0 16

Fig. 23, cont'd

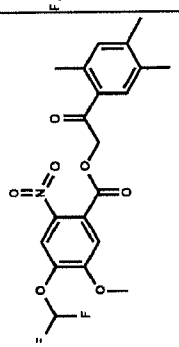
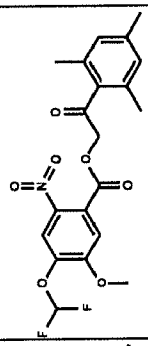
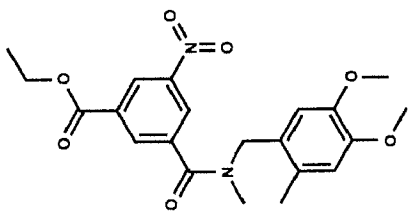
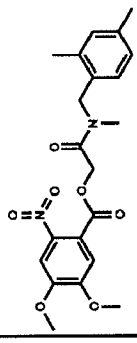
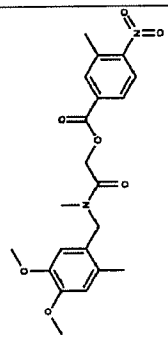
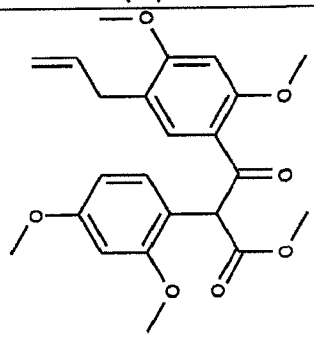
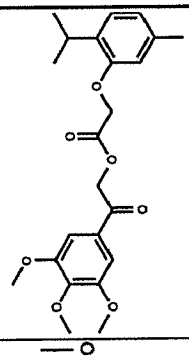
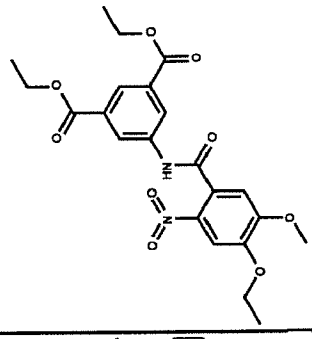
617	618	619	620
			
46676072_0 16	46676073_0 16	8376873_0 16	8952474_0 16
621	**622**	**623**	**624**
			
9199273_0 16	42598458_0 16	23821464_0 16	26771702_0 16

Fig. 23, cont'd

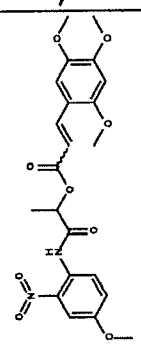
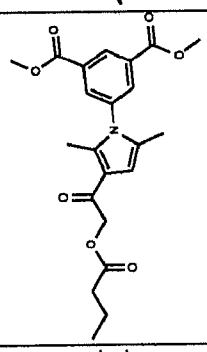
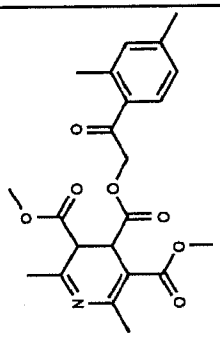
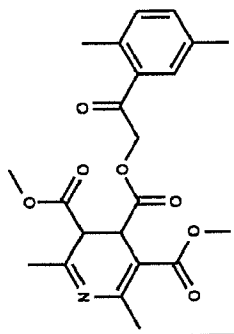
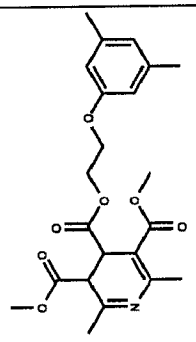
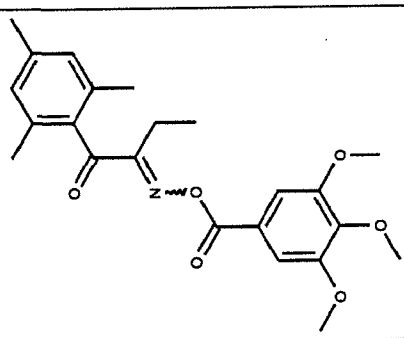
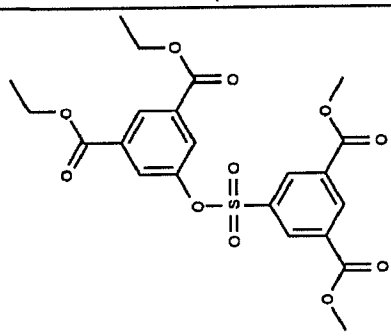
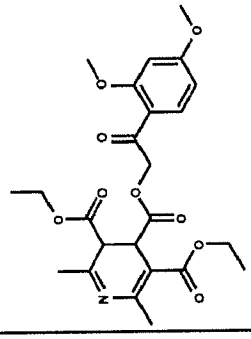
625	626	627	628
			
46625236_0 16	24362649_0 16	7226046_0 16	7226029_0 16
629	630	631	632
			
8124907_0 16	1365253_0,5349180	24419421_0 16	41297287_0 16

Fig. 23, cont'd

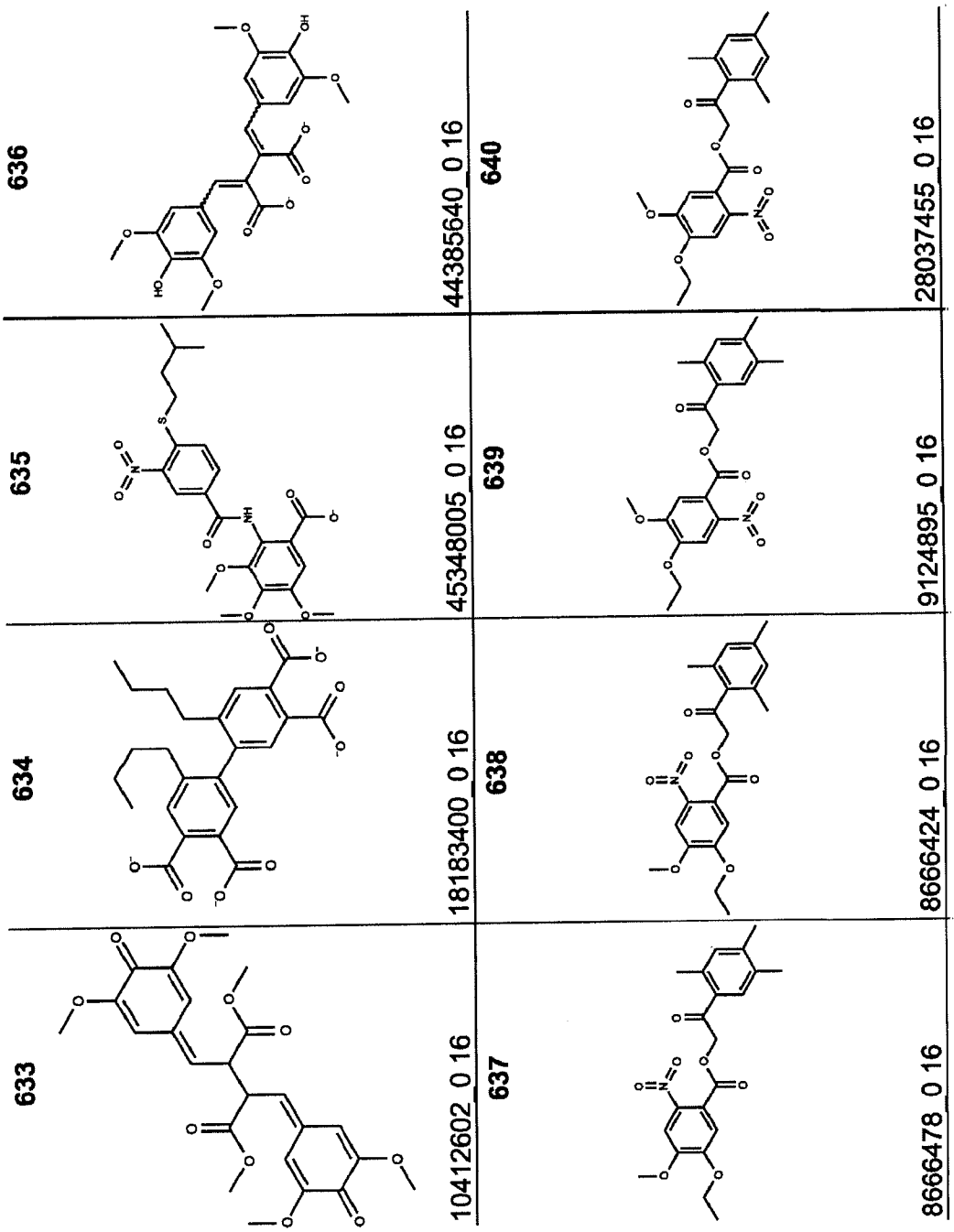

633
634
635
636
10412602_0 16
637
18183400_0 16
638
45348005_0 16
639
44385640_0 16
640
8666478_0 16
8666424_0 16
9124895_0 16
28037455_0 16

Fig. 23, cont'd

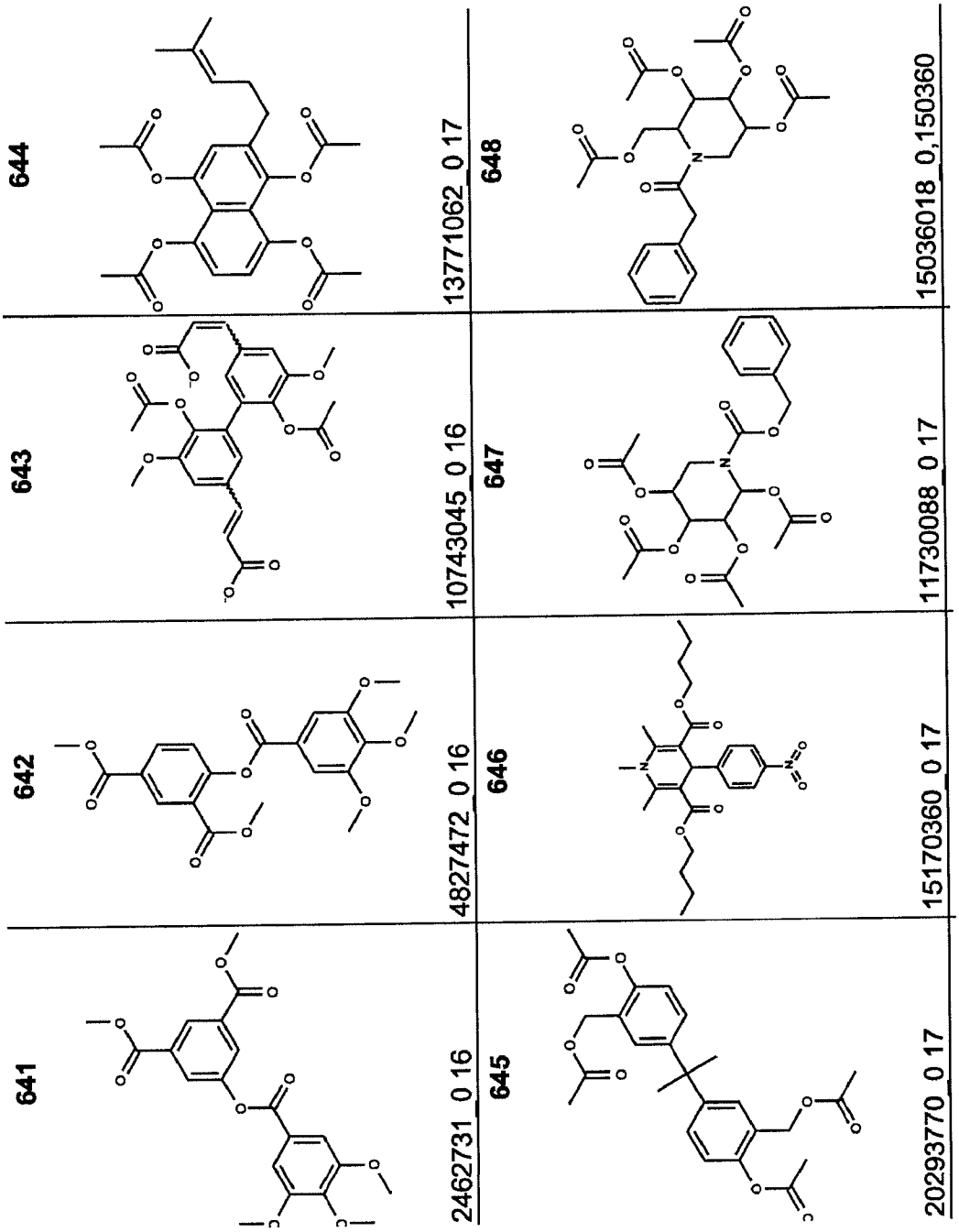

641
642
643
644
2462731_0 16
4827472_0 16
10743045_0 16
13771062_0 17
645
646
647
648
20293770_0 17
15170360_0 17
11730088_0 17
15036018_0,150360

Fig. 23, cont'd

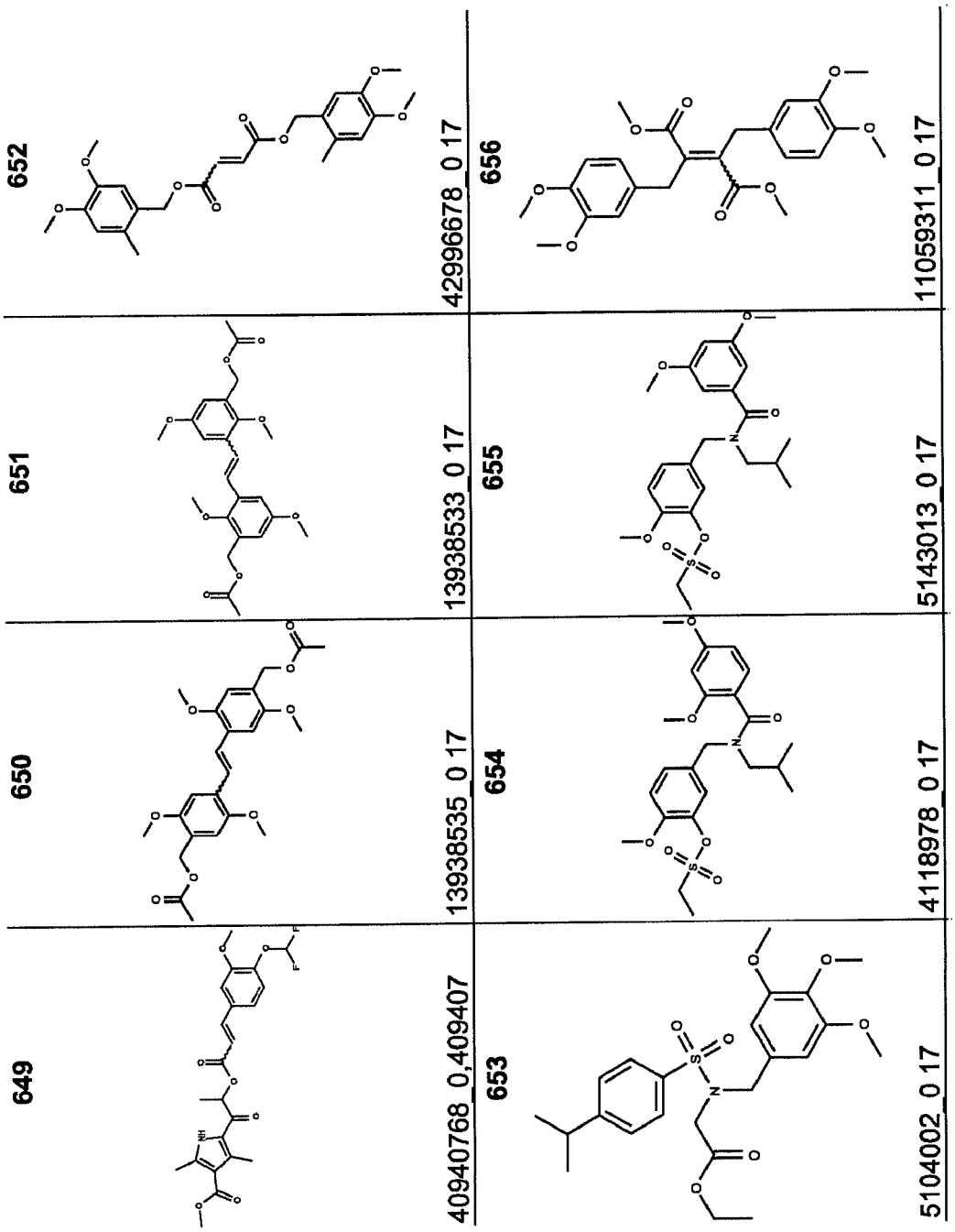

649
650
651
652
40940768_0,409407
13938535_0 17
13938533_0 17
4296678_0 17
653
654
655
656
5104002_0 17
4118978_0 17
5143013_0 17
11059311_0 17

Fig. 23, cont'd

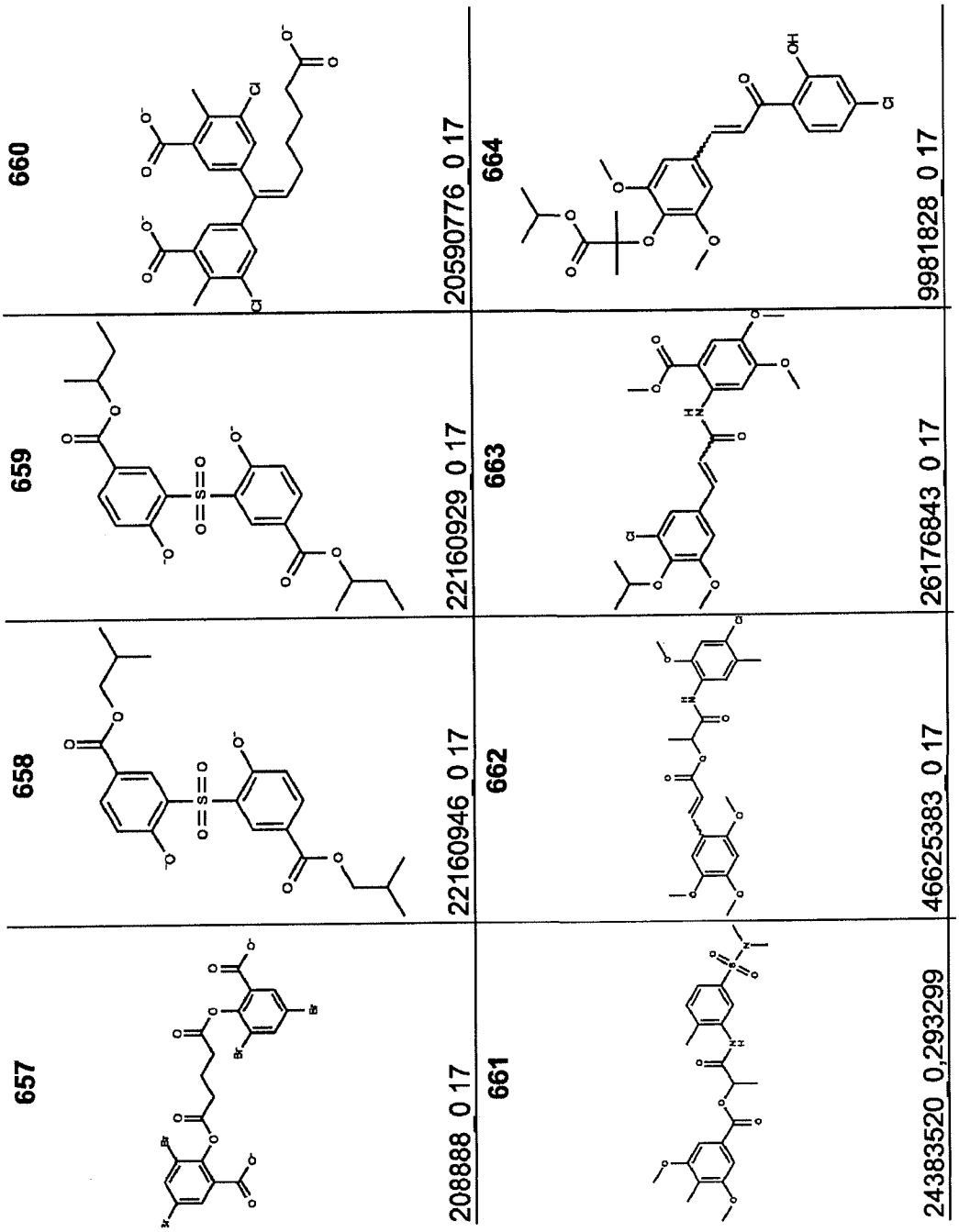

657
208888_0 17
658
22160946_0 17
659
22160929_0 17
660
20590776_0 17
661
24383520_0,293299
662
46625383_0 17
663
26176843_0 17
664
9981828_0 17

Fig. 23, cont'd

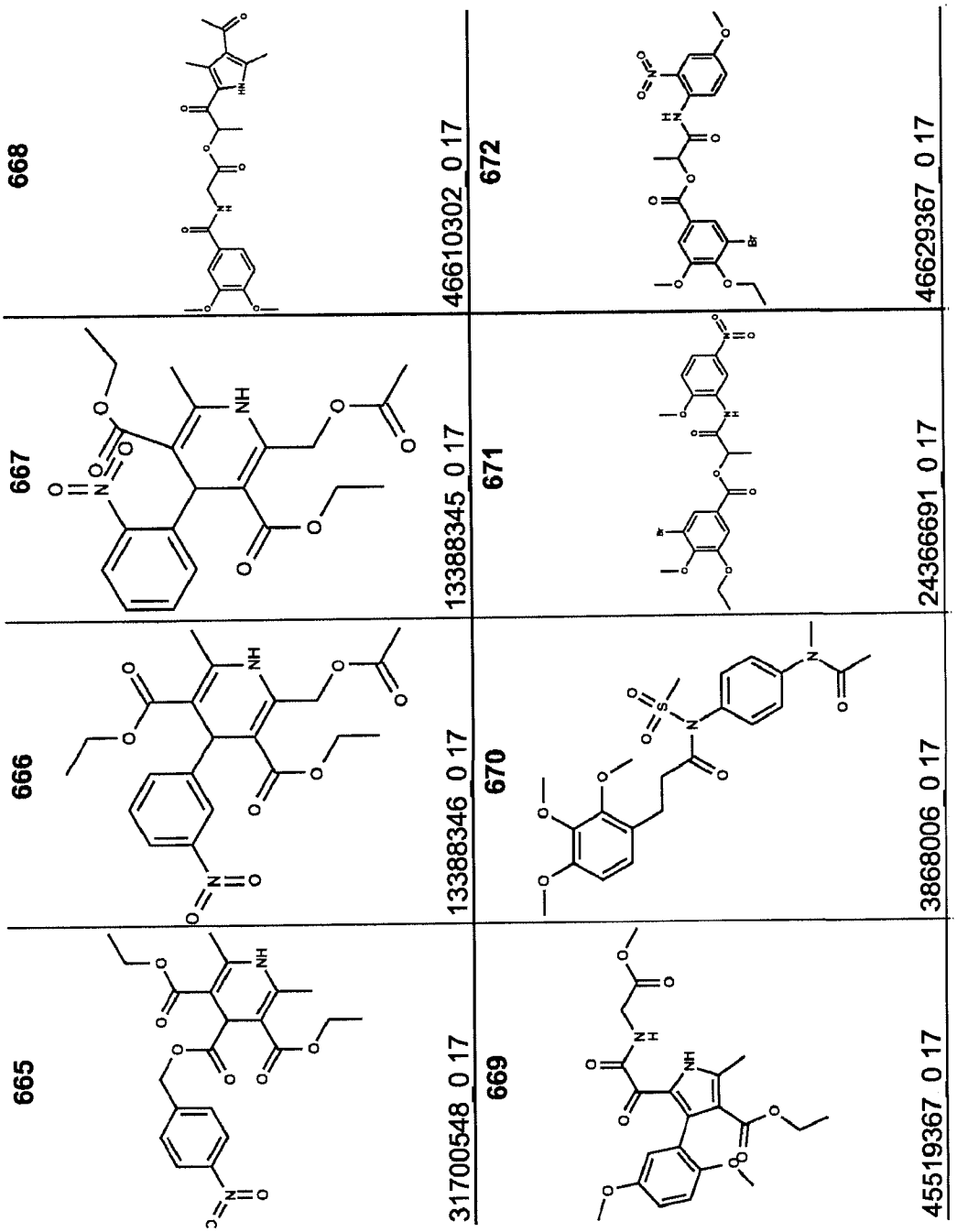

665
666
667
668
31700548_0 17
669
13388346_0 17
670
13388345_0 17
671
46610302_0 17
672
45519367_0 17
3868006_0 17
24366691_0 17
46629367_0 17

Fig. 23, cont'd

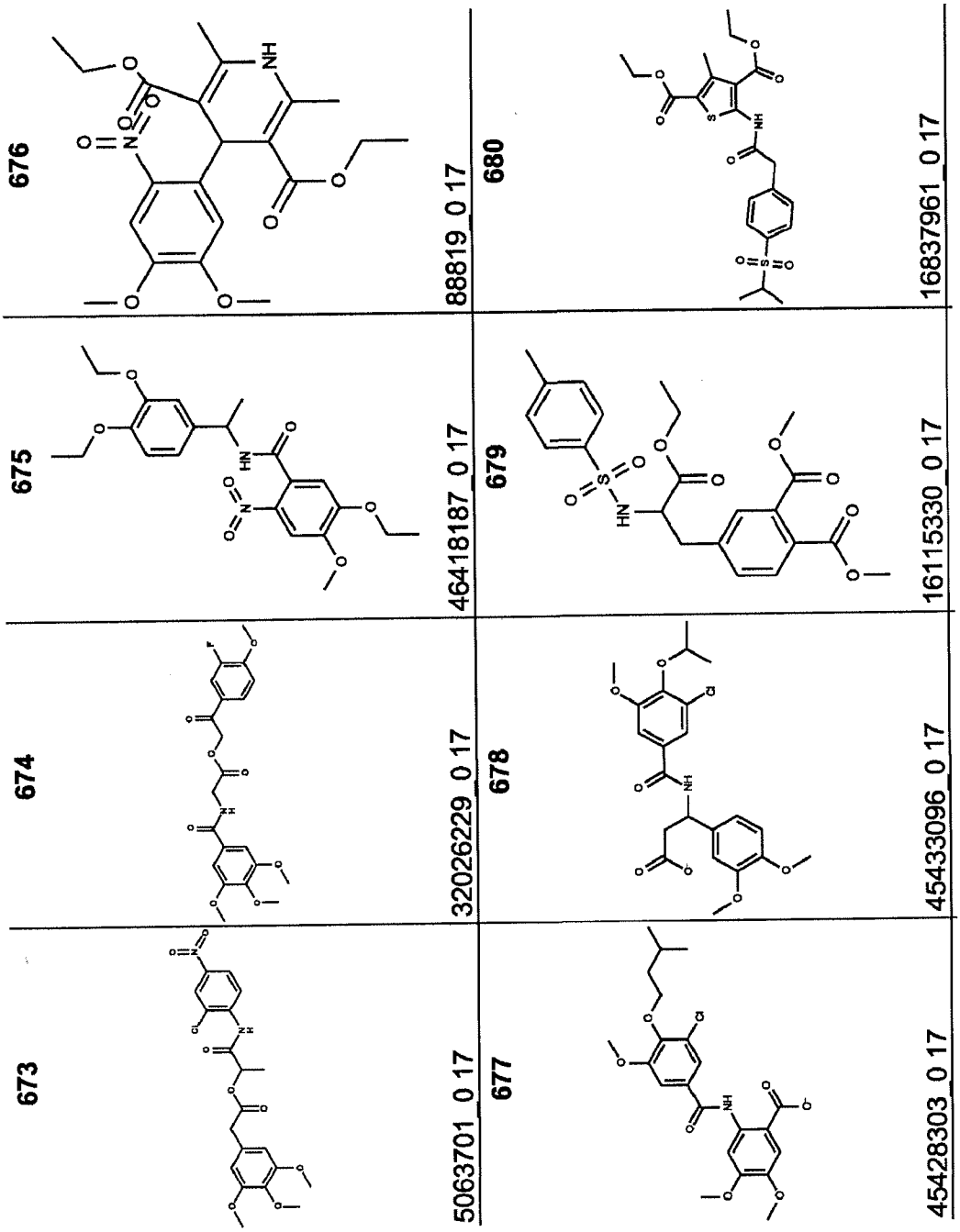

673
674
675
676
5063701_0 17
677
32026229_0 17
678
46418187_0 17
679
88819_0 17
680
45428303_0 17
45433096_0 17
16115330_0 17
16837961_0 17

Fig. 23, cont'd

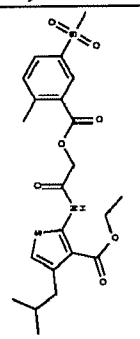
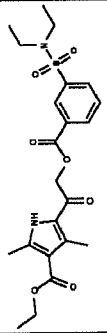
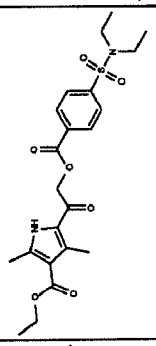
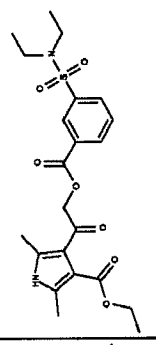
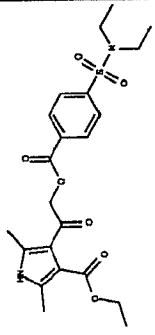
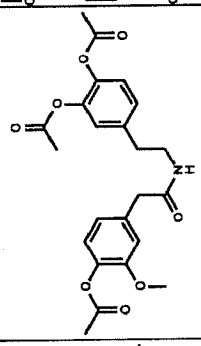
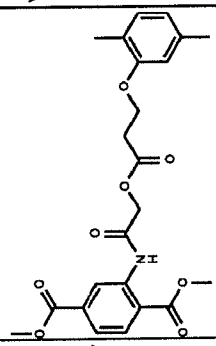
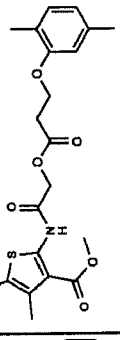
681	682	683	684
			
16518186_0 17	3464279_0 17	2557292_0 17	2125707_0 17
685	**686**	**687**	**688**
			
2430004_0 17	586444_0 17	16286887_0 17	32342384_0 17

Fig. 23, cont'd

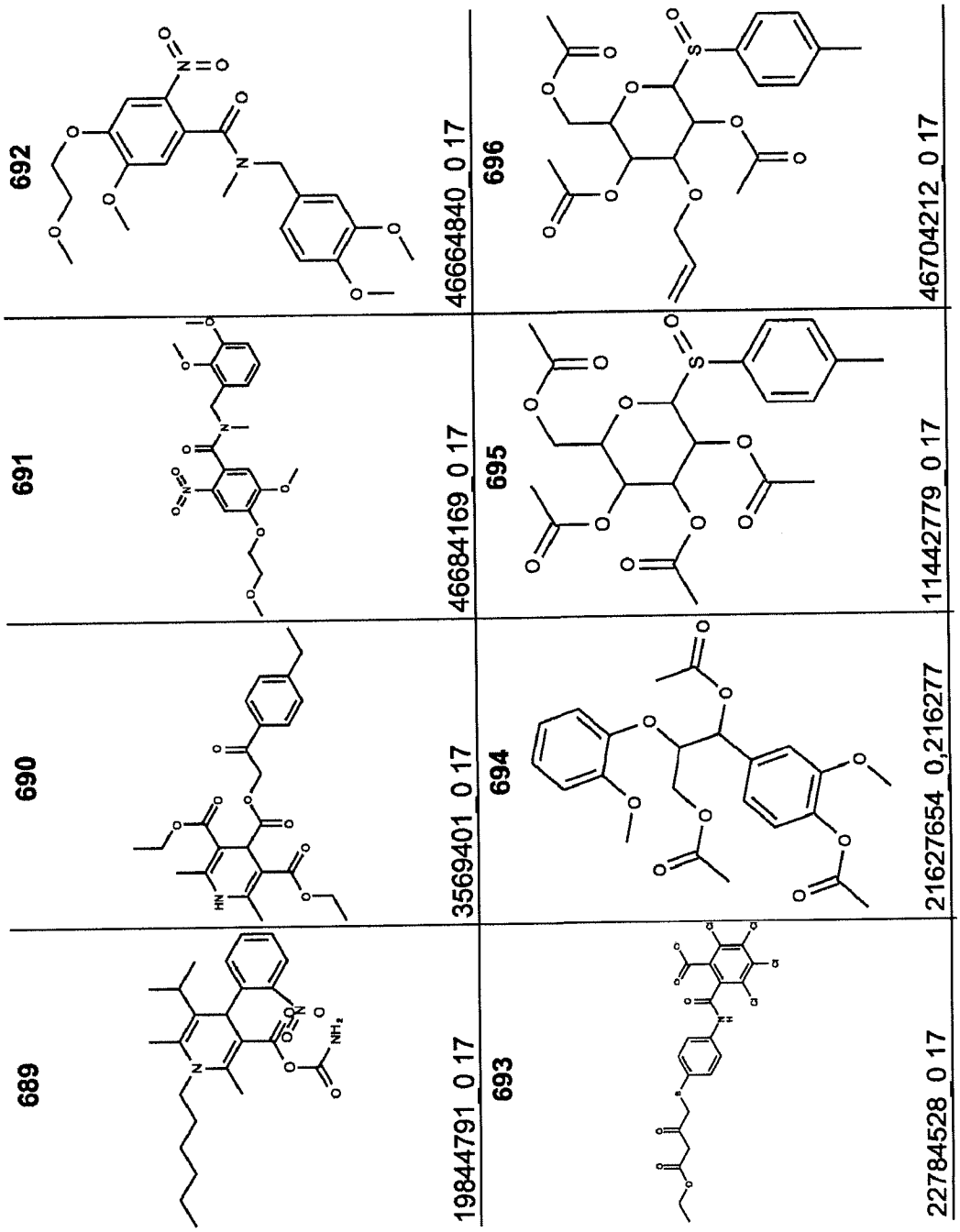

689
690
691
692
693
694
695
696
19844791_0 17
3569401_0 17
46684169_0 17
46664840_0 17
22784528_0 17
21627654_0,216277
11442779_0 17
46704212_0 17

Fig. 23, cont'd

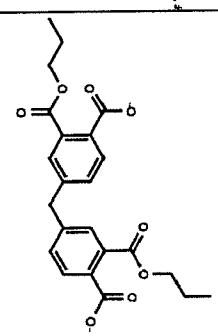
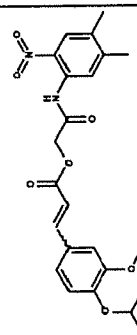
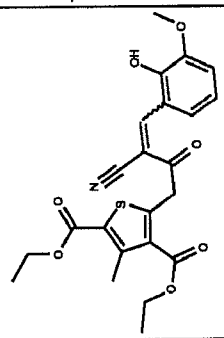
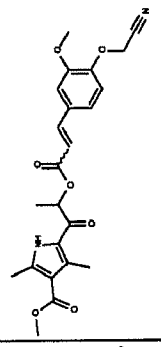
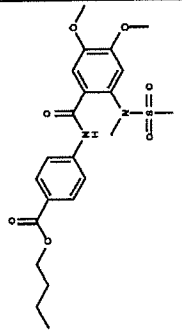
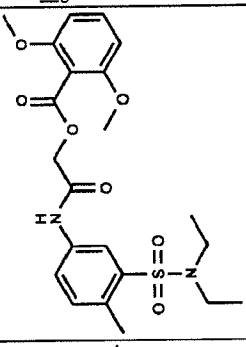
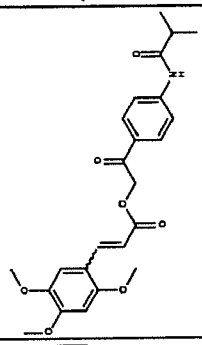
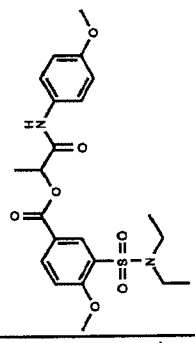
697	698	699	700
			
20321782_0 17	3882939_0,5946128	3963815_0 17	42976504_0 17
701	**702**	**703**	**704**
			
17635350_0 17	24351466_0 17	29471622_0 17	27949610_0,279496

Fig. 23, cont'd

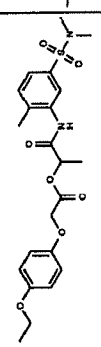
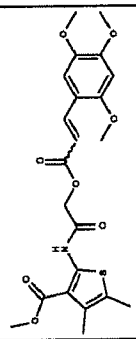
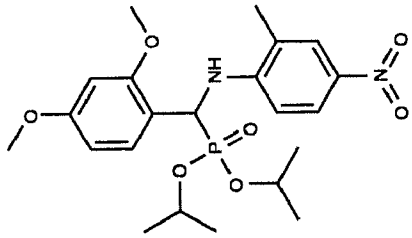
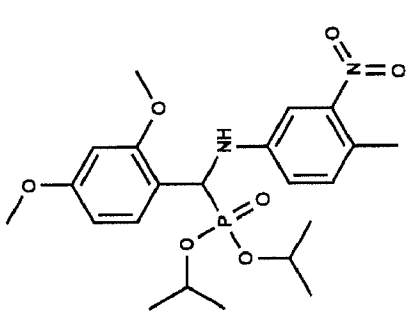
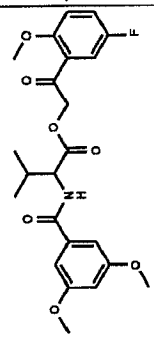
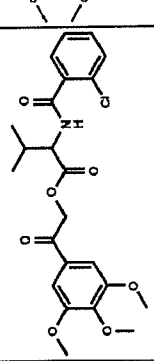
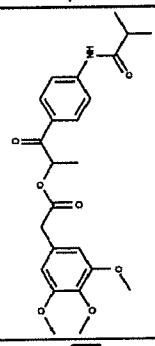
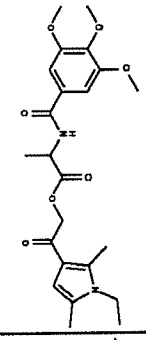
705	706	707	708
			
29333561_0,293335	31983610_0 17	21210945_0 17	21210944_0 17
709	710	711	712
			
46508712_0 17	16564493_0 17	24453236_0,293494	25691566_0,256915

Fig. 23, cont'd

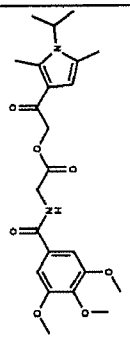
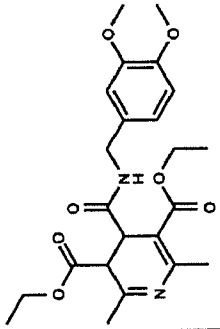
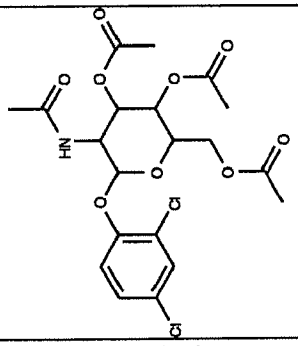
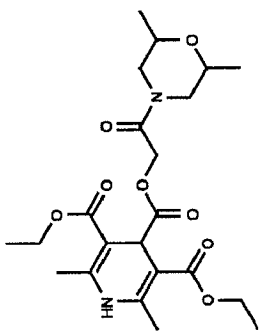
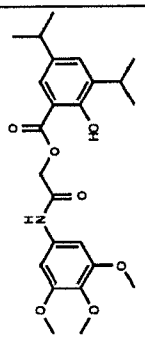
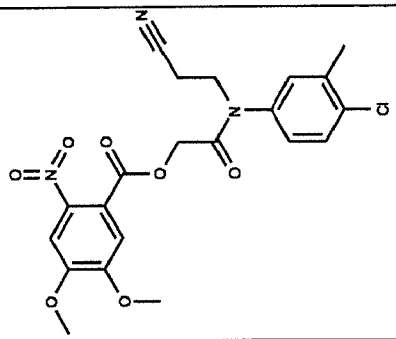
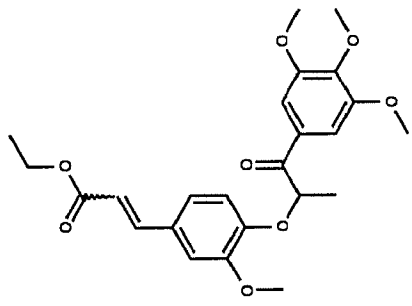
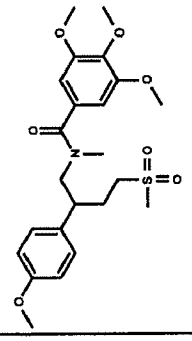
713	714	715	716
			
24367332_0 17	27276765_0 17	16398291_0,188051	32493181_0,324931
717	**718**	**719**	**720**
			
24384287_0 17	24567510_0 17	11236127_0 17	21223820_0 17

Fig. 23, cont'd

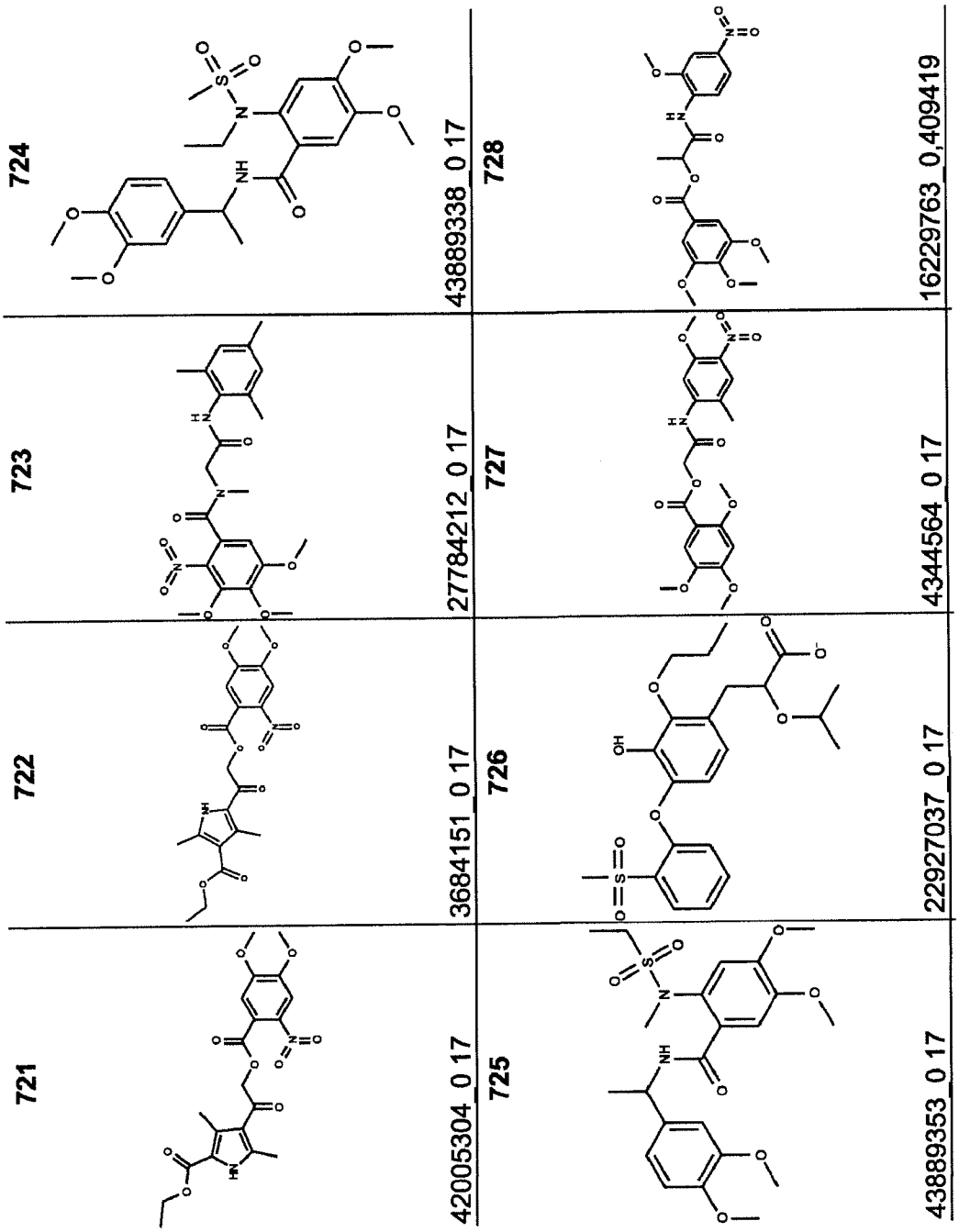

721
722
723
724
42005304_0 17
3684151_0 17
27784212_0 17
43889338_0 17
725
726
727
728
43889353_0 17
22927037_0 17
4344564_0 17
16229763_0,409419

Fig. 23, cont'd

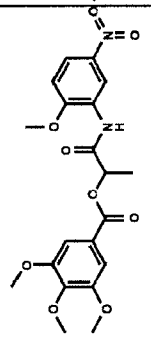
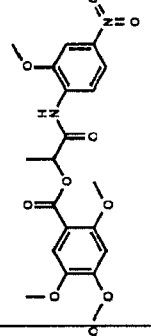
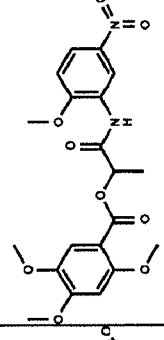
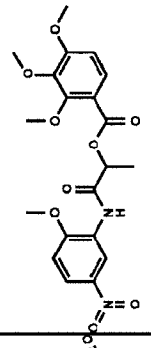
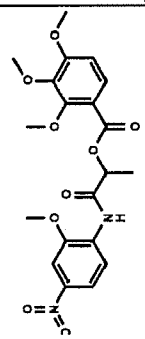
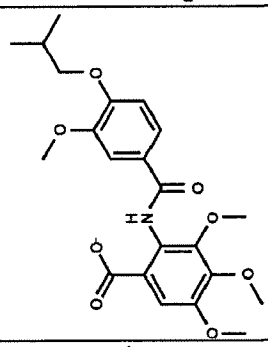
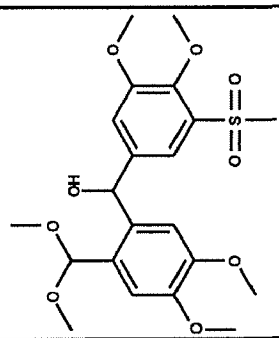
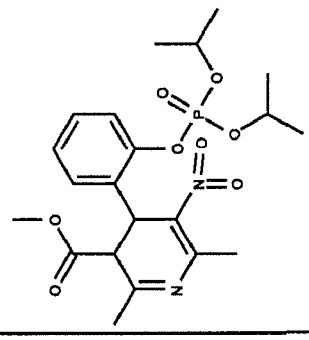
729	730	731	732
			
2355200_0,2355201	16252816_0,411798	18774945_0,256600	18774929_0 17
733	734	735	736
			
18774928_0 17	45348070_0 17	10503989_0 17	7073417_0,7073418

Fig. 23, cont'd

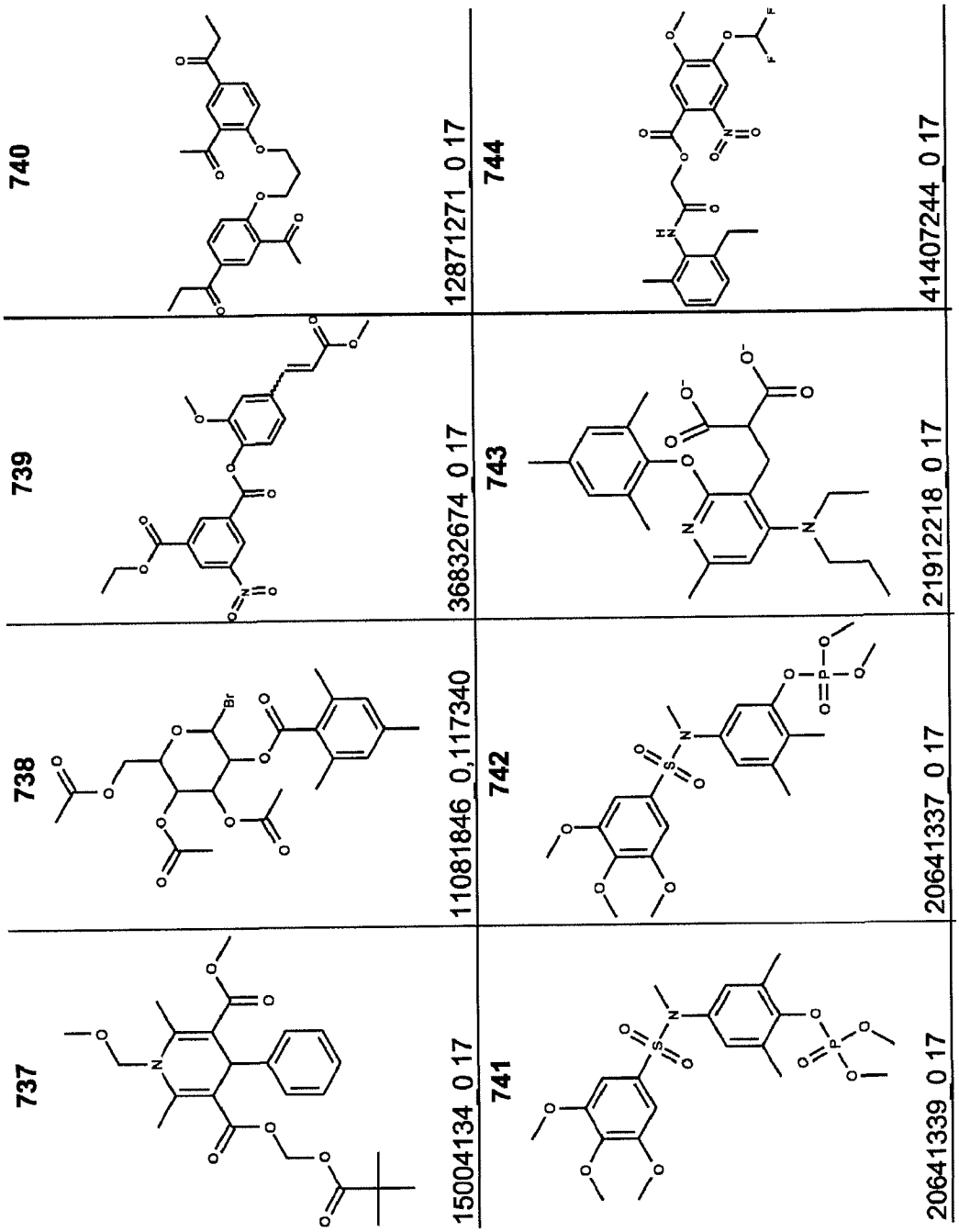

737
738
739
740
15004134_0 17
11081846_0,117340
36832674_0 17
12871271_0 17
741
742
743
744
20641339_0 17
20641337_0 17
21912218_0 17
41407244_0 17

Fig. 23, cont'd

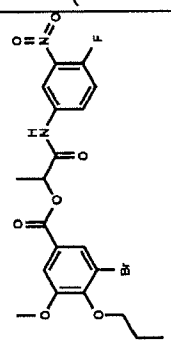
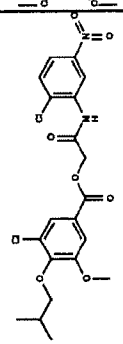
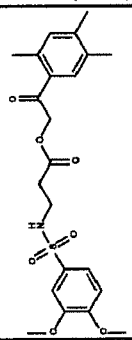
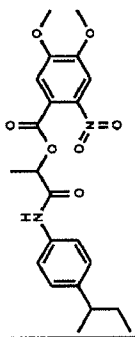
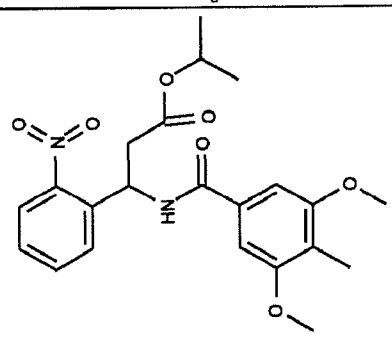
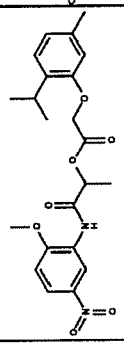
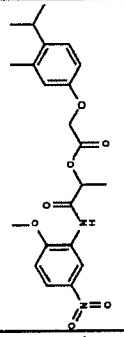
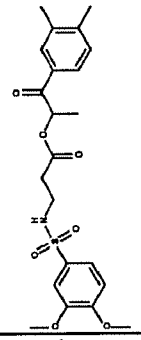
745	746	747	748
			
42974276_0 17	41278808_0 17	28048366_0 17	2651930_0,2651931
749	750	751	752
			
46657493_0 17	45705257_0 17	29182877_0,291828	46809188_0 17

Fig. 23, cont'd

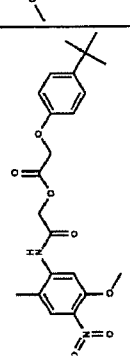
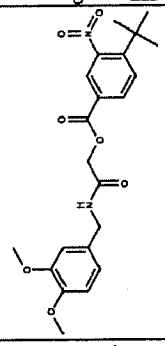
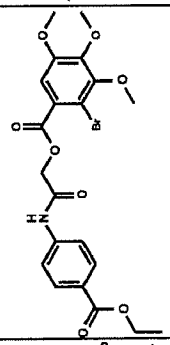
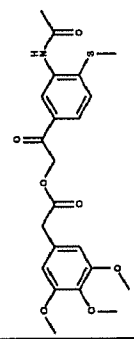
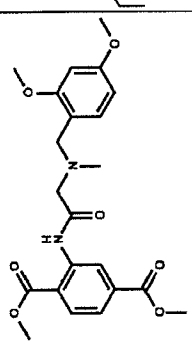
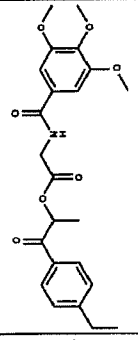
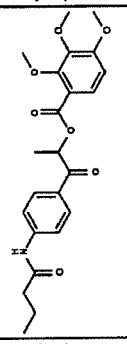
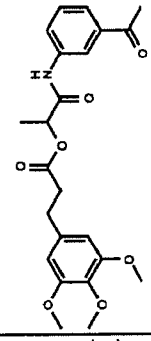
753	754	755	756
			
3667962_0 17	18283203_0 17	1194605_0 17	27312563_0 17
757	758	759	760
			
2698988_0 17	24367376_0,291913	24438028_0,309272	45689354_0 17

Fig. 23, cont'd

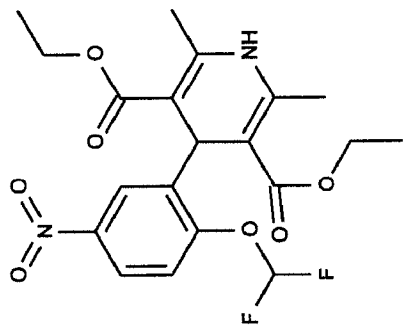
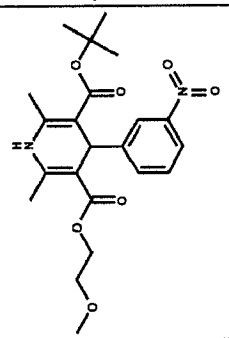
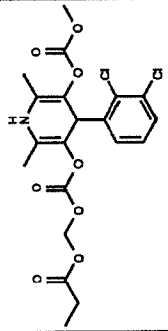
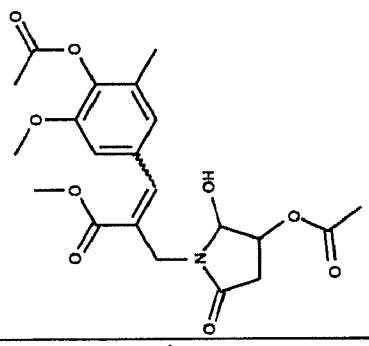
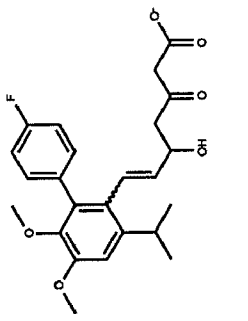
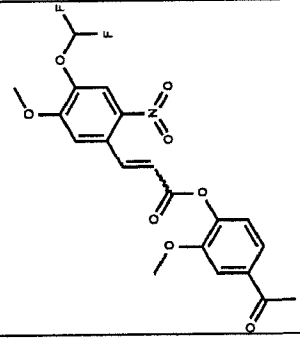
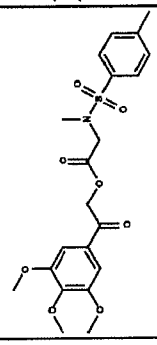
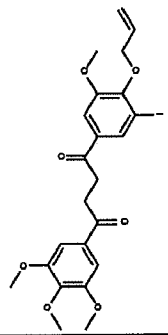
761	762	763	764
			
4140979_0 17	5198133_0 17	23215648_0 17	11732830_0 17
765	**766**	**767**	**768**
			
23352481_0,233524	24581288_0 17	4851447_0 17	15718026_0 17

Fig. 23, cont'd

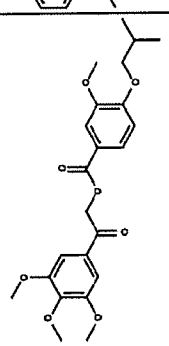
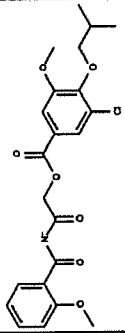
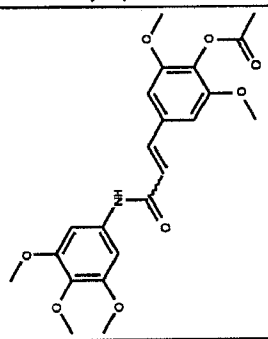
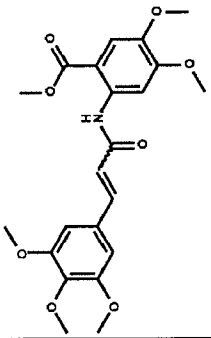
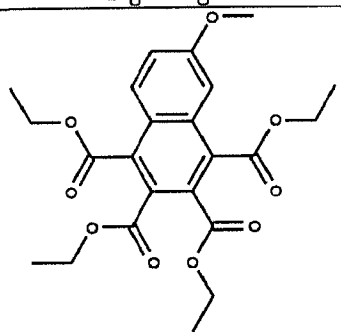
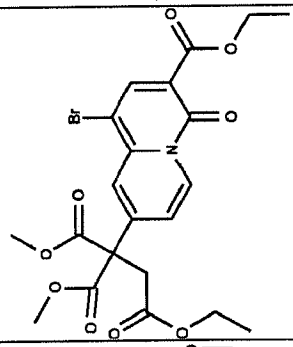
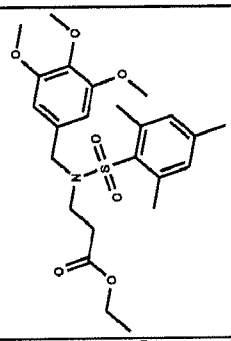
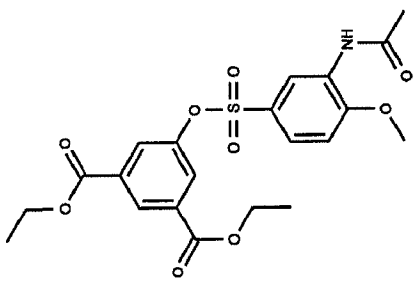
769	770	771	772
			
16503166_0 17	31192710_0 17	46177362_0 17	26176946_0 17
773	**774**	**775**	**776**
			
11733003_0 17	20634150_0 17	5103999_0 17	24464952_0 17

Fig. 23, cont'd

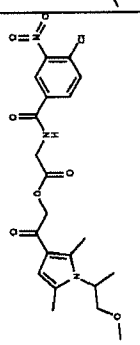
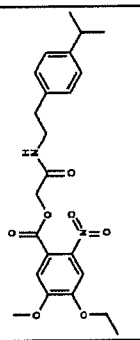
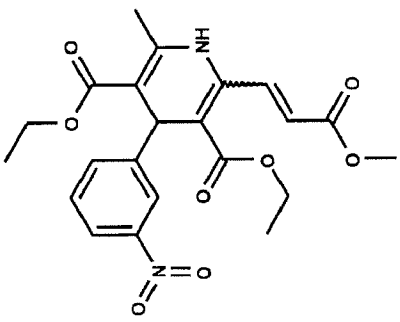
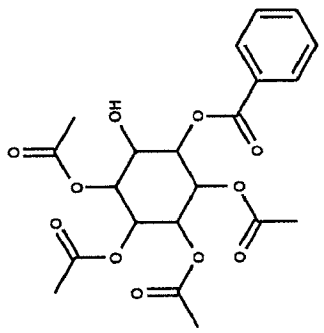
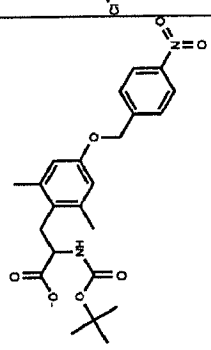
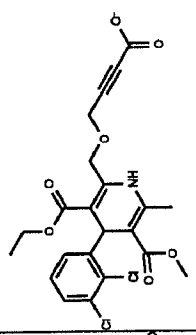
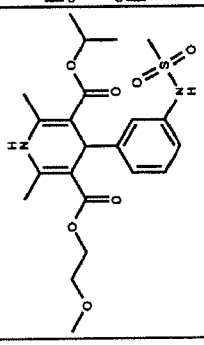
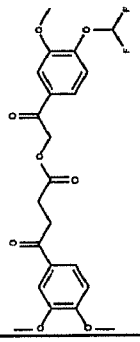
777	778	779	780
			
29245658_0,292456	24485575_0 17	46887806_0 17	320734_0 17
781	**782**	**783**	**784**
			
10321231_0 17	22165626_0 17	11839446_0,284260	42988497_0 17

Fig. 23, cont'd

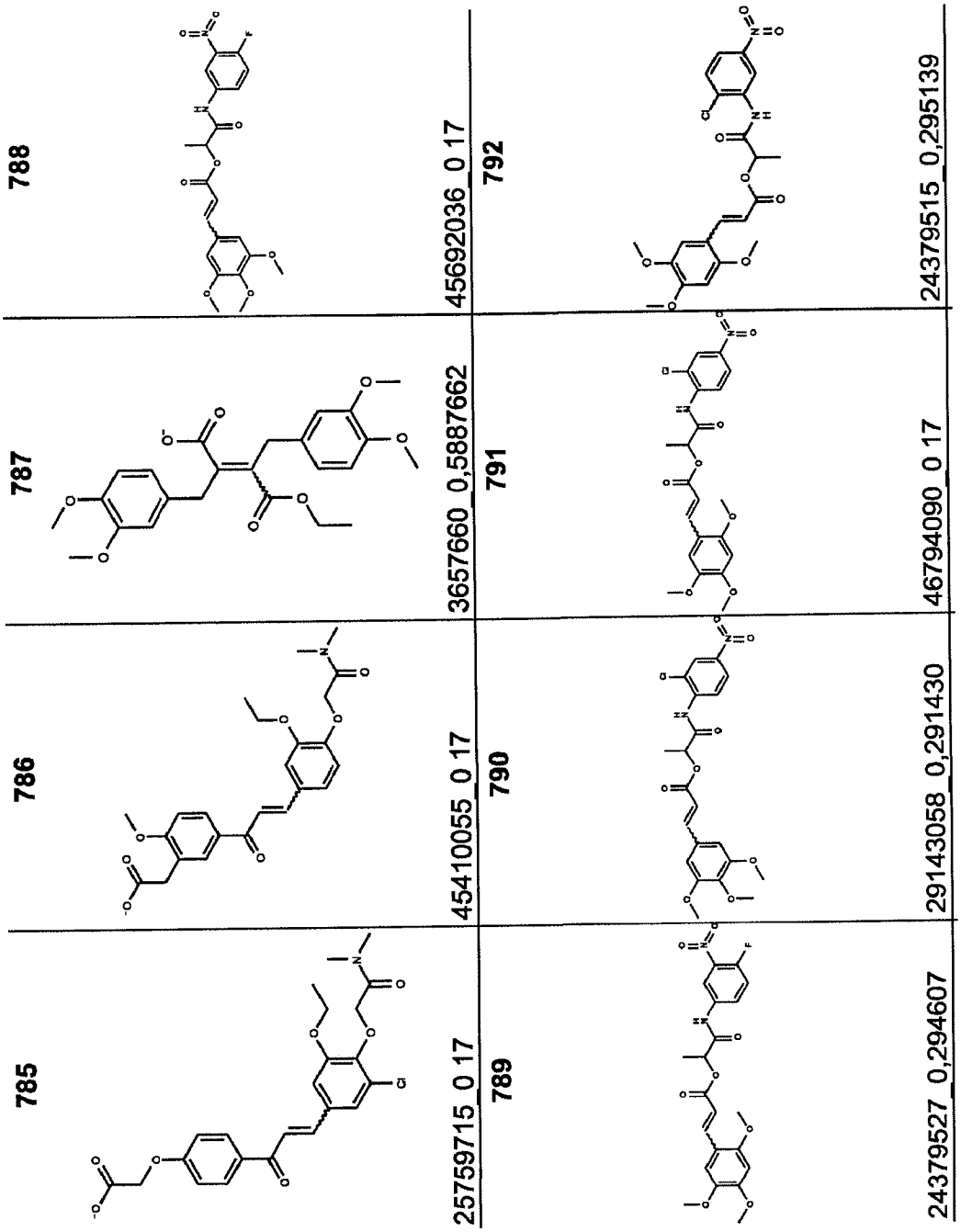

785
786
787
788
25759715_0 17
45410055_0 17
3657660_0,5887662
45692036_0 17
789
790
791
792
24379527_0,294607
29143058_0,291430
46794090_0 17
24379515_0,295139

Fig. 23, cont'd

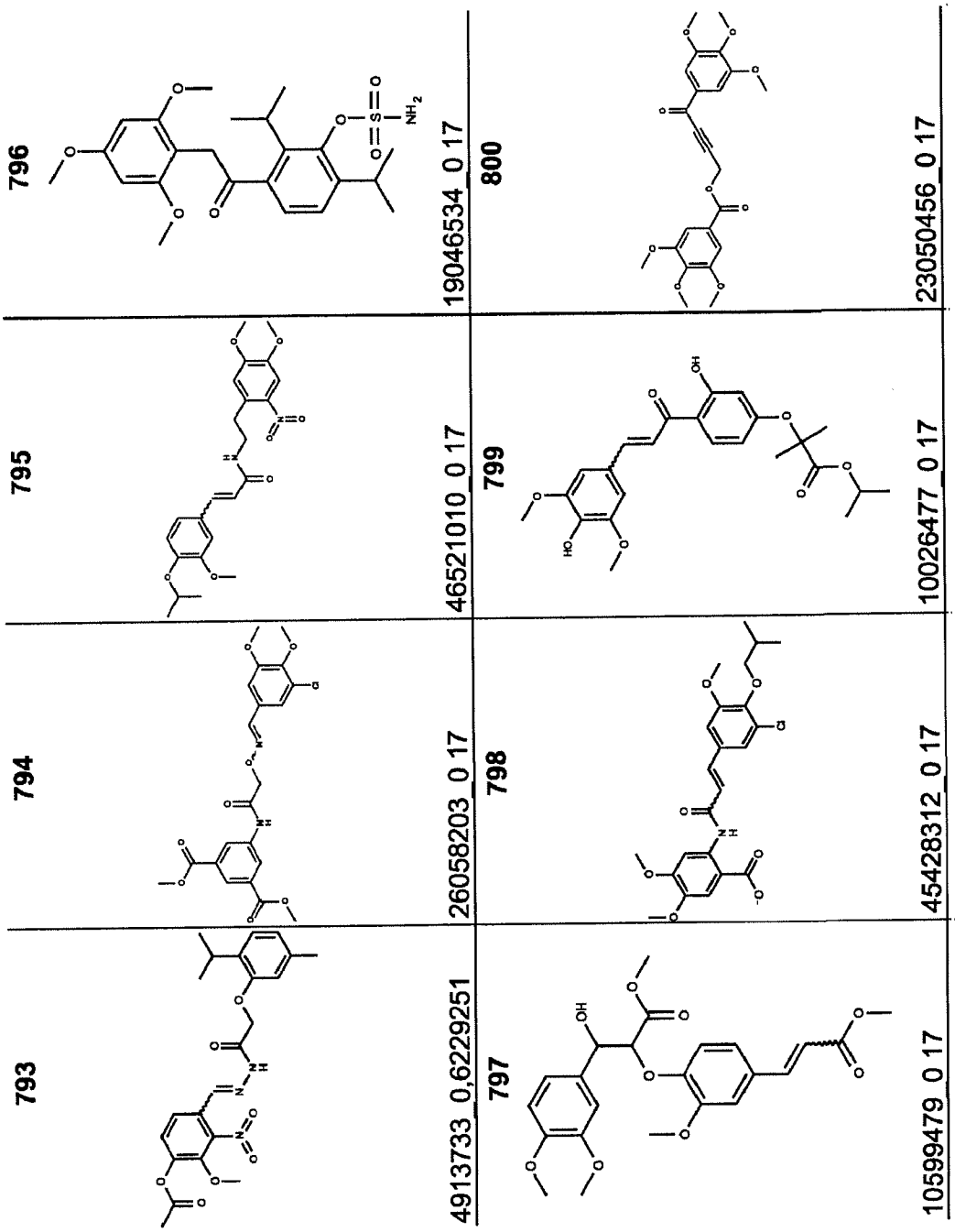

793
4913733_0,6229251
794
26058203_0 17
795
46521010_0 17
796
19046534_0 17
797
10599479_0 17
798
45428312_0 17
799
10026477_0 17
800
23050456_0 17

Fig. 23, cont'd

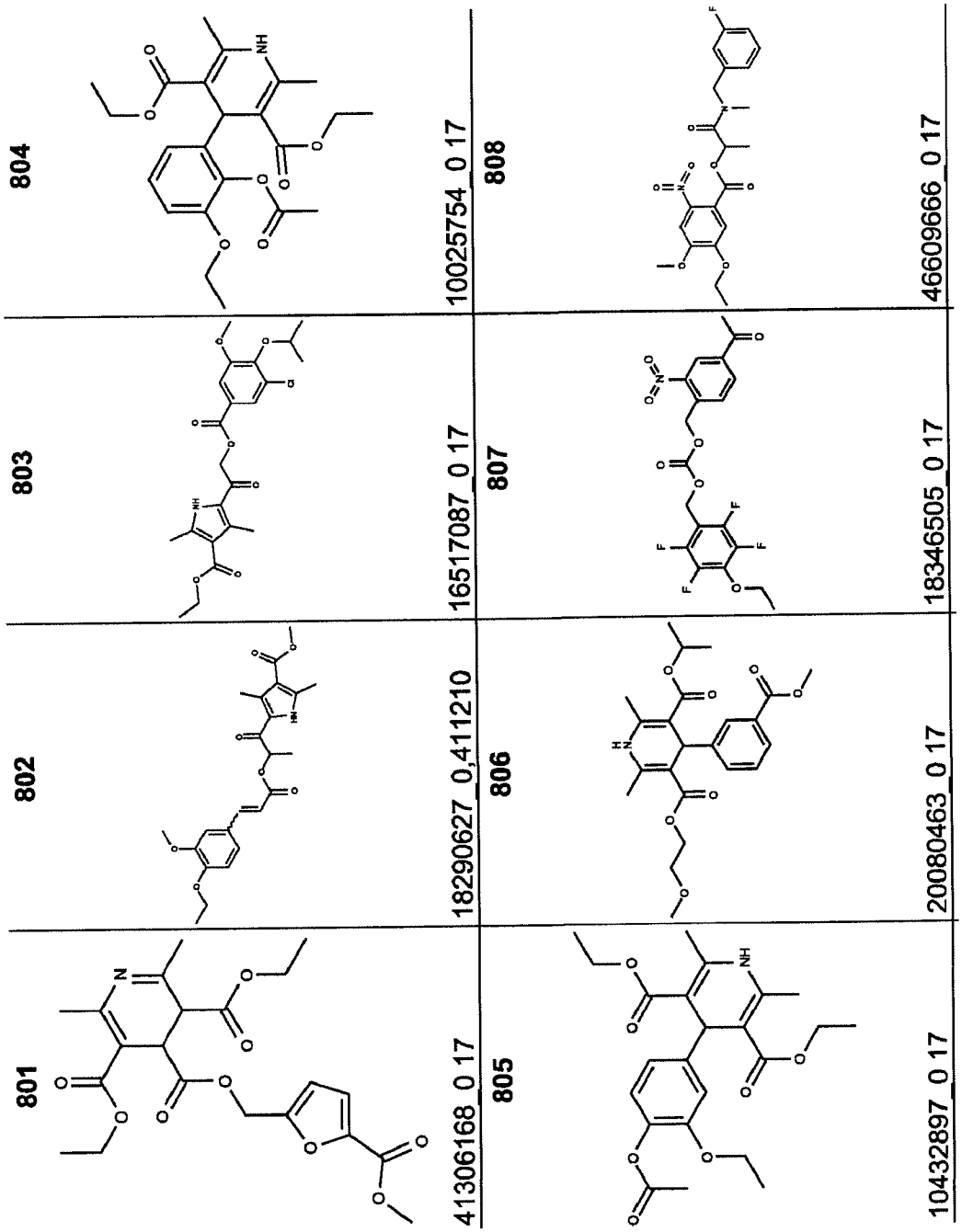

801
802
803
804
41306168_0 17
18290627_0,411210
16517087_0 17
10025754_0 17
805
806
807
808
10432897_0 17
20080463_0 17
18346505_0 17
46609666_0 17

Fig. 23, cont'd

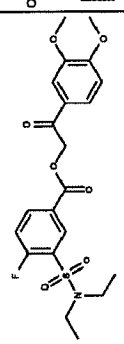
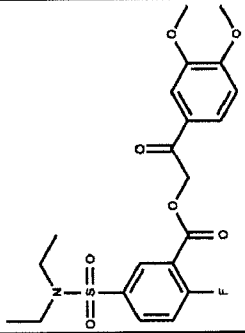
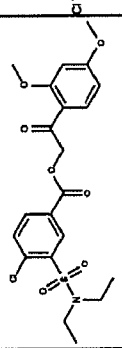
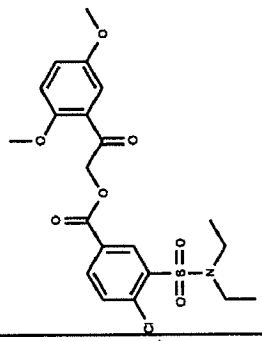
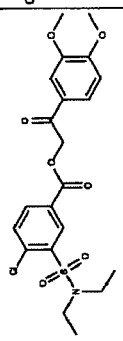
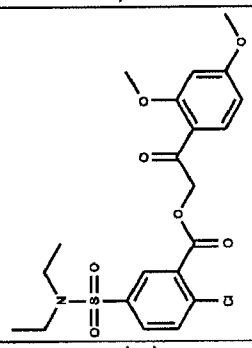
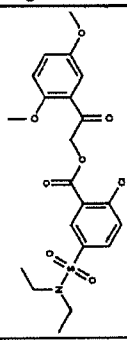
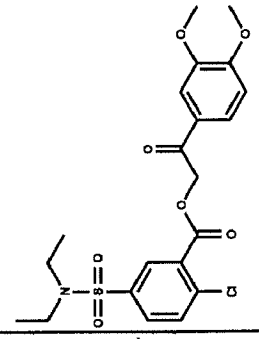
809	810	811	812
			
16529918_0 17	16512439_0 17	2458498_0 17	23940193_0 17
813	**814**	**815**	**816**
			
2510455_0 17	2460514_0 17	30687427_0 17	2509923_0 17

Fig. 23, cont'd

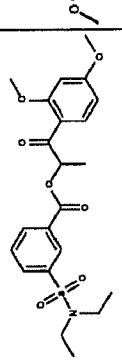
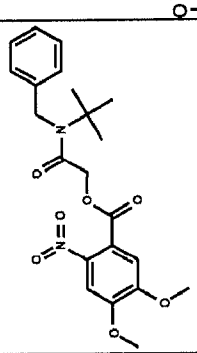
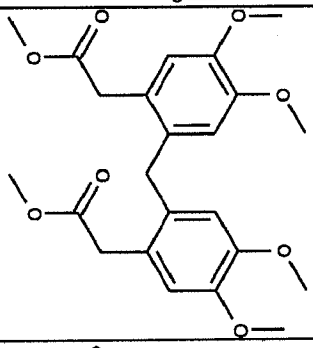
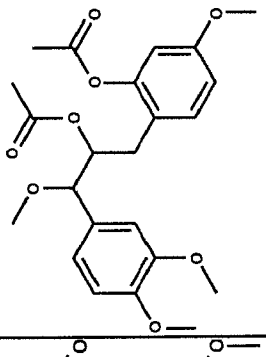
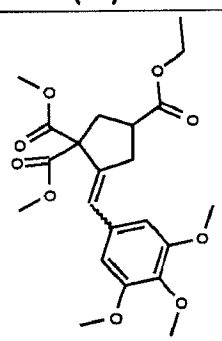
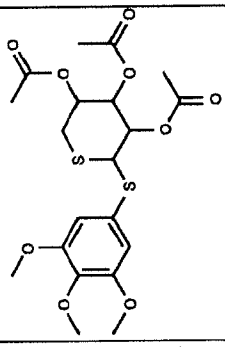
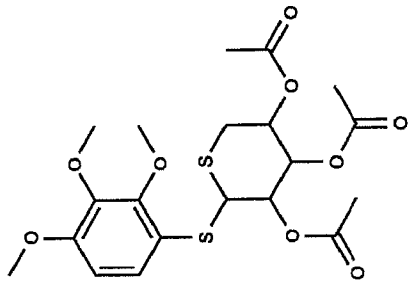
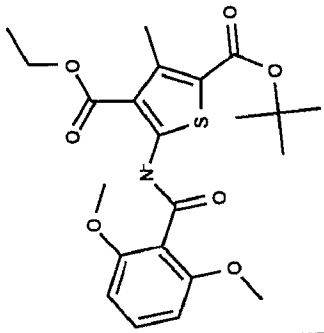
817	818	819	820
			
2625925_0,2625927	2483014_0 17	1352009_0 17	602327_0 17
821	822	823	824
			
23631843_0 17	14795350_0 17	21650636_0 17	4421662_0 17

Fig. 23, cont'd

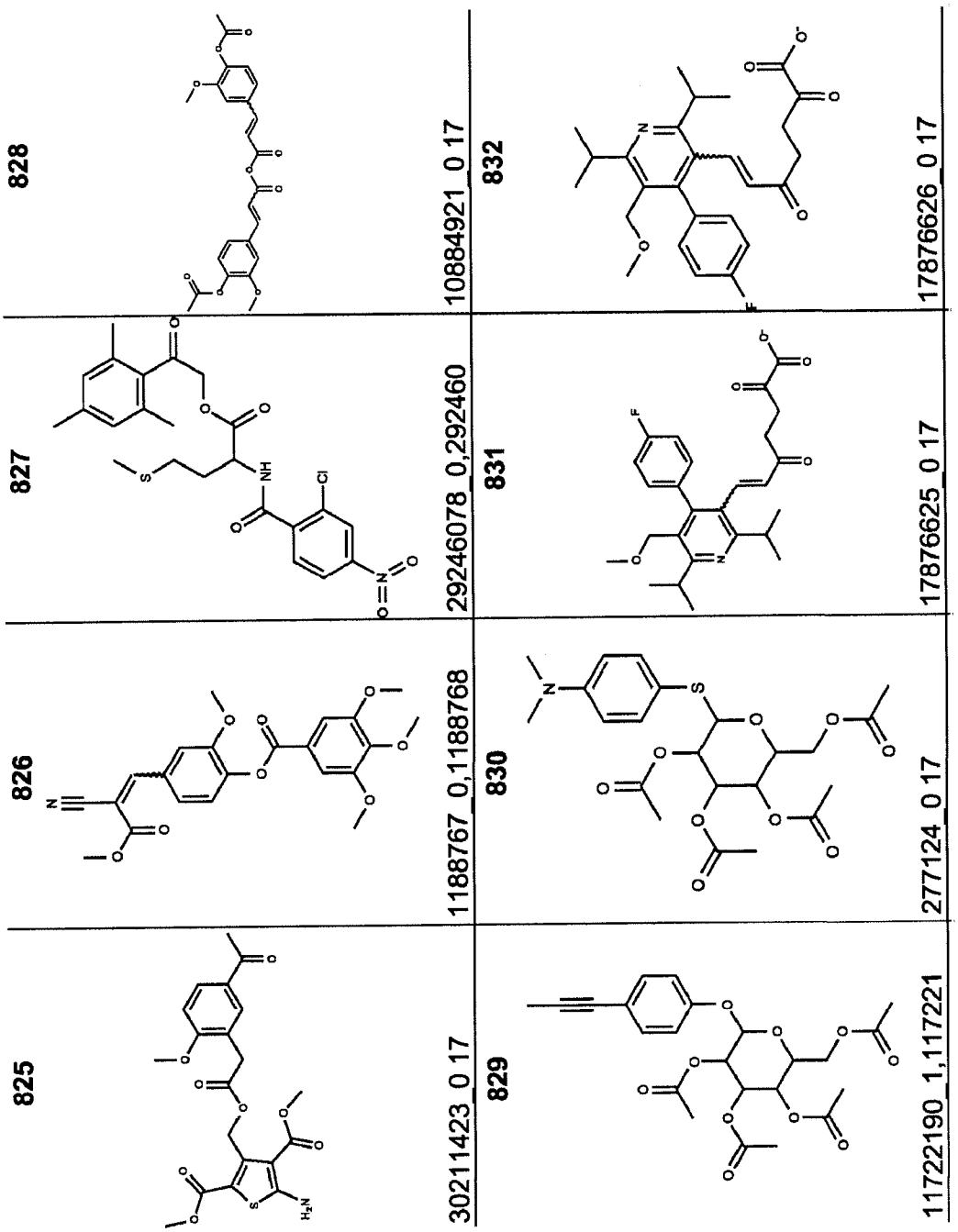

825
826
827
828
30211423_0 17
1188767_0,1188768
29246078_0,292460
10884921_0 17
829
830
831
832
11722190_1,117221
277124_0 17
17876625_0 17
17876626_0 17

Fig. 23, cont'd

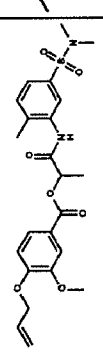
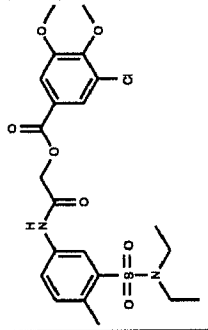
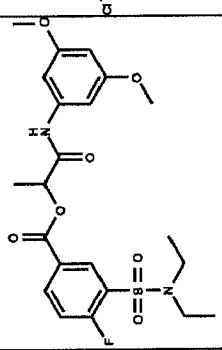
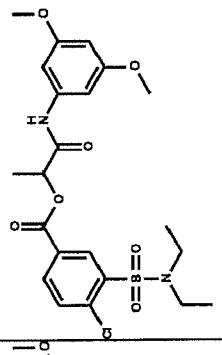
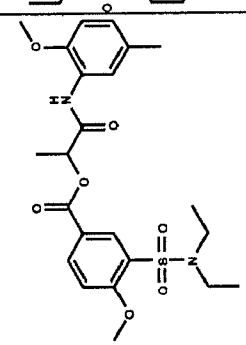
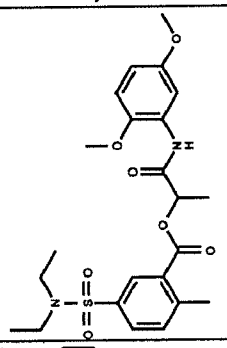
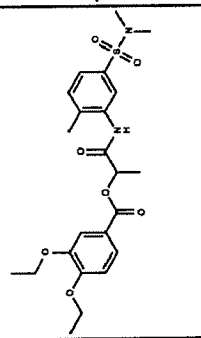
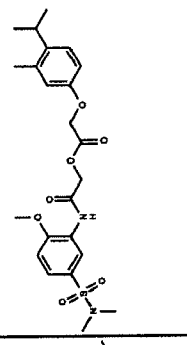
833	834	835	836
			
16576065_0 17	42979654_0 17	16530006_0 17	16521875_0 17
837	**838**	**839**	**840**
			
27949624_0,279496	42986541_0 17	16527901_0 17	24379166_0 17

Fig. 23, cont'd

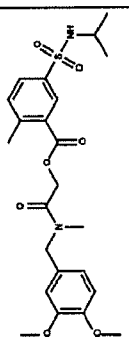
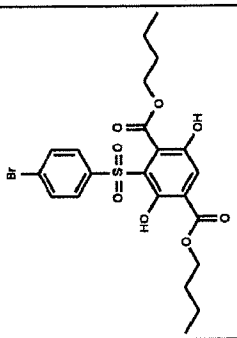
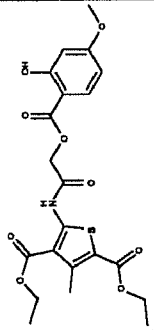
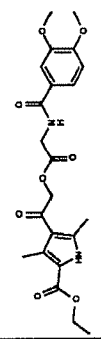
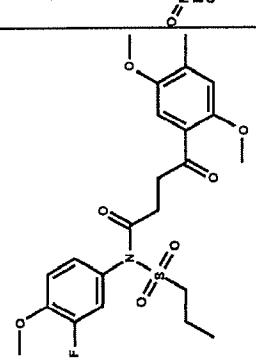
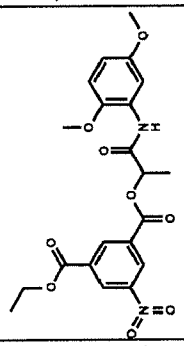
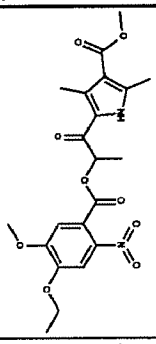
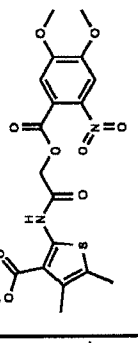
841	842	843	844
			
30011855_0 17	20144746_0 17	24380493_0 17	41492185_0 17
845	**846**	**847**	**848**
			
3753023_0 17	24348557_0 17	46683510_0 17	2569979_0 17

Fig. 23, cont'd

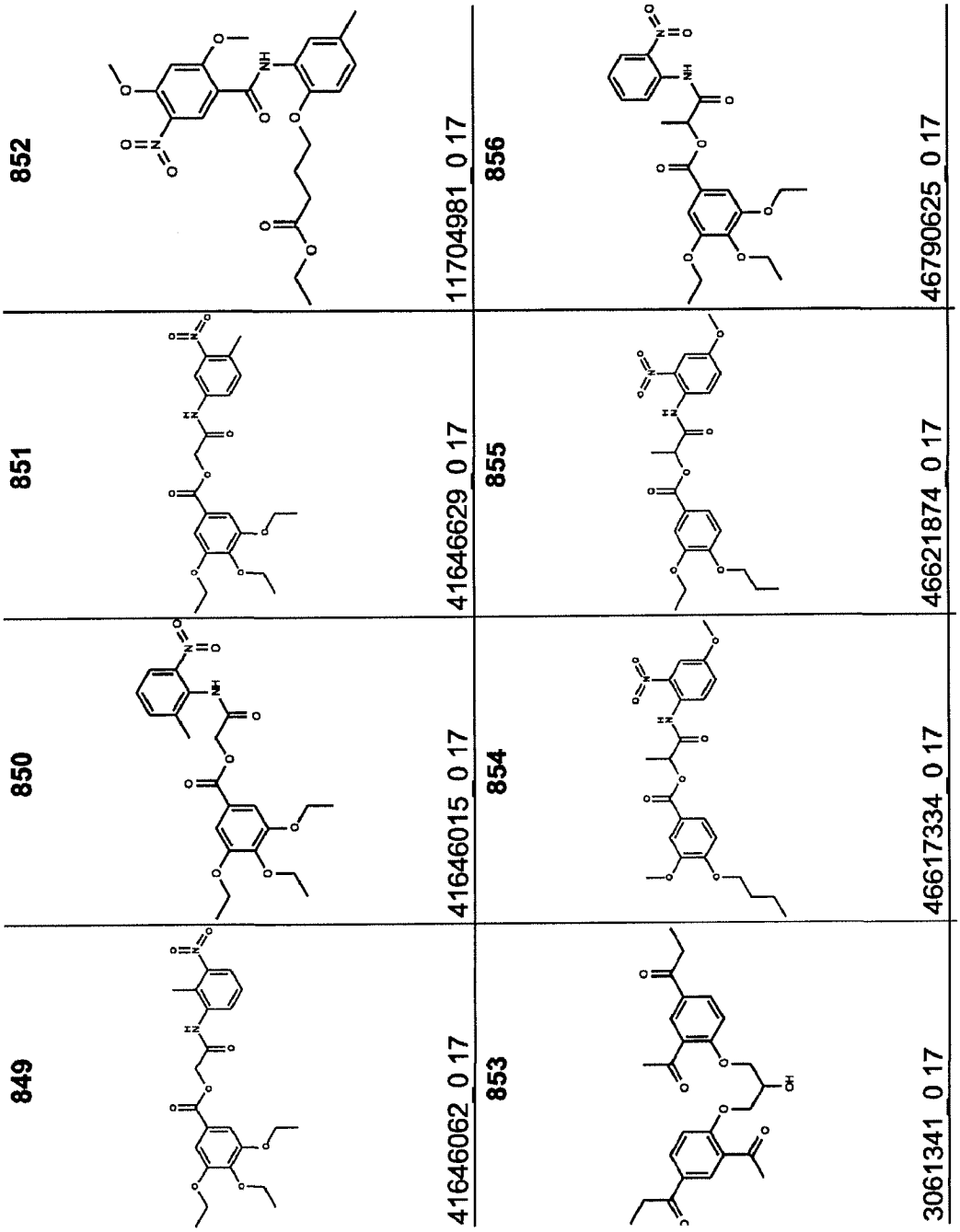

849
850
851
852
41646062_0 17
41646015_0 17
41646629_0 17
1170481_0 17
853
854
855
856
3061341_0 17
46617334_0 17
46621874_0 17
46790625_0 17

Fig. 23, cont'd

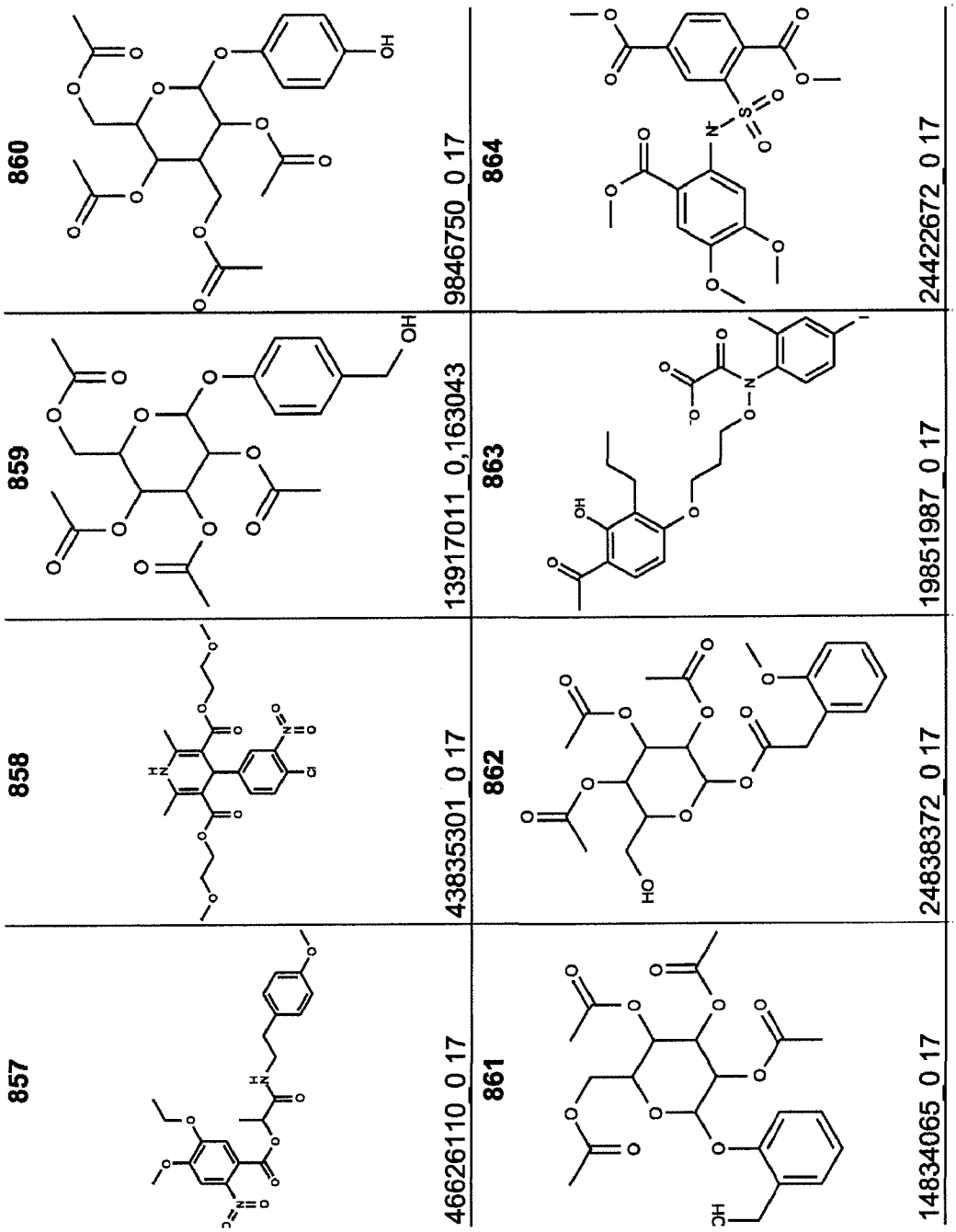

857
858
859
860
4662611 0 17
43835301 0 17
13917011 0,163043
9846750 0 17
861
862
863
864
14834065 0 17
24838372 0 17
19851987 0 17
24422672 0 17

Fig. 23, cont'd

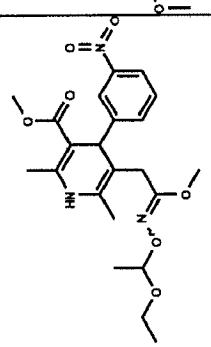
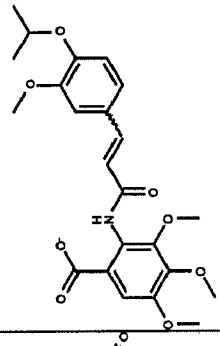
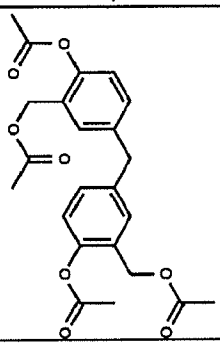
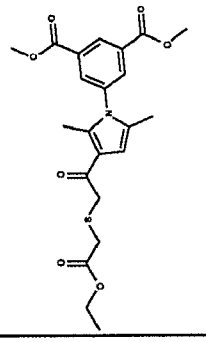
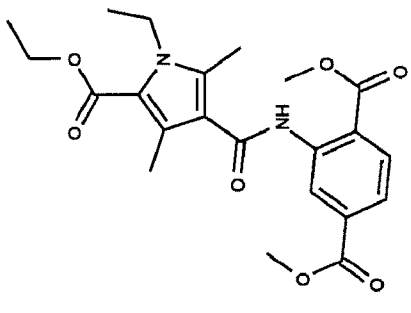
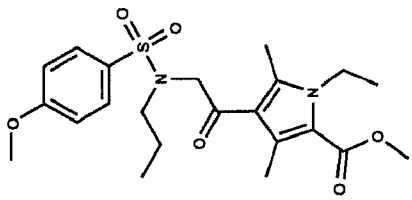
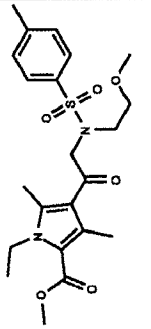
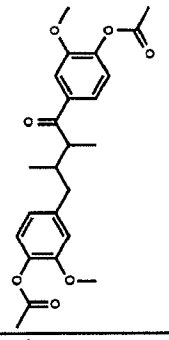
865	866	867	868
			
18596568_0,204024	45348019_0 17	20293789_0,203878	30549627_0 17
869	**870**	**871**	**872**
			
43954157_0 17	42678027_0 17	42823553_0 17	11743316_0 17

Fig. 23, cont'd

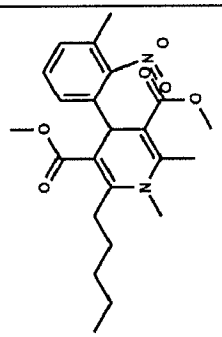
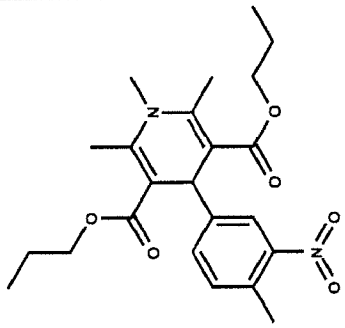
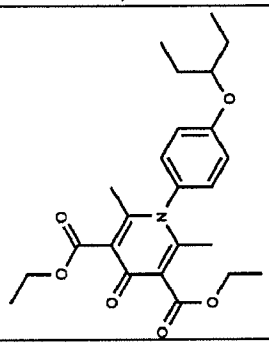
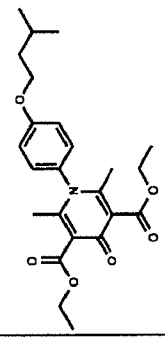
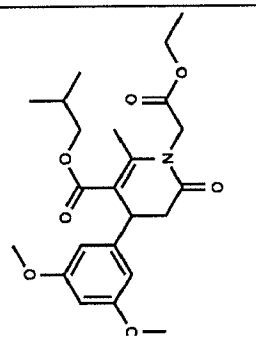
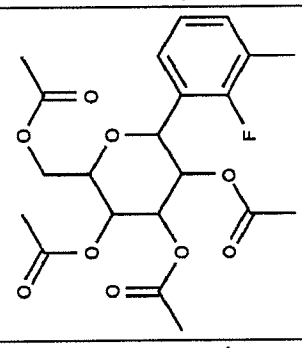
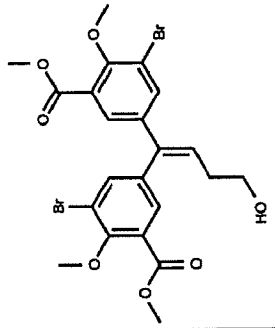
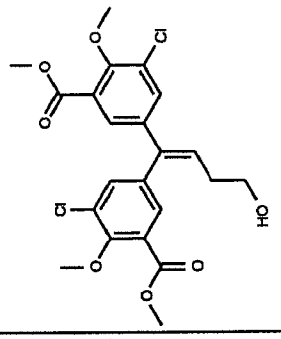
873	874	875	876
			
22558236_0 17	15170375_0 17	21515588_0 17	21515582_0 17
877	**878**	**879**	**880**
			
42854886_0 17	23080593_0 17	392998_0 17	391573_0 17

Fig. 23, cont'd

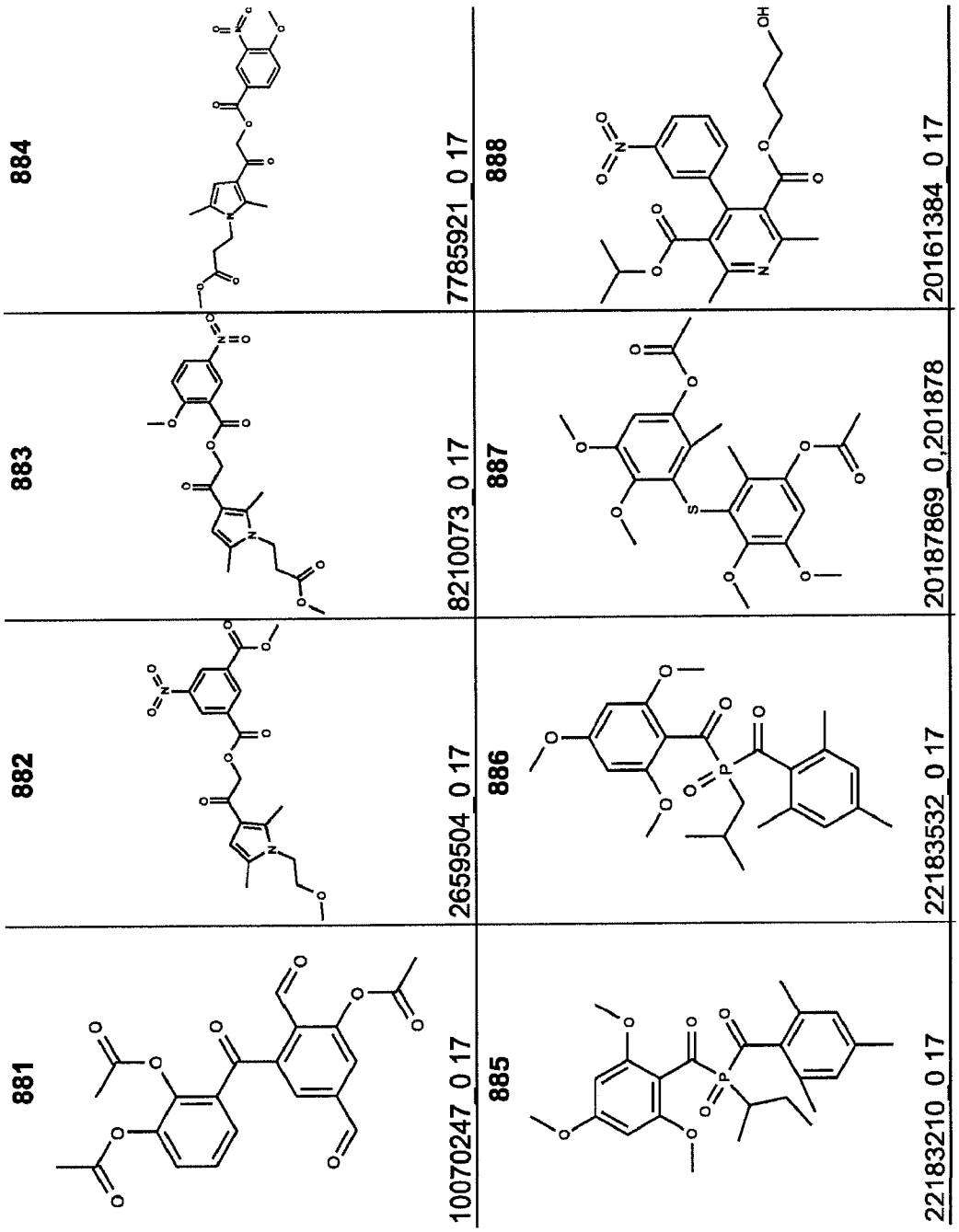

881
882
883
884
10070247_0 17
2659504_0 17
8210073_0 17
7785921_0 17
885
886
887
888
22183210_0 17
22183532_0 17
20187869_0,201878
20161384_0 17

Fig. 23, cont'd

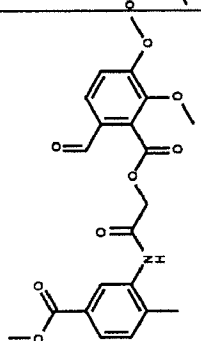
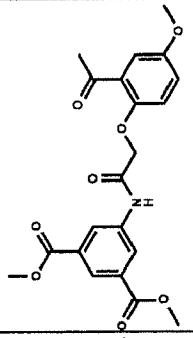
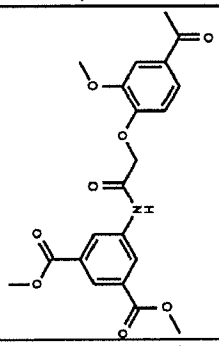
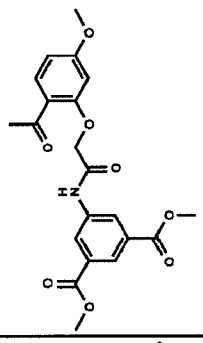
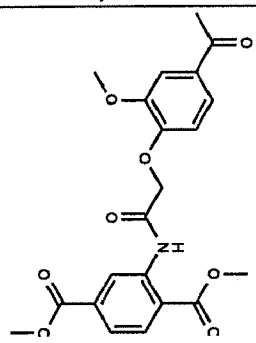
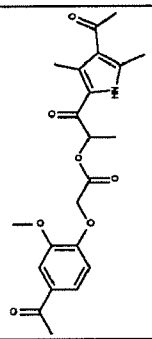
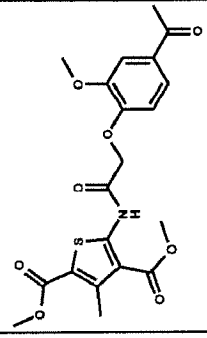
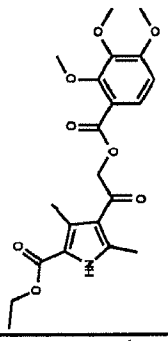
889	890	891	892
			
8370096_0 17	24387952_0 17	2709031_0 17	2507163_0 17
893	**894**	**895**	**896**
			
8308431_0 17	8849875_0 17	18161524_0 17	25939443_0 17

Fig. 23, cont'd

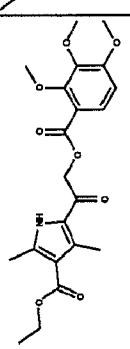
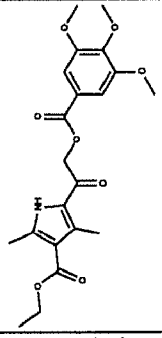
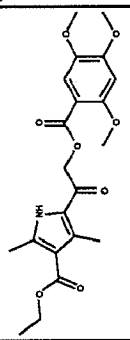
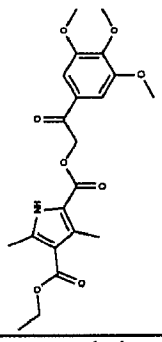
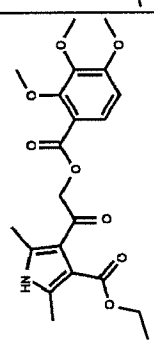
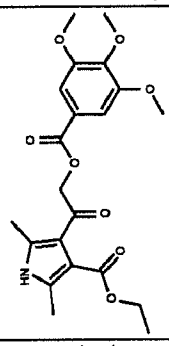
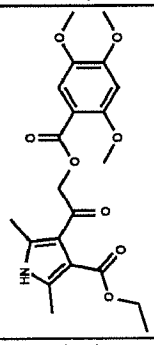
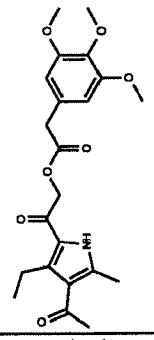
897	898	899	900
			
4002812_0 17	3517718_0 17	4016932_0 17	16508601_0 17
901	**902**	**903**	**904**
			
7758345_0 17	8013083_0 17	2365302_0 17	48233519_0 17

Fig. 23, cont'd

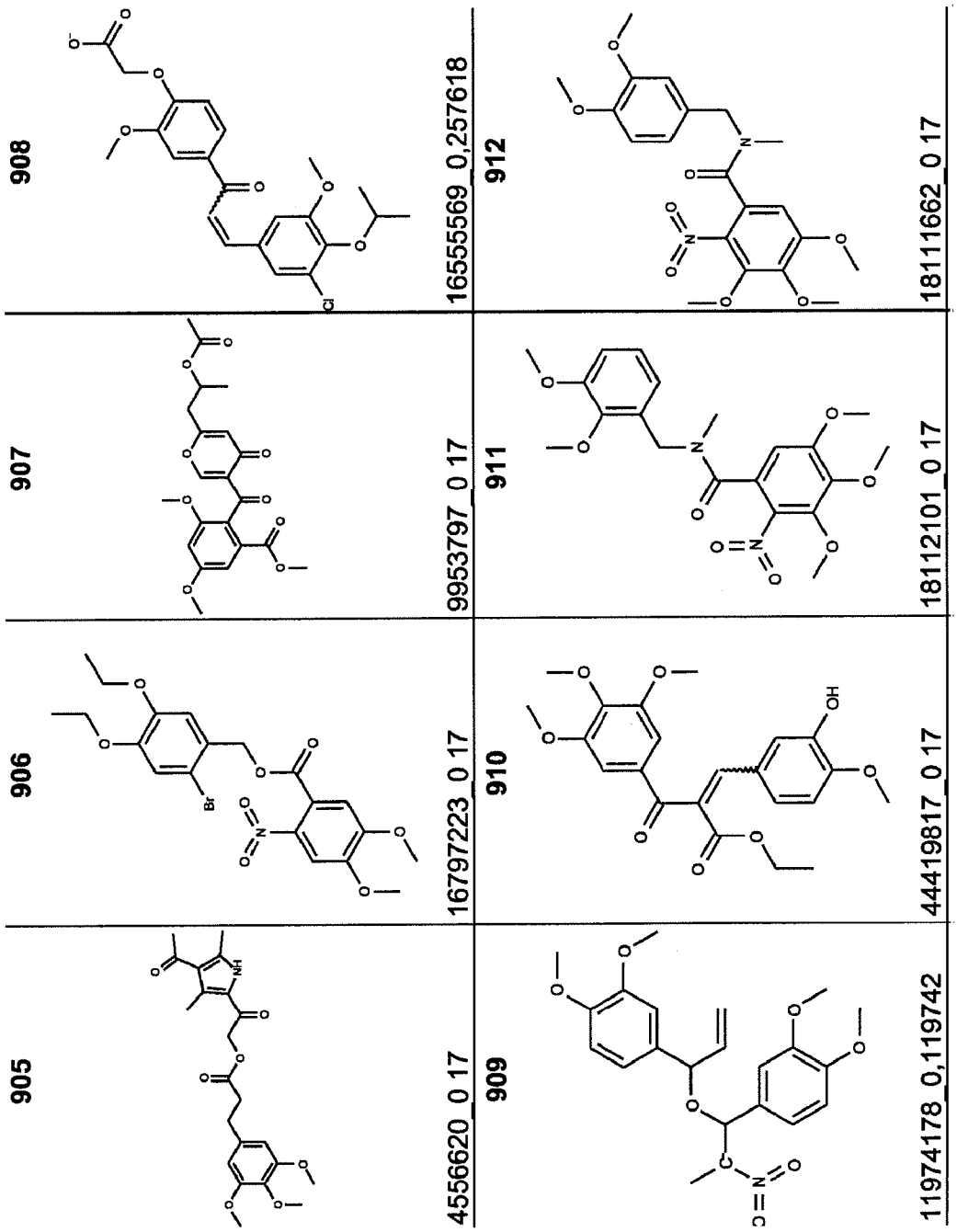

905
906
907
908
4556620_0 17
16797223_0 17
9953797_0 17
16555569_0,257618
909
910
911
912
11974178_0,119742
44419817_0 17
18112101_0 17
18111662_0 17

Fig. 23, cont'd

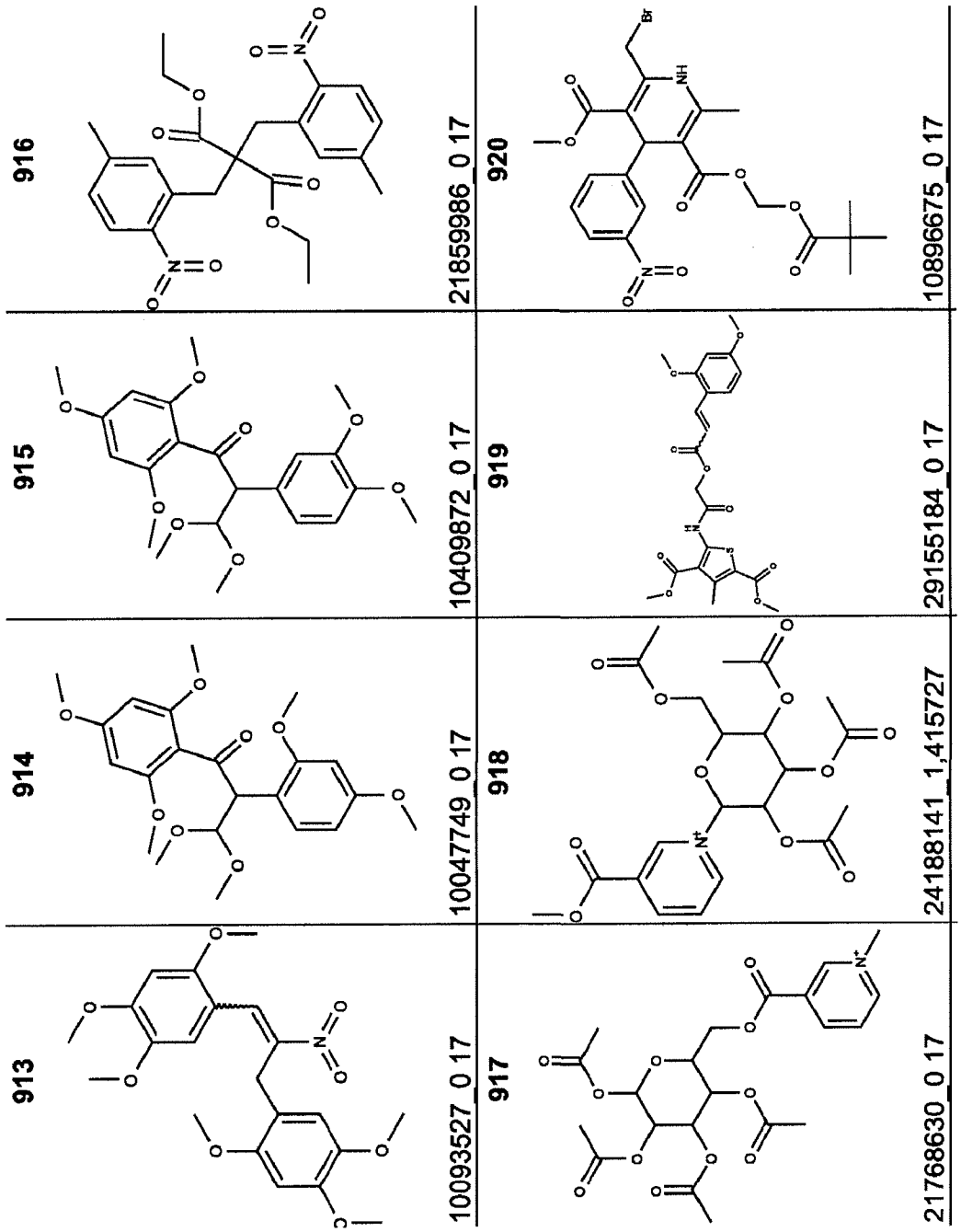

913
914
915
916
917
918
919
920
10093527_0 17
10047749_0 17
10409872_0 17
21859986_0 17
21768630_0 17
24188141_1,415727
29155184_0 17
10896675_0 17

Fig. 23, cont'd

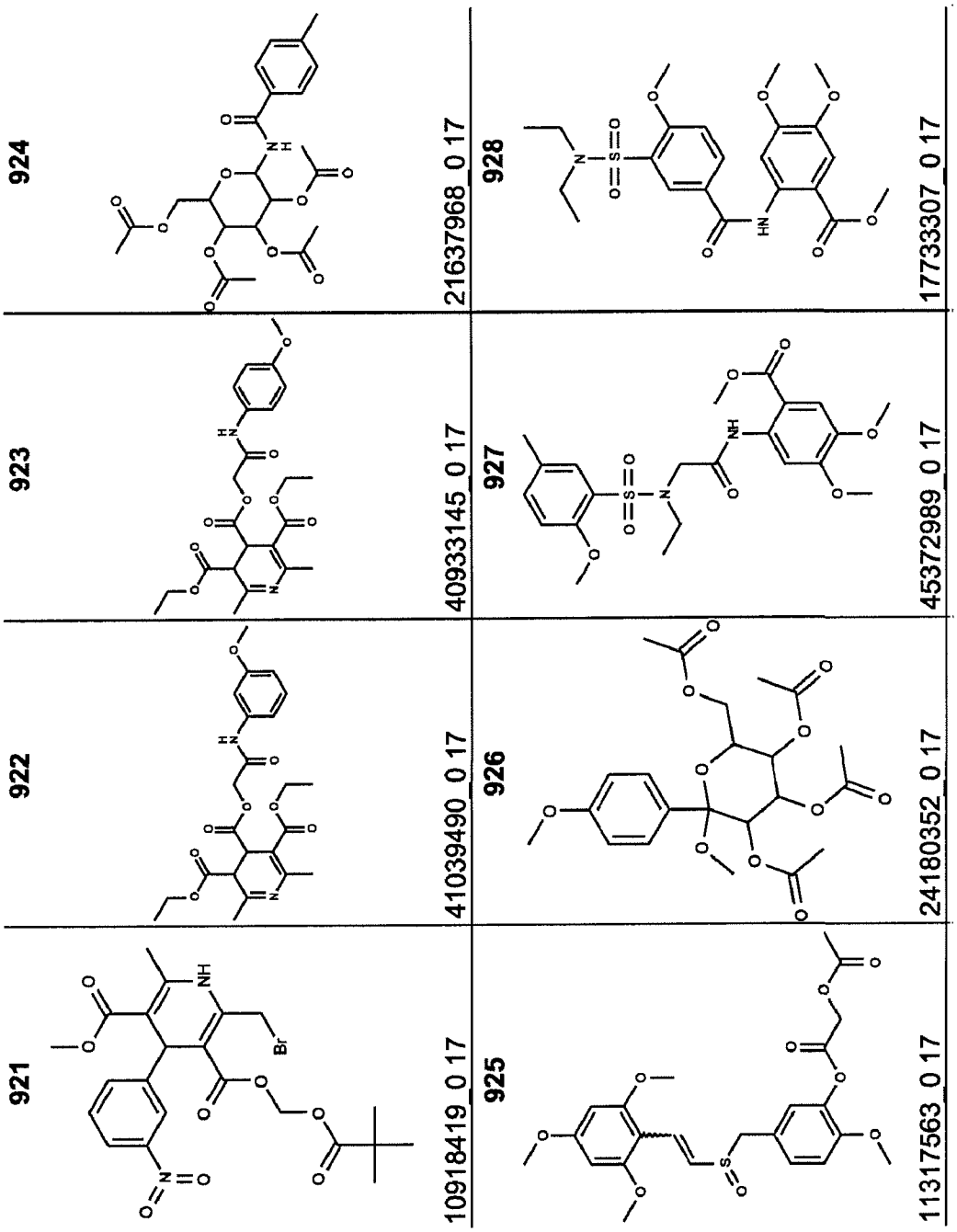

921
10918419_0 17
922
41039490_0 17
923
40933145_0 17
924
21637968_0 17
925
11317563_0 17
926
24180352_0 17
927
45372989_0 17
928
17733307_0 17

Fig. 23, cont'd

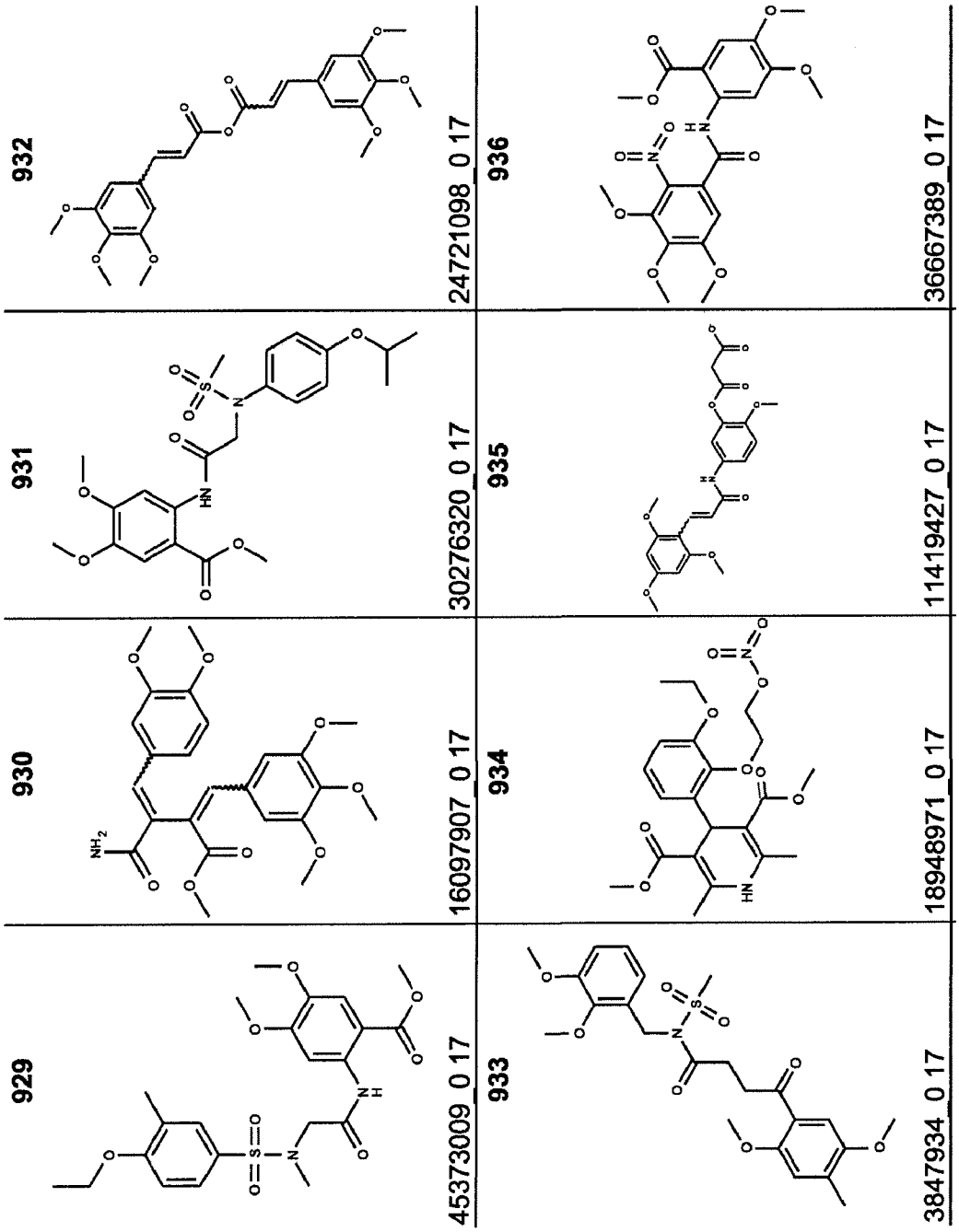

929
4537300 9_0 17
930
16097907_0 17
931
30276320_0 17
932
24721098_0 17
933
3847934_0 17
934
18948971_0 17
935
11419427_0 17
936
36667389_0 17

Fig. 23, cont'd

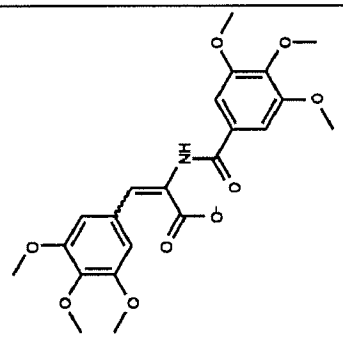
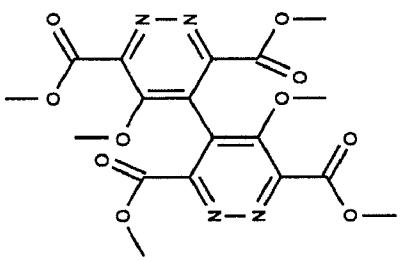
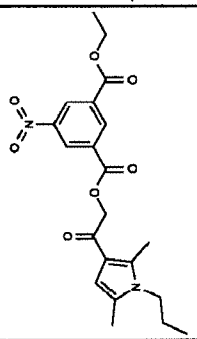
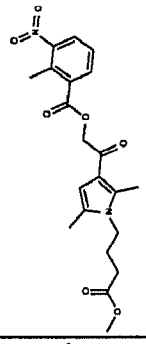
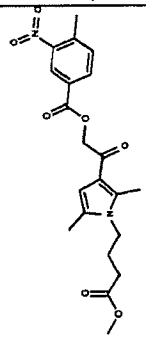
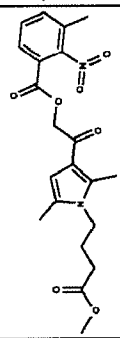
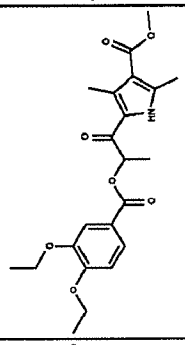
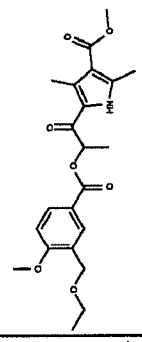
937	938	939	940
			
2063676_0,2063677	11048629_0 17	24348575_0 17	8710062_0 17
941	**942**	**943**	**944**
			
8177157_0 17	7569425_0 17	16527908_0,778578	8619305_0,8619306

Fig. 23, cont'd

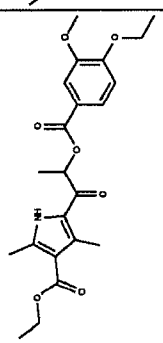
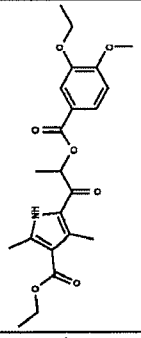
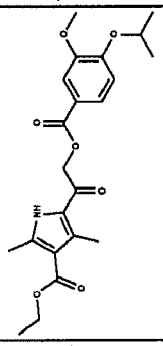
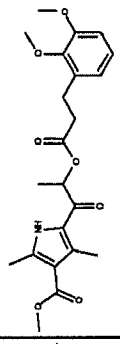
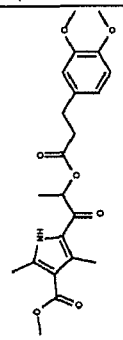
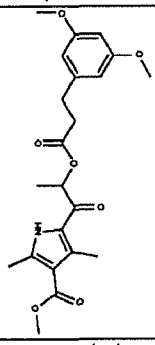
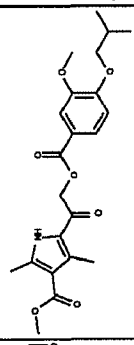
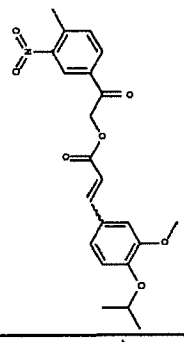
945	946	947	948
			
16516106_0 17	22829803_0,790361	16501059_0 17	46812684_0 17
949	**950**	**951**	**952**
			
8311189_0,8311191	8372312_0,8372313	24332023_0 17	7726381_0 17

Fig. 23, cont'd

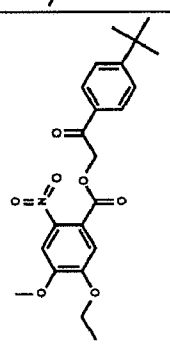
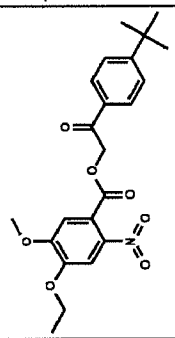
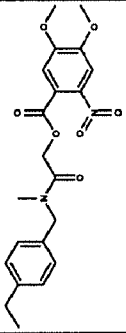
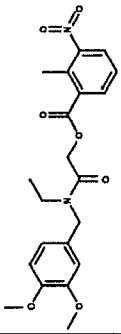
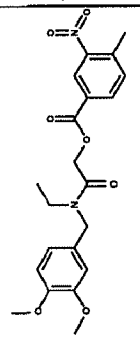
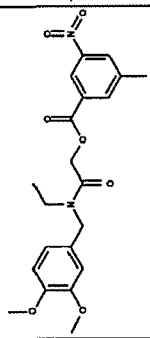
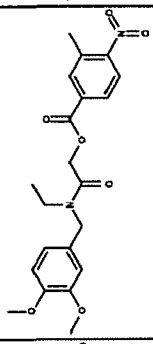
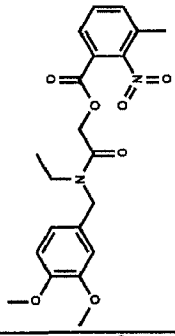
953	954	955	956
			
8666426_0 17	9124824_0 17	8847787_0 17	9289732_0 17
957	**958**	**959**	**960**
			
9339503_0 17	48700661_0 17	9199276_0 17	40752620_0 17

Fig. 23, cont'd

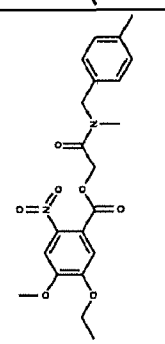
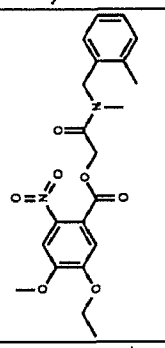
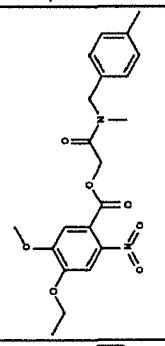
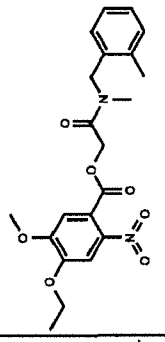
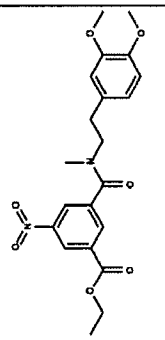
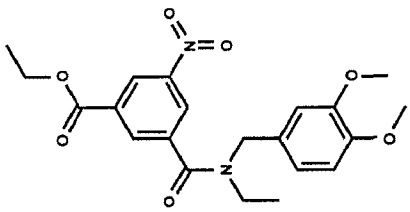
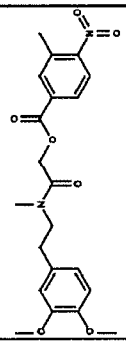
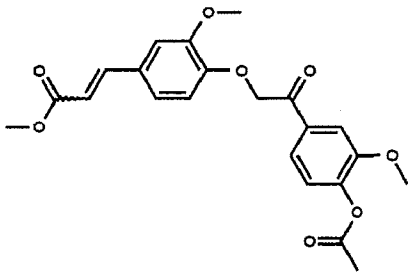
961	962	963	964
			
8666665_0 17	8666661_0 17	9125113_0 17	9125106_0 17
965	**966**	**967**	**968**
			
9468462_0 17	33183206_0 17	8629778_0 17	11026073_0 17

Fig. 23, cont'd

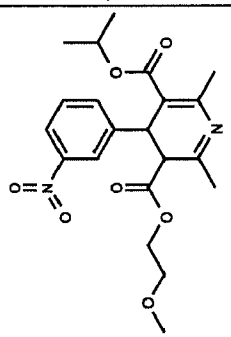
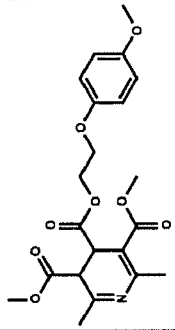
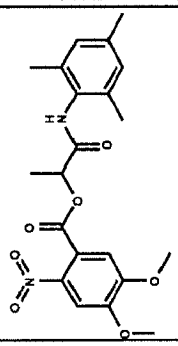
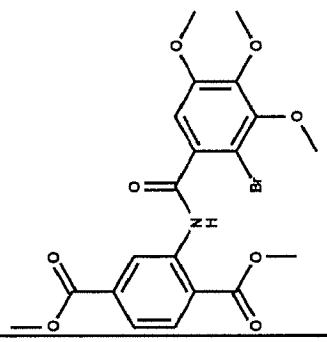
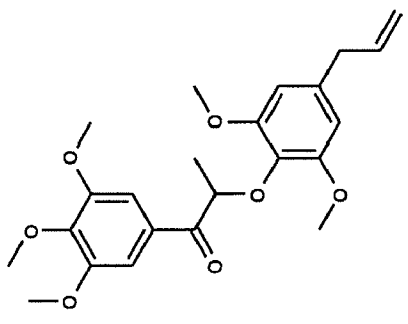
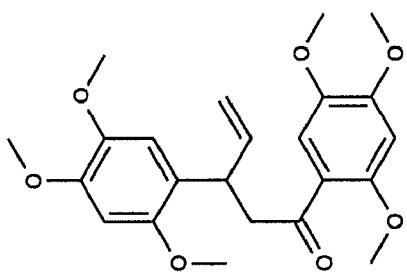
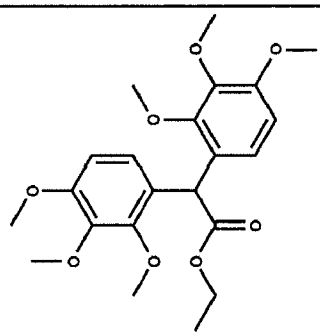
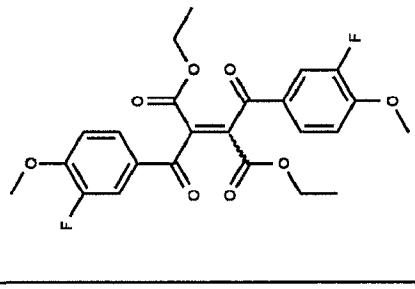
969	970	971	972
			
6992029_0,7048573	7586940_0 17	2615325_0,2615328	19172244_0 17
973	**974**	**975**	**976**
			
14236591_0 17	10001953_0 17	11384619_0 17	12127721_0 17

Fig. 23, cont'd

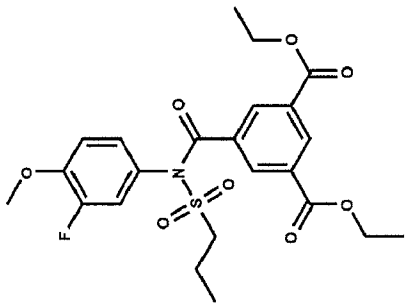
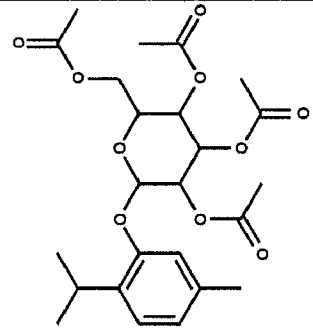
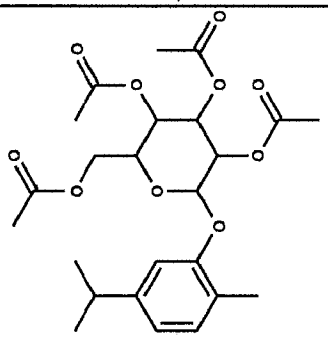
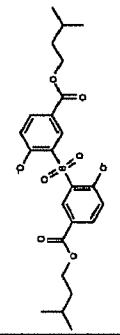
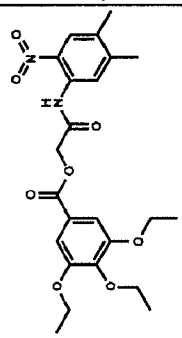
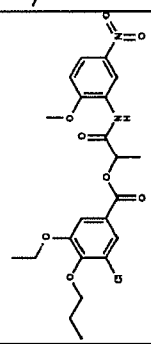
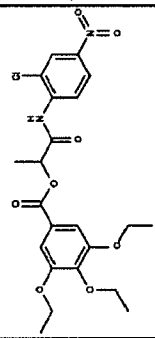
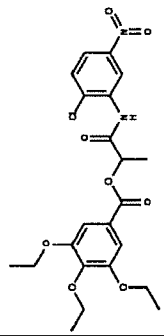
977	978	979	980
			
3771753_0 17	11835562_0,228414	27077272_0,270772	22160923_0 17
981	**982**	**983**	**984**
			
23987786_0 17	16958614_0,411852	24363386_0,416459	46790742_0 17

Fig. 23, cont'd

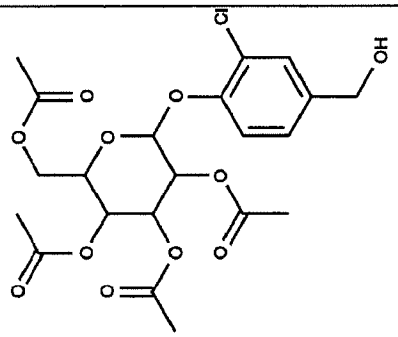
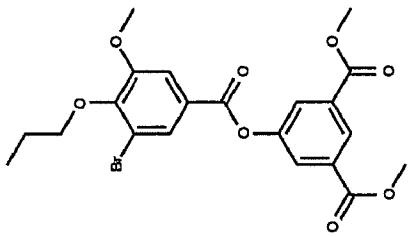
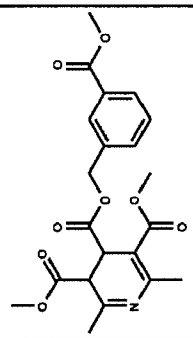
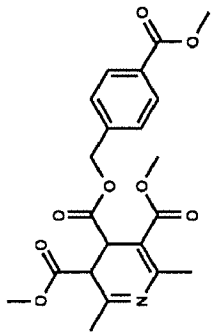
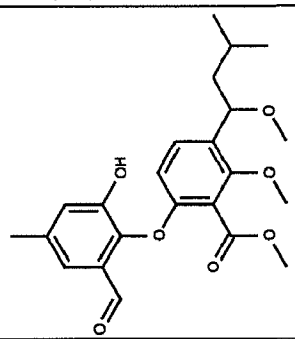
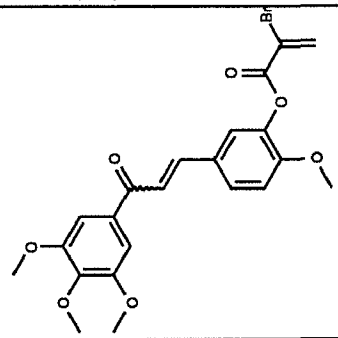
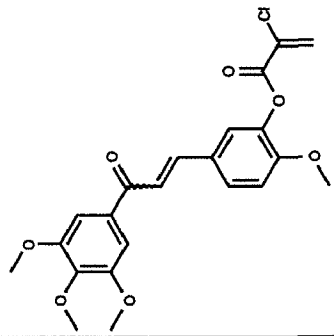
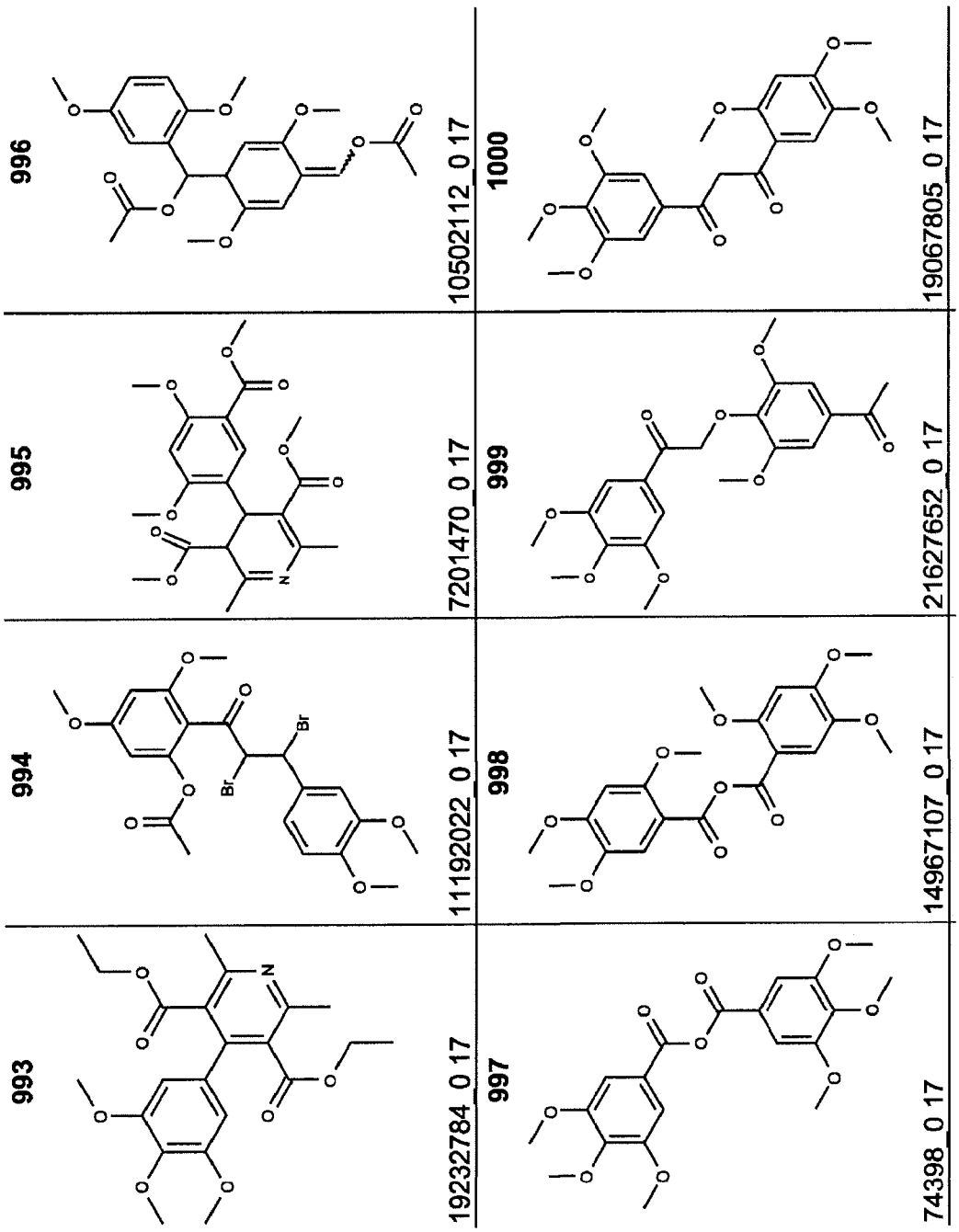
985	986	987	988
			
19420303_0 17	4849106_0 17	7587160_0 17	7587095_0 17
989	**990**	**991**	**992**
			
7586988_0 17	11796173_0 17	24815446_0 17	24815445_0 17

Fig. 23, cont'd


993
994
995
996
1000
999
998
997
1923278_4_0 17
11192022_0 17
7201470_0 17
10502112_0 17
19067805_0 17
21627652_0 17
14967107_0 17
74398_0 17